IMPACT OF DIETARY AND MICROBIAL FATTY ACIDS ON THE BIOAVAILABILITY OF PHENOLICS

KERSTIN ZIEGLER

Submitted in accordance with the requirements for the degree of

Doctor of Philosophy

The University of Leeds

School of Food Science and Nutrition

November, 2014

The candidate confirms that the work submitted is her own, except where work which has formed part of jointly-authored publications has been included. The contribution of the candidate and the other authors to this work has been explicitly indicated below. The candidate confirms that appropriate credit has been given within the thesis where reference has been made to the work of others.

Chapter 7 contains work which has also been used in the publication

'Asymmetric catalysis by UDP-glucuronosyltransferase 1A8 shows functional localisation to the cell surface'

Authors: Kerstin Ziegler, Gary Williamson

submitted to the Journal of Biological Chemistry

Chapter 4 contains work which has also been used in the publication

'Butyric acid increases transepithelial transport of ferulic acid through upregulation of the monocarboxylate transporters SLC16A1 (MCT1) and SLC16A3 (MCT4)'

Authors: Kerstin Ziegler, Laure Poquet, Gary Williamson

manuscript in preparation

Acknowledgements

I would like to thank my supervisor Gary Williamson for giving me the opportunity to work on this project and for his guidance and support. I would also like to thank Laure Poquet for her support at the Nestlé Research Center and kind encouragement. To the Nestlé Research Center for funding the PhD studentship and to the members of the Nutrient Bioavailability group for their help with the cell lipid analysis. I would also like to thank Asimina Kerimi, Sarka Tumova and Lynn McKeown for sharing their knowledge of molecular biology with me and for their continuous advice. I am also grateful to my colleagues Ebru Cetin, Jeab Charoensuk, Yuanlu Shi, Dila Jailani, Rui Pimpao and especially Kayleigh Clarke for their inspiration and to Nicolai Kraut for his help with the LC-MS/MS, the thesis submission and many interesting discussions about the quality of data.

Abstract

The current work addresses the possible impact of dietary and microbial fatty acids on the absorption of phenolics at the intestinal epithelium. The Caco-2 cell culture model of small intestinal enterocytes was optimised to mimic the chronic supplementation with physiological concentrations of fatty acid. Treatment with polyunsaturated fatty acids (PUFA) changed the fluidity of the brush border membrane, but this modification did not affect transepithelial transport of the test compounds caffeic acid, ferulic acid and epicatechin. PUFA supplementation did however increase paracellular diffusion of caffeic acid and epicatechin in apical to basolateral (a→b) transport direction. Epicatechin efflux was reduced by arachidonic acid and decosahexaenoic acid (DHA) supplementation, most likely by reducing either expression or activity of the ATP-binding cassette transporter family member C2. Transepithelial transport of ferulic acid in a→b direction was increased by PUFA supplementation, most likely through upregulation of an apical uptake transporter, whose identity could not be determined here. Supplementation of cells with the microbial metabolite butyric acid upregulated gene expression of monocarboxylate transporters 1 and 4, which resulted in increased ferulic acid uptake and metabolism. Metabolism of epicatechin was also affected by PUFA supplementation of cells. An unusual pattern of epicatechin glucuronidation by UDP-glucuronosyl transferase (UGT) 1A8 was observed in the intestinal cell line HT29-MTX. UGT activity was highly polarised within the cell, resulting in up to fifty times higher metabolite levels when the substrate reached the cell layer from what *in vivo* would be the serosal side, than from the side corresponding to the intestinal lumen. Consequent immunofluorescence staining revealed the presence of UGT1A8 in the basolateral plasma membrane. These *in vitro* results suggest a possible impact of dietary and microbial fatty acids on the absorption and metabolism of phenolic compounds.

List of figures

List of tables

Abbreviations

ABC	ATP-binding cassette
AGPAT	acylglycerol-3-acyltransferase
ASBT	Apical sodium dependent bile acid transporter
BBMV	brush border membrane vesicle
BCA	bicinchoninic acid
C8	caprylic acid
C16:0	palmitic acid
C16:1	palmitoleic acid
C18:0	stearic acid
C18:1	oleic acid
C18:2	linoleic acid
C18:3	α-linolenic acid
C20:0	arachidic acid
C20:3	eicosatrienoic
C20:4	arachidonic acid
C20:5	eicosapentaenoic acid
C21:0	heneicosanoic acid
C22:6	decosahexaenoic acid
C23:0	tricosanoic acid
C24:0	lignoceric acid
C24:1	nervonic acid
CD36	cluster of differentiation 36
CDPD	CDP-diacylglycerol
CDP	Cytidyldiphosphate
CDS	phosphatidate cytidylyltransferase
CoASH	Coenzyme A
COMT	Catechol-O-methyltransferase

CTP	Cytidyltriphosphate
DAD	diode array detector
DAG	diacylglycerol
DAPI	4',6-diamidino-2-phenylindole
DB	double bond
DBI	double bond index
DHA	decosahexaenoic acid
DMEM	Dulbecco’s modified Eagle’s medium
DRM	detergent resistant membrane
EC	(-)-epicatechin
ECG	epicatechin gallate
EGC	epigallocatechin
EGCG	epigallocatechin gallate
EFA	essential fatty acid
ELOVL	elongation of very long chain
EPA	eicosapentaenoic acid
EPT	CDP-ethanolamine:1,2-diacylgylcerol ethanolaminephosphotransferase
ER	endoplasmatic reticulum
FABP	fatty acid binding protein
FADS	fatty acid desaturase
FAME	fatty acid methylester
FAS	fatty acid synthase
FBS	foetal bovine serum
FFA	free fatty acid
FI	flame ionisation
FLD	fluorescence detector
G3P	glycerol-3-phosphate

GC	gas chromatography
GPAT	glycerol-3-phosphate acyltransferase
GTC	green tea catechins
HPT	Human peptide transporter
HUFA	highly unsaturated fatty acid
IgG	Immunoglobulin G
JAM	junctional adhesion molecule
LPA	lysophosphatidic acid
MAG	monoacylglycerol
MCT	monocarboxylate transporter
MEM	modified Eagle’s medium
MGAT	monoacylglycerol acyltransferase
MTT	3-(4,5-dimethylthiazol-2-yl)-2,5-diphenyltetrazolium bromide
MUFA	monounsaturated fatty acid
MW	molecular weight
OAT	Organic anion transporter
OATP	Organic anion transporting peptide
OCT	Organic cation transporter
OCTN	Organic cation transporter, novel
OST	organic solute transporter
PA	phosphatidic acid
PBS	Phosphate buffered saline
PC	phosphatidylcholine
PE	phosphatidylethanolamine
PepT	Peptide transporter
PI	phosphatidylinositol
PS	phosphatidylserine
PSD	phosphatidylserine decarboxylase

PSS	phosphatidylserine synthase
PUFA	polyunsaturated fatty acid
RIPA	radioimmunoprecipitation assay
RT	room temperature
SCFA	short chain fatty acid
SLC	solute carrier
SMCT	sodium coupled monocarboxylate transporter
SFA	saturated fatty acid
siRNA	small interfering RNA
SOAT	sodium-dependent organic anion transporter
SULT	Sulfotransferase
TAG	triacylglycerole
TBS	Tris-buffered saline
TEER	transepithelial electrical resistance
TMA-DPH	N,N,N-Trimethyl-4-(6-phenyl-1,3,5-hexatrien-1-yl)-phenylammonium p-toluenesulfonate
UDPGA	Uridine-diphosphate glucuronic acid
UGT	UDP-glucoronosyltransferase
WGA	wheatgerm agglutinin
ZO	zona occludens

Chapter 1: Introduction

The current work focuses on the interaction of two types of food components: lipids and polyphenols. Accordingly, this chapter consists of two parts. In the first part, a very brief overview of the great variety of phenolic compounds is given and then the mechanisms of their intestinal absorption and metabolism are highlighted. After that, the phenolics which were investigated in the current work, are introduced in more detail. In the second part of this chapter, the absorption and metabolism of dietary lipids is detailed and routes of incorporation of dietary fatty acids into cellular structures are explained.

1.1 Polyphenols

1.1.1 Classification

Polyphenols are a diverse group of compounds which are found in plants. In our diet they are therefore present in all plant derived foods, but their concentration will vary depending on the degree of processing the food has undergone and with the type and also with the part of the plant it was derived from (1). As the name suggests, polyphenols are characterised by the presence of at least one phenol group in their structure. The simplest representatives of this family of compounds are the hydroxycinnamic and hydroxybenzoic acids. They comprise one phenol ring, a carboxylic acid moiety and a different number of hydroxyl groups, connected to the aromatic ring. Most polyphenols belong to the class of flavonoids, which can be split into subgroups of flavones, isoflavones, flavanols, flavanones, anthocyanins, catechins and procyanidins (2). Figure 1.1 shows representatives of each category. Flavonoids are often conjugated to sugars and can also polymerise to form complex structures, as shown on a small scale for the procyanidin B2.

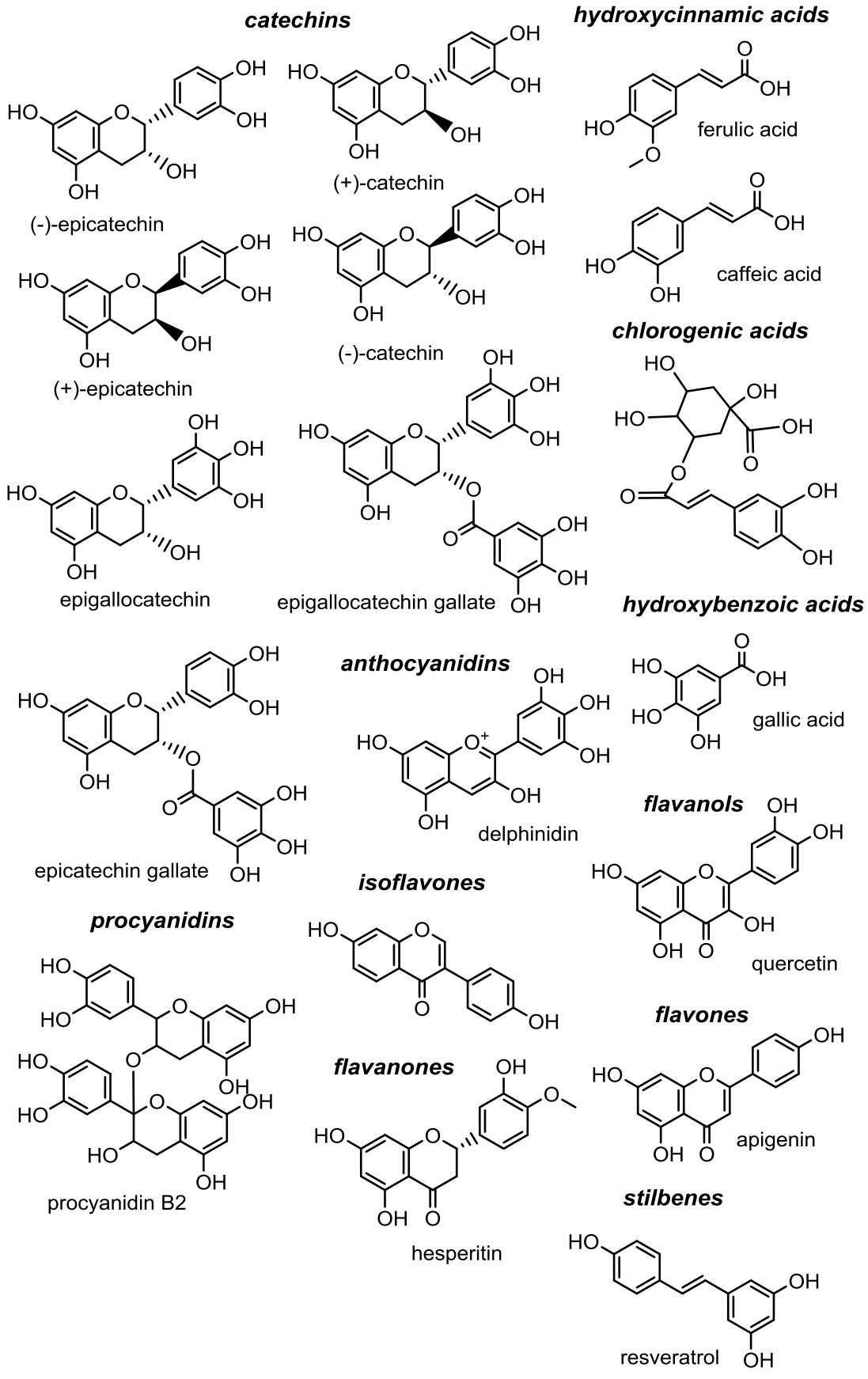

Figure 1.1; Examples structures of different polyphenol classes.

1.1.2 Transport and metabolism

Absorption of polyphenols at the intestinal epithelium occurs via three different routes of uptake: paracellular diffusion, transcellular passive diffusion and transporter mediated uptake (figure 1.2).

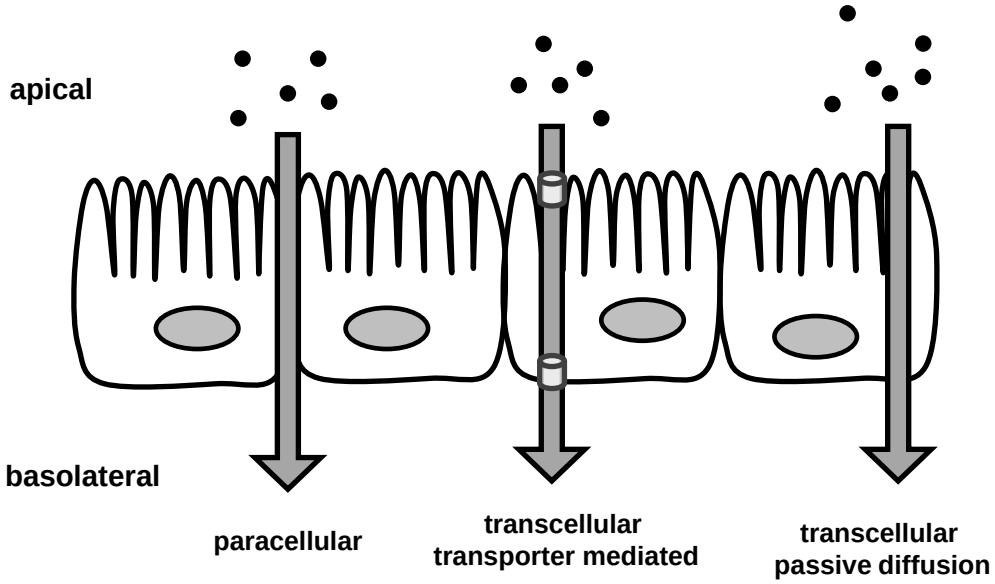

Figure 1.2; Transport routes of polyphenols across the intestinal epithelium.

Molecules that cross the intestinal lining by paracellular diffusion do not enter the cells of the epithelium but move between them. Diffusion through this intercellular space is controlled by tight junctions. These are complexes made up of different protein families that connect cells of the epithelium and regulate the passage of solutes and ions. They have also been suggested to regulate the segregation of apical and basolateral membrane proteins (3). The tight junction complex is located at the very apical end of lateral plasma membranes. Enterocytes are the most abundant cell type in the epithelium, other types include goblet cells, paneth cells, tuft cells or microfold cells (4). With such a high number of different kinds of cells in the intestinal lining, it is important that tight junctions are not only formed between the same cell type, but that there is a continuous connection, as otherwise there

would be abundant opportunity for unregulated invasion of the underlying tissue by the intestinal microflora and also potentially detrimental xenobiotics (5). Along the intestine, paracellular permeability decreases from the duodenum towards the colon, probably reflecting the increase in microbial population along this axis (6).

The tight junction complex is made up of different transmembrane proteins (the claudin family, occludin, junctional adhesion molecule (JAM)) and peripheral proteins (zonula occludens (ZO) proteins). Occludin has four transmembrane domains, two extracellular loops, one intracellular loop and one long, cytosolic C-terminal end. The extracellular loops, projecting into the paracellular space of neighbouring cells, bind to each other and hinder diffusion of larger molecules and particles. The C-terminus interacts with ZO proteins in the cytosol which in turn are linked to the actin cytoskeleton (3, 7). Though much smaller, claudins have a structure that is very similar to occludin. Whereas only a single form of occludin has been discovered, claudins are a larger protein family for which 24 members have been reported in humans. Just as described for occludin, their extracellular loops interact with each other in the intercellular space. Different members of the claudin family have been shown to have different functions in the tight junction complex. Claudin 1, claudin 3 and claudin 5 have been reported to help seal the tight junction barrier, wheras claudin 2, claudin 10b and claudin 15 are believed to form cation selective pores in the paracellular space. Claudin 10a and claudin 17 on the other hand, were shown to form anion selective pores. Unfortunately the last two family members are not well studied and there is no information on their expression in the intestine, which would be highly relevant to the work described here (8). Tight junctions between the cells of the intestinal epithelium have been reported to be smaller and more restrictive towards the tip of the villi than between crypt cells. The tight junction channel radius was shown to increase from ~ 6 to 60 Å in that direction (9) When Caco-2 monolayers were investigated regarding their pore diameter, it became apparent that there is a distinct size barrier to parracellular

diffusion. Molecules with a radius of over ~4 Å could easily diffuse across the cell layer but compounds above 4 Å exhibited much lower permeation rates, although diffusion of these larger compounds was not completely inhibited (10). These findings agree with the concept that there are two different diffusion pathways across tight junctions: a high capacity pore pathway and low capacity leak pathway (11). Members of the claudin family can also form heterodimers. On the cytoplasmic site, claudins are linked to the cytoskeleton via ZO proteins (3, 7). JAM have a single extracellular strand with two immunoglobulin (Ig) domains and a cytoplasmic tail that also links the to the actin skeleton via ZO proteins. They form homodimeres with JAM of neighbouring cells but have also been reported to interact with other types of proteins, for example integrins (12).

Cells are not only connected by tight junctions but also by gap junctions and desmosomes. But these two types of connection do not primarily serve the purpose of sealing the intercellular space and preventing diffusion, but they facilitate communication between cells and provide a stable connection. Gap junctions consist of small channels made up from proteins of the connexin family, through which neighbouring cells can exchange ions and small molecules (13, 14). Desmosomes on the hand, provide a very strong connection between cells of a tissue, helping to resist mechanical stress. They are protein complexes made up of membrane spanning cadherins, that bind to cadherin strands of neighbouring cells, and of intracellular connections that link desmosomes to the cytoskeleton (15). In the lateral space between cells of the intestine, gap junctions and desmosomes are located more towards the basolateral membrane than tight junctions. Small phenolic compounds like gallic acid (16) or caffeic acid (17) are most likely to cross the intestinal epithelium by paracellular diffusion.

Transepithelial transport of compounds across intestinal enterocytes, that are to large or polar to cross by paracellular route, can be facilitated either by uptake transporters located at the apical membrane or by efflux transporters at the

basolateral membrane. Many polyphenols are allocrites (substrates) of members of the SLC transporter family. Apical uptake in enterocytes is mostly facilitated by the transporters Organic cation transporter 3 (OCT3), Peptide transporter 1 (PepT1), Organic anion transporting peptide A and B (OATPA/B), Organic cation transporter, novel 1 and 2 (OCTN1/2), Human peptide transporter 1 (HPT1) and Apical sodium dependent bile acid transporter (ASBT). Basolateral efflux is mainly mediated by members of the ATP-binding cassette (ABC) transporter family (18, 19).

But transporters are not only involved in uptake of phenolics from the intestinal lumen and excretion on the serosal side, but they can also limit the bioavailability of polyphenols through active excretion back into the intestinal lumen. Such apical efflux transporters are mostly members of the ABC family. Especially ABCB1, ABCC2 and ABCG2 have been shown to facilitate excretion of xenobiotics and their phase II metabolites. These transporters are highly expressed in enterocytes of the small intestine (20).

Phase II metabolism of phenolics mainly comprises conjugation by sulfotransferases (SULT), catechol-*O*-methyltransferase (COMT) and UDP-glucuronosyltransferases (UGT).

In vertebrates, the UGT protein is spanning the endoplasmic reticulum (ER) membrane with the active site facing the ER lumen (21). UGTs catalyse the transfer of glucuronic acid from the co-factor UDP-glucuronic acid (UDPGA) to a nucleophilic group of the substrate, increasing the compound’s polarity and thus enabling active transport and excretion (22).

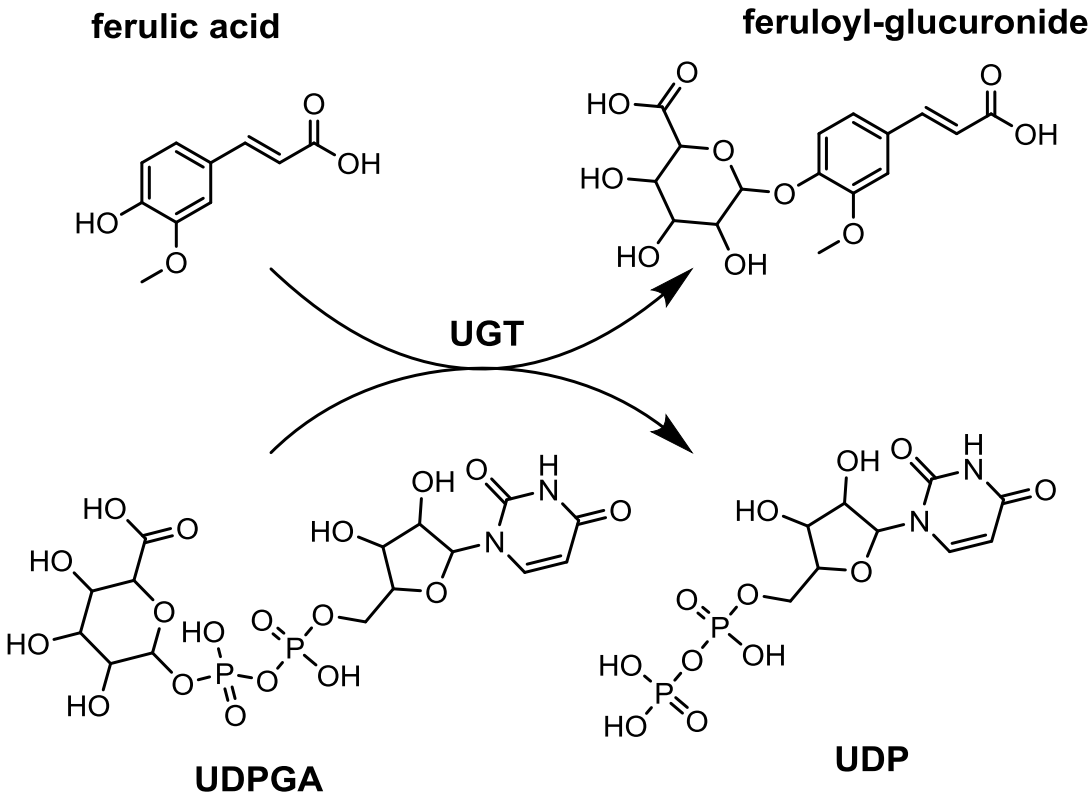

Figure 1.3; Glucuronic acid conjugation of ferulic acid catalysed by UDP-glucuronosyltransferase (UGT). UDPGA = UDP-glucuronic acid, UDP = Uridine-diphosphate

UGTs display broad substrate specificity ranging from drugs (23, 24) to environmental pollutants (25-27) and endogenous compounds (28-31). Many polyphenols are glucuronic acid conjugated (32-34). Glucuronidation affects the bioavailability and activity of polyphenols and with that, their potential health effect (32). In vertebrates four UGT families have been described: UGT1, UGT2, UGT3 and UGT8. So far, no function could be observed for UGT8. Members of the UGT3 family do not have UDPGA as their co-factor but instead catalyse the transfer of glucose-, xylose- or N-acetylglucosamine moieties. However, UGT3 activity only plays a minor role in phase II metabolism which is almost entirely facilitated by the UGT1A and UGT2B families (35). The highest UGT activity is found in liver and intestine. Ohno and Nakajin analysed samples from various tissues for relative mRNA abundance of different UGT isoforms. Overall, they found much higher levels of UGT2B than UGT1A forms, except for UGT1A9 which is highly expressed in

kidney. The main UGT2B isoforms in hepatic tissue are UGT2B4 and UGT2B15, the main UGT1A forms are UGT1A1 and UGT1A9. In the intestine they found UGT2B7, UGT2B17, UGT1A1 and UGT1A10 to be most abundant (36).

SULTs catalyse the transfer of a sulfonyl-moiety from the co-factor 3ˈ-phosphoadenosin-5ˈ-phosphosulfate (PAPS) to hydroxyl- or amine groups of a substrate. Reaction products are the sulfonated substrate and 3ˈ-phosphoadenosine-5ˈ-phosphate (PAP) (figure 1.4). The strongest SULT activity is found in liver. There are two major SULT families, the cytosolic SULTS and the membrane bound SULTs. Membrane bound SULTs are mainly located at the trans-Golgi site and are involved in posttranslational modification. Membrane bound SULTs have glycoproteins, lipids and peptides as substrates. Cytosolic SULTS are involved in inactivation and regulation of hormones and neurotransmitters, for example sterols and catecholamines, but they are also crucial enzymes of phase II metabolism. The major SULT forms expressed in the human small intestine are SULT1A3, SULT1A1 and SULT1B1. As with glucuronic acid conjugation, sulfonation increases the polarity and size of a compound and makes it thus a more likely allocrite of ABC efflux transporters in the intestine. (37-39)

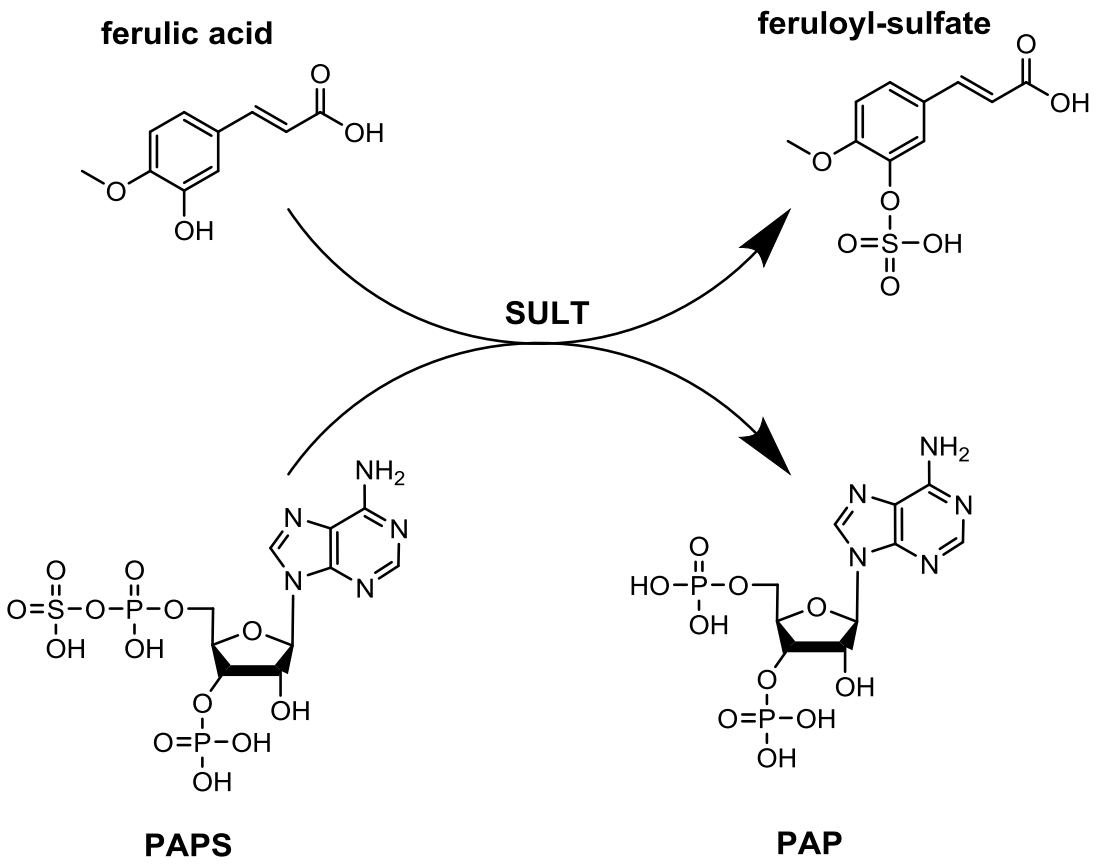

Figure 1.4; Conjugation reaction catalysed by sulfotransferases (SULT) with the example of ferulic acid. PAPS = 3ˈ-phosphoadenosin-5ˈ-phosphosulfate, PAP = 3ˈ-phosphoadenosine-5ˈ-phosphate

COMT activity is highest in intestine, liver, kidney and brain. There are two forms, the cytosolic COMT (C-COMT) and membrane bound COMT (MB-COMT). The latter is highly expressed in brain tissue, but in all other organs C-COMT is the major form. COMT catalyses the formation of an ether bond between a hydroxyl group of the xenobiotic and a methyl group donated by the co-factor S-adenosyl methionine (figure 1.5) (40).

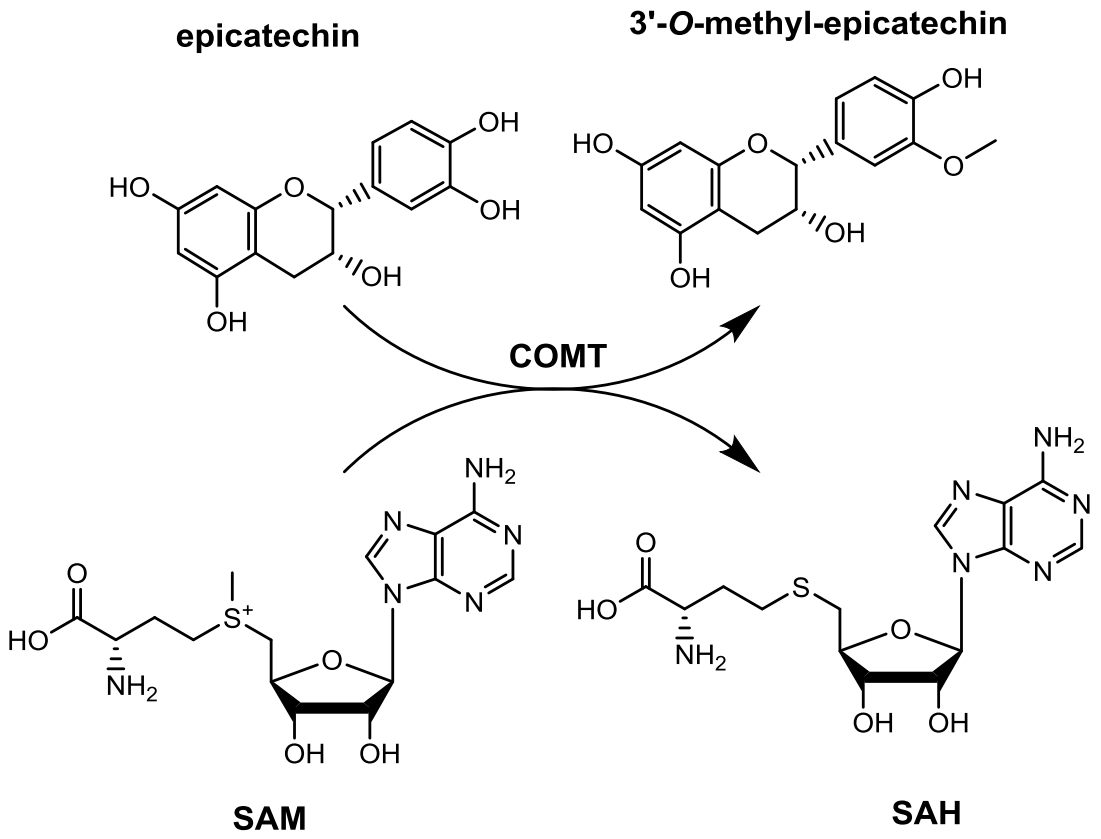

Figure 1.5; Methylation of epicatechin by Catechol-*O*-methyltransferase (COMT). SAM = S-adenosyl methionine, SAH = S-adenosyl-L-homocysteine

1.1.3 Ferulic and caffeic acid

Ferulic acid is most abundant in whole grain cereals, coffee, chocolate and berry fruits (41, 42). In whole grains, ferulic acid is mostly esterified to arabinose side chains of hemicellulose strands in the plant cell wall and is the most abundant phenolic from cereals (43), but only traces of ferulic acid are found in the endosperm (44). Since only this part is used for the production of white flour, foods made from this type of flour do not contain significant amounts of phenolic acids (45). In its bound form, ferulic acid cannot be absorbed in the small intestine, the fibre fraction first has to undergo enzymatic hydrolysis before the free acid can be absorbed at the intestinal mucosa. Cells of the mammalian gastrointestinal tract only have low cinnamoyl esterase activity (46), but several species of the colon microflora are able

to hydrolyse these ester bonds efficiently (47, 48) and the released phenolic acid is then absorbed in the large intestine. Most ferulic acid from cereals is present in the bound form, but there is a small fraction which is present as the free acid, and this can be readily absorbed in the small intestine (49). A similar distribution of free and esterified ferulic acid is also found in coffee. Here the major part of ferulic acid occurs in form of chlorogenic acid, in which ferulic acid is esterified to quinic acid, but there is also a small percentage of free ferulic acid present (50). Chlorogenic acids can also be hydrolysed by microbial esterases in the large intestine to release the free acid. Whether a compound is absorbed in the small or large intestine can be seen from their pharmacokinetic profile. Absorption in the small intestine occurs rapidly, the maximum plasma concentration is usually observed within the first two hours after ingestion, whereas phenolic acids released in the large intestine will only enter the bloodstream five to ten hours after food consumption (42). Here the matrix and the form of administration can play a role in the exact time profile, for example, ferulic acid from a morning coffee drunk on an empty stomach will reach the small and also the large intestine much faster than ferulic acid from wholemeal bread that is part of a large dinner. Absorption of ferulic acid from coffee occurs in two phases, the first maximum plasma concentration is reached within one hour due to the compound being taken up from the lumen of the stomach and small intestine. After that, the concentration in plasma decreases again, until about five hours after coffee consumption, when ferulic acid released in the colon results in a second rise plasma concentration (51).

Another phenolic acid that is present in coffee but also fruits, salad and spices is caffeic acid (41, 42). Absorption of caffeic acid from coffee and apple cider has been shown to occur rapidly, the maximum plasma concentration was reached within two and one hour, respectively (51-53). In coffee, caffeic acid is also mainly present in form of its quinic acid ester.

1.1.4 Epicatechin

The best source of (-)-epicatechin is chocolate, but it is also found in a range of fruits, green tea and broad beans (41). But even though with an average of 70 mg/100 g dark chocolate is the food with the highest concentration of (-)-epicatechin, it might not contribute the highest amount to the diet if one considers portion sizes. 100 g of chocolate equals to an entire bar, which is probably not eaten on a regular basis. Green tea infusions on the other hand, might contain a lower concentration with about 8 mg/100 mL, but regular tea drinkers will consume much more than this every day (41). Even with black tea, which contains about half the amount of (-)-epicatechin compared to green tea, habitual consumption will most likely contribute more than the occasional chocolate snack (54). (-)-Epicatechin is one of four stereoisomers that naturally occur for this compound (see figure 1.1), but it is the most abundant one in tea and chocolate. Especially in green tea, (-)-epicatechin is also accompanied by epicatechin gallate (ECG), epigallocatechin (EGC) and epigallocatechin gallate (EGCG) (see figure 1.1). These other members of the catechin family also occur in other types of food, but their combination and high amount is characteristic for green tea which is why they are collectively called green tea catechins (GTC) together with the (-)-epicatechin stereoisomer (+)-catechin. Most human bioavailability studies of (-)-epicatechin have been conducted using either green tea or green tea extracts. In tea infusions EGCG is usually the most abundant GTC followed by EGC. (-)-Epicatechin and ECG are only present in lower amounts (55, 56). The different types of GTC vary in their bioavailability. (-)-Epicatechin is absorbed best and found in plasma and urine almost exclusively in form of its phase II metabolites whereas EGCG is absorbed least and mostly present in the free form (56, 57). Absorption of GTC occurs in the small intestine and is dose dependent. Maximum plasma concentrations are usually observed within two hours of ingestion. High total concentrations of (-)-epicatechin and its metabolites were reached in plasma when high doses were administered.

When plasma levels were investigated after consumption of green tea infusions of varying strength, tea containing 0.13 mmole (-)-epicatechin resulted in total plasma concentration of 0.13 µM and 0.38 mmole of (-)-epicatechin resulted in 0.22 µM of that compound in plasma (58). When green tea extracts, which contain much higher GTC levels than the tea infusions, were administered, total plasma concentrations of (-)-epicatechin increased correspondingly. With the extract, 11, 19 and 65 µM (-)-epicatechin were detected in plasma after consumption of 5, 13 and 26 mmole of the compound, respectively (56, 59). In comparison to that, the concentration of free (-)-epicatechin was only about 0.15 nM after consumption of 581 mg green GTC (60), whereas individual metabolites were present in over 100 fold higher concentrations (55). Using chocolate instead of green tea as an (-)-epicatechin source, similar dose relationships were observed with 28 and 56 mmole consumption,which gave rise to plasma concentrations of 35 and 68 µM respectively (61). These total concentrations of epicatechin only include metabolites that are formed from (-)-epicatechin absorbed in the small intestine. Only about 5 - 10 % of the administered (-)-epicatechin dose was found in urine (55, 57), suggesting that the major part of the compound reaches the colon. Here all GTC are digested by the colon microflora and absorbed in form of two valerolactone break-down products termed M4 and M6 (62). But since all tea catechins can be broken down to yield these two metabolites, it is not possible to determine the part each individual compound contributes to the overall amount when a combination of catechins was administered.

1.2 Lipids

1.2.1 Intestinal absorption and metabolism

Lipids are the most energy dense part of our diet. In the Western diet fat accounts for 30 - 40 % of the total energy intake (63-67). The major lipid components of food are triacylglycerols which provide 90 - 95% of energy from all dietary lipids (68). Other components are cholesterol, phospholipids, sterolesters and free fatty acids (FFA). Since the current work focuses on non-sterol lipids, only the absorption and metabolism of triacylglycerols and free fatty acids are reviewed.

Digestion of lipids starts in the mouth. Lingual lipase, which hydrolyses triacylglycerols to two molecules FFA and one molecule monoacylglycerol, is secreted by salivary glands of the tongue. Lingual lipase secretion has been shown to be stimulated by chewing and the lipid composition of foods (69). Digestion of lipids continues in the stomach which secretes gastric lipase that differs from other members of this enzyme family by being stable and fully active at the very low pH prevalent in the stomach. It also does not require the cofactor colipase, as pancreatic lipase does (70).

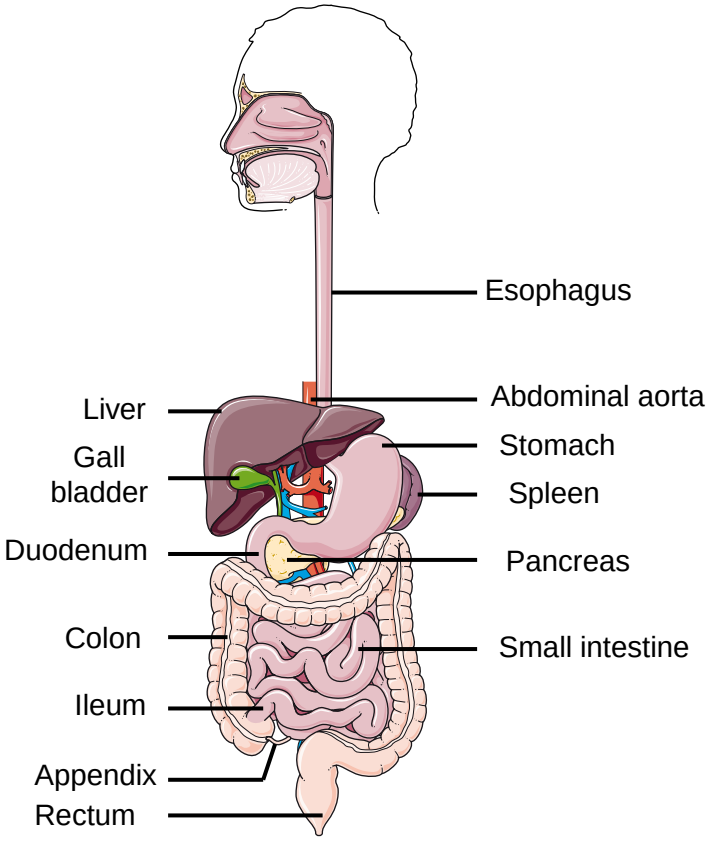

Figure 1.6; Overview of the gastrointestinal tract anatomy. Adapted from (71)

In the stomach, lipids are already emulsified by the stomach acid and when the chymus is emptied into the duodenum, these lipid droplets are then further dispersed and mixed with bile, which is produced by the liver and stored in the gall bladder from where it is released into the duodenum upon stimulation by gastric emptying. The main components of bile are bile acids, phospholipids and cholesterol, which help to disperse dietary lipids into small micelles and enhance the oil/water surface area at which water soluble lipases can catalyse the hydrolysis of triacylglycerols. Bile acids are reabsorbed along the small intestine via the sodium-dependent bile acid transporter (72) and transported back to the liver where they are filtered out and secreted again with the bile (73, 74). Pancreatic lipase, which is the more active than its lingual and gastric family members, is also secreted into the duodenum, together with the cofactor colipase which prevents the enzyme from being inhibited by bile acids. The pancreas also secretes phospholipase and

carboxylester lipase which are able to hydrolyse phospholipids, lysophospholipids and sterol esters (68, 75).

The main sites of lipid absorption are the duodenum and ileum. The concentration of FFA in enterocytes of the small intestine remains low as upon entering the cell, they are very rapidly bound by fatty acid binding protein (FABP). This mechanism ensures that the concentration gradient of FFA is maintained so that even low amounts of this energy dense nutrient can always freely diffuse into the cell. FFA absorption is dependent on chain length and saturation. Increasing chain length reduces absorption and increasing desaturation increases absorption. The medium chain fatty acids myristic and palmitic acid are almost entirely absorbed but the long chain fatty acid stearic acid much less and arachidic acid with an acyl chain length of 20 carbon atoms is only taken up by about 25 %. Whereas arachidonic acid, which is the same length as arachidic acid, but contains five double bonds, is almost completely absorbed again (76). FFA uptake has also been suggested to occur by transporters cluster of differentiation 36 (CD36) and fatty acid transport protein (FATP), but it was subsequently shown that these proteins do not influence the net absorption of lipids in the intestine but are more important in directing absorbed fatty acids to specific pathways of lipoprotein formation (68, 77). Caveolae mediated endocytosis has also been identified as a possible fatty acid uptake mechanism (78).

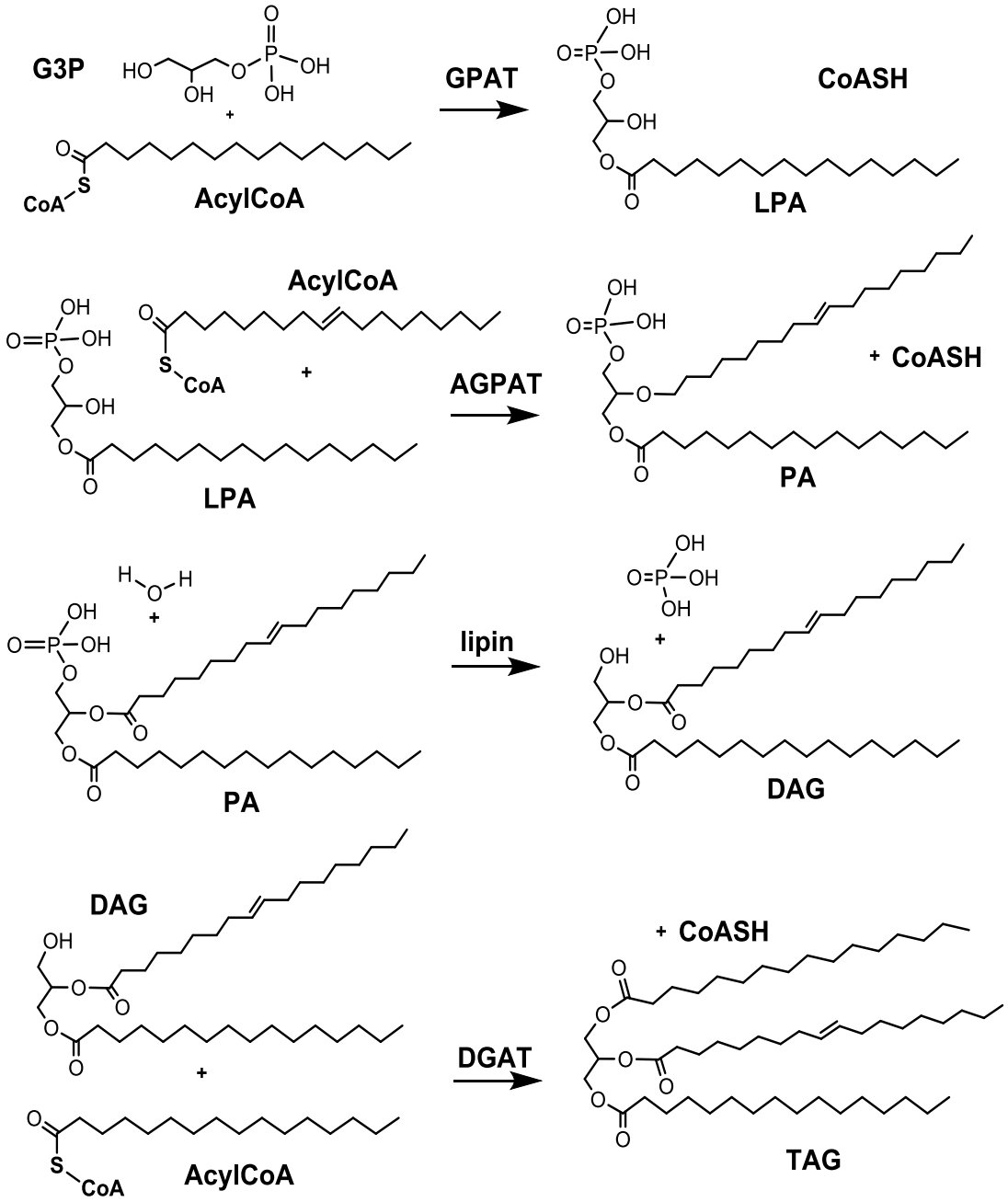

Figure 1.7; The glycerol-3-phosphate pathway of triacylglycerol synthesis. GPAT = glycerol-3-phoshate acyltransferase, AGPAT = acylglycerol-3-acyltransferase, DGAT = diacylglycerol acyltransferase, CoASH = Coenzyme A, G3P = glycerol-3-phosphate, LPA = lysophosphatidic acid, PA = phosphatidic acid, DAG = diacylglycerol, TAG = triacylglycerol

All cell types have the ability to synthesise triacylglycerols via the glycerol-3-phosphate pathway and intestinal enterocytes are no exception. Triacylglycerol synthesis via this pathway is illustrated in figure 1.7. The first step in this series of reactions is the transfer of a fatty acid moiety, that has been activated

through conjugation to Coenzyme A (CoA) by acylCoA synthase (ACS), to glycerol-3-phosphate at the n-1 position, resulting in the formation of lysophosphatidic acid (75, 77). This reaction is catalysed by the enzyme glycerol-3-phoshate acyltransferase (GPAT). Four different forms of GPAT were identified, GPAT 1 and 2 reside in the outer mitochondrial membrane and GPAT 3 and 4 reside in the ER membrane (79). Lysophosphatidic acid is then esterified with one further acylCoA molecule resulting in phosphatidic acid. This reaction is catalysed by acylglycerol-3-acyltransferase (AGPAT). This reaction occurs in the ER. In the next step, phosphatidic acid is dephosphorylated to diacylglycerol by members of the lipin family. This step occurs in the ER lumen but the three members of the lipin family with phosphatase activity that have been identified in humans, are also present in the cytosol. Enzyme translocation to the ER is regulated by the cytosolic concentration of acylCoA and insulin. In the final step of the glycerol-3-phosphate pathway, another fatty acid is transferred to diacylglycerol by diacylglycerol acyltransferase (DGAT) to form triacylglycerol (79-81).

However, in the postprandial phase, high concentrations of not only FFA but also monoacylglycerol are available in enterocytes of the small intestine. These are primarily re-esterified into triacylglycerol through the monoacylglycerol pathway (illustrated in figure 1.8) that is unique to this cell type. The monoacylglycerol pathway is essentially the reverse of the lipase activity. It contains two steps, in the first a CoA activated FFA is transferred to monoacylglycerol, catalysed by monoacylglycerol acyltransferase (MGAT). The second step is identical to the last step of the glycerol-3-phosphate pathway, the formation of triacylglycerol from diacylglycerol and fatty acid CoA. This step is also catalysed by DGAT. Both reactions occur in the ER (68, 79-81). This pathway of triacylglycerol synthesis from monoacylglycerole and acylCoA is very fast and occurs within seconds of absorption of the monomers (78).

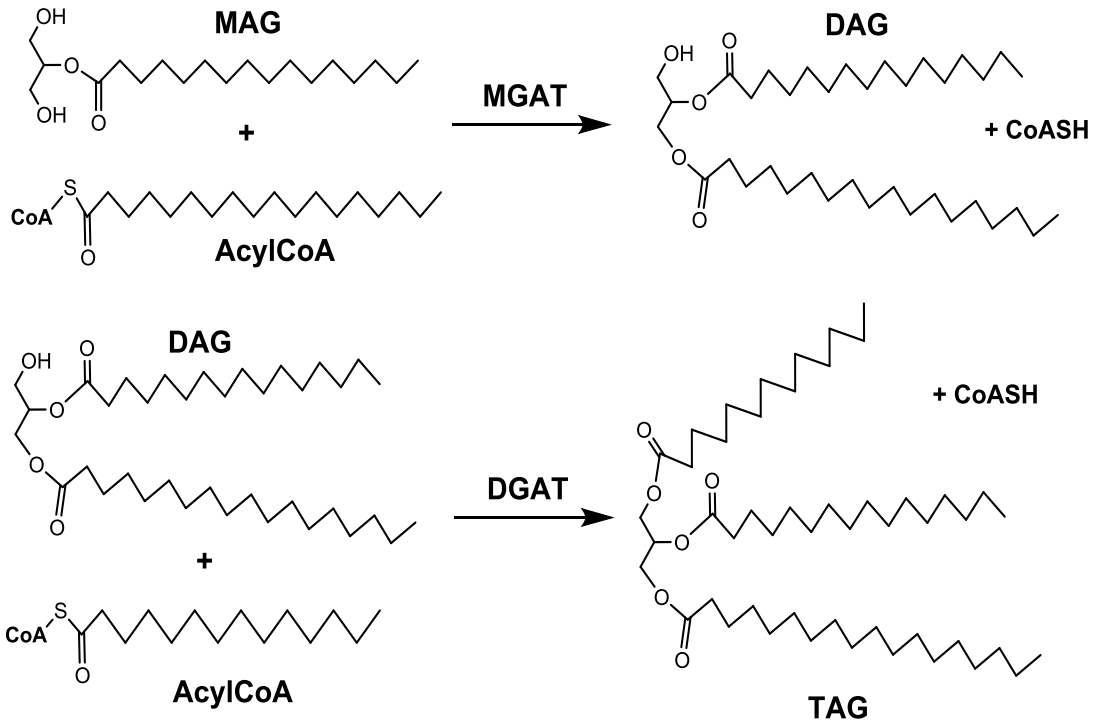

Figure 1.8; The monoacylglycerol pathway of triacylglycerol synthesis. CoASH = Coenzyme A, DAG = diacylglycerol, DGAT = diacylglycerol acyltransferase, MAG = monoacylglycerol, MGAT = monoacylglycerol acyltransferase, TAG = triacylglycerol

Triacylglycerols formed from dietary lipids in the small intestine are either stored in form of lipid droplets or packed into lipoproteins and excreted at the serosal side into the lymph or blood for systemic distribution. While the liver mainly synthesises very low density lipoprotein (VLDL), the intestine mainly synthesises chylomicrons. These are the largest type of lipoproteins with a lipophilic core made up of triacylglycerols, cholesterol and sterolesters. These neutral lipids are surrounded by a single phospholipid layer that contains different coat proteins of the apolipoprotein (Apo) family. Formation of chylomicrons starts in the ER lumen. During extrusion of ApoB48 from the translocon into the ER lumen, the protein attracts and binds triacylglycerols at the inner ER membrane surface and eventually folds around the lipid molecules and buds of as a nascent ApoB48 rich particle (82). This process is assisted by the microsomal triglycerol transfer protein (MTTP) but the exact mechanism is not clear (77). The ApoB48 particle then fuses with lipid droplets made up of triacylglycerols, cholesterol and phospholipids formed in the ER, which

causes it to expand and become less protein dense. This pre-chylomicron is then transported to the Golgi, in pre-chylomicron transfer vesicles (PCTV), which are unique to cells of the small intestine, and during migration though the Golgi, further Apo coat proteins are added and glycosylated (68, 75). As mentioned above, there is evidence that CD36 is involved in directing triacylglycerols to incorporation into chylomicrons instead of VLDL, as deficiency in that protein was associated with decreased chylomicron and increased VLDL synthesis in the intestine. CD36 is found in PCTVs but is also ubiquitously expressed throughout the body. CD36 deficiency also results in decreased uptake of lipids into cells which leads to prolonged circulation of lipoproteins in plasma (68, 77, 78, 83).

Triacylglycerols synthesised in the small intestine can also be stored in form of cytosolic lipid droplets. Transient storage of dietary lipids in the postprandial phase is a common mechanism that prevents hyperlipidaemia due to a surge of lipoproteins entering the bloodstream after a meal (75). The mechanism of lipid droplet formation is still not resolved and several modes of droplet initiation have been proposed. The most widely accepted one is the accumulation of triacylglycerols between the two sheets of the ER membrane, attracting more and more neutral lipids while growing and eventually budding off into the cytosol. This mechanism would explain that lipid droplets are surrounded by a single phospholipid layer and not by a bilayer like all other organelles (84). It is also under discussion to what extend lipid droplets stay in contact with the ER. Proteomic analysis of proteins extracted from the lipid droplet phospholipid coat, have shown the presence of a number of lipid processing enzymes, like DGAT, ACS, lysophosphatidylcholine acyltransferase and monoglyceride lipase, suggesting a role of these storage organelles in lipid metabolism (85-87).

But lipids are not only turned over into triacylglycerols to be used for storage and energy production but they also constitute the building material of all cellular membranes. Each cell and each organelle is surrounded by a lipid bilayer that is

mainly made up of phospholipids and cholesterol. Phospholipids are composed of a glycerol backbone with different fatty acids attached at n-1 and n-2 position and a headgroup linked to the carbon 3 via a phosphate moiety. There is a variety of different headgroups and together with different acyl chains, there are hundreds of possible combinations varying slightly in their physical properties which makes it possible that different membranes can exhibit unique properties regarding their thickness, polarity, fluidity, curvature and other characteristics, tailoring them for a variety of tasks and environments. In human ileum samples, the most abundant lipid classes, besides cholesterol, were phosphatidylcholine and phosphatidylethanolamin but also phosphatidylserine and phosphatidylinositol and some sphingomyelin and ceramide (88). Synthesis of those phospholipids is illustrated in figure 1.9 and the general structure of the two sphingolipids is shown in figure 1.10. Phospholipids are synthesised from either phosphatidic acid or diacylglycerol. In both cases reactants are activated by conjugation with cytidine diphosphate (CDP). The difference is that with phospholipids based on phosphatidic acid, the lipid is CDP conjugated and then the nucleotide is exchanged for the headgroup, as shown for the synthesis of phosphatidylinositol, whereas with phospholipids based on diacylglycerol, the headgroup is activated by CDP conjugation and then reacts with the lipid, as shown for phosphatidylcholine and phosphatidylserine formation (89). Interestingly, it was shown that intestinal cells process absorbed lipids differently depending on whether they were taken up from the basolateral or from the apical side. Lipids entering the cell from the basolateral side are more likely to be incorporated into phospholipids instead of triacylglycerols compared to lipids taken up from the apical side (90-92).

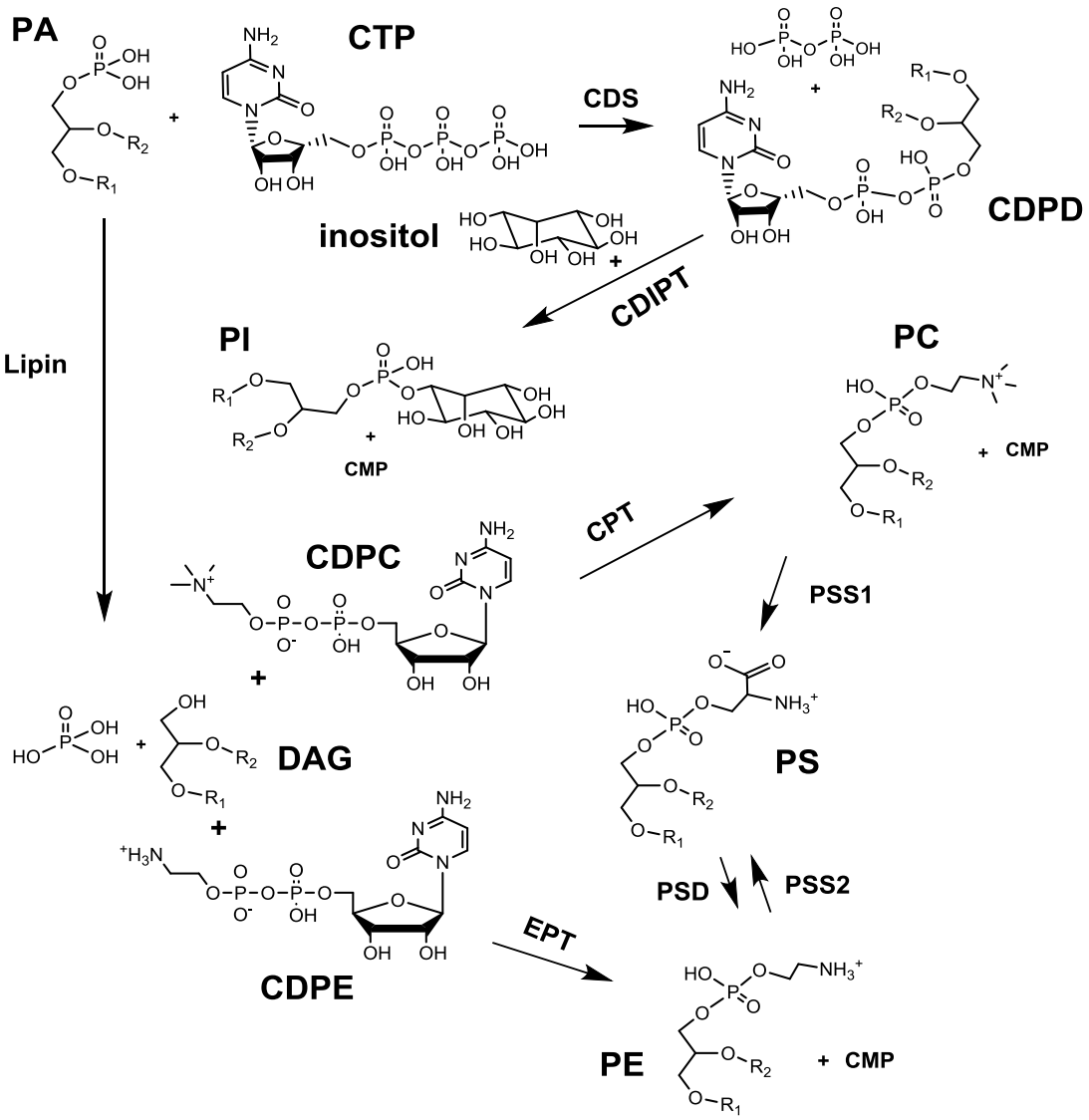

Figure 1.9; synthesis of phospholipids from intermediates of the glycerol-3-phosphate pathway. CDIPT = CDP-diacylglycerol inositol phosphatidyltransferase, CDP = cytidyldiphosphate, CDPD = CDP-diacylglycerol , CDPE = CDP-ethanolamin, CDS = phosphatidate cytidylyltransferase, CMP = cytidine monophosphate, CDPC = CDP-choline, CPD = CDP-choline: 1,2-diacylgylcerol cholinephosphotransferase, CTP = Cytidyltriphosphate, DAG = diacylglycerol, CDP-ethanolamine:1,2-diacylgylcerol ethanolaminephosphotransferase PA = phosphatidic acid, PC = phosphatidylcholine, PE = phosphatidylethanolamin, PI = phosphatidylinositol, PS = phosphatidylserine, PSD = phosphatidylserine decarboxylase, PSS = phosphatidylserine synthase

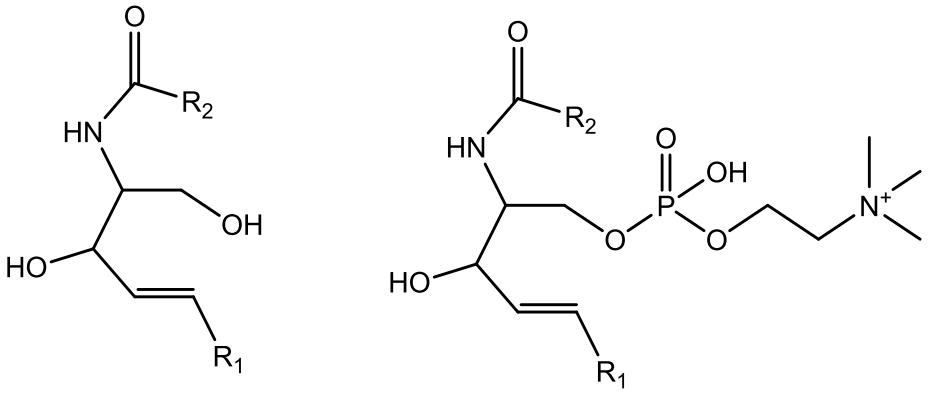

ceramide **sphingomyelin**

Figure 1.10; Structure of ceramides and sphingomyelins. R = acyl chain

Cells of the small intestine are well supplied with fatty acids from the diet but other cell types, especially in liver and adipose tissue, also synthesise fatty acids *de novo*. Fatty acids up to a chain length of 16 carbon atoms are synthesised in the cytoplasm by the multi-enzyme complex fatty acid synthase (FAS) and then further elongated in the ER. Via these two routes, fatty acids with up to 26 carbon atoms can be synthesised *de novo*. There are six different elongases in mammals termed elongation-of-very-long-chain-fatty-acids (ELOVL) 1-6 (93, 94). Different members of that family are expressed in different tissues and have varying substrate specificity. For example, ELOVL5 preferentially elongates fatty acids with a chain length of 18 - 20 carbon atoms, whereas ELOVL2 has the highest activity towards fatty acids with a chain length of 20 to 24 carbon atoms (95, 96). All fatty acids produced by these enzymes are saturated fatty acids (SFA). In humans, double bonds can be introduced to the acyl chains by four members of the desaturase enzyme family, Δ4-, Δ5-, Δ6- and Δ9 desaturase, resulting in monounsaturated fatty acids (MUFA). Fatty acids taken up from the diet can also be processed further through elongation and desaturation. Since mammals do not have the ability to synthesise highly unsaturated fatty acids (HUFA) *de novo*, they have to rely on supplementation with the diet. But not all HUFA need to be present in the diet to the extent they are required by tissues, some can be synthesised from the polyunsaturated fatty acid

(PUFA) precursors linoleic acid and α-linolenic acid. Below is a list of the most abundant fatty acids that are found in tissue and in the diet:

SFA		MUFA		PUFA	
C8:0	caprylic				
C10:0	capric				
C12:0	lauric				
C14:0	myristic				
C16:0	palmic	C16:1	palmitic (n-7)		
C18:0	stearic	C18:1	oleic (n-9)	C18:2	linoleic (n-6)
				C18:3	α/γ-linolenic (n-3/6)
C20:0	arachidic	C20:1	gondoic (n-7)	C20:3	eicosatrienoic (n-6)
				C20:4	arachidonic (n-6)
				C20:5	EPA (n-3)
C22:0	behenic	C22:1	cetoleic (n-11)	C22:6	DHA (n-3)
C24:0	lignoceric	C24:1	nervonic (n-9)		

Table 1.1; The most common dietary and tissue fatty acids. The short form is given as CX**:**Y with X = number of carbon atoms in the acyl chain and Y = number of double bonds in the acyl chain. After the trivial name, n-Z denotes the carbon atom Z at which the first double bond is located counting from the n or omega (ω) end of the chain which is the opposite of the delta (Δ) or alpha (α) end that bears the carboxylic acid moiety. SFA = saturated fatty acid, MUFA = monounsaturated fatty acid PUFA = polyunsaturated fatty acid

Most PUFA either belong to the n-3 or the n-6 series. All n-3 PUFA can be endogenously synthesised from α-linolenic acid and all n-6 PUFA can be synthesised from linoleic acid, but these two smallest members of their series have to be taken up with the diet and are therefore termed essential fatty acids (EFA)

(94). The sequence of reactions leading from those EFA to HUFA is illustrated below:

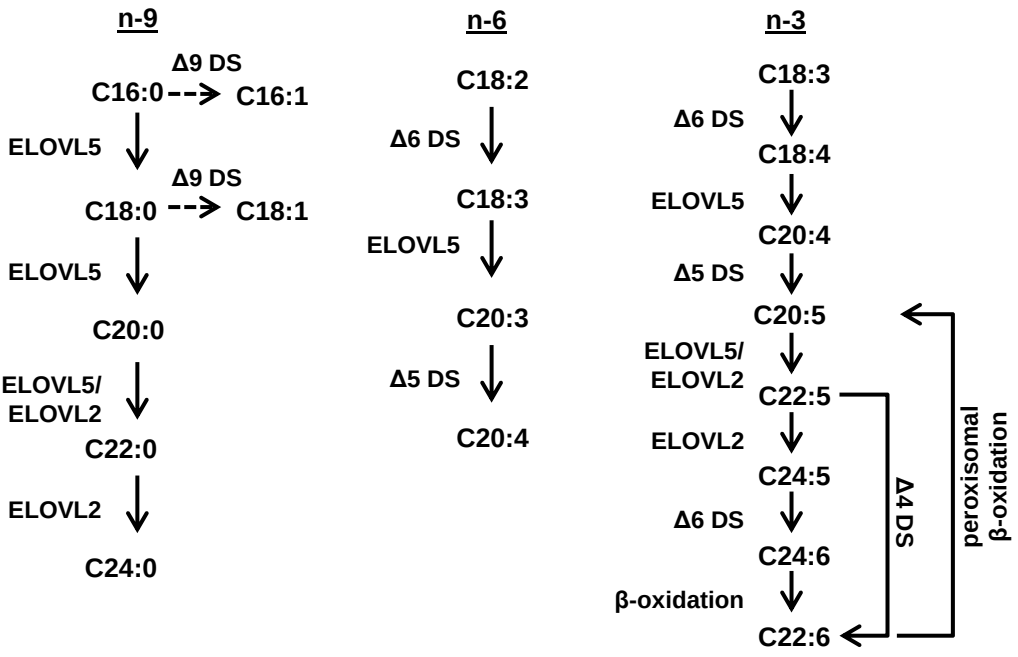

Figure 1.11; Fatty acid anabolism pathways in humans. DS = desaturase, ELOVL = elongation-of-very-long-chain

While enterocytes of the small intestine are exposed to high concentrations of dietary fatty acids, the mucosa of the large intestine is exposed to high concentrations of microbial fatty acids. The short chain fatty acids with an acyl-chain length of one to six carbon atoms are produced by the colon microflora mainly from dietary fibre (47). The most abundant short chain fatty acids in the large intestine are acetic acid (C2:0), propionic acid (C3:0) and butyric acid (C4:0) reaching concentrations in the millimolar range (97). Short chain fatty acids are readily taken up into colonocytes where they are mainly used for energy production, but a part is also excreted from the basolateral side, enters the bloodstream and is taken up by the liver where they are also used for lipid synthesis (98). Uptake and excretion occurs via passive diffusion and transporter mediated diffusion, facilitated by members of the monocarboxylate transporter (MCT) family at both apical and basolateral side (97).

1.2.2 Dietary sources and tissue modulation

Vegetable oils and animal fats contribute the greatest part of dietary fatty acids. But there are differences in the percentage of individual fatty acids depending on the source of fat. For example, palm and coconut oil, which are much used in south-east Asia, contain mostly saturated medium chain fatty acids, lauric and myristic acid in coconut and palmitic but also the MUFA oleic acid in palm oil. Olive oil, which is a highly characteristic part of the Mediterranean diet, is mostly made up of oleic acid (> 70 %) but also some palmitic and linoleic acid. Corn oil, which is more popular in the US also contains high levels of oleic acid together with linoleic acid. In general, vedgetable oils are rich in oleic, linoleic, and palmitic acid, with only little content of n-3 PUFA. Lipid rich vegetable foods like avocado, pistachios or walnuts share the distribution pattern of the pure oil, only with lower overall percentage of fat. The fatty acid composition of animal fat depends on the source of lipids. Butter, which is made from milk, exhibits a typical milk fat composition with a wide range of saturated fatty acids, mainly palmitic, stearic and myristic acid, a small percentage of short chain fatty acids and also some oleic acid. Another good source of milk fat is cheese, which has the same fatty acid profile as butter. In contrast to milk fat, the animal fat lard reflects more the composition of adipose tissue, where triacylglycerols are synthesised containing oleic, palmitic and linoleic acid. The fat content of meat itself varies depending on the animal source and which part of the animal tissue was removed from. Muscle tissue mainly contains oleic, palmitic and linoleic acid, similar to adipose tissue. Just as with meat, the fat content of fish depends on the species. Muscle tissue from some white fish like cod have a very low lipid content, whereas oily fish like herring or sardines is high in fat. Apart from unsaturated fatty acids like oleic and linoleic acid, oily fish also contributes HUFA like DHA and EPA to the diet as well as some more unusual fatty acids, like gondoic and cetoleic acid from herring, for example. (All nutritional information was obtained from the USDA National Nutrient Database (99).)

The examples given above show that there is a great variation in the fatty acid content of foods and that depending on cultural background and personal preferences, the type and amount of fatty acid that is absorbed can differ substantially between individuals. Since dietary fatty acids are not only used for energy production but also as cellular building material, the lipid composition of the diet is to some extent also reflected in the lipid composition of cells. It has been shown that supplementation with specific dietary lipids will increase the abundance of that particular lipid and its metabolic products, not only in the small intestine, but through systemic distribution of dietary fatty acids by chylomicrons also in other organs. For example, mice fed with a diet based on herring were shown to have a different lipoprotein and fatty acid composition than mice fed with a diet based on beef. Liver tissue of fish fed mice contained less MUFA, more n-3 PUFA and less n-6 PUFA than meat fed mice (100). When mice were fed a diet with added fish oil or safflower oil, compared to coconut oil, the fatty acid composition of platelets was reflecting the high content of linoleic acid and EPA/DHA of those lipid sources. Membrane fluidity was also significantly higher in platelets from mice fed with safflower or fish oil than in platelets from mice fed with coconut oil (101). This example shows that the modulation of fatty composition of cells by dietary fatty acids has an impact on the physical properties of the membrane. Supplementation with fish oil has also been shown to increase the percentage of HUFA in phospholipids and triacylglycerols of platelets, blood immune cells, serum lipids, muscle tissue, heart tissue and adipose tissue of human volunteers in a concentration dependent manner (102-109) and that a regular supplementation with lower doses is more effective then intermittent supply of high doses (110). A diet enriched with vegetable oil high in oleic or α-linolenic acid was also shown to change plasma serum levels of MUFA and PUFA in humans (111).

1.2.3 Impact on absorption

In the pharmaceutical industry, lipids are employed as drug carriers and absorption enhancers. Their popularity in this context is partly due to the fact that they can be synthesised with a great range of physical properties from liquid to solid and also different polarity and hydrophobicity. Lipophilic drugs administered in an oil matrix are more likely to be incorporated into mixed micelles and therefore more finely dispersed and likely to reach the intestinal wall for absorption. Popular lipid vehicles are FFA, triacylglycerols of medium and long chain fatty acids and fatty acid ethyl esters. Phospholipids are also used as emulsifiers (74, 112). There are many published examples on drug bioavailability enhancement by lipids, for example, passive diffusion of doxorubicin into endothelial cells of the aorta was increased after concomitant injection of lipid analogues made up of short-chain sphingolipids (113).

Increase of polyphenol bioavailability through incorporation into liposomes has also been investigated. For example, curcumin plasma concentration in mice was several fold higher when incorporated into liposomes compared to the pure compound (114). Similar results were obtained for liposomal preparations of quercetin. Here, the presence of lipids delayed maximum plasma concentration of the compound and quercetin remained in circulation for longer, resulting in a several fold increased area under the curve (AUC) for the plasma and tissue concentration profile (115).

But the examples given above are all based on short term modulation of physical properties. As mentioned in the previous section, dietary fatty acids are incorporated into biomembranes and such change in lipid composition can yield a change in plasma membrane fluidity. Many polyphenols are reported to cross the intestinal epithelium by passive diffusion. A change in membrane fluidity could thus affect the diffusion rate of phenolics and with that their pharmacokinetics. In pig intestinal cells, a PUFA deficient diet drastically changed the fatty acid composition of plasma triacylglycerides and also decreased the fluidity of isolated brush border membrane

vesicles (BBMV) (116). Brush border membrane fluidity increases along the intestinal tract (117).

But not only passive diffusion can be influenced by membrane fatty acid modification, membrane spanning proteins are also affected. Calcium (Ca^{2+}), magnesium (Mg^{2+}) and sodium/potassium-ATPase (Na^{+}/K^{+}-ATPase) activity has also been shown to be sensitive to the membrane lipid environment (118). Incorporation of linoleic acid into hepatocyte plasma membranes increased membrane fluidity and concomitantly decreased Mg^{2+}-, Ca^{2+}- and Na^{+}/K^{+}-ATPase activity by about 25% (119). In erythrocytes and fibroblasts glucose transport was also demonstrated to be dependent on the lipid environment. A decrease in membrane fluidity of about 8% increased transport of glucose, but any further decrease in fluidity reversed this effect (120). The inverted response to membrane fluidity was shown for Ca^{2+} uptake at the intestinal brush border of rabbits. Here a small increase in fluidity by about 5 % through incorporation of oleic acid was shown to increase Ca^{2+} uptake, whereas a larger increase in fluidity by about 15 % drastically decreased Ca^{2+} uptake (121). Another group of transporters that have been reported to be sensitive to their lipid microenvironment are of the ABC-family (122-124). Since these transporters have been shown to recognise phase II conjugates of many xenobiotics, these proteins could also play a substantial role in the first pass elimination of polyphenols. But it is not only lipids that can exert an effect on integral membrane proteins, but proteins also modulate their lipid environment. Membrane lipids in immediate vicinity to the protein are called annular lipids (from Latin ‘annulus’ = ring-shaped (125)). They form a distinct shell of lipids around the peptide region spanning the hydrophobic membrane core. To match the hydrophobic and hydrophilic domains of the inserted protein, annular lipids can be distorted in their packing density by stretching or compression to yield a conformation that is less favourable in terms of lipid-lipid packing, but will result in stronger van der Waals attraction between the protein and lipids, thus ‘dissolving’

the protein in the membrane. The distinction between annular lipids and bulk lipids is mostly characterised by this conformational change but not by a difference in lipid composition compared to the bulk lipids. The annular lipid shell is not a rigid structure but highly dynamic with an average residing time of a lipid molecule in the shell of 10^{-7} s before diffusing back into the bulk lipid phase (126-128).

Membrane lipid composition was also shown to affect the pathway of cellular uptake of water soluble compounds by endocytosis. It was reported that incorporation of long chain saturated fatty acids resulted in a decrease in membrane fluidity of macrophages which also caused a decrease in pinocytosis rates (129).

1.3 Project aims

Dietary lipids have been shown to affect cellular lipid composition through incorporation of fatty acids from food into cellular triacylglycerol and phospholipid structures. Especially the small intestine is regularly exposed to high quantities of fatty acids which will differ in their chain length and saturation depending on food preferences. Changes in plasma membrane lipid composition have been shown to affect transepithelial transport via paracellular and transcellular routes. The impact of lipids on the absorption of polyphenols has been reported regarding improved solubility of phenolic compounds when co-ingested with lipids but so far it has not been investigated how long term changes of membrane composition could affect polyphenol bioavailability. In the current study, this gap of knowledge was addressed. The main objectives of the work were:

- To establish and characterise an *in vitro* model of the impact of chronic lipid supplementation on enterocytes of the small intestine.
- To test whether chronic fatty acid supplementation affects transepithelial transport of polyphenols across the intestinal epithelium, using the phenolic acids caffeic acid and ferulic acid and the flavanol epicatechin as model substrates.
- To identify the mechanism by which fatty acids affect transport of phenolics.
- To test whether fatty acid supplementation will affect phase II metabolism of selected polyphenols.

Chapter 2: Materials, methods and equipment

2.1 Materials

All cell culture consumables, acetonitrile, formic acid, stearic, linolenic and arachidonic acid, (-)-epicatechin (from here on only called epicatechin), 3,4-dimethoxycinnamic acid, ascorbic acid, CelLytic M buffer, caprylic, lauric, palmitic, stearic, linolenic, linolenic and arachidonic acid, 1-oleoyl-*rac*-glycerol, L-α-lysophosphatidylcholine, L-α-phosphatidylcholine, α-tocopherol, glycodeoxycholic acid, taurodeoxycholate, taurocholate hydrate, ferulic acid, caffeic acid, hesperetin, metoprolol, estrone-3-sulfate, ibuprofen, diglycine, methyl-β-cyclodextrin, 1-(4-trimethylammoniophenyl)-6-phenyl-1,3,5-hexatriene *p*-toluenesulfonate (TMA-DPH), lucifer yellow, 3,4-dimethoxycinnamic acid, 3-(4,5-dimethylthiazol-2-yl)-2,5-diphenyltetrazolium bromide (MTT) and protease inhibitor cocktail were purchased from Sigma-Aldrich (St. Louis, USA), RIPA buffer, EZ-Link Sulfo-NHS-LC-Biotin, High Capacity Streptavidin Agarose Resin and bicinchoninic acid (BCA) kit were purchased from Pierce Biotechnology (Rockford, USA), cholesterol detection kit, EPA and DHA were purchased from Cayman Chemical (Ann Harbour, USA), all protein simple consumables and reagents were purchased from protein simple (Santa Clara, USA). Baculovirus infected insect cells expressing human UGT isoforms were purchased from BD Bioscience (Woburn, USA). The Caco-2 cell line (HTB-37) and the HepG2 cell line (HB-8065) were obtained from ATCC (Manassas, USA), the HT29-MTX cell line (130) was a generous gift from the Nestlé Research Center (Lausanne, Switzerland). Cy3-conjugated donkey anti-mouse IgG and Alexa488-conjugated donkey anti-rat IgG were obtained from Jackson Immuno Research (West Grove, USA), fluorescein conjugated wheatgerm agglutinin (WGA) from Vector laboratories (Burlingame, USA), ProLong Gold antifade reagent mounting medium from molecular probes (Carlsbad, USA) all TaqMan primer/probe sets, Lipofectamine RNAiMAX, siRNA and Opti-MEM from life technologies (Carlsbad, USA).

2.2 Cell culture

Caco-2 cells were routinely cultured in low glucose (5 mM) Dulbecco's Modified Eagle's Medium (DMEM) supplemented with 15% Fetal Bovine Serum (FBS), 100 units/mL penicillin, 0.1 mg/mL streptomycin and 0.25 µg/mL amphotericin B (full medium) at 37°C with 5% CO_2 in humidified atmosphere. Cells were subcultured when reaching ~ 90% confluence (after 3 - 5 days) and seeded into flasks at a density of 1 x 10^4 cm^{-2} (as recommended by the supplier (131)). Cells were received from ATCC at passage number 23 and used for experiments between passage number 35 and 50.

HT29-MTX cells were cultured the same way as Caco-2 cells but with 10 % FBS instead of 15 % and cells were seeded into flasks at a density of 2.4 x 10^4 cm^{-2}. Cells were received at passage number 17 and used for experiments between passage numbers 27 to 35.

HepG2 cells were grown in Minimum Essential Medium (MEM) supplemented with 10 % FBS, non-essential amino acids, 100 µM sodium pyruvate, 100 units/mL penicillin and 0.1 mg/mL streptomycin. Cells were subcultured when reaching ~ 90 % confluence and seeded into flasks at a density of 1 x 10^5 cm^{-2}. Cells were received from ATCC at passage number 74 and used for experiments between passage number 80 and 90.

For all cell lines, cell numbers were determined using a haemocytometer.

2.3 Fatty acid treatment

For experiments, cells were supplemented with 50 µM fatty acid or 1000 µM butyric acid, unless stated otherwise. Stock solutions of fatty acids were prepared in 100 % ethanol and controls were supplemented with the corresponding amount of solvent. For treatments with EPA and DHA, an additional 100 µM of α-tocopherol (vitamin E) was added to the medium to prevent oxidation of the fatty acid. Corresponding controls were treated with the same amount of vitamin E and ethanol. Final ethanol

concentrations in the medium were 0.5 % (108 mM) and 0.6 % (130 mM) for DHA and EPA treatments. The medium was changed every other day. Different batches of FBS were used and there was no control for batch to batch variation in lipids.

For chronic supplementation, cells were seeded into fatty acid containing medium. For acute treatments, cells were grown in full medium containing 10 % FBS and changed to fatty acid containing medium 24 h (for results described in section 3.3.1) or 48 h (for results described in section 3.3.2 and in chapter 4) before the transport study or harvesting. Caco-2 and HT29-MTX cells were used for experiments on day 22 or day 23 after seeding. The last medium change was always performed 24 h before the experiment.

Micelles were prepared by dissolving monoolein, lyso-phosphatidylcholine, phosphatidylcholine and α-tocopherol and FFA in chloroform with a final concentration of 0.2 mM, 0.3 mM, 0.1 mM, 0.01 mM and 0.05 mM respectively. This lipid mixture was dried under nitrogen flow and mixed with bile salts glycodeoxycholic acid (0.8 mM), taurodeoxycholic acid (0.46 mM) and taurocholate hydrate (0,75 mM) dissolved in serum free DMEM medium. Bile salts and lipids were then vortexed and sonicated for 30 min. 1 mL aliquots were taken for analysis.

For transport experiments, cells were seeded into 6-well Transwell plates (0.4 µm pore size, polycarbonate) at 6×10^4 cm^{-2}. Caco-2:HT29-MTX co-cultures were seeded at a ratio of 76:24 unless stated otherwise. With this seeding density, cells were usually confluent within 24 h.

For preliminary experiments described in section 3.3.1, cells were grown in Transwell plates and for experiments described in section 3.3.2 cells were grown in flasks with a growth area of 75 cm^{-2}, due to the high cost of the permeable supports. Cells used for fluidity measurements were grown in petri dishes (ø = 10 cm). The two culture types (solid vs. permeable support) resulted in a slightly different fatty acid composition of cells. Mainly, cells grown on permeable supports had a higher content of the saturated fatty acids palmitic (C16:0) and stearic acid (C18:0) but less

of the monounsaturated fatty acids palmitoleic (C16:1) and oleic acid (C18:1), as shown in table 2.1.

	percentage [%]	
fatty acid	solid	permeable
16:0	20	24
16:1	9	4
18:0	11	20
18:1	38	24
18:2	5	3
18:3	2	1
20:4	5	7
205	2	3
22:6	4	5

Table 2.1; Fatty acid composition of differentiated Caco-2 cells grown on solid and permeable supports. solid: n = 3, permeable: n = 1; For details on analysis see section 2.14.

For gene expression studies and protein quantification cells were seeded into 6-well plastic plates as preliminary studies had shown a very similar response to fatty acid treatment in cells grown on permeable and solid supports.

	expression change [$2^{-\Delta\Delta C_T}$]	
gene	solid	permeable
ABCB1	1.1 ± 0.09	1.3 ± 0.11
ABCC2	0.9 ± 0.03	0.9 ± 0.06
ABCG2	1.1 ± 0.05	1.2 ± 0.08

Table 2.2; Changes in gene expression after chronic DHA [50 µM] treatment of Caco-2 cells grown on solid or permeable supports. Values are given as cycle threshold (C_T) of the gene of interest in samples from treated cells normalised to the C_T of the reference gene GAPDH and to the C_T of the gene of interest in samples from untreated cells. See section 2.8 for calculations.

For siRNA silencing cells were either seeded into 6-well or 12-well plastic plates and not Transwell inserts, as they were analysed five days after seeding, which is too short a time for full differentiation to occur.

Cells used for fluorescence microscopy were grown in Millicell cell culture inserts (12-well, PET 0.4 µm pore size, Millipore).

HepG2 cells were grown in 6-well plastic plates at a seeding density of 1×10^5 cm^{-2} for all experiments. Cells were used for experiments 5 days after seeding by which time they were about 95 % confluent.

2.4 Transport studies

Transport studies were conducted with cells grown on Transwell inserts, which are illustrated below.

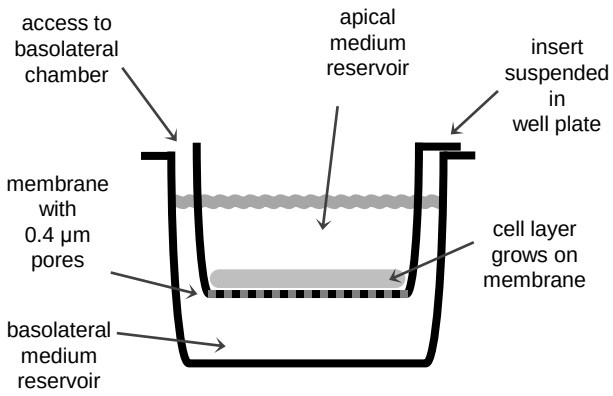

Figure 2.1; Structure of Transwell inserts

For transport studies, cell monolayers were washed twice with Hank's Balanced Salt Solution (HBSS) and the Transepithelial Electrical resistance (TEER) of the cell layer was measured in HBSS containing 1.8 mM calcium chloride (HBSS + $CaCl_2$). Calcium chloride was added to maintain tight junction integrity (132). TEER values are indicative of the differentiation state of the cell layer. With increasing time in culture, the TEER of a cell layer increases due to the formation of tight junctions. Figure 2.2 shows the development of TEER in Caco-2 cultures over time. On the basis of this data, a TEER value of 300 Ω was chosen as a minimum for cell layers to be used for transport studies.

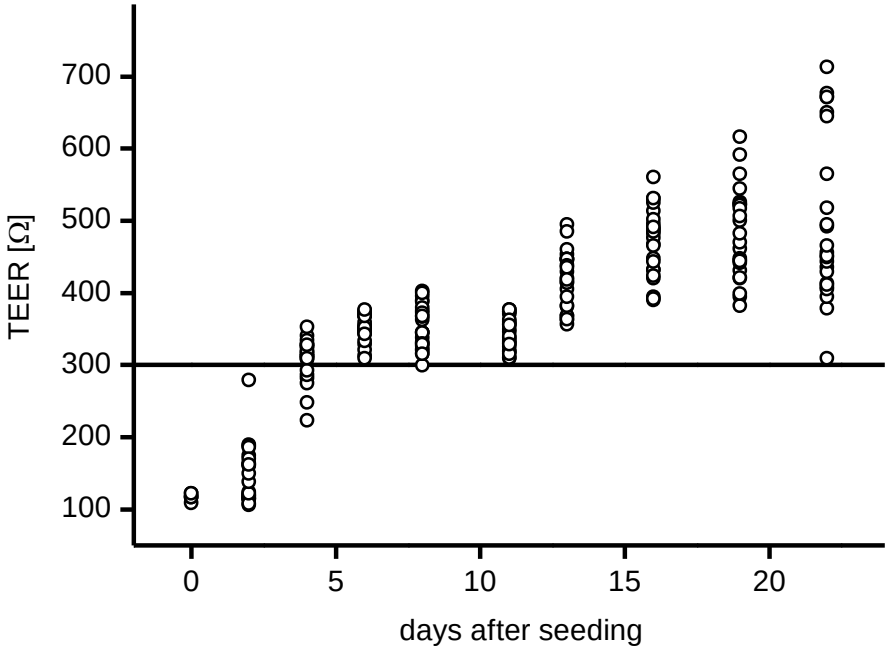

Figure 2.2; Transepithelial electrical resistance (TEER) of Caco-2 cell layers grown in Transwell inserts over time in culture. Each data point represents the average TEER of one Transwell insert measured at three different areas of the cell layer. The TEER value of 300 Ω was selected as a minimum value for cell layers used in transport studies. TEER values at day 0 are from membranes immersed in full medium, before seeding of cells.

Monitoring the tight junction integrity is especially important for cell layers used in transport studies as it determines diffusion of a compound by the paracellular route. Figure 2.3 shows the correlation between TEER of Caco-2 cell layers 22 - 23 days after seeding and the permeability of the paracellular transport marker lucifer yellow in apical to basolateral direction.

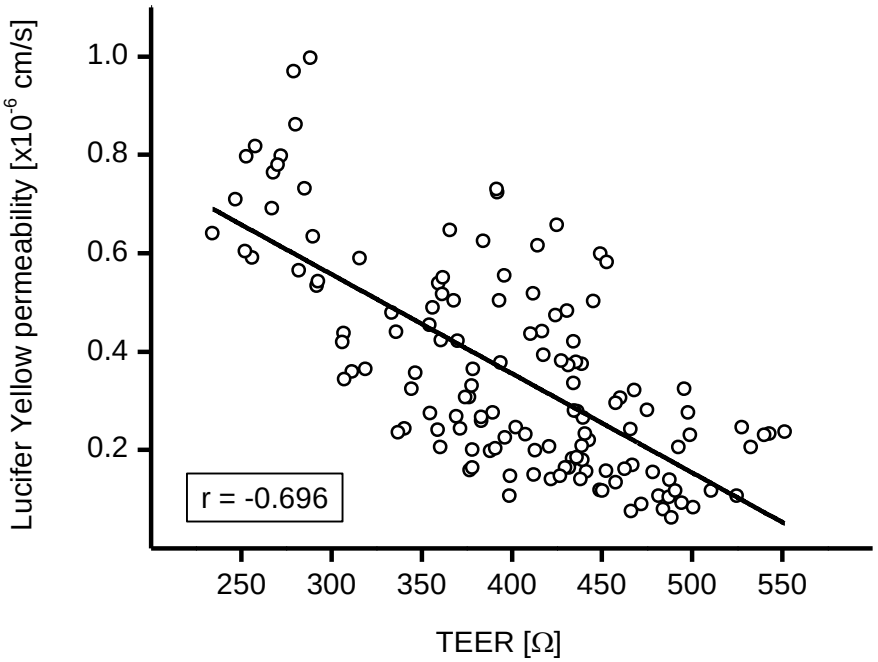

Figure 2.3; Correlation between transepithelial electrical resistance (TEER) of Caco-2 cell layers grown in Transwell inserts and diffusion rate of paracellular permeability marker lucifer yellow in apical to basolateral direction. For details on lucifer yellow analysis see section 2.6. r = Pearson's correlation coefficient.

After TEER measurement, the buffer was aspirated and replaced by 2 mL aglycone dissolved in HBSS + $CaCl_2$ in the donor chamber and 2 mL HBSS + $CaCl_2$ in the receiver chamber. For transport experiments with epicatechin, 100 µM ascorbic acid were additionally added to donor and receiver chamber to prevent oxidation of the compound. The concentration of compounds used for transport experiments in the donor chamber was dictated by the sensitivity of the analysis method and by the prerequisites of transport experiments using the Caco-2 model. In general, diffusion of a compound is described by Fick's first law as:

$$J = -D\frac{d_c}{d_x}$$

with J = flux, D = diffusion coefficient, d_c = change in concentration and d_x = length of diffusion pathway. In Caco-2 transport assays, results are usually calculated as 'apparent permeability' (P_{app}), which is derived from D in Fick's law, using the following equation:

$$P_{app} = \frac{c_r}{t} * \frac{V}{A * c_d}$$

with c_r = concentration of the analyte in the receiver chamber in µM, t = transport time in s, V = volume of the receiver chamber in cm^3, A = growth area in cm^2 and c_d = concentration of the analyte in the donor chamber in µM. However, there are several prerequisites regarding the assay set-up for using this equation. Figure 2.4 shows a cross section schematic of such transport assay set-up with different flux pathways marked.

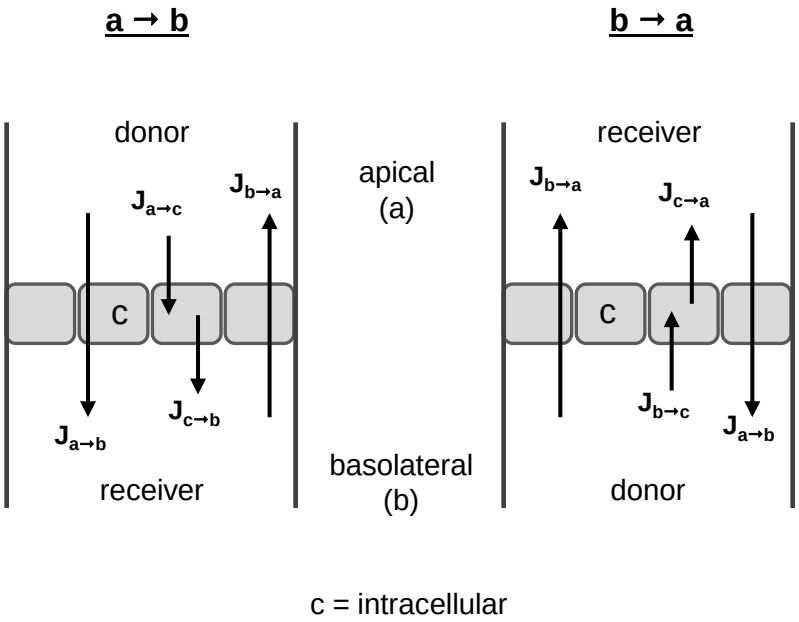

Figure 2.4; Overview of flux in Caco-2 transport assays. J = flux, a = apical, b = basolateral, c = intracellular

The main assumption made for calculating P_{app} is that the concentration of the transport compound in the donor chamber (c_d) does not change during the transport experiment and that the flux back from the receiver to the donor chamber ($J_{r→d}$) is negligibly low. In practice these two conditions are met by selecting the compound concentration in the donor chamber and the transport time so that only a small fraction of the compound is crossing into the receiver chamber ($c_d >> c_r$). Ideally this can be achieved by using radiolabeled compounds of interest which can be detected

in trace amounts with the appropriate method. However, the compounds tested in the current work were not readily available in a radiolabeled form, so the aglycones were analysed by HPLC with either diode array detection or fluorescence detection, where possible. As these detection methods are less sensitive, higher concentrations and longer incubation times were used in the assay. The detection limit for hesperetin, caffeic and ferulic acid was ~ 1 µM, therefore they were used at a concentration of 500 µM and with an incubation time of 60 min. With these conditions, ~ 0.8% of the original load of caffeic acid and 8 - 9% of the original load of ferulic acid and hesperetin were detected in the receiver chamber after transport. The detection limit of epicatechin was ~ 0.05 µM and since this compound was reported to be cytotoxic in Caco-2 cultures at a concentration of > 250 µM (133) a concentration of 200 µM was chosen for transport studies. With an incubation time of 90 min, the percentage of original load that was detected in the receiver chamber was ~ 0.1% and ~ 1% for a → b and b → a transport, respectively. The detection limit for the paracellular marker lucifer yellow was ~ 0.02 µM and the concentration of 100 µM was chosen for transport experiments. With an incubation time of 60 min 0.2 - 0.5% of the original load were found in the receiver chamber, dependent on tight junction integrity. The detection limit for the passive diffusion model compound, metoprolol was < 0.5 µM and using a concentration of 500 µM and an incubation time of 10 min, ~ 5% of the original load were detected in the receiver chamber.

After incubation, 1.5 mL samples of the donor and receiver chambers were collected, acidified with 10 mM acetic acid and 100 µM ascorbic acid, 50 µM internal standard 3,4-hydroxycinnamic acid was added and the samples were analysed by HPLC and/or LC-MS/MS. After sample collection, cells were either used for viability testing or washed three times with HBSS + $CaCl_2$ and lysed with 80% methanol containing 100 µM ascorbic acid and 5 µM internal standard. After vigorous mixing, cell lysates were centrifuged, the supernatant was dried under vacuum and reconstituted in 100 µL LC-MS/MS solvent A.

When the impact of transport inhibitors was investigated, these compounds were added to the donor and acceptor chamber at the following concentrations: 300 µM phloretin, as the presence of this concentration gave a 80% inhibition of mevalonate and 90% inhibition of pyrovate uptake via MCT1 (134); 10 µM apigenin, 25 µM MK571 and 25 µM cyclosporine A, as described previously for inhibition of apical efflux-transporters ABCB1, ABCC2 and ABCG2 (135). Possible inhibitors of ferulic acid transport were also used at previously suggested concentrations: 500 µM ibuprofen (136), 1000 µM diglycine (137) and 500 µM estrone-3-sulfate (138).
All replicates of transport studies were conducted on the same day with usually n = 6 and therefore N = 1.

2.5 Viability test

After transport experiments, 2 mL of 0.5 mg/mL MTT in serum free medium was added to the apical side and 2 mL of HBSS + $CaCl_2$ was added to the basolateral side of the cell layer. After 4 h incubation, solutions were aspirated, the cells were lysed in 2 mL of 10% Triton X-100 and 0.1 M hydrochloric acid in isopropanol and the absorption of the lysate was read at λ = 595 nm on a microplate reader. Results are given as fold change:

$$Fold\ Change = \frac{average\ absorbance\ test\ sample}{average\ absorbance\ control\ sample}$$

To monitor tight junction integrity during experiments, TEER before and after transport was compared. With a 60 min incubation time, TEER dropped by 85 Ω and with a 90 min incubation time TEER dropped by 108 Ω on average. Cell layers that had a TEER value of above 300 Ω before the transport experiment but were below that value afterwards, were still included.

2.6 HPLC analysis

After transport experiments, aglycone concentrations were determined using an Agilent 1200 series HPLC equipped with diode array detector (DAD) and fluorescence detector (FLD). Separation was achieved on an Agilent ZORBAX Eclipse Plus C18 column (2.1 x 100 mm, particle size 1.8 µm). Solvent A consisted of 95% deionised water, 5% acetonitrile and 0.1% formic acid. Solvent B consisted of 95% acetonitrile, 5% deionised water and 0.1% formic acid.

The solvent gradient profile for the analysis of ferulic acid, caffeic acid and hesperetin was as follows: 0 – 12 min linear gradient from 0% solvent B to 50% solvent B; 12 – 18 min linear gradient from 50% solvent B to 100% solvent B; 18 – 24 min 100% solvent B; 24 – 31 min 0% solvent B. The flow rate was 0.2 mL/min. The peak areas detected at 320 nm by DAD were used to quantify ferulic acid, caffeic acid and the internal standard 3,4-dimethoxycinnamic acid hesperetin was detected at 287 nm.

The solvent gradient profile for the analysis of epicatechin and metoprolol was the following: A linear increase from 0 % solvent B to 50 % solvent B in the first 18 min, then increase to 100 % solvent B between 18 and 18.5 min, holding of 100 % solvent B for 3 min, a linear decrease to 0 % solvent B between 21.5 and 24 min with a subsequent column equilibration at 0 % solvent B for 7 min. The flow rate was 0.2 mL/min. Epicatechin was detected using the FLD at an excitation wavelength of λ = 230 nm and an emission wavelength of λ = 321 nm. Metoprolol was detected with an excitation wavelength of λ = 225 nm and an emission wavelength of λ = 320 nm. The internal standard was monitored at λ = 320 nm using the DAD.

The paracellular transport marker lucifer yellow was quantified by FLD with an excitation wavelength of λ = 425 nm and an emission wavelength of λ = 515 nm. Samples from transport studies without lucifer yellow did not exhibit any background signal within this spectrum. Therefore the transport marker was analysed without chromatographic separation on a column. The autosampler was directly connected

to the FLD and 5 µL of sample were injected. The mobile phase was PBS and the flow rate was 0.085 mL/min.

2.7 LC-MS/MS analysis of metabolites

Samples were analysed for ferulic acid metabolites as described previously (139) with the following modifications: Solvent A consisted of 95% deionised water, 5% acetonitrile and 0.5% formic acid, solvent B consisted of 95% acetonitrile, 5% deionised water and 0.5% formic acid. A solvent gradient was run with the following profile: 0% solvent B from 0 to 3 min, a linear increase from 5% to 30% solvent B from 3 min to 15 min, 100% solvent B from 15.1 min to 17.5 min and 0 % solvent B from 17.6 min to 21.5 min. The flow rate was 0.3 mL/min and 15 µL of sample were injected. Separation was achieved on an Agilent ZORBAX Eclipse Plus C18 column (2.1 x 100 mm, particle size 1.8 µm). Ferulic acid and its metabolites were identified and quantified by comparison to original standards. Ion traces were monitored in negative ionisation mode and two traces were monitored for each metabolite. In the list below, the first trace was used for quantification.

m/z = 369 → 113;	m/z = 369 → 193	for feruloyl-glucuronide
m/z = 273 → 178;	m/z = 273 → 193	for feruloyl-sulfate
m/z = 195 →121;	m/z = 195 → 136	for dihydroferulic acid,
m/z = 193 → 178;	m/z = 193 → 134	for ferulic acid and
m/z = 207 → 103		for 3,4-dimethoxycinnamic acid

For LC-MS/MS analysis of epicatechin metabolites an LC-MS/MS method for analysis of green tea catechin metabolites in urine (140) was adopted and optimised for analysis of epicatechin metabolites in cell culture samples. Separation was achieved with an Agilent 1200 series HPLC using a Phenomenex Kinetex C18 column with particle size of 2.6 µM. The injection volume was 10 µL. Solvent A consisted of 95% Millipore water, 5% acetonitrile and 0.5% formic acid. Solvent B

consisted of 95% acetonitrile, 5% Millipore water and 0.5% formic acid. The solvent gradient was the following: 0% solvent B from 0 to 3 min, a linear increase to 50% solvent B from 3 to 16 min, 100% solvent B from 16 to 20 min and 0% solvent B from 20 to 23 min. The flow rate was 0.4 mL/min

Ion traces were monitored in negative ionisation mode and chromatograms obtained for the first of the following traces were used for determination of peak areas:

m/z = 303 → 137;	m/z = 303 → 165	for *O*-methyl-epicatechin
m/z = 369 → 289;	m/z = 369 → 245	for epicatechin-sulfate
m/z = 383 → 303;	m/z = 383 → 137	for *O*-methyl-epicatechin-sulfate
m/z = 465 → 289;	m/z = 465 → 245	for epicatechin-β-D-glucuronide
m/z = 479 → 303;	m/z = 479 → 137	*O*-methyl-epicatechin-β-D-glucuronide
m/z = 289 → 245;	m/z = 289 → 203	for epicatechin
m/z = 207 → 103		for 3,4-dimethoxycinnamic acid

For results shown in figures 4.6, 5.14, 6.12 - 6.14, 6.20, 7.2, 7.3, 7.5, and 7.12 the concentrations were adjusted to the original volume of the compartment they were drawn from. The volume of a cell monolayer was estimated through immunofluorescence staining of the cell membrane (see section 2.10). The distance between apical and basolateral membrane was measured by confocal microscopy and was an average of 15 µm for both Caco-2 and HT29-MTX cells, estimated from 13 independent experiments for Caco-2 and 24 independent experiments for HT29-MTX cells. With a growth area of 4.67 cm^2 for Transwell plates and 9.5 cm^2 for solid 6-well plates, the volume of a cell monolayer was calculated as 7 µL and 14 µL respectively. As cell lysates were reconstituted in 100 µL solvent B, metabolites were diluted by the factor 14.3 and 7.15 respectively. For cell lysate samples, the concentration obtained by LC-MS/MS analysis was multiplied by this dilution factor. For samples collected from the apical or basolateral well, the dilution

factor was 1 as those samples were injected without further processing. For the total amount, peak areas were multiplied by the total sample volume (2000 µL for apical and basolateral and 100 µL for intracellular amounts) and divided by the injection volume. For epicatechin metabolism by HepG2 cells, peak areas obtained for epicatechin conjugates, presented in figures 5.14, 5.15 and 7.1, were normalised to protein concentration determined by the BCA assay. For that, cell layers were lysed with 1 M sodium hydroxide, neutralised with 1 M hydrochloric acid and the BCA assay was performed according to the manufacturer's protocol.

2.8 Gene expression analysis

Cells were seeded into solid 6-well plates and maintained as for transport experiments. On day 22 after seeding (Caco-2 and HT29-MTX) or day 5 after seeding (HepG2 and Caco-2 after siRNA gene silencing), cells were washed twice with ice cold PBS, scraped and mRNA was extracted using the ambion RNAqueous kit, according to the manufacturer's protocol. RNA was transcribed to cDNA using the Applied Biosystems high capacity RNA to cDNA kit and then gene expression was determined by TaqMan real-time PCR using the Applied Biosystems TaqMan gene expression assay and TaqMan gene expression master mix according to the manufacturer's protocol on a StepOnePlus real-time PCR system. The Applied Biosystems ID of the primer/probe sets were:

SLC16A1: Hs00161826_m1,

SLC16A3: Hs00358829_m1

SLC16A4: Hs01006127_m1

SLC5A8: Hs00377618_m1

SLC22A7: NM_002046.3

ABCB1: Hs00184500_m1

ABCC2: Hs00166123_m1

ABCG2: Hs01053790_m1*UGT1A1*: Hs02511055_s1,

UGT1A8: Hs01592482_m1,

UGT1A9: Hs02516855_sH

GAPDH: NM_002046.3

Each well of the PCR plate contained a primer/probe set specific to the gene of interest with the probe conjugated to the fluorescent dye 6-carboxyfluorescein (FAM, absorption at λ_{max} = 494 nm, emission λ_{max} = 518 nm) and a primer probe set specific for the reference gene GAPDH with the probe conjugated to the fluorescence dye VIC (chemical structure not disclosed by Applied Biosystems, absorption at λ_{max} = 538 nm, emission λ_{max} = 554 nm). Because of the two different fluorophores, CT values for gene of interest and reference gene can be determined simultaneously in the same sample and well. The relative expression of a gene of interest in fatty acid treated cells compared to non-treated control cells was calculated as follows:

$$relative\ gene\ expression = 2\text{^} - \left(\frac{1}{n} \times \sum_{i=1}^{n} [\Delta C_{T1i} - \Delta C_{T2}]\right)$$

$$\Delta C_{T1} = C_{TFIi} - C_{TFRi}$$

$$\Delta C_{T2} = \frac{1}{n} \times \sum_{i=1}^{n} [C_{TCIi} - C_{TCRi}]$$

with n = number of replicates, C_{TFI} = C_T value of gene of interest in fatty acid treated sample, C_{TFR} = C_T value of reference gene in fatty acid treated sample, C_{TCI} = C_T value of gene of interest in control sample, C_{TCR} = C_T value of reference gene in control sample. In figure 7.7 only the expression of the gene of interest relative to GAPDH is given as:

$$relative\ gene\ expression = 2\text{^} - \left(\frac{1}{n} \times \sum_{i=1}^{n} [C_{TCIi-}\ C_{TCRi}]\right)$$

2.9 SiRNA silencing of efflux transporters

Gene silencing was achieved by reverse transfection of Caco-2 cells with ABCB1 (s10418), ABCC2 (s3227) or ABCG2 (s18056) or negative control (AM4611) siRNA. All reagents were used according to the manufacturer's protocol.

50 µM siRNA stocks were prepared in molecular biology grade water. SiRNA was mixed with the low serum medium Opti-MEM at a ratio of 1 in 250 and Lipofectamine RNAiMAX was mixed with Opti-MEM at a ratio of 1 in 17 and both were incubated for 5 min at RT. Then diluted RNA and diluted transfection reagent were mixed 1 in 2 and incubated for 5 min at RT. An aliquot of the mixture was then transferred into a well and overlaid with a cell suspension in Opti-MEM. Final reagent concentrations were 2.63 pmol siRNA per cm^2 and 0.79 µL Lipofectamine RNAiMAX per cm^2. Cells were plated at a density of 0.178 x 10^6 cm^{-2}. After 24 h, the medium was replaced with 10 % FBS in DMEM, without added penicillin, streptomycin or amphotericin B.

For gene expression analysis, cells were grown in 12-well plates, for metabolism experiments, cells were grown in 6-well plates. All experiments were carried out 5 days after seeding.

2.10 Staining and microscopy

Caco-2 or HT29-MTX cells were seeded into Millicell cell culture inserts at a density of 6 x 10^4 cm^{-2}. Before staining, cells were fixed with 4 % para-formaldehyde in PBS for 20 min. Caco-2 cells were then incubated with fluorescein conjugated wheatgerm agglutinin for 10 min. Then both cell lines were permeabilised with 0.1 % Triton X-100 for 20 min and incubated with either mouse MCT1 (sc-365501) or mouse MCT4 (sc-376139) for Caco-2, or rabbit UGT1A (sc-25847) and mouse ABCC1 (sc-18835) antibody for HT29-MTX cells, all at a dilution of 1:50 for 1 h. After washing with PBS, Caco-2 cells were further incubated with Cy3-conjugated donkey anti-mouse IgG and HT29-MTX cells were incubated with Cy3-conjugated

donkey anti-mouse IgG and Alexa488-conjugated donkey anti-rat IgG at a 1:300 dilution in PBS for 1 h. Then cell layers were stained with 0.2 mg/mL DAPI and mounted on microscopy slides with ProLong Gold antifade reagent mounting medium. Cells were imaged using a Zeiss LSM510 confocal microscope with an Plan-Apochromat 63x oil immersion objective with a numerical aperture of 1.4. Images in figure 4.10 were acquired with a Z-stack consisting of 11 slices with a depth of 20 µm, for images in figure 4.11, 10 slices with a depth of 18 µm were acquired, for images presented in figure 7.10, 15 slices with a slice depth of 28 µm were acquired.

Widefield images of Caco-2/HT29-MTX co-cultures were acquired using the Leica EL6000 microscope with a 10x HI PLAN dry objective with a numerical aperture of 0.25. Percentage of each cell line in the monolayer at day 21 was calculated from widefield images using the ImageJ software.

2.11 Surface biotinylation and protein detection

HT29-MTX cells grown on permeable supports were washed twice with ice cold PBS and 0.25 mg/mL EZ-Link Sulfo-NHS-LC-Biotin dissolved in HBSS + $CaCl_2$ from either apical or basolateral side. After 4 h of incubation on ice, the reaction was stopped by addition of 40 mM Tris. Cells were washed twice with Tris-Buffered Saline (TBS) and lysed with RIPA buffer containing 0.5% protease inhibitor cocktail. After rocking on ice for 20 min, lysates were centrifuged at 14 000xg for 10 min and the supernatant was incubated with 25 µL High Capacity Streptavidin Agarose Resin over night at 8°C with constant gentle shaking. The supernatant was removed, the resin washed three times with TBS and samples were eluted in 20 µL of 4x protein simple sample buffer containing 0.2 M DTT. 10 µL sample were used for analysis by capillary electrophoresis.

For UGT1A protein detection, HT29-MTX cells grown on solid supports were washed with PBS, scraped and lysed in RIPA buffer containing 0.5% protease inhibitor cocktail by gently rocking the samples in ice for 30 min. Afterwards the

lysate was centrifuged at 14 000xg for 10 min and the protein concentration of the supernatant was determined by BCA microplate assay according to the manufacturer's instructions. Protein analysis was carried out using the automated capillary electrophoresis system 'Simon'. Samples, size protein molecular weight markers, primary and secondary antibodies, separation and stacking matrix and a luminol/horseraddish-peroxidase mixture are transferred to separate wells of a 384-well plate and inserted into a tray of the machine. Protein separation and detection occurs in capillaries which are handled by a robot and automatically loaded with the help of a vacuum pump. After loading of separation matrix, stacking matrix and sample, capillaries are connected to running buffer reservoirs on both ends and a direct current of 250 volts is applied which starts the separation of peptides based on their molecular weight, similar to separation of peptides by SDS-PAGE. After separation, sample peptides are immobilised at the capillary wall and then detection occurs with the help of immunoprobes, analogue to traditional Western blotting. The chemoluminescence signal is detected by a camera and the signal intensity was analysed by the software Compass v2.3.7. All analysis parameters were used as recommended by the manufacturer, except that loading time of the stacking matrix was increased to 17.0 s, loading time of the sample was increased to 12.0 s and separation time to 47.0 min, to achieve a higher sensitivity.
Samples were denatured by incubation with DTT containing protein simple sample buffer at room temperature for 30 min. All primary antibodies were used at a dilution of 1:100. For results presented in figure 7.9, samples were loaded at a protein concentration of 0.8 mg/mL.

2.12 Membrane fluidity

Impact of chronic fatty acid supplementation on brush border membrane fluidity of Caco-2 cells was determined using the fluorescent probe TMA-DPH. For that, the brush border membrane was isolated as described previously (141). Briefly, cells were washed with ice-cold PBS, scraped and homogenized in 0.1 M mannitol, 2 mM

HEEPES/Tris buffer by passing ten times through a 21 gauge needle. 10 mM $MgCl_2$ was added and after gentle rocking on ice for 30 min the homogenate was centrifuged at 3 000xg for 15 min. The supernatant was removed, centrifuged at 30 000xg for 30 min and the resulting pellet of brush border membrane vesicles (BBMV) was reconstituted in 0.3 M mannitol, 0.1 mM $MgSO_4$ and 20 mM HEPES/Tris buffer. The protein concentration of the BBMV suspension was determined by BCA assay and each sample was adjusted to a protein concentration of 0.1 mg/mL with reconstitution buffer.

BBMV fluidity was determined by incubating BBMV suspensions with 1 µM TMA-DPH at different temperatures and reading parallel and perpendicular fluorescence intensity using the PHERAstar FS microplate reader in fluorescence polarisation mode at an excitation wavelength of λ = 355 nm and an emission wavelength of λ = 460 nm. Samples were allowed to equilibrate for 15 min after each temperature increase of 2 K. Fluorescence anisotropy (r) was calculated according to the following equation:

$$r = \frac{I_{\parallel} - I_{\perp}}{I_{\parallel} + 2I_{\perp}}$$

where $I_{\parallel}$ is the fluorescence intensity emitted in parallel to the direction of the polarized light and $I_{\perp}$ is the fluorescence intensity emitted in the perpendicular direction.

Results are given as the percentage change of anisotropy between fatty acid treated cells and controls:

$$\% \text{ change} = \frac{r_{\text{treatment}}}{r_{\text{control}}}$$

2.13 Membrane cholesterol removal and quantification

Cholesterol was removed from the plasma membrane of differentiated Caco-2 monolayers by incubation with 10 mM methyl-β-cyclodextrin dissolved in HBSS + $CaCl_2$ for 30 min. Afterwards, cell layers were washed twice and transport

experiments were carried out as described in section 2.4. After transport, cells were washed and scraped into microcentrifuge tubes. For analysis of cholesterol content, cells were dispersed in 100 µL PBS and extracted three times with chloroform:methanol 2:1. Combined extracts were dried under vacuum and reconstituted in 100 µL of ethanol. Cholesterol content was quantified using the Cayman Chemical Cholesterol Fluorometric Assay Kit according to the manufacturer's instructions. Efficiency of the solvent extraction was 92 %, determined by cholesterol spiking of samples.

2.14 Fatty acid analysis

Caco-2 cells grown on solid supports were supplemented with 50 µM fatty acid as described in section 2.3. On day 22 after seeding, cells were detached using 0.05% trypsin in HBSS, washed twice by repeated re-suspension in HBSS and spinning down and the final cell pellet was stored at -80°C until analysis. Cells were allowed to thaw on ice and were than mixed with CelLytic M lysis buffer at a w/w ratio of 1:10 cells:buffer and homogenised by passing ten times through a 21gauge needle. Homogenised cell suspension was mixed with the internal standards methyl heneicosanoic acid (FAME C21:0) and 1,2-ditricosanoyl-sn-glycero-3-phosphocholine (PC C23:0), methanol, 3 N hydrochloric acid in methanol and hexane. The samples were mixed vigorously and incubated at 100°C for 90 minutes. After they reached room temperature HPLC grade water was added, the samples were mixed again and then centrifuged to aid phase separation. The organic phase was collected and analysed by gas chromatography (GC) with flame ionisation (FI) detection using an injection volume of 2 µL. Separation was achieved using a Varian CP-Sil 88 capillary column on an Agilent 7890A gas chromatograph with 1:25 split injection. The carrier gas was hydrogen at a flow rate of 2.5 mL/min. The oven temperature programme was the following: 60°C for 5 min, then increase to 165°C at a rate of 15 K/min with subsequent hold time of 1 min then increase to 195°C at a rate of 2 K/min with a subsequent hold time of 20 min and then an increase to 215°C

at a rate of 5 K/min with a subsequent hold time of 8 min. The temperature of the FI detector was set to 300°C. Fatty acids were quantified using response factors to the internal standards as described previously (142).

The double bond index was calculated as follows:

$$DBI = \sum_{i=1}^{n} (\%_{FAi} \times n_{DBi})_i$$

with $\%_{FAi}$ being the molar percentage of a fatty acid, n_{DBi} the number of double bonds in that fatty acid.

Results of the fatty acid analysis are given as a relative weight percentage of the overall fatty acid content and not as absolute values. This way of presentation was chosen because the initial weight of the sample was very low and could thus only be measured with a high probability of inaccuracy, especially in the case of cell samples harvested from permeable supports.

2.15 *In vitro* glucuronidation

Activity of different UGT isoforms towards epicatechin was tested using recombinant human enzymes expressed in insect microsomes. In vitro glucuronidation assay was performed as described in Wong *et al*., 2010 (143). In short, an amount of BD Bioscience UGT supersomes corresponding to 0.5 µg protein was incubated at 37°C in 100 mM phosphate buffer (pH = 7.4) with 100 µM ascorbic acid, 1 mM UDPGA, 5 mM saccharolactone, 0.025 mg/mL alamecithin and 50 µM ferulic acid for 1 h. The reaction was stopped by adding 10 µL of 500 mM ice cold hydrochloric acid in acetonitrile. Then samples were centrifuged for 10 min at 17 000xg and the supernatant was analysed by LC-MS/MS as described in section 2.7.

2.16 Statistics

All values shown are the mean of n independent experiments ± standard error of the mean. For analysis of statistical significance, unpaired Students t-test and ANOVA with Bonferroni test for means comparison (where indicated) were used, except for

results presented in sections 3.3.1 and 3.3.2, where the Mann Whitney U Test was chosen as only two samples were analysed for most conditions and the standard distributions in treatment groups were much larger than in control groups. Correlation was analysed using Pearson's correlation.

2.17 Equipment

- StepOne Real time PCR System, Applied Biosystems, Life Technologies Ltd, Cheshire, UK.
- Hettich Universal 320R centrifuge, Andreas Hettich GmbH & Co., Tuttlingen, Germany
- PHERAstar FS microplate reader, BMG Labtech, Ortenberg, Germany
- Multiskan Ascent 96-well plate reader, Thermo Fisher Scientific, Waltham, USA
- MS 6410 triple quadrupole LC-MS/MS, Agilent Technologies, Santa Clara, USA
- HPLC Agilent 1200 system, Agilent Technologies, Dorset, UK
- 'Simon' automated capillary electrophoresis system, Protein Simple, San Jose, USA
- Nanodrop ND-1000 spectrophotometer, Thermo Scientific, Loughborough, UK
- Zeiss LSM510 META upright confocal microscope, Carl Zeiss Microscopy, Cambridge, UK
- Leica EL6000 microscope Leica Microsystems Ltd, Milton Keynes, UK
- GC Agilent 7890A, Agilent Technologies, Santa Clara, USA
- Genevac EZ-2 plus, Fisher Scientific Ltd, Leicestershire, UK
- Milli-Q water purifying system, Millipore, Hertfordshire, UK

Chapter 3: The impact of fatty acid supplementation on the Caco-2 cell model

3.1 Abstract

To investigate the impact of dietary lipids on polyphenol absorption, a cell culture model of the small intestine was used. First, different culturing conditions were tested regarding their efficiency to modify cellular fatty acid composition. Incubation with fatty acids bound to FBS albumin proved to be a more robust and easier method for changing lipid composition than incubation with mixed micelles. Also chronic incubation for 22 days resulted in more pronounced and diverse changes than incubation for 24 h or 48 h. Fatty acid treatment of cells induced formation of lipid droplets, an effect that was intensified when lipid treatment was performed in glucose growth medium. However, lipid treatment had no cytotoxic impact on cells, when viability was assessed by MTT assay. On the contrary, treatment with PUFA even enhanced apparent viability. Tight junction integrity assessed by measuring TEER was also not affected. Treatment with PUFA did change plasma membrane fluidity significantly: linoleic, α-linolenic and arachidonic acid increased and EPA decreased fluidity. Therefore it is concluded, that the chronic treatment of Caco-2 cells constitutes a good model to study the effect of long term fatty acid supplementation on the intestinal epithelium.

3.2 Introduction

A critical property that determines the bioavailability of a compound is its capacity to cross the cells of the intestinal epithelium, the first line of defence in a complex machinery that nature has created to protect an organism from absorbing potentially harmful substances. In order to investigate the impact of lipids on such ability of phenolics to cross the intestinal lining, most work was carried out using the Caco-2 cell culture model, which is widely used and well characterised. This cell line was derived from a colon adenocarcinoma, but cells will spontaneously differentiate into small intestinal, enterocyte like cell monolayers with a polar morphology and function that includes well developed tight junctions, and microvilli on the apical side (144). Cells express many key enzymes of lipid (145) and polyphenol (146) metabolism and also most uptake and efflux transporters (147) that are found in enterocytes of the small intestine, making it a good model to study intestinal polyphenol uptake. However, the Caco-2 cell line is still a heterogeneous cell population that includes a minor amount of flat undifferentiated cells (148), sub-populations with a morphology varying in the organisation of the action cytoskeleton, the composition of membrane glycoproteins, in viability and marker enzyme density (149, 150). There are a number of studies that used Caco-2 cells to investigate lipid absorption (151, 152) and metabolism (85, 91, 153) and it has been shown that the lipid composition of these cells can be modified by incubation with free fatty acids (154, 155). In the current study the emphasis was placed on a long term impact of different dietary lipids on transport across the intestinal epithelium. Therefore the Caco-2 small intestinal model was first characterised regarding the impact of such long term fatty acid supplementation on some key parameters related to physical properties that determine epithelial permeability.

3.3 Results

The impact of different incubation methods on the fatty acid composition of cells was compared to identify optimal assay conditions. Then the effect of fatty acid modification was analysed regarding the impact on cell viability, lipid storage and membrane fluidity.

3.3.1 Impact of fatty acid presentation as part of micelles or albumin complexes on cellular lipid profile

Previous publications have shown that the lipid composition of cells in culture can be modulated by supplementing the growth medium with free fatty acids. *In vivo*, free fatty acids are presented to intestinal cells either from the luminal side of the intestine in the form of mixed micelles with bile acids or from the serosal side, bound to albumin circulating in the blood stream. Both forms of fatty acid presentation are also used *in vitro*. To investigate whether these two different incubation methods result in the same changes in cellular fatty acid composition, the lipid composition of differentiated Caco-2 cells treated for 24 h with either 50 µM stearic acid, oleic acid or DHA, presented as micelles or albumin bound, was analysed by gas chromatography with flame ionisation detection. Table 3.1 shows the concentration of the main fatty acids present in the incubation medium. Both micelle and FBS incubation medium contained not only the supplemented fatty acid, but also other background lipids that stem from either the FBS or the mixed micelles. 10% FBS medium already contained 15 to 35 µM of palmitic, stearic and oleic acid. These concentrations increased to over 50 µM when further stearic or oleic acid were added, but not to the expected amount of around 70 µM. No DHA could be detected in 10% FBS medium and after adding 50 µM of that fatty acid this concentration was also detected. A ten times higher content of palmitic and oleic acid was detected in the medium containing micelles, compared to the FBS incubation medium. The stearic acid content of micelle medium was five times higher than that of FBS

medium and also ~ 20 µM of linoleic acid were detected in micelle medium but not FBS medium. Just as with the 10 % FBS medium, no DHA was detected in the micelle control solution and the added fatty acid was recovered. The addition of neither stearic nor oleic acid to micelles changed the content of those fatty acids in the final incubation medium, indicating that these fatty acids were not incorporated.

	fatty acid [µM]				
incubation medium	C16:0	C18:0	C18:1	C18:2	C22:6
10% FBS medium	34	19	24	n.d.	n.d.
10% medium + 50 µM C18:0	34	57	23	n.d.	n.d.
10% medium + 50 µM C18:1	35	16	59	n.d.	n.d.
10% medium + 50 µM C22:6	34	21	23	n.d.	48
micelle medium	224	94	243	23	n.d.
micelles + 50 µM C18:0	221	93	271	22	n.d.
micelles + 50 µM C18:1	211	87	231	22	n.d.
micelles + 50 µM C22:6	215	92	265	23	53

Table 3.1; Fatty acid content of incubation medium with and without fatty acid supplementation. An aliquot of the medium prepared as described in chapter 2.3 was taken before the start of the experiment and frozen immediately. Lipid content was analysed as described in chapter 2.14. C16:0 = palmitic acid, C18:0 = stearic acid, C18:1 = oleic acid, C18:2 = linoleic acid, C22:6 = DHA; n = 1; n.d. = not detected

It can therefore be concluded that the fatty acid profile of the incubation medium differed between the two incubation techniques and that the micelle solution had a much higher lipid background than the FBS medium. Even though no PUFA were detected in 10 % FBS medium, they were present when the lipid composition of undiluted FBS was analysed. After 1:10 dilution in medium, some fatty acids from FBS were below the detection limit of ~ 10 µM. Calculating from the undiluted FBS,

DHA, arachidonic acid, linoleic acid and α-linolenic acid should be present in 10 % FBS medium at the concentrations of 2, 7, 3 and 6 µM, respectively.

To investigate whether the different amounts of background lipids were able to modulate cellular fatty acid content on their own, three different control incubations were carried out. Cells were either incubated with serum free medium, 10% FBS supplemented medium or micelle solution without added free fatty acid and the fatty acid composition of whole cell lipid extracts was analysed (Figure 3.1).

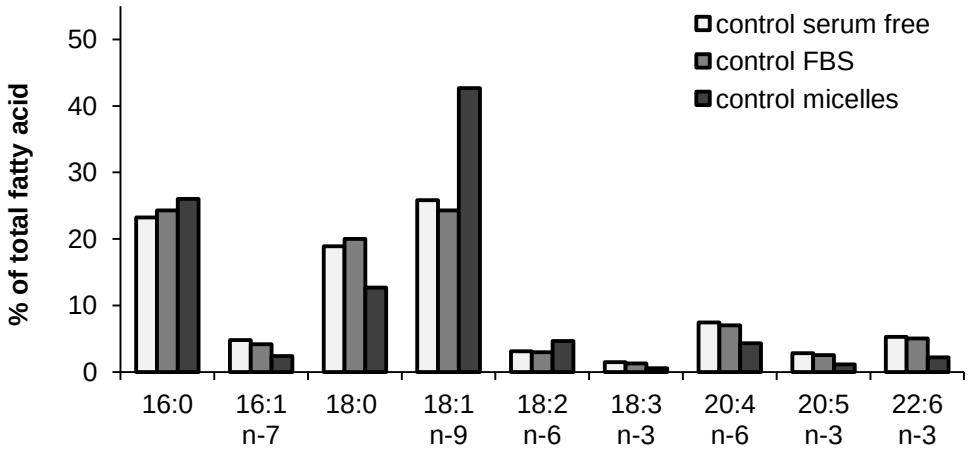

Figure 3.1; Comparison of fatty acid composition of Caco-2 cells grown on permeable supports, incubated with serum free medium, 10% FBS in medium or micelle solution without added fatty acid. 16:0 = palmitic acid, 16:1 = palmitoleic acid, 18:0 = stearic acid, 18:1 = oleic acid, 18:2 = linoleic acid, 18:3 = linolenic acid, 20:4 = arachidonic acid, 20:5 = EPA, 22:6 = DHA; n = 1; For conditions and analysis sections 2.3 and 2.14.

Cells incubated with micelle solution contained 19% more oleic acid but interestingly, 7% less stearic acid than cells incubated with 10% FBS medium and the percentage of linoleic acid was also slightly increased with micelle treatment. The increase in oleic and linoleic acid content could be due to the high concentration of these fatty acids in the micelle solution (table 3.1). However, the concentration of stearic acid was also higher in micelle solution than 10 % FBS medium, but the stearic acid content of Caco-2 cells was much lower after incubation with micelles. These results show that not all background fatty acids from micelle preparations are

equally available to be taken up by the cell. Cells incubated with serum free medium had a very similar fatty acid composition to cells incubated with 10% FBS medium which is not surprising as cells were incubated in 10 % FBS medium for the previous 21 days and only switched to serum free medium for the last 24 h. These experiments demonstrate that the lipid background of the control medium alone already resulted in a modification of cellular fatty acid composition.

The lipid composition of cells, incubated for 24 h with stearic acid, oleic acid or DHA bound to serum albumin or incorporated into mixed micelles, is shown in figures 3.2 to 3.4, with panel A showing the results for incubation with micelles and panel B showing the results for incubation with fatty acids bound to albumin.

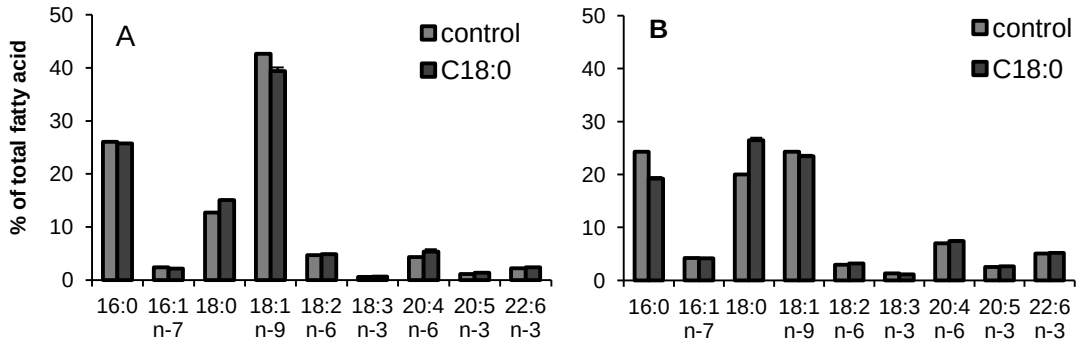

Figure 3.2; Impact of 24 h incubation of differentiated Caco-2 monolayers grown on permeable supports with 50 µM stearic acid on fatty acid composition of cell samples. Panel **A** shows incubations with fatty acids incorporated into micelles, panel **B** shows incubations with fatty acids added to medium containing 10% FBS. 16:0 = palmitic acid, 16:1 = palmitoleic acid, 18:0 = stearic acid, 18:1 = oleic acid, 18:2 = linoleic acid, 18:3 = linolenic acid, 20:4 = arachidonic acid, 20:5 = EPA, 22:6 = DHA; n = 2, N = 1; For conditions and analysis see sections 2.3 and 2.14.

Treatment with 50 µM stearic acid in 10 % FBS medium increased the content of that fatty acid in Caco-2 cells by 7 % and decreased the palmitic acid content by 6.8 % (figure 3.2B). Incubation with stearic acid incorporated into micelles increased

the percentage of that fatty acid by 2.8 % and decreased the percentage of oleic acid by 3.1 %, without a change in palmitic acid percentage (figure 3.2A).

Treatment with oleic acid incorporated into micelles had no effect on cellular fatty acid composition (figure 3.3A). This result is in accordance with the analysis of the incubation medium, which showed that addition of free oleic acid did not change the concentration of that fatty acid in the micelle solution. Adding oleic acid to medium with 10 % FBS resulted in an 11 % increase of that fatty acid in the cellular lipid extract and a 4 % decrease of each palmitic acid and stearic acid (figure 3.3B).

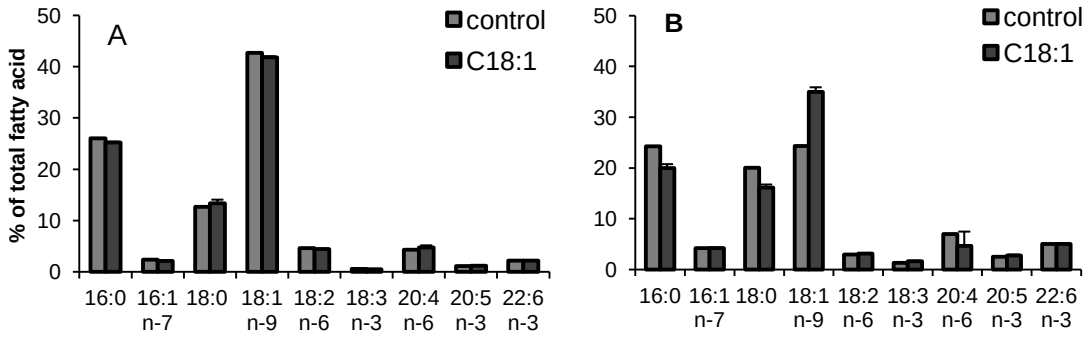

Figure 3.3; Impact of 24 h incubation of differentiated Caco-2 monolayers grown on permeable supports with 50 µM oleic acid on fatty acid composition of cell samples. Panel **A** shows incubations with fatty acids incorporated into micelles, panel **B** shows incubations with fatty acids added to medium containing 10% FBS. 16:0 = palmitic acid, 16:1 = palmitoleic acid, 18:0 = stearic acid, 18:1 = oleic acid, 18:2 = linoleic acid, 18:3 = linolenic acid, 20:4 = arachidonic acid, 20:5 = EPA, 22:6 = DHA; n = 2, N = 1; For conditions and analysis see sections 2.3 and 2.14.

Figure 3.4 shows that incubation with 50 µM DHA greatly increased the concentration of that fatty acid in the cell lipid extract with both incubation methods. With micelle incubation the percentage of DHA rose from 2 % to 8 % and reduced the content of oleic acid by 6 % (figure 3.4A). With FBS incubation, the percentage of DHA rose from 5 % to 21 % and reduced the content of palmitic, stearic and oleic acid by 5 %, 4 % and 5 %, respectively (figure 3.4B).

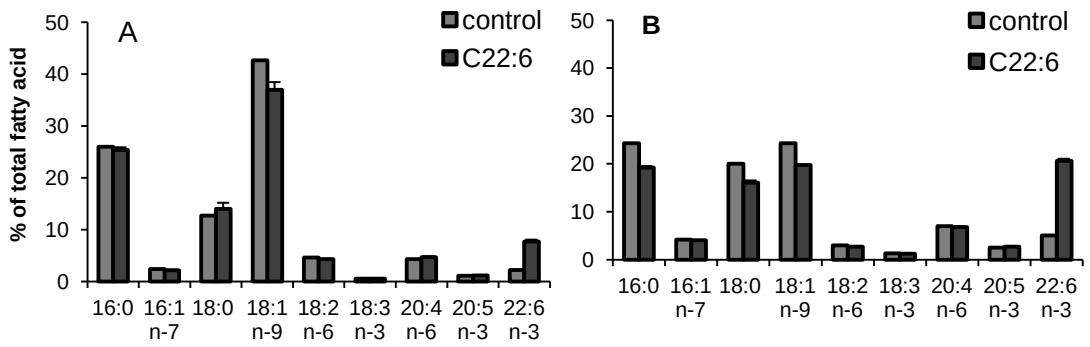

Figure 3.4; Impact of 24 h incubation of differentiated Caco-2 monolayers grown on permeable supports with 50 µM DHA on fatty acid composition of cell samples. Panel **A** shows incubations with fatty acids incorporated into micelles, panel **B** shows incubations with fatty acids added to medium containing 10% FBS. 16:0 = palmitic acid, 16:1 = palmitoleic acid, 18:0 = stearic acid, 18:1 = oleic acid, 18:2 = linoleic acid, 18:3 = linolenic acid, 20:4 = arachidonic acid, 20:5 = EPA, 22:6 = DHA; n = 2, N = 1; For conditions and analysis see sections 2.3 and 2.14.

Overall incorporation of selected fatty acids was more pronounced when fatty acids were bound to FBS albumin than when incorporated into micelles. Also the micelle medium had a high background of other fatty acids that dominated the desired change in cellular fatty acid composition. Therefore the incubation condition with 10 % FBS medium was chosen for all further studies.

3.3.2 Modification of cellular fatty acid content by chronic and acute incubation with fatty acids bound to serum albumin

Most studies investigating the impact of lipid supplementation on the fatty acid profile of cells in culture have used an incubation time of a few hours to a few days, whereas animal studies addressing the same question were usually carried out with a feeding period of several weeks. It is generally assumed that cells *in vitro* will respond in a very similar way to changing fatty acid availability as *in vivo*, but in a much shorter time. However, so far it has not been reported whether the response of cells in culture to changing lipid availability varies with the length of the incubation period. This question was addressed by comparing the pattern of changes occurring

with acute fatty acid supplementation of Caco-2 cells for 48 h and chronic incubation of cells over their entire differentiation time of 22 to 23 days.

Table 3.2 shows the change in overall percentage of the most abundant cellular fatty acids in supplemented cells, compared to cells incubated with 10 % FBS medium only. In general, most changes were similar with acute and chronic treatment but the impact was more pronounced in cells supplemented for their entire differentiation time. Some of the most interesting modifications of individual fatty acids are highlighted in table 3.2. The most prominent impact of supplementation was the incorporation of high amounts of all unsaturated fatty acids, that were additionally supplied, into the cellular lipid profile of up to + 32 % of overall fatty acid content with chronic arachidonic acid supplementation (table 3.2, frame a). Supplementation with stearic acid had no impact on cellular stearic acid content.

	supplementation													
%	C18:0		C18:1 n-9		C18:2 n-6		C18:3 n-3		C20:4 n-6		C20:5 n-3		C22:6 n-3	
Fatty acid	chronic	acute	chronic	acute	chronic	acute	chronic	acute	chronic	acute	chronic	acute	chronic	acute
C16:0	- 0.7	-1.2	- 4.2	- 1.6	+ 0.1	- 0.2	+ 1.5	- 0.5	+ 1.5	- 1.5	+ 9.6		+ 4.3	+ 0.3
C16:1 n-7	+ 0.3	+1.4	- 3.6	- 1.2	- 4.9	- 2.2	- 6.3	- 0.9	- 7.4	- 2.0	- 6.4		- 7.0	- 0.7
C18:0	+ 1.2	+ 2.4	- 3.4	- 0.9	- 0.3	+ 1.2	+ 4.9	+ 0.6	+ 9.1	+ 0.1	+ 7.1		+ 5.8	- 0.1
C18:1 n-9	+ 6.6	+ 2.6	+ 17.5	+ 8.6	- 17.8	- 6.3	- 22.7	± 0	- 27.7	- 3.2	- 24.2		- 27.2	- 7.2
C18:2 n-6	- 3.6	- 3.4	- 2.5	- 2.3	+ 23.2	+ 9.4	- 0.5	-4.1	- 2.7	- 1.2	- 1.5		- 2.9	- 3.6
C18:3 n-3	- 0.4	- 0.2	+ 1.3	- 0.8	- 0.3	- 0.3	+ 20.5	+ 7.7	- 1.7	+ 0.2	- 0.8		- 1.3	- 0.4
C20:4 n-6	- 1.7	- 0.8	- 2.5	- 1.4	+ 0.2	-0.9	- 2.0	-1.7	+ 31.9	+ 9.2	- 2.0		- 2.7	- 1.3
C20:5 n-3	- 1.1	- 0.4	- 1.2	- 0.6	- 2.1	- 0.9	+ 4.7	-2.1	- 2.1	- 1.3	+ 20.5		+ 9.0	+ 0.2
C22:6 n-3	- 1.3	- 0.5	- 1.9	- 0.7	- 1.7	- 0.9	- 1.4	-1.3	- 1.9	- 1.6	- 1.1		+ 21.9	+ 12.2
SFA	+ 1.8	+ 2.3	- 7.3	- 1.7	+ 0.9	+ 2.4	+ 7.6	+ 2.4	+ 11.5	+ 0.6	+ 16.7		+ 11.2	+ 1.0
MUFA	+ 6.7	+ 2.8	+ 14.3	+ 7.4	- 22.9	- 8.5	- 29.5	- 1.1	- 35.7	- 5.2	- 30.9		- 34.8	- 8.2
Σ PUFA	- 8.4	- 5.0	- 6.8	- 5.6	+ 22.0	+ 6.2	+ 22.1	- 1.3	+ 24.4	+ 4.8	+ 14.3		+ 23.6	+ 7.3
n-6 PUFA	- 5.7	- 4.0	- 5.2	- 3.5	+ 26.1	+ 8.2	- 1.8	- 5.6	+ 30.0	+ 7.4	- 4.2		- 6.0	- 4.8
n-3 PUFA	- 2.8	- 1.1	- 1.7	- 2.1	- 4.2	- 2.0	+ 23.8	+ 4.3	- 5.7	- 2.7	+ 18.5		+ 29.6	+ 12.0
n	2	1	2	1	1	1	2	1	2	1	1	0	2	1

Table 3.2; Impact of chronic and acute supplementation on change in overall percentage of cellular fatty acids. Cells were grown on solid supports and incubated with 50 µM fatty acid for 22 - 23 days or 48 h as described in section 2.3 and analysed as described in section 2.14. C16:0 = palmitic acid, C16:1 = palmitoleic acid, C18:0 = stearic acid, C18:1 = oleic acid, C18:2 = linoleic acid, C18:3 = linolenic acid, C20:4 = arachidonic acid, C20:5 = EPA, C22:6 = DHA, SFA = saturated fatty acid, MUFA = monounsaturated fatty acid, PUFA = polyunsaturated fatty acid

	supplementation							
Fatty acid [%]	control	C18:0	C18:1 n-9	C18:2 n-6	C18:3 n-3	C20:4 n-6	C20:5 n-3	C22:6 n-3
C16:0	20.1 ± 0.9	19.4 ± 2.0	**15.9 ± 0.3**	20.1	21.6 ± 1.4	21.6 ± 1.3	29.6	**24.4 ± 2.5**
C16:1 n-7	9.2 ± 0.7	9.5 ± 0.9	**5.6 ± 0.4**	4.3	**2.9 ± 0.7**	**1.8 ± 0.1**	2.8	**2.2 ± 0.04**
C18:0	10.5 ± 0.6	11.7 ± 1.8	**7.1 ± 0.3**	10.2	**15.4 ± 0.3**	**19.6 ± 1.6**	17.6	**16.3 ± 1.0**
C18:1 n-9	38.3 ± 0.6	**44.9 ± 3.0**	**55.8 ± 0.7**	20.5	**15.6 ± 1.9**	**10.6 ± 0.2**	14.1	**11.1 ± 1.3**
C18:2 n-6	4.8 ± 0.1	**1.2 ± 0.3**	**2.3 ± 0.6**	28.0	**4.3 ± 0.2**	**2.1 ± 0.7**	3.3	**1.9 ± 1.0**
C18:3 n-3	2.0 ± 0.1	1.6 ± 0.5	**3.3 ±0.001**	1.7	**22.5 ± 6.5**	**0.3 ± 0.3**	1.2	**0.7 ± 0.2**
C20:0	nd	0.6 ± 0.6	0.6 ± 0.05	0.9	**0.7 ± 0.03**	**0.7 ± 0.1**	nd	**0.7 ± 0.1**
C20:3 n-6	0.7 ± 0.4	0.3 ± 0.3	0.5 ± 0.05	0.8	0.6 ± 0.1	1.4 ± 0.4	nd	0.8 ± 0.3
C20:4 n-6	5.1 ± 0.5	3.4 ± 1.0	**2.6 ± 0.2**	5.3	**3.1 ± 0.1**	**37.0 ± 3.7**	3.1	**2.4 ± 0.2**
20:5 n-3	2.1 ± 0.2	**1.0 ± 0.1**	**0.9 ± 0.04**	nd	**6.8 ± 3.2**	nd	22.6	**11.1 ± 1.2**
C24:0	1.1 ± 0.1	**1.8 ± 0.1**	1.0 ± 0.1	1.6	1.4 ± 0.2	**1.5 ± 0.2**	1.1	**1.8 ± 0.2**
C24:1 n-9	1.2 ± 0.1	1.0 ± 0.1	**1.6 ± 0.00**	1.0	**0.7 ± 0.1**	**0.6 ± 0.05**	0.8	**0.6 ± 0.04**
C22:6 n-3	3.6 ± 0.5	**2.3 ± 0.5**	**1.7 ± 0.01**	1.9	**2.2 ± 0.2**	**1.7 ± 0.1**	2.5	**25.5 ± 3.4**
SFA	33.0 ± 0.3	34.8 ± 0.2	25.7 ± 0.8	33.9	40. ± 1.3	44.5 ± 3.0	49.7	44.2 ± 3.3
MUFA	48.7 ± 1.2	55.4 ± 1.9	63.0 ± 1.1	25.8	19.2 ± 2.7	13.0 ± 0.3	17.8	13.9 ± 1.4
Σ PUFA	18.2 ± 1.5	9.8 ± 2.1	11.4 ±0.3	40.2	40.3 ± 4.0	42.6 ± 3.2	32.5	41.8 ± 1.9
n-6 PUFA	10.6 ± 1.1	4.8 ± 1.6	5.4 ± 0.9	36.7	8.7 ± 0.6	40.6 ± 4.5	6.3	4.6 ± 1.5
n-3 PUFA	7.7 ± 0.8	4.9 ± 1.0	6.0 ± 0.1	3.5	31.5 ± 9.8	2.0 ± 0.4	26.2	37.3 ± 4.7
DBI	112	91	101	122	152	169	156	216
N	3	2	2	1	2	2	1	2

Table 3.3; Lipid composition of Caco-2 cells grown on solid supports and treated with 50 µM of different fatty acids for 22 - 23 days. Results are given as weight percentage of total fatty acids. Numbers in bold differ significantly from control cells grown in 10% FBS medium with p = 0.083. nd = not detected, All replicate samples were obtained on different days, partly from different batches of cells (N = 1, 2 or 3). For conditions and analysis see sections 2.3 and 2.14. C16:0 = palmitic acid, C16:1 = palmitoleic acid, C18:0 = stearic acid, C18:1 = oleic acid, C18:2 = linoleic acid, C18:3 = linolenic acid, C20:4 = arachidonic acid, C20:5 = EPA, C22:6 = DHA, SFA = saturated fatty acid, MUFA = monounsaturated fatty acid, PUFA = polyunsaturated fatty acid

Supplementation with n-3 PUFA reduced the percentage of n-6 PUFA and vice versa (table 3.3). Treatment of cells with linoleic or arachidonic acid resulted in a decrease in EPA content to the below detection limit.

Supplementation with PUFA also led to a decrease in MUFA and an increase in SFA levels. Palmitic and stearic acid together make up 96 % of all cellular SFA. 98 % of MUFA are palmitoleic and oleic acid (table 3.3). These four fatty acids can all be synthesised endogenously, but palmitic, stearic and oleic acid are also supplied with the medium (table 3.1). Palmitic acid levels are not affected by PUFA supplementation (table 3.2 frame b and table 3.4) indicating that fatty acid treatment has no impact on endogenous synthesis involving cytosolic FAS. Palmitic acid levels are unchanging but the desaturation of palmitic to palmitoleic acid is affected by PUFA treatment, resulting in decreased palmitoleic acid levels, which contributes to the overall decrease in MUFA with PUFA supplementation. The enzyme catalysing this reaction is the Δ^9-desaturase. These results would indicate that PUFA supplementation is affecting either the expression or activity of Δ^9-desaturase.

	chronic supplementation					acute supplementation				
	control	C18:2	C18:3	C20:4	C22:6	control	C18:2	C18:3	C20:4	C22:6
C16:0	20.1	20.1	21.6	21.6	24.4	20.1	19.9	19.5	18.6	20.4
C16:1	9.2	4.3	2.9	1.8	2.2	9.2	7.0	8.3	7.2	8.5
Σ C16	29.3	24.5	24.5	23.4	26.6	29.3	26.9	27.8	25.8	28.9

Table 3.4; Impact of chronic and acute PUFA supplementation on cellular palmitic and palmitoleic acid content. Excerpt from table 3.3. For conditions and analysis see sections 2.3 and 2.14. C16:0 = palmitic acid, C16:1 = palmitoleic acid, C18:2 = linoleic acid, C18:3 = linolenic acid, C20:4 = arachidonic acid, C22:6 = DHA

While the content of the SFA palmitic acid remained unchanged, the content of the SFA stearic acid increased with all PUFA treatments except linoleic acid (table 3.2 frame c). Cells can take up stearic acid from the medium, mainly by passive diffusion and, to a much lesser extent, by caveolin-mediated endocytosis and via the

uptake transporter CD36 (78). But as none of these mechanisms are selective for one type of fatty acid over another, it is not plausible that a change in fatty acid uptake from the medium is responsible for changing stearic acid levels while the palmitic acid content remains stable. Therefore this effect is more likely due to an impact of PUFA on endogenous synthesis of stearic acid, involving the enzyme ELOVL6. The precursor of stearic acid is palmitic acid. Since palmitic acid levels are not affected by PUFA treatment, such changes in stearic acid levels are not due to a change in substrate availability for ELOVL6, but instead it seems that PUFA have an impact on the enzyme's activity or expression. However, looking more closely at the data, it becomes apparent that the increase in cellular stearic acid content is correlated with a decrease in oleic acid levels (table 3.5). Endogenous synthesis of oleic acid requires the precursor stearic acid and the enzyme Δ^9-desaturase. The sum of cellular oleic and stearic acid concentrations remains the same with all PUFA treatments. It therefore seems that all PUFA treatments reduced the oleic acid content by ~ 20 % and then the saturation level of the remaining ~ 30 % of stearic + oleic acid is regulated by an impact of individual PUFA on the Δ^9-desaturase activity, as already observed with the desaturation of palmitic to palmitoleic acid.

	chronic supplementation					acute supplementation				
	control	C18:2	C18:3	C20:4	C22:6	control	C18:2	C18:3	C20:4	C22:6
C18:0	10.5	10.2	15.4	19.6	16.3	10.5	11.7	11.1	10.6	10.4
C18:1	38.3	20.5	15.6	10.6	11.1	38.3	32	38.3	35.1	31.1
Σ C18	48.8	30.7	31.0	30.2	27.4	48.8	43.7	49.4	45.7	41.5

Table 3.5; Impact of chronic and acute PUFA supplementation on cellular stearic and oleic acid content. Excerpt from table 3.3. For conditions and analysis see sections 2.3 and 2.14. C18:0 = stearic acid, C18:0 = oleic acid, C18:2 = linoleic acid, C18:3 = linolenic acid, C20:4 = arachidonic acid, C22:6 = DHA

The effect of PUFA on palmitic and stearic acid desaturation is mainly observed in chronic but not acute treatment (tables 3.4 and 3.5), indicating that these are cellular

responses which are not induced by acute lipid doses but more with long term changes in dietary patterns.

Supplementation with linoleic or α-linolenic acid did not result in a large increase in downstream reaction products although those two EFA should be elongated and desaturated to yield highly unsaturated fatty acids (HUFA) of the n-3 and n-6 pathway (table 3.2 frame d). *In vivo*, these reactions occur mainly in liver and adipose tissue and to a much lesser extend in enterocytes. But ELOVL5 and ELOVL7, which catalyse the chain elongation, are expressed ubiquitously and FADS2, which catalyses the desaturation, the rate limiting step in this process, is also expressed in Caco-2 cells. Moreover, Caco-2 cells have previously been shown to be able to process EFA to HUFA (156). One pathway of fatty acid processing that is well observed here is the retro-conversion of DHA to EPA through peroxisomal β-oxidation (table 3.2 frame e).

Fatty acid supplementation did not only affect the percentage of individual cellular fatty acids but also dramatically changed the profile of SFA, MUFA and PUFA. Supplementation with PUFA increased the percentage of cellular PUFA to ~ 40 % while decreasing the percentage of MUFA to about one third of the control value and increasing the percentage of SFA by about one third. The relationship between these three groups of fatty acids is shown in figure 3.5.

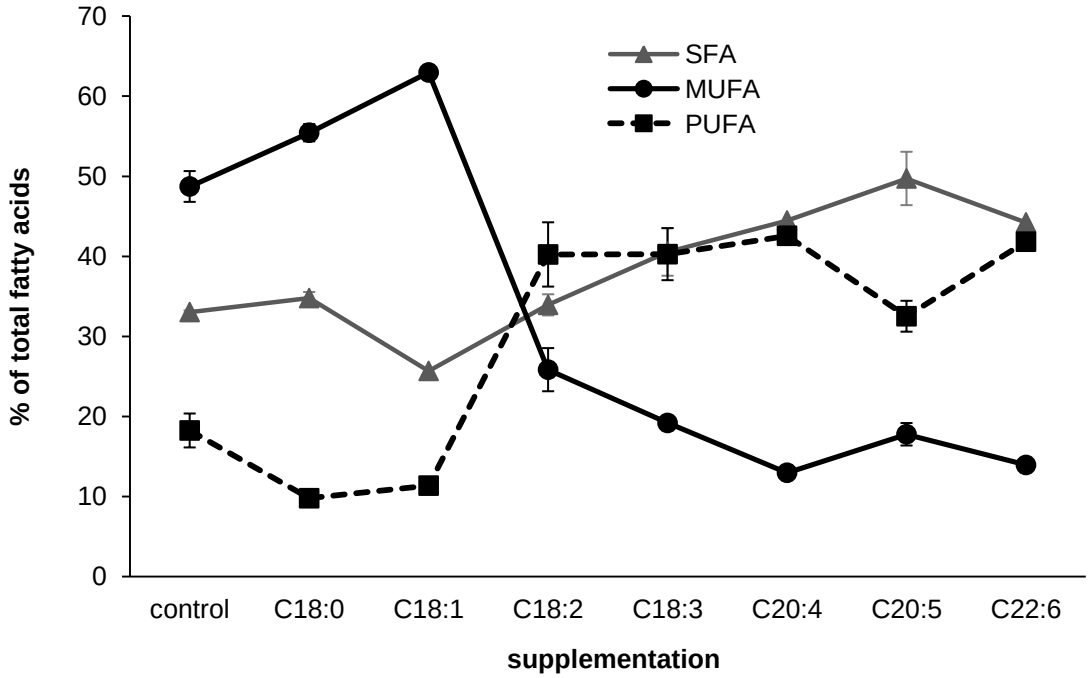

Figure 3.5; Impact of fatty acid supplementation (as indicated on the abscissa) on desaturation profile. For conditions and analysis see sections 2.3 and 2.14. C18:0 = stearic acid, C18:1 = oleic acid, C18:2 = linoleic acid, C18:3 = linolenic acid, C20:4 = arachidonic acid, C20:5 = EPA, C22:6 = DHA

There is a clear inverse correlation between the percentage of MUFA and the percentage of PUFA in cellular lipids. The correlation between the three groups of unsaturation in different treatments is shown in figures 3.6 to 3.8.

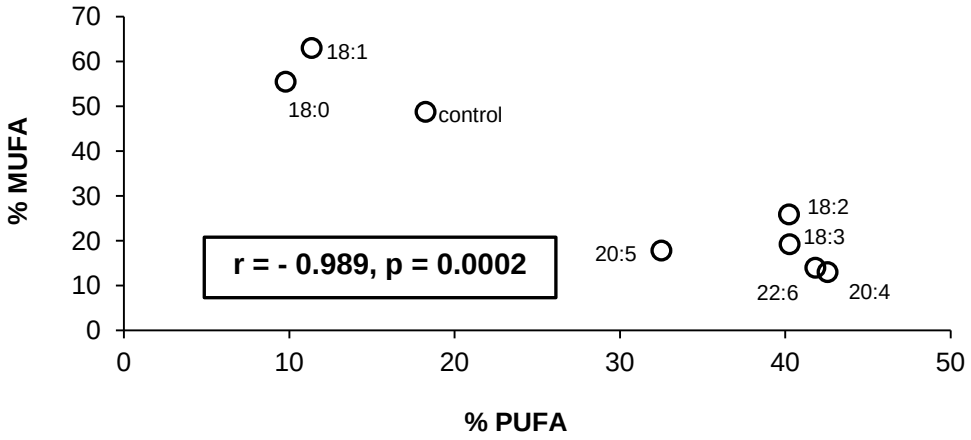

Figure 3.6; Correlation between MUFA and PUFA in Caco-2 cells grown on solid supports and chronically treated with 50 µM fatty acid. Each data point represents an incubation with a different fatty acid as indicated in the label. For conditions and analysis see sections 2.3 and 2.14. r = Pearson correlation coefficient; C18:0 = stearic acid, C18:1 = oleic acid, C18:2 = linoleic acid, C18:3 = linolenic acid, C20:4 = arachidonic acid, C20:5 = EPA, C22:6 = DHA

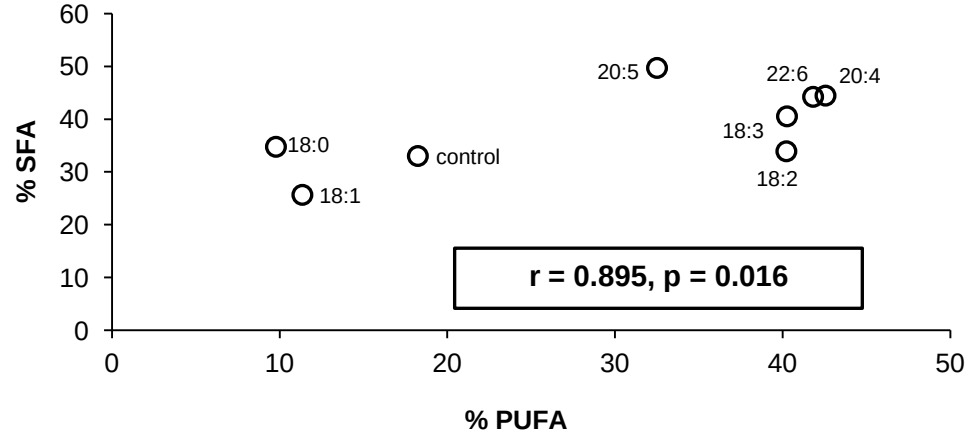

Figure 3.7; Correlation between SFA and PUFA in Caco-2 cells grown on solid supports chronically treated with 50 µM fatty acid. Each data point represents incubation with a different fatty acid as indicated in the label. For conditions and analysis see section 2.3 and 2.14. r = Pearson correlation coefficient; C18:0 = stearic acid, C18:1 = oleic acid, C18:2 = linoleic acid, C18:3 = linolenic acid, C20:4 = arachidonic acid, C20:5 = EPA, C22:6 = DHA

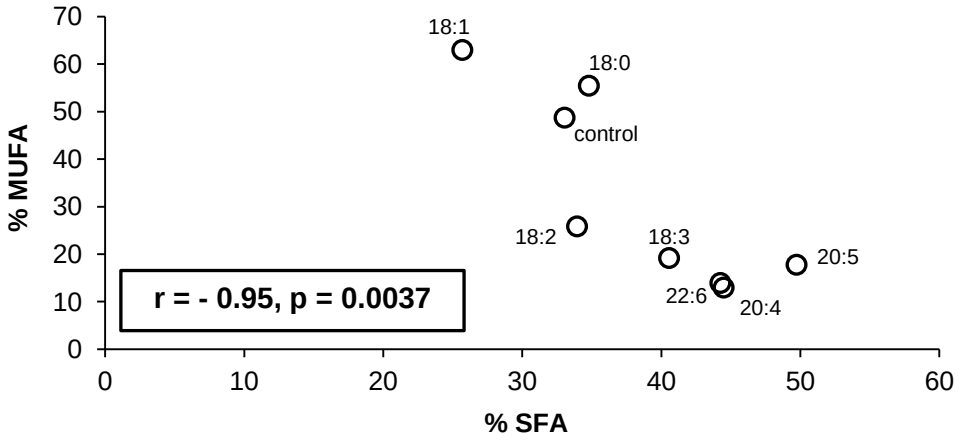

Figure 3.8; Correlation between MUFA and SFA in Caco-2 cells grown on solid supports and chronically treated with 50 µM fatty acid. Each data point represents incubation with a different fatty acid as indicated in the label. For conditions and analysis see sections 2.3 and 2.14. r = Pearson correlation coefficient; C18:0 = stearic acid, C18:1 = oleic acid, C18:2 = linoleic acid, C18:3 = linolenic acid, C20:4 = arachidonic acid, C20:5 = EPA, C22:6 = DHA

With a coefficient of correlation of – 0.959, there is a strong dependence of MUFA on PUFA content in fatty acid supplemented cells (figure 3.6), mainly due to the above described decrease of oleic acid levels. The slightly less strong correlation between MUFA and SFA (figure 3.8) is probably also reflecting the PUFA impact on desaturation of stearic to oleic acid, as discussed above (figure 3.5). Interestingly, supplementation with stearic acid has the same effect as supplementation with oleic acid on the overall degree of unsaturation of cellular lipids. Both fatty acids decrease the double bond index of whole cell lipid extracts whereas all other treatments increase this parameter (table 3.3).

3.3.3 Impact of fatty acid supplementation on cell viability

The results described above indicate that the fatty acid content of Caco-2 cells can be modified by addition of free fatty acids to FBS containing medium and that chronic treatment results in greater changes than acute treatment.

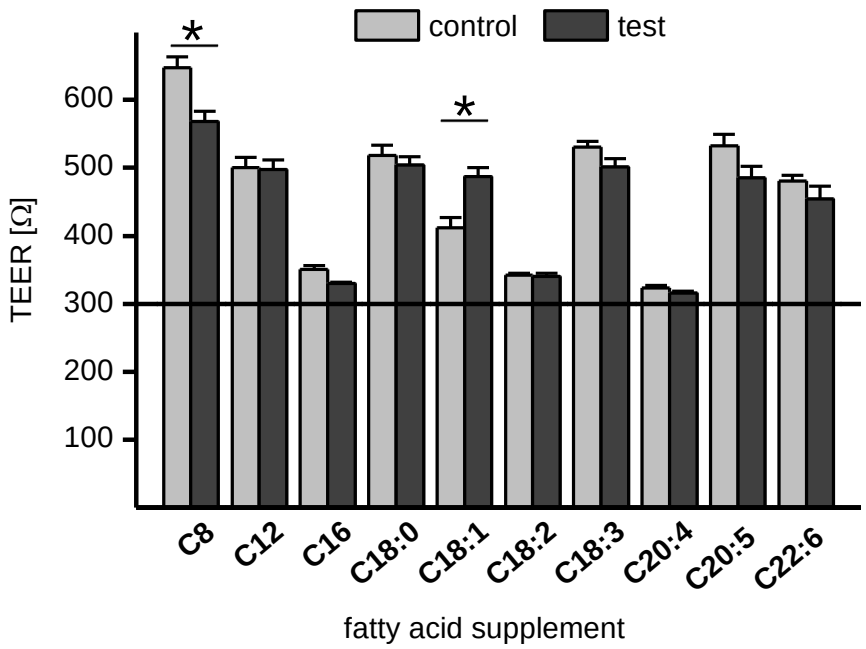

Figure 3.9; Impact of chronic fatty acid supplementation on viability assessed by TEER fold change. For further information see sections 2.3 and 2.5. C8 = octanoic acid, C12 = lauric acid, C16 = palmitic acid, C18:0 = stearic acid, C18:1 = oleic acid, C18:2 = linoleic acid, C18:3 = linolenic acid, C20:4 = arachidonic acid, C20:5 = EPA, C22:6 = DHA; n = 6, N = 1; * = $p < 0.05$;

Figure 3.9 shows the impact of chronic incubation with different fatty acids on TEERvalues, indicating tight junction integrity and figure 3.10 shows the impact of fatty acid supplementation on cell viability, determined by MTT assay. Only the medium chain fatty acid caprylic acid decreased TEER and treatment with oleic acid increased TEER slightly. Interestingly, all PUFA treatments increased apparent viability of cells, indicating that chronic PUFA supplementation had no cytotoxic effect. Only oleic acid treatment decreased viability.

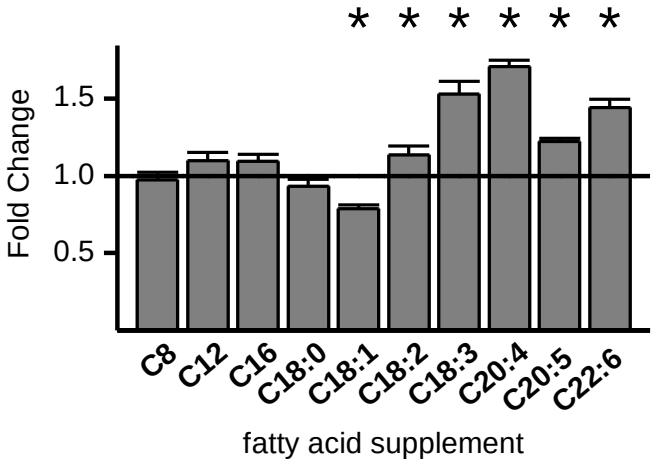

Figure 3.10; Impact of fatty acid supplementation on viability assessed by MTT assay. For further information see sections 2.3 and 2.5. C8 = octanoic acid, C12 = lauric acid, C16 = palmitic acid, C18:0 = stearic acid, C18:1 = oleic acid, C18:2 = linoleic acid, C18:3 = linolenic acid, C20:4 = arachidonic acid, C20:5 = EPA, C22:6 = DHA; n = 6, N = 1; * = $p < 0.05$

3.3.4 Cellular lipid accumulation

It has previously been reported that cells in culture are prone to store supplemented fatty acids in form of triacylglycerides in intracellular lipid droplets. PUFA such as DHA and EPA have been associated with reduced lipid droplet accumulation in adipocytes (157). To investigate whether chronic supplementation of Caco-2 cells with 50 µM fatty acid, as performed here, leads to lipid droplet formation, cells were treated with DHA for their entire differentiation period and then stained with the hydrophobic probe nile red to identify intracellular storage lipids. It was assumed that if DHA incubation, which is usually reported to reduce lipid accumulation, induces lipid droplets, then other fatty acids will have a similar effect.

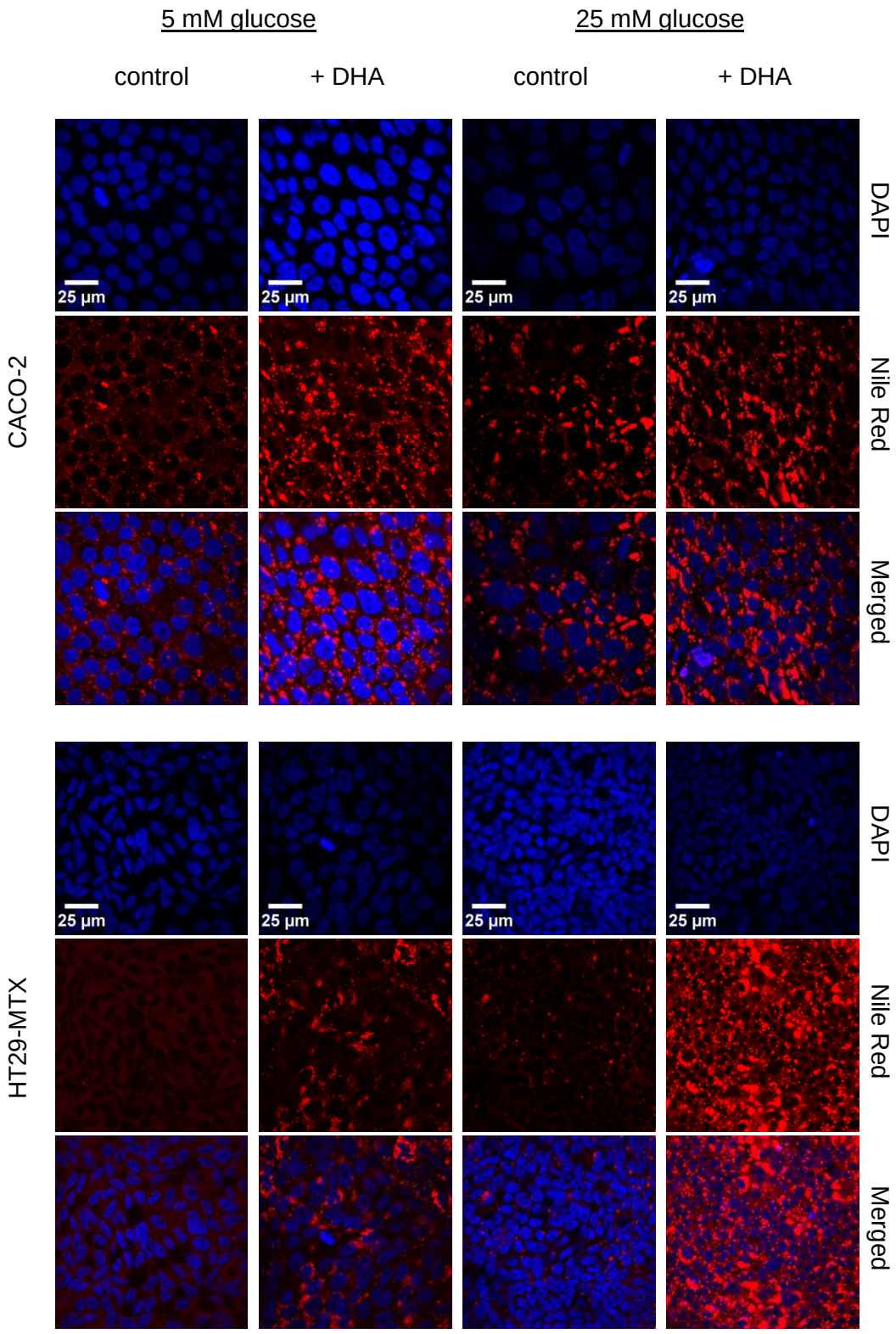

Figure 3.11, Lipid droplet formation in Caco-2 and HT29-MTX cells grown on permeable supports in high or low glucose medium and treated with 50 µM DHA for 22 days. Nuclei are shown in blue, lipid deposits in red. Representative images of three independent experiments are shown (n = 3, N = 1). For conditions and analysis see sections 2.3 and 2.10.

Figure 3.11 shows the impact of glucose concentration and DHA supplementation on lipid accumulation in the two intestinal cell lines used in this study. Different glucose concentrations were tested because both medium with high (25 mM) and physiological (5 mM) glucose concentration is routinely used to culture Caco-2 cells.

Nile red is a fluorescence probe that will selectively integrate into hydrophobic structures and its fluorescence signal is quenched in an aqueous environment (158). It will therefore give a strong signal when dissolved in the neutral lipid core of lipid droplets, but will also show a weak signal when incorporated into cellular membranes, as especially clearly observed with the low glucose control incubation of HT29-MTX cells.

Figure 3.11 shows that Caco-2 cells which had not been fatty acid supplemented already contained some intracellular lipid deposits when grown in either low or high glucose medium, but there was a stronger fluorescence signal with high glucose medium. With DHA supplementation, cells grown in low glucose medium, as well as cells grown in high glucose medium, developed pronounced intracellular lipid bodies. With high glucose, lipid droplets were of larger size than with low glucose medium.

HT29-MTX cells showed no lipid accumulation when grown in low glucose control medium and only very little when grown in high glucose control medium. With DHA addition, HT29-MTX cells grown in low glucose medium developed some intracellular lipid droplets but with high glucose medium there was a dramatic accumulation of lipid bodies.

Since especially HT29-MTX cells accumulated substantially more lipids with high glucose medium in combination with fatty acids, low glucose medium was chosen for all further experiments.

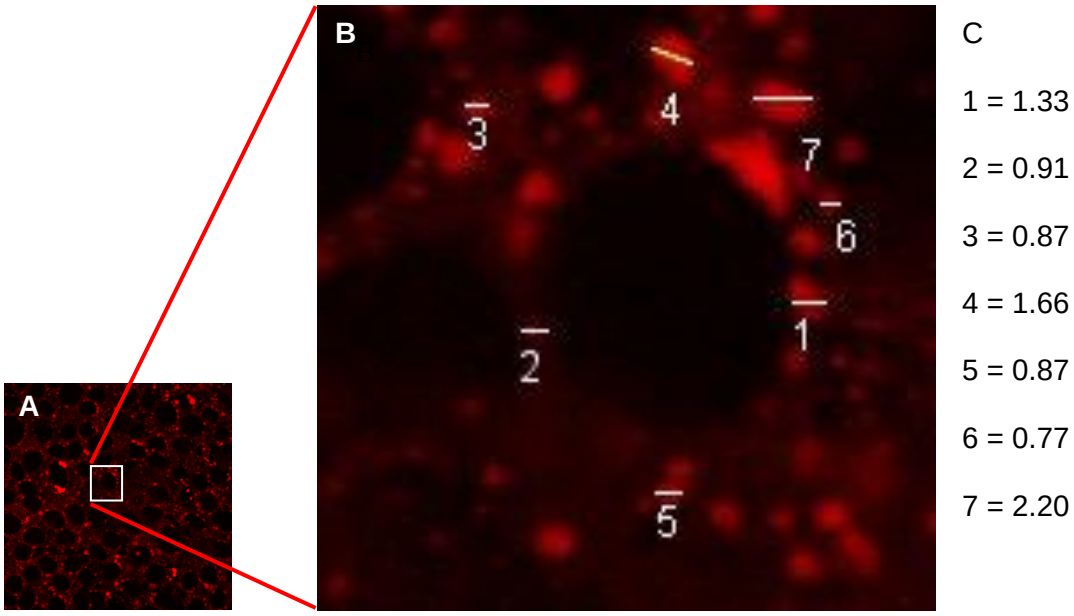

Figure 3.12; Size of intracellular lipid bodies in Caco-2 cells grown on permeable supports in 10 % FBS medium for 22 days. A) Image of Nile Red stained Caco-2 cells as shown in figure 3.10. B) Detail of image A) showing intracellular lipid accumulations and scale bars. C) length of scale bars shown in B) in µM.

Most fatty acids that are taken up from the luminal side of small intestinal enterocytes are re-esterified into triacylglycerols and can be either transiently stored in cytosolic lipid droplets or assembled into lipoproteins or chylomicrons and released into the bloodstream. Caco-2 cells are also able to excrete lipoproteins and chylomicrons into the medium (145, 159). Chylomicrons have a size of 0.08 – 1.2 µm whereas lipid droplets, in non adipose tissues, can reach a diameter of up to 6 µm (75). Figure 3.11 shows a typical example image of the nile red staining, where the area surrounding the nucleus has been enlarged to show the lipid staining in more detail. Most of the lipid bodies observed here had a diameter of < 1 µm which could make them either large chylomicrons or lipid droplets. Some had a diameter of > 1.3 µm which clearly identifies them as lipid droplets (figure 3.12). Most of the nile red fluorescence signal seems to cluster around the nucleus indicating ER localisation. Lipid droplets localise to the cytoplasm but they are formed and bud from the ER (75, 86). It can therefore not definitively be determined

whether the small lipid bodies observed around the nucleus are indeed lipid droplets or whether they are lipoproteins assembled in the secretory pathway.

3.3.5 Impact of chronic fatty acid supplementation on membrane fluidity

The impact of chronic fatty acid supplementation of Caco-2 cells on membrane fluidity was assessed using the fluorescence probe TMA-DPH (figure 3.13). To assess this parameter there are a number of different probes available which insert into the membrane in different ways and at different depth, giving information on the fluidity at this precise localisation. TMA-DPH was chosen as it mimics phospholipid components well, with a polar headgroup and a non-polar chain, it has a general structure that is similar to membrane lipids (160).

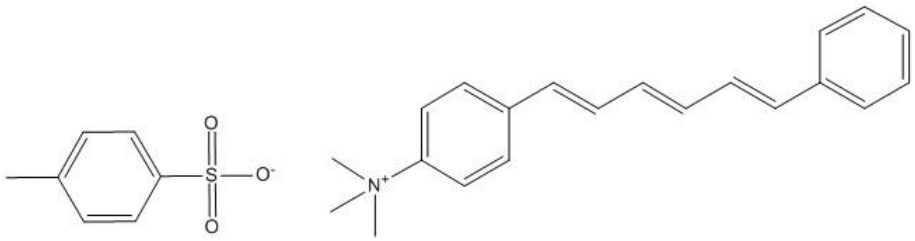

Figure 3.13; Chemical structure of fluorescence probe N,N,N-Trimethyl-4-(6-phenyl-1,3,5-hexatrien-1-yl)phenylammonium p-toluenesulfonate (TMA-DPH).

BBMV were isolated from differentiated cells chronically supplemented with 50 µM fatty acid and incubated with TMA-DPH. The fluorescence probe was then excited with polarised light and the ratio of signal emitted in parallel and perpendicular direction was determined, which reflects the degree of restriction that the membrane exerts on the free movement of the probe. Fluorescence anisotropy was assessed at an array of temperatures ranging from 25°C to 45°C. Figure 3.14 shows the temperature dependence of and the effect of different fatty acids on fluorescence anisotropy in BBMV. Anisotropy decreased with increasing temperature and with supplementation of cells with unsaturated fatty acids.

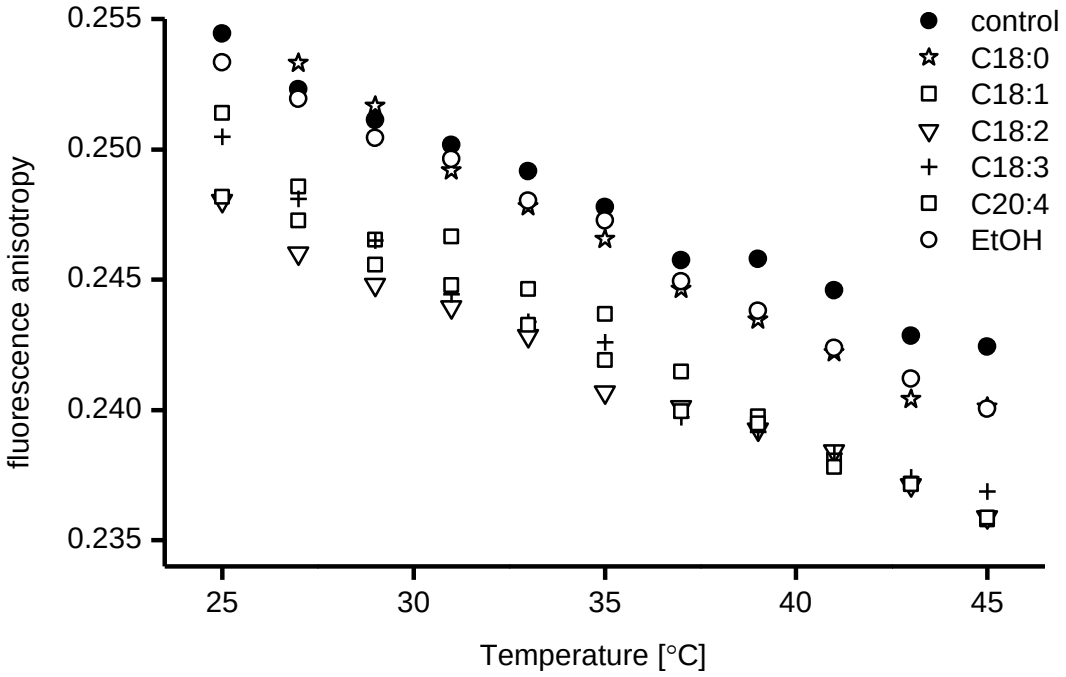

Figure 3.14; Fluorescence anisotropy of brush border membrane vesicles isolated from differentiated Caco-2 cells that were grown on solid supports and either chronically supplemented with 50 µM fatty acid or solvent vehicle (EtOH) or untreated (control). C18:0 = stearic acid, C18:1 = oleic acid, C18:2 = linoleic acid, C18:3 = linolenic acid, C20:4 = arachidonic acid; n = 4, N =2; For clarity of the graph, error bars were omitted (see figure 3.15). For details on culture, isolation and analysis see section 2.2, 2.3 and 2.12.

All treatments, except for EPA and DHA, were compared to membrane fluidity of BBMV isolated from Caco-2 cells grown in 10 % FBS medium. Cells treated with EPA or DHA were also supplemented with 100 µM of the antioxidant vitamin E to prevent oxidation of the HUFA in the growth medium, which would induce oxidative stress of cells. Vitamin E supplementation of cells differentially lowered membrane anisotropy, with no change compared to non-supplemented cells at 25°C, but decreased with increasing temperatures. Because of that, anisotropy of cells supplemented with DHA or EPA was normalised to cells grown in 10 % FBS medium supplemented with 100 µM vitamin E, as shown in figure 3.15.

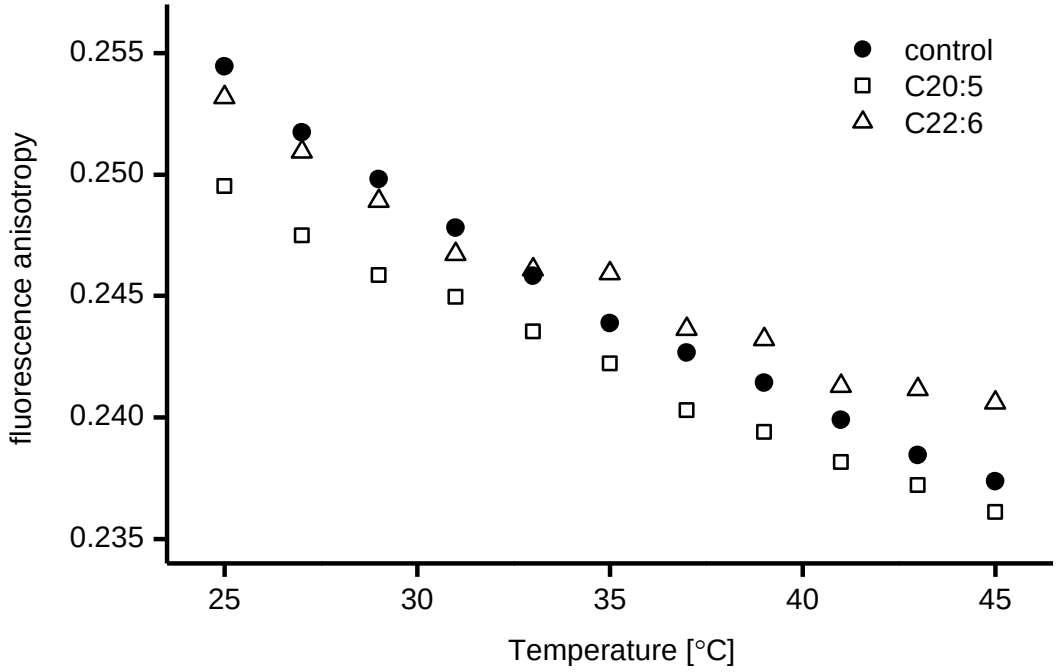

Figure 3.15; Fluorescence anisotropy of brush border membrane vesicles isolated from differentiated Caco-2 cells that were grown on solid supports and chronically treated with 100 µM vitamin E and either 50 µM EPA (C20:5) or DHA (C22:6) or solvent vehicle. For clarity of the graph, error bars were omitted (see figure 3.15). n = 4, N = 2 For details on culture, isolation and analysis see section 2.2, 2.3 and 2.12.

For several anisotropy curves an inflexion point was noted, which indicates a phase change in the lipid membrane from gel phase to liquid crystalline phase at that temperature. Therefore anisotropy values were plotted against the reciprocal temperature and linear regression lines were fitted to find the approximate temperature value at which such a phase change occurs in different lipid treatment groups (figure 3.16). The results are summarised in table 3.6 together with the P-values obtained from ANOVA analysis of significant differences in fluorescence anisotropy between BBMV isolated from untreated and lipid supplemented Caco-2 cells.

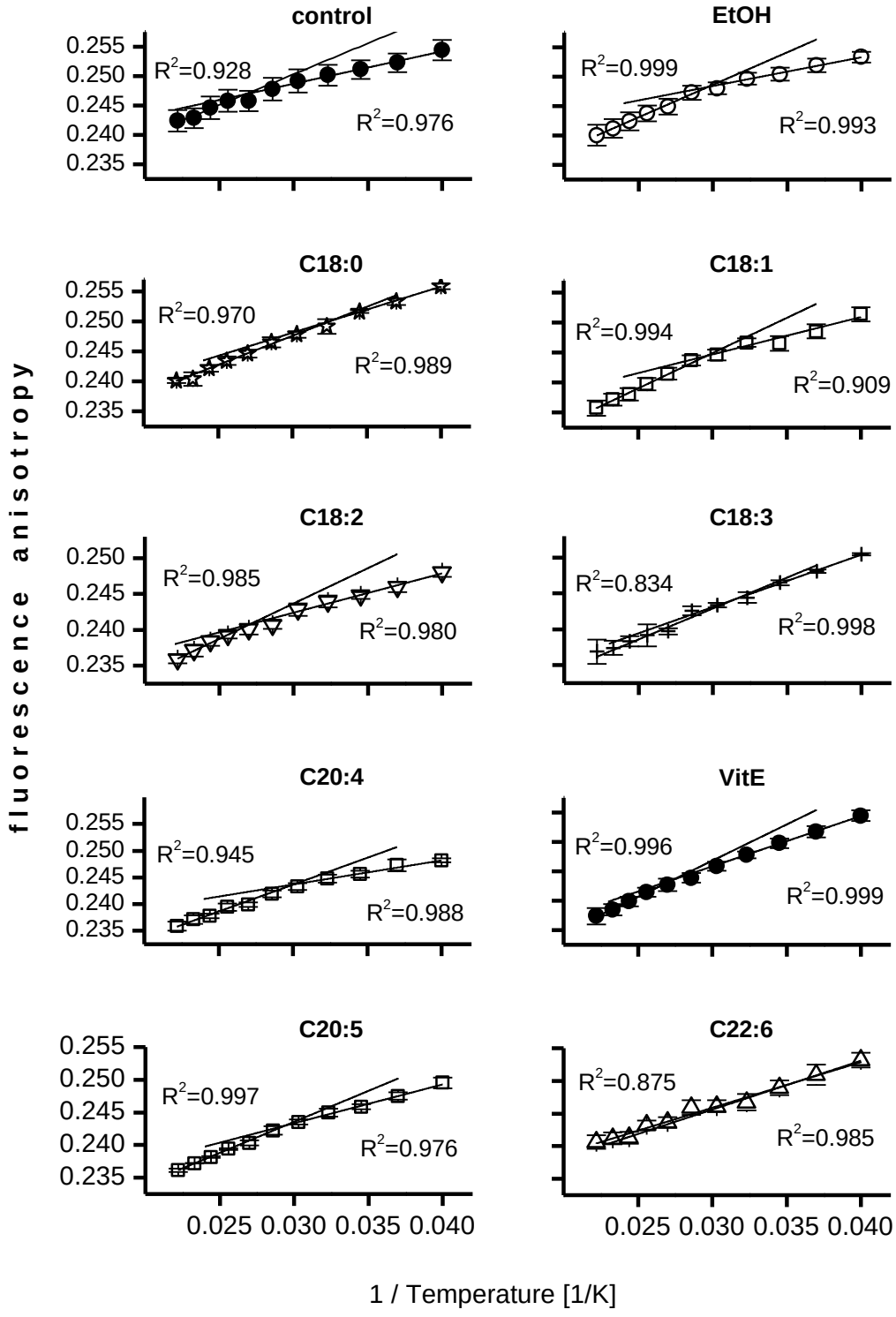

Figure 3.16; Fluorescence polarisation of individual lipid treatment groups in relation to the reciprocal temperature. C18:0 = stearic acid, C18:1 = oleic acid, C18:2 = linoleic acid, C18:3 = linolenic acid, C20:4 = arachidonic acid, C20:5 = EPA, C22:6 = DHA, VitE = vitamin E, EtOH = ethanol. For details on conditions and analysis see sections 2.2, 2.3, 2.12 and 2.16.

Supplementation of the growth medium with linoleic, α-linolenic and arachidonic acid resulted in a significant decrease in fluorescence anisotropy, which corresponds to an increase in membrane fluidity. Stearic acid, oleic acid, EPA and DHA had no significant effect. Ethanol was used for preparing fatty acid stock solutions and was present in treatment groups and also in control groups for transport experiments at a concentration of ~ 100 mM. It has been reported that ethanol increases membrane fluidity (161). To test whether the presence of the solvent has an impact on membrane fluidity here, the fluorescence anisotropy of BBMV isolated from chronically ethanol supplemented Caco-2 cells were compared to BBM isolated from cells grown without supplementation of solvent or fatty acid. Membrane fluidity was slightly increased in ethanol treated samples at higher temperature, but these changes were not significant.

supplementation	P-value	~ T inflexion point [°C]
control		37
EtOH	0.883	34
C18:0	1	31
C18:1	0.066	34
C18:2	0.0006	37
C18:3	0.036	?
C20:4	0.012	33
VitE		36
C20:5	0.412	34
C22:6	0.731	?

Table 3.6; Membrane fluidity significance level and phase transition temperature for brush border membrane vesicles isolated from Caco-2 cells chronically supplemented with different fatty acids. All treatments were compared to brush border membrane vesicles isolated from untreated control cells, except EPA and DHA treatments, which were compared to samples obtained from cells chronically supplemented with vitamin E. C18:0 = stearic acid, C18:1 = oleic acid, C18:2 = linoleic acid, C18:3 = linolenic acid, C20:4 = arachidonic acid, C20:5 = EPA, C22:6 = DHA, VitE = vitamin E, For details on analysis see sections 2.12 and 2.16.

A possible phase transition point in BBMV was analysed as shown in figure 3.16. Even though ethanol had no significant impact on membrane fluidity it reduced the phase transition temperature by ~ 3 K. Stearic acid, oleic acid and EPA also reduced the phase transition temperature, but no obvious inflexion point could be observed in BBMV isolated from linolenic acid or DHA supplemented cells.

3.4 Discussion

Different incubation conditions were tested for a long term, dietary pattern cell culture model and the impact of modification of the cellular fatty acid composition on basic parameters was assessed.

Previous reports have shown that fatty acids incorporated into micelles are taken up much faster and more efficiently than fatty acids bound to albumin and that uptake from the apical side of Caco-2 cells occurs at a higher rate than uptake from the basolateral side (162-164). Such studies were usually carried out with the help of isotopically labelled free fatty acids which are then traced through different compartments and metabolic pathways. While this approach gives valuable insight into the preferred incorporation of supplemented fatty acids into different lipid classes (triglycerides, phospholipids, etc.) and into eventual intracellular storage or excretion in form of different lipid particles, it does not provide information on overall changes in cellular lipid composition induced by the treatment. Mixed micelles are made up of different kinds of lipids and bile acids but since it is only the free fatty acid which is isotopically labelled, the impact of other fatty acid moieties cannot be monitored. The lipid component of mixed micelles is typically made up of a monoglyceride (in the present study that was monoolein), phosphatidylcholine and lysophosphatidylcholine, where the fatty acid composition is usually not well defined as they are extracted from natural sources like egg yolk or soybean and contain a mixture of different acyl moieties. Not only free fatty acids, but also monoacylglycerols, can be absorbed by Caco-2 cells and used for phospholipid and triacylglycerol synthesis. Caco-2 cells display low level phospholipase and lysophospholipase activity (165) and therefore the fatty acids derived from those micelle components can also be taken up and turned over. Such impact of other micelle lipid components has been observed in the current study where micelle treatment of Caco-2 cells resulted in a cellular lipid modification dominated by the monoacylglycerol component and only to a lesser extent by the free fatty acid. A

much more controlled lipid modification was achieved when fatty acids were presented in the form of albumin complexes.

For short term incubations of a few minutes to a few hours, fatty acids are usually complexed to lipid free bovine serum albumin (BSA) at high concentrations in buffer and afterwards diluted to the final concentration, and then sterile filtered (166). With this method, there is a precisely defined concentration of fatty acids and nutrients in the experimental set-up. But with long term incubation, as employed here, this approach is very cumbersome as other factors that are needed for cell growth and development, which are contained in FBS (such as growth and adhesion factors, trace elements and vitamins), would have to be added individually to the serum free medium. Adding fatty acids dissolved in ethanol directly to FBS-containing growth medium under sterile conditions, as chosen here, is a much easier method, but will not result in a precisely defined nutrient composition of the medium. However, since a model of chronic dietary pattern was sought, it would be a highly artificial situation to incubate enterocytes with only one single type of fatty acid as the entire source of lipids and would ultimately lead to EFA deficiency in the model. Since FBS contains low levels of PUFA, a domination of the metabolic impact of EFA deficiency over the desired effect of the provided fatty acid is avoided with the here chosen method of incubation. However, the here employed method does not replicate the conditions in which fatty acids are presented to intestinal enterocytes in vivo, which is complexed to albumin from the basolateral and incorporated into micelles from the apical side. With short term incubations, the ratio of fatty acid to BSA is usually set between 1 and 6 to 1 as albumin has a very high capacity of fatty acid binding of up to 13 mole fatty acid per mole albumin (167). FBS contains albumin at a concentration of 20 - 36 g/L (168). The fatty acid concentration used in the current study is 50 µM, which corresponds to a fatty acid to albumin ratio of about 1.4 to 1 in 10 % FBS medium. Since albumin has a much higher fatty acid binding capacity than that, it

was assumed that all supplemented fatty acid was bound, even with the presence of additional background fatty acids as listed in table 3.1.

There are numerous reports that the fatty acid profile of the plasma membrane can be modulated in animal studies with selective fatty acid feeding and that this effect can also be reproduced *in vitro*. The chemical nature of the acyl chains esterified to the glycerol backbone of phospholipids, together with the type of headgroup and cholesterol content, determines plasma membrane fluidity, which in turn can have an impact on the passive diffusion rate of a compound across the lipid bilayer. One of the objectives of the current study was to assess such impact of acyl chain modification on passive diffusion of phenolics. Cell culture studies on incorporation of fatty acids are typically performed with an exposure time of 24 or 48 h, which is very short for the Caco-2 cell culture model, where transport studies are usually carried out at day 21 to 25 after seeding, by which time the cells will have spontaneously differentiated to small intestinal, enterocyte-like cell monolayers. During differentiation there occurs not only a structural change, characterised by development of a distinctly polar morphology, but also a functional change, resulting in a shift in expression and activity of many key enzymes, receptors and nutrient transporters (169). The activity of some important enzymes for lipid metabolism is also changing during differentiation of Caco-2 cells. Activity of MOGAT and of acyl-CoA synthase increases with differentiation as well as excretion of triacylglycerols, whereas phospholipid secretion decreases over time. Excretion of HDL is unaffected by differentiation but more VLDL and less LDL is released with increasing time in culture (145). Also, with increasing differentiation time, supplemented fatty acids are more likely incorporated into phospholipids and less into triacylglycerols (170). The consequence of these changes in metabolism is that fatty acids supplemented at the beginning of cell differentiation will most likely be metabolised in a slightly different way and might have a different impact on cell proliferation than when supplemented after differentiation is almost complete. Also

short term treatment will simulate an acute exposure to certain lipids but not the long term impact of dietary patterns, as was sought here. It was therefore of interest to compare how acute treatment and chronic treatment differentially modulate lipid composition of Caco-2 cells. In animal models it has been shown that the response to long term exposure can vary over a longer feeding period. For example, one study that analysed the fatty acid composition of subcellular membranes after 3, 8 and 12 weeks of feeding rats with different oil enriched diets reported dynamic changes in cellular lipid composition over time (171). At first, a diet rich in linoleic acid but poor in α-linolenic acid caused a drastic decrease in n-3 fatty acid levels, but those levels recovered to values of the control group over the course of the 12 week feeding period. A cod liver oil diet, rich in n-3 PUFA, caused a great drop in n-6 PUFA levels but levels of linoleic acid slowly recovered whereas arachidonic acid levels remained constantly low. With the same diet, levels of DHA increased over time, but levels of oleic acid dropped slowly. By week 12, the double bond indices of all feeding groups, except for the cod liver oil group, were very similar, but at week 3 double bond indices of membranes obtained from rats fed with a lard, soybean or sunflower oil enriched diets were much lower than that of the control group. Such changes in fatty acid composition are not accompanied by changes in phospholipid headgroup distribution (172). Adaptation to changing fatty acid availability is hardly ever seen in short term cell culture studies, where usually only an increase in the percentage of the fatty acid that was supplemented with, is noted (155, 173). But the longer the supplementation period, the more a cellular adjustment to the additional fatty acid can be observed (174-177). In that respect, the Caco-2 model is of great advantage as cell monolayers are typically maintained for a long period of time. In general, a supplementation with n-3 PUFA will decrease the content of n-6 PUFA and vice versa and such effects are dose dependent (178-180). Exogenous fatty acid supply can inhibit endogenous synthesis (181). In the current study, a decrease in MUFA concentrations was observed in cells

supplemented with PUFA with a concomitant increase in the corresponding SFA levels. This is very likely due to a decrease in Δ^9-desaturase expression caused by the PUFA supplementation as has been described before (178, 182-184). Another metabolic pathway, which is usually not observed in cell culture studies, but was observed here, is the retro-conversion of DHA to EPA through peroxisomal β-oxidation (185). The fact that these cellular adaptations to fatty acid supplementation, which are typically only seen *in vivo*, were observed here, shows that chronic fatty acid supplementation of Caco-2 cultures is a good model to study the impact of fatty acid supplementation on enterocytes *in vitro*, despite the fact that there is only little turnover of EFA to HUFA. But this anabolic pathway is also not consistently observed in animal models, some studies do report an increase in HUFA after EFA feeding (186), but some do not (187). Perhaps, since in the current study different HUFA are supplied at low levels with the FBS, there are sufficient amounts available and therefore the cell is reluctant to waste ATP by producing more than necessary.

Since only the whole cell fatty acid composition was assessed, it was not possible to determine into which lipid classes the supplemented fatty acids were incorporated. Since the aim was to change membrane fluidity, it would be necessary for the supplemented fatty acid to be incorporated into the membrane phospholipid fraction. But since the accumulation of intracellular lipid bodies was observed, it cannot just be assumed that supplemented fatty acids were incorporated into phospholipids, but the possibility must be considered, that all additional fatty acids are simply stored in lipid droplets and no membrane modification has taken place.

Lipid droplet accumulation is a typical process in enterocytes of the small intestine in the postprandial phase. After a fat containing meal, high amounts of lipid are taken up and transiently stored in enterocytes in form of triacylglycerole droplets to prevent hyperlipidaemia. Over time, fatty acids are then slowly released from lipid droplets and excreted in form of lipoproteins or chylomicrons (75). *In vivo,* excreted lipid

particles are carried in the bloodstream to other organs where they are hydrolysed and fatty acids can be taken up and used. *In vitro* there are no vessels to take away lipoproteins between medium changes, so they accumulate in the basolateral medium and can be re-absorbed. In pig small intestinal explants, lipid droplets were observed in the basolateral cytoplasm of enterocytes, even without any lipid treatment, and addition of a pre-digested oil and bile salt mixtures resulted in formation of lipid droplets in the apical part of enterocytes within one hour (188). In cultured fibroblasts, lipid droplets could already be observed after five minutes of fatty acid exposure and volume and number of lipid bodies increased with prolonged incubation period (189). A nine day treatment of Caco-2 cells with palmitic, stearic or oleic acid also resulted in accumulation of triacylglycerols and all treatments resulted in the same level of lipid body accumulation, independent of acyl chain length and saturation (154). The core of lipid droplets mainly consists of neutral lipids (triglycerides and sterol esters) and is surrounded by a single, outer layer of phospholipids, mainly consisting of phosphatidylcholine. In published reports, where a similar experimental set-up, as used in the current study, was employed and where differential incorporation of supplemented fatty acids into phospholipid and neutral lipid fraction was analysed, the composition of both lipid classes was modified by exogenous fatty acid treatment. Not only SFA but also PUFA induced lipid droplet formation, but supplemented EPA and DHA were preferentially incorporated into phospholipids and less into triacylglyceroles (190). In lymphocytes, supplemented long chain fatty acids were incorporated into both phospholipids and neutral lipids. SFA were preferentially incorporated into neutral lipids e.g. treatment with stearic acid resulted in a rise of that fatty acid in the neutral lipid fraction from 15 % to 36 % and in the phospholipid fraction from 20 % to 30 %. PUFA were preferentially incorporated into phospholipids e.g. DHA rose from 1.3 % to 23 % in the phospholipid fraction and from 0.8 % to only 8 % in the neutral lipid fraction (191, 192). These studies, given here as an example of a number of reports on this topic,

lead to the conclusion that even though in the current study the fatty acid composition of phospholipids and neutral lipids was not analysed separately, it can be assumed that supplemented fatty acids, especially PUFA, were incorporated into the membrane phospholipid fraction and not only stored in lipid droplets.

As discussed above, short term *in vitro* incubations with fatty acids often only contain one specific type of lipid but with an incubation with 10 % FBS in medium, as was used here, there are about 100 µM of background lipids present. FBS is serum, which means the fatty acids it contains will mostly be esterified as triacylglycerols, phospholipids and sterolesters and present in form of lipoproteins and chylomicrons. Additionally supplemented fatty acids, on the other hand, are free fatty acids. Pazouki *et al*. analysed the lipid composition of FBS in detail and found that it contained mostly palmitic and stearic acid (both 130 µM) and also oleic acid (105 µM), arachidonic acid (32 µM), DHA (30 µM) and linoleic acid (13 µM). Of course these values will vary depending on the product's place of origin and the associated vegetation and perhaps animal breed. Nevertheless, concentrations of fatty acids reported by Pazouki *et al.* roughly correlate with the concentrations of fatty acids measured for one batch of FBS used in the current study. It was further reported that 78 % of FBS fatty acids exist in form of phospholipids, 6 % as triacylglycerols and 16 % as free fatty acids, though this distribution varied with different types of fatty acid. Only 47 % of palmitoleic acid were found in the phospholipid fraction, whereas 23 % occurred in triacylglycerols and 30 % as free fatty acids. Distribution of DHA showed a very different pattern, here 91 % were esterified as phospholipids, no DHA was found in the triacylglycerol fraction and 9 % occurred as free fatty acids. In general, serum PUFA were mainly present as part of phospholipids whereas triacylglycerols were entirely made up of myristic, palmitoleic, oleic and palmitic acid (193). It is important to know in which form those background fatty acids are present, since only free fatty acids and monoacylglycerols can be taken up by the cell. Since most fatty acids are not in a

freely available form, they will have to be hydrolysed in order to be taken up. *In vivo*, the activity of pancreatic lipase determines the hydrolysis of triacylglycerols in the small intestine, but in absence of this enzyme, endogenous lipolytic activity of enterocytes becomes crucial *in vitro*. As already mentioned above, Caco-2 cells do have the capacity to hydrolyse phospholipids and triacylglycerols, but the enzyme activity is much lower than *in vivo*. Therefore it can be assumed that the supplemented free fatty acids and those that stem from FBS have a greater impact on cell lipid composition than the esterified lipids. It has been reported that fatty acids were incorporated much more efficiently when bound to BSA in lipid free medium (27 - 37 % of supplemented fatty acid incorporated in 24 h) than in medium with 10% FBS (5 - 7 % of supplemented fatty acid incorporated in 24 h) (194). Another study, investigating competition between different fatty acids regarding cellular uptake and incorporation, found that increasing concentrations of background lipids had no impact on uptake of EPA or linoleic acid (195), which could indicate that it is not the lipid component of FBS that inhibits fatty acid uptake. They did however observe, that increasing amounts of background lipids affect the incorporation into different lipid classes. The higher the concentration of background lipids, the more of the fatty acid of interest was found in the neutral lipid fraction (195).

A great weakness of the current study is the low number of replicates that was analysed for lipid composition, due to very limited access to the analysis equipment. Because there were only two replicates per treatment group, the data could not be tested for normal distribution and no parametric test could be applied to determine statistical significance. Therefore Mann Whitney U test was chosen and due to the nature of this test, a p value of ≤ 0.05 cannot be reached with only five samples (three control and two test samples). However, even though only a statistical significance of $p \leq 0.1$ could be obtained here, most of the fatty acid changes have a large effect size, for example, with DHA treatment, the effect size for cellular DHA

content is $r = 0.775$. Replicates of cell samples that were analysed for lipid composition were not grown simultaneously, but a few weeks apart and often different batches of cells and fatty acid standards were used. Such a way of obtaining sample replicates probably resulted in an increased variance, but it indicates that the observed modulation of cell composition is reproducible. Together with the large effect size, this supports the credibility of the data.

Passive diffusion across a cell layer is dependent on partition of a compound between the membrane lipophilic core and the aqueous surrounding, which constitutes the rate limiting step for this mechanism of absorption. The degree of unsaturation (position and number of double bonds) of the acyl chains in the membrane core determines the packing density and strength of the lateral van der Waals attractions in that membrane region. Melting points of pure fatty acids reveal their packing density, which decreases from oleic acid ($T_m = 10°C$) to linoleic acid ($T_m = - 8°C$), α-linolenic acid ($T_m = - 10°C$), arachidonic acid ($T_m = - 49.5°C$), DHA ($T_m = - 44.5°C$) and EPA ($T_m = - 54.4°C$) (118). Exchanging fatty acids of the hydrophobic membrane core will result in a changed cohesion and fluidity. Membrane fluidity can be assessed using fluorescence probes that insert into the bilayer, mimicking membrane components. That way, the movement of molecules within the membrane can be investigated with different techniques, the most widely used being assessment of anisotropy using the fluorescence probes DPH or TMA-DPH. In the current study, experiments on plasma membrane fluidity were performed on isolated BBMV and not on whole cells. It has been reported that fluorescence polarisation of membrane probes in whole cells is strongly correlated with lipid body accumulation. Polarisation dropped drastically when lipid droplet formation was induced but when isolated membranes from cells with and without lipid bodies were used in the assay, no difference could be observed (196). Since lipid accumulation was observed in the current study, BBMV were used for measuring cell membrane fluidity, even though this approach could also result in

several inaccuracies. Isolated membranes can be perturbed during the isolation process and do not reflect the added structural stability that the cytoskeleton provides in whole cell assays. But apart from the interferences of lipid droplets, in whole cell assays the probe can also diffuse into other subcellular membranes and organelles, where a different lipid composition is prevalent, resulting in a difficult to interpret mixture of fluorescence signals (192). Membrane fluidity can change with cell differentiation (117, 197) and also with culturing conditions. For example, it has been shown that growing Caco-2 cells in high glucose medium results in an increase in membrane fluidity compared to cells grown in low glucose medium (198). Reports on the impact of *in vitro* incubation with fatty acids on membrane fluidity vary in their conclusion. For example, supplementing Caco-2 cells with EPA was once reported to have no effect on fluidity (199) and another time, under the same conditions, an increase in fluidity was observed (155). This variation could stem from the short incubation time of 24 h and 20 h respectively, or because whole cells were used for the assay. Other *in vitro* studies also do not report a change with short term fatty acid supplementations (192, 200), but in animal models, fatty acid feeding usually results in altered membrane fluidity. For example a diet with safflower oil rich in oleic and linoleic acid decreased fluorescence polarisation in rat synaptosomal membranes (201) and membrane anisotropy of rat urothelium plasma membrane exhibited a dose dependent, inverse correlation with the percentage of DHA present in the diet (202). Chronic fatty acid supplementation of Caco-2 cells resulted in a significant change in plasma membrane fluidity, similar to that observed in animal studies. These results again show that Caco-2 cells are a good model to study the impact of lipids on transport across the intestinal epithelium. But the question remains whether the observed changes in fluidity stem from the modification of phospholipid acyl chains or from other factors. Interestingly, the PUFA linoleic, α-linolenic and arachidonic acid have the opposite effect on fluidity as DHA and EPA. This behaviour could indicate that there are different mechanisms

that contribute to the overall impact of PUFA on fluidity. As already mentioned above, it is not only the fatty acid composition of membrane lipids that affects fluidity but also the cholesterol content and phospholipid headgroup distribution. It has been reported that fatty acid feeding does not change the abundance of different headgroups, but it was shown that PUFA can reduce cholesterol synthesis and increase cellular cholesterol efflux (203-207). Such reduced content of cholesterol in the plasma membrane will also have an impact on membrane fluidity. Which membrane component exactly is the cause for the observed change in fluidity cannot be determined from the present data, this would require a more in-depth analysis of membrane composition regarding content of different fatty acids and cholesterol.

Except for oleic acid, none of the fatty acids tested impaired cell viability; on the contrary, all PUFA even increased apparent viability as assessed by the MTT assay. This assay is based on the cellular uptake of a yellow tetrazolium salt and consequent intracellular reduction of the compound to a dark purple formazan product. An increase in product formation rate in this assay is usually interpreted as an increase in cell proliferation. However, in the case of the Caco-2 cell model, this interpretation is not plausible as by the time the assay is performed, cells are differentiated, no longer dividing and completely fill the available growth area. It is more likely that the supplemented fatty acid either has an impact on the reduction reaction itself or on the intracellular concentration of the substrate MTT. It is still not entirely clear which enzymes exactly are catalysing the formation of the formazan product. Early studies concluded that MTT is reduced by enzymes of the mitochondrial respiratory chain with succinate acting as the electron donor (208) and in rat tissue samples intracellular formazan crystals, co-localising with mitochondria, were observed (209). *In vitro* studies, using isolated mitochondria and selective inhibitors, revealed that the reduction of MTT occurs somewhere between ubiquinone binding to complex II and cytochrome c binding to complex IV within the

chain of reactions occurring at the inner mitochondrial membrane, but the exact mechanism is still unclear (210, 211). Later studies found that mitochondrial MTT reduction constitutes only a minor pathway and that cytosolic NADH and NADPH are much more potent electron donors in this reaction. In contrast to studies using subcellular fractions, performing the assay with whole cells showed that respiratory chain inhibitors had no impact on overall formazan production and most of the product was found in the cytosol (211, 212). Also formazan granules formed in the cytoplasm of HeLa cells were reported not to co-localise with lysosomes or mitochondria (213). Another study revealed that formazan production is not impaired in cell lines with dysfunctional mitochondria (214). Also it was shown that the assay is much dependent on the cell line used and also on culturing conditions, for example the concentration of glucose in the culturing medium and the presence of pyruvate or lactate (210). PUFA could have an impact on activity or expression of a cellular reductase, and in that way, increase its own turnover. One possible candidate for this reaction could be glutathione S-transferase which has been shown to reduce MTT *in vitro* (215) and which is induced by several PUFA (216). Another factor that could come into play here is the occurrence of intracellular lipid bodies with fatty acid treatment. It was reported that due to its hydrophobic nature, the formazan product specifically localises in lipid droplets and emits a higher intensity signal than when formed in the cytosol of cells that do not contain any lipid bodies (213). However, it is unlikely that the presence of lipid droplets contributes to the increase in apparent viability that was observed here, as this effect only occurred in cells treated with PUFA and it is unlikely that there was lipid droplet formation in cells treated with, for example, EPA but not in cells treated with stearic or palmitic acid. Also when the formazan product was extracted with organic solvent, the difference in intensity due to the hydrophobic environment of the lipid core would be lost, since all samples are dissolved in the same medium after extraction. A further potential impact on formazan production is the uptake or efflux of the substrate. The

MTT molecule in solution is very polar and also ionic. It is therefore highly improbable that this greatly hydrophilic molecule can cross the cell membrane simply by passive diffusion. Most likely the uptake will require a plasma membrane spanning transporter but it seems the identification of such has never been attempted. The only report on active transport of MTT has been concerning the possible impact of ATP-binding-cassette efflux transporters. The presence of selective inhibitors of ABCB1 and ABCC2 correlated with an increase in apparent viability measured by MTT assay. This increase could stem from the inhibition of active MTT efflux and consequent increased intracellular concentration of substrate (217). Since there is some evidence that PUFA can decrease expression and activity of ABCB1 (181, 218) such modulation of intracellular substrate concentration could also account for the increase in apparent viability observed in the current study.

In conclusion, it was shown that the chronic supplementation of Caco-2 cells, with fatty acids bound to FBS albumin, in medium with physiological glucose content, will result in a change in cell fatty acid composition. Chronic treatment does not impair cell viability but it does have an impact on plasma membrane fluidity. The model can therefore be employed to investigate the impact of dietary fatty acids on polyphenol absorption.

Chapter 4: Butyric acid increases transepithelial transport and metabolism of ferulic acid through upregulation of monocarboxylate transporters SLC16A1 and SLC16A4

4.1 Abstract

Ferulic acid is highly abundant in whole grain products where it is covalently linked to fibres of the plant cell wall. The free acid is released in the colon by microbial fermentation and taken up by the colon mucosa along with other metabolites produced by the intestinal microflora, especially short chain fatty acids (SCFA). Butyric acid is one of the three most abundant SCFA in the large intestine. Chronic treatment of intestinal Caco-2 cells resulted in increased expression of monocarboxylate transporters (MCT) 1 and 4, which have also been suggested as a pathway of ferulic acid absorption. Acute SCFA treatment only resulted in upregulated expression of MCT4. Both chronic and acute treatment increased transepithelial transport of ferulic acid in uptake but not in efflux direction. Chronic treatment also increased intracellular concentrations of ferulic acid, which in turn resulted in increased levels of ferulic acid metabolites. Immunofluorescence staining of cells revealed the uniform distribution of MCT1 protein in the cell membrane, whereas MCT4 was only detected in the lateral plasma membrane sections of Caco-2 cells. These results suggest a novel transport mechanism for ferulic acid across colonic enterocytes, which is that ferulic acid is taken up into the cytosol by MCT1 and transported out across the basolateral membrane by MCT4.

4.2 Introduction

As described in chapter 1, whole grain is a good source of ferulic acid and the free acid is released in the colon by microbial esterases. Therefore the main site of ferulic acid uptake from whole grain foods is the colon after fermentation by the colon microflora (46, 48). Fermentation of fibre also results in the production of large quantities of short chain fatty acids (SCFA). These fatty acids with a chain length of one to five carbon atoms together can reach concentrations of 30 to 100 mM in the colon (47, 219). One of the major SCFA produced is butyric acid. Butyric acid is absorbed in the large intestine either by passive diffusion of the free acid or via the apical uptake transporters monocarboxylate transporter 1 (MCT1) and sodium coupled monocarboxylate transporter (SMCT) (220, 221). MCT1 and SMCT transport SCFA by facilitated diffusion and co-transport of either protons, along the proton gradient created by the luminal pH of 6 to 7 (MCT1), or of sodium ions, along the sodium gradient maintained by basolateral sodium/potassium pumps (SMCT). SCFA constitute the major energy source for cells of the large intestine colonocytes (222, 223).

After synthesis of the nascent peptide chain into the ER, the MCT1 transporter is assembled as a heterodimer with the chaperone peptide CD147, also known as basigin. CD147 directs MCT1 insertion into the plasma membrane and the continued association of the two proteins is essential for ensuring functionality of the transporter. MCT1 can also bind to another chaperone called embigin, but CD147 is the preferred partner (224). There is no report of SMCT forming a similar complex (225)

Butyric acid has been associated with a broad range of beneficial health effects. It is reported to protect from colon cancer by induction of cell differentiation and apoptosis and it also has anti-inflammatory properties and protects the mucosa through stimulation of mucus secretion and tight junction integrity (226, 227). Some of these effects are mediated through increased concentrations of butyric acid in

colonic enterocytes caused by upregulated expression of MCT1 and its chaperone CD147 and consequent increased absorption (228-232). In the small intestine, which, compared to the colon, is only sparsely populated by bacteria, concentrations of SCFA are low and it is this difference in SCFA concentration that is believed to be the reason for the great difference in MCT1 abundance between the large and the small intestine (233).

In chapter 3 it was shown that dietary fatty acids are able to modulate the composition and some biophysical properties of Caco-2 cells. SCFA like butyric acid are much more abundant in the intestine than dietary fatty acids, but they are solely used for energy production and do not serve as building materials for membranes, and hence, will not change membrane composition. However, through their ability to upregulate transporter expression, they could still affect ferulic acid bioavailability as MCT1 and SMCT have also been suggested as a pathway of ferulic acid uptake (234, 235). It was therefore investigated whether there is a link between physiological butyric acid levels, as present in the colon, and the uptake of ferulic acid via MCT1 and SMCT, using the Caco-2 intestinal cell culture model.

4.3 Results

4.3.1 Impact of butyric acid pre-treatment of enterocytes on bidirectional transport of ferulic acid

The influence of increasing concentrations of butyric acid on ferulic acid transport was investigated using the intestinal Caco-2 cell culture model. Figure 4.1 shows that only the concentration of 1000 µM was able to significantly modulate ferulic acid transport in apical to basolateral direction (control: P_{app} = 9.0 cm/s, chronic 1000 µM butyrate: P_{app} = 11.4 cm/s). Chronic butyric acid supplementation had a greater effect than acute butyric acid treatment

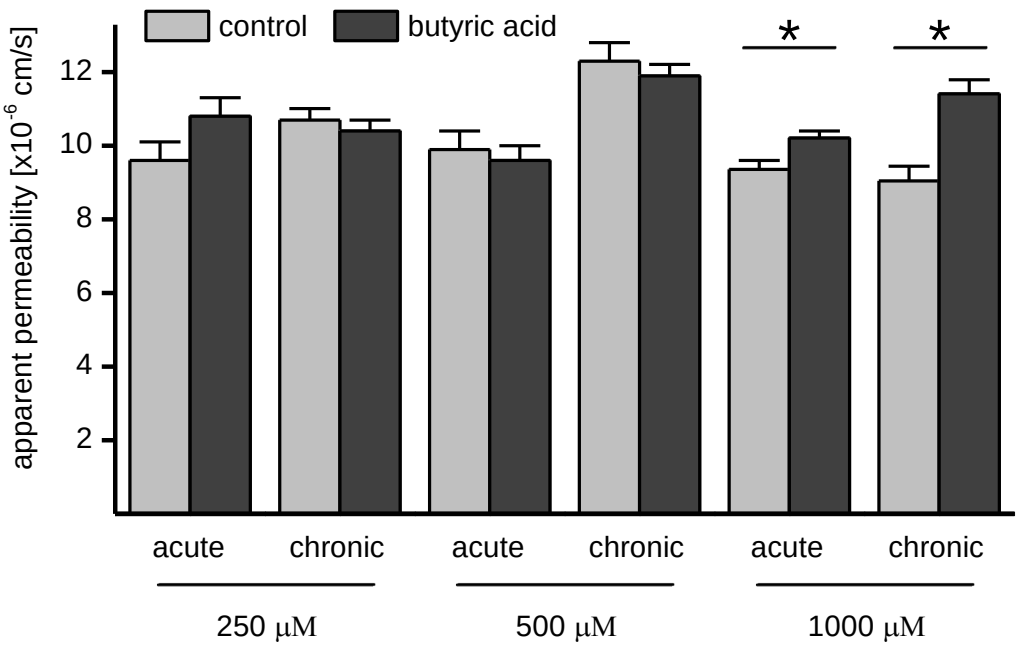

Figure 4.1; Impact of supplementation of Caco-2 cells with different concentrations of butyric acid on transepithelial transport of ferulic acid (500 µM) in apical to basolateral direction. Cells were either incubated for their entire differentiation time of 21 days (chronic) or for 24 h starting at day 20 after seeding (acute). Butyric acid was dissolved in ethanol (final concentration 0.5% for 250 and 1000 µM and 1% for 500 µM butyric acid before addition to 10 % FBS medium. Controls were incubated with the corresponding amount of ethanol for the corresponding time. The pH of the transport solution was 7.4 in both receiver and acceptor chamber. n = 6, N = 1; * = $p \leq 0.05$, For conditions and analysis see sections 2.3, 2.4 and 2.6.

In the next step, transport in apical to basolateral ($J_{a \rightarrow b}$) direction was compared to transport in efflux basolateral to apical ($J_{b \rightarrow a}$) direction after chronic supplementation of Caco-2 cells with 1000 µM butyric acid (figure 4.2).

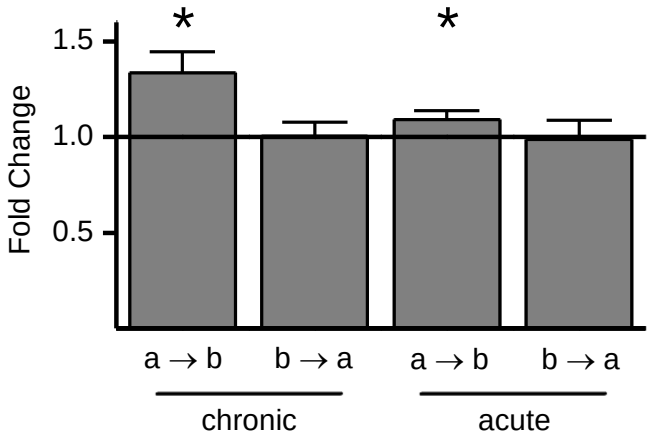

Figure 4.2; Butyric acid treatment only affects ferulic acid (500 µM) transport in $J_{a\rightarrow b}$ direction (apical to basolateral) not in $J_{b\rightarrow a}$ direction (basolateral to apical). Cells were either incubated for their entire differentiation time of 21 days (chronic) or for 24 h starting at day 20 after seeding (acute). n = 6, N = 1; * = $p \leq 0.05$; For conditions and analysis see section 2.3, 2.4 and 2.6.

Butyric acid only increased transport in the uptake direction, whereas efflux of ferulic acid was unaffected.

Ferulic acid has been described to be mainly taken up by passive diffusion and, as a minor pathway, also by facilitated diffusion via MCT1. A directional change in transport as shown in figure 4.2 does not support a change in passive diffusion but instead it suggests that the transport via MCT1 is increased by the butyric acid treatment. This hypothesis was tested by performing transport experiments in the uptake direction in the presence and absence of the MCT1 inhibitor phloretin, after chronic supplementation of Caco-2 cells with 1000 µM butyric acid (figure 4.3).

A

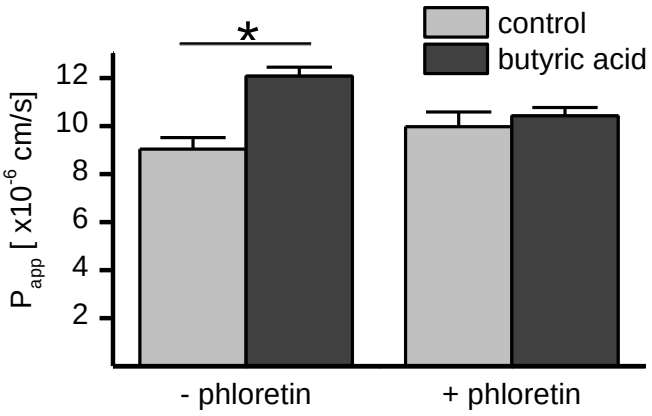

B

treatment 1	treatment 2	p-value
b- p-	b- p+	1
b+ p+	b- p+	1
b+ p+	b- p-	0.416
b+ p-	b- p+	0.057
b+ p-	b- p-	0.002
b+ p-	b+ p+	0.192

Figure 4.3; **A** Impact of MCT inhibitor phloretin (300 µM), applied to both sides of the cell monolayer, on apical to basolateral transport ($J_{a\rightarrow b}$) of ferulic acid (500 µM) across chronically butyric acid (1000 µM) supplemented Caco-2 monolayers. n = 6, N = 1; * = $p \leq 0.05$, **B** Statistical significance between treatment groups analysed with one-way ANOVA. b- = no butyric acid, b+ = butyric acid supplemented, p- = no phloretin, p+ = phloretin supplemented. For conditions and analysis see sections 2.3, 2.4 and 2.6.

The presence of 300 µM phloretin abolished the effect of butyric acid pre-treatment, indicating that MCT1 is involved in the ferulic acid transport increase.

According to the literature, MCT1 is located in the apical membrane of Caco-2 cells, facilitating transport from the apical lumen to the cytosol. Such localisation would explain the asymmetrical impact of butyric acid on transport. In consequence, there should be an increase in intracellular ferulic acid concentration when uptake transport is assessed, but no change with efflux transport. However, when intracellular ferulic acid concentrations were analysed, a very different picture emerged (figure 4.4).

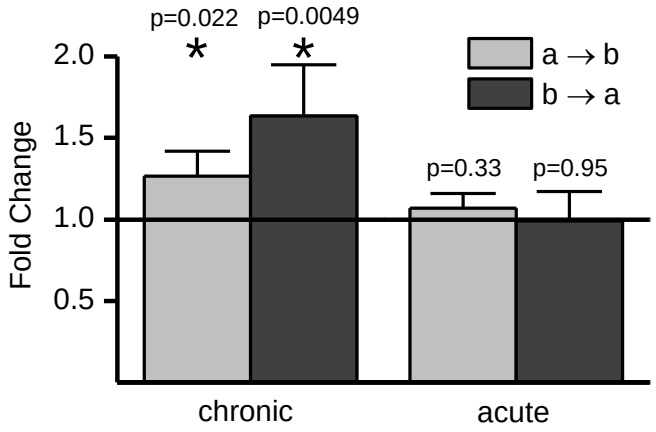

Figure 4.4; Changes in intracellular ferulic acid concentrations induced by chronic and acute butyric acid supplementation. The extracellular concentration of ferulic acid was 500 µM. n = 6, N = 1; For conditions and analysis see sections 2.3, 2.4 and 2.7.

Ferulic acid concentrations were higher when 500 µM of the compound were applied from the basolateral side (111 ± 12 µM), than when applied from the apical side (70 ± 5 µM) and butyric acid treatment increased intracellular concentrations with transport in both directions. The increase even was much higher in efflux direction (+ 63 %) than in uptake direction (+ 26 %). Acute butyric acid treatment did not change intracellular ferulic acid concentrations.

4.3.2 Impact of butyric acid on metabolism of ferulic acid

To explore the impact of butyric acid on ferulic acid transport further, it was investigated whether the change in intracellular ferulic acid concentrations, shown in figure 4.4, is also reflected in the metabolism of ferulic acid, since increasing intracellular concentrations of the aglycone would constitute an increase in substrate availability for metabolising enzymes.

To achieve this, an LC-MS/MS method was developed to quantify the three main ferulic acid metabolites in Caco-2 cells, feruloyl-glucuronide, feruloyl-sulfate and dihydroferulic acid. Metabolite traces in cell culture samples were identified and

concentration was assessed by comparison to original standards. Example chromatograms of standards are shown in figure 4.5.

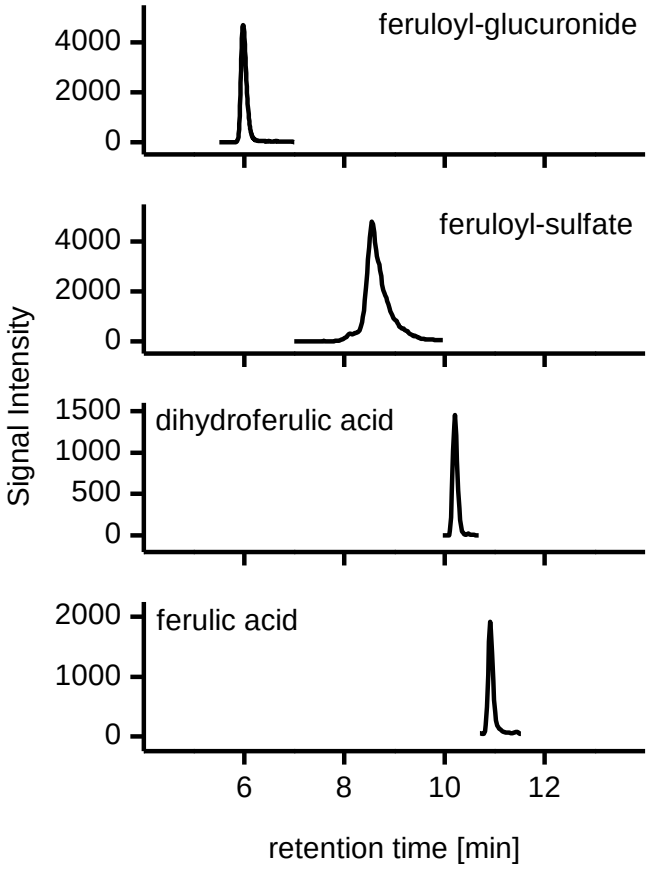

Figure 4.5; Chromatogram of ferulic acid metabolite standards analysed by LC-MS/MS. All standards were injected at a concentration of 1000 µM. Ion traces shown: feruloyl-glucuronide m/z = 369 → 113; feruloyl-sulfate m/z = 273 → 178; dihydroferulic acid m/z = 195 → 121; ferulic acid m/z = 193 → 178. For details see section 2.7.

After transport experiments, samples were taken from the apical and basolateral chamber and the Caco-2 cell layer was washed, lysed, collected and analysed. Concentrations obtained by LC-MS/MS analysis were adjusted for the original volume of the sample (2000 µL for apical and basolateral, 7 µL for cell lysate samples, see chapter 2.4).

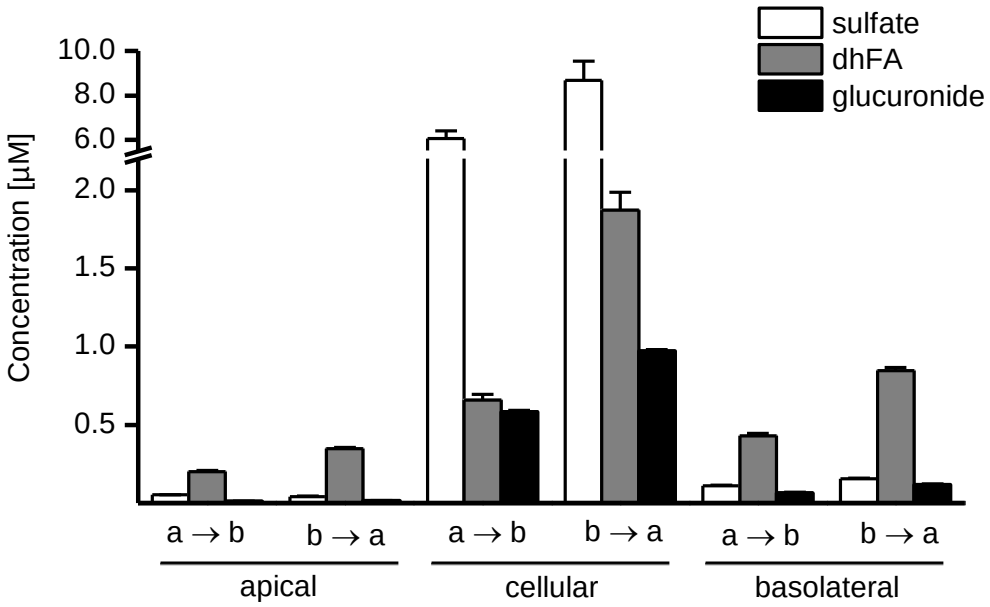

Figure 4.6, Ferulic acid metabolism by Caco-2 cells. Concentration of metabolites detected in apical, basolateral and cell lysate samples after ferulic acid (500 µM) transport in uptake (a → b) or efflux (b → a) direction. n = 6, N = 1; For details on conditions, analysis and calculation see sections 2.4 and 2.7.

All metabolites were more abundant in the basolateral than the apical well (two-way ANOVA analysis: apical $c_{a\rightarrow b}$ vs. $c_{b\rightarrow a}$ $p = 0.013$, cellular $c_{a\rightarrow b}$ vs. $c_{b\rightarrow a}$ $p = 0.033$, basolateral $c_{a\rightarrow b}$ vs. $c_{b\rightarrow a}$ $p = 0.009$) but the highest concentrations were found intracellularly (see section 2.7 for calculation of intracellular concentrations). Dihydroferulic acid was the most abundant metabolite in the donor and acceptor chamber but intracellularly the most abundant metabolite was ferulic acid sulfate, reaching high concentrations of up to 9 µM. In general, metabolite concentrations were higher when ferulic acid was applied to the basolateral side (b → a) than when ferulic acid was applied to the apical side (a → b). In that respect, metabolite levels correlated with intracellular ferulic acid levels.

Figure 4.7 shows the changes in metabolite levels induced by chronic butyric acid supplementation, figure 4.8 shows changes induced by acute treatment. Overall, chronic butyric acid supplementation had a high impact on metabolism, acute treatment only very little.

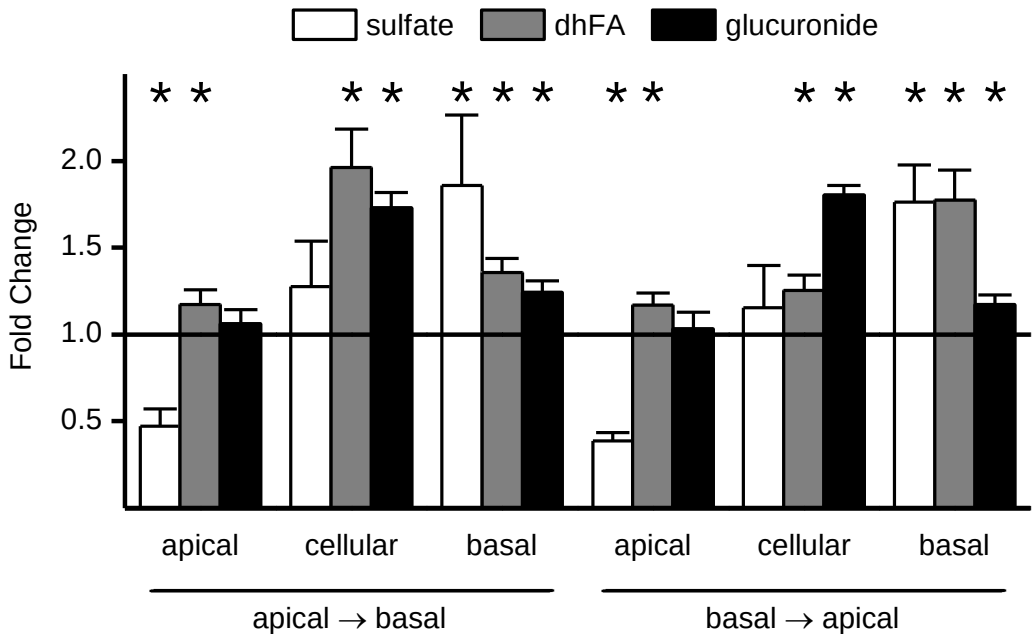

Figure 4.7, Ferulic acid metabolism by Caco-2 cells. Change in metabolite formation after chronic butyric acid (1000 µM) treatment. Ferulic acid metabolite content was analysed in apical, basolateral and cell lysate samples after ferulic acid (500 µM) transport in uptake (apical → basal) or efflux (basal → apical) direction. n = 6, N = 1; * = $p \leq 0.05$ according to ANOVA analysis; For details see sections 2.3, 2.4 and 2.7.

With chronic butyric acid supplementation, levels of all metabolites increased, except for feruloyl-sulfate, where apical levels decreased but intracellular and basolateral levels also increased (figure 4.7). Overall abundance of the glucuronide and of dhFA increased significantly (glucuronide: $J_{a\rightarrow b}$ p = 0.0141, $J_{b\rightarrow a}$: p = 0.0142; dhFA: $J_{a\rightarrow b}$ p = 0.008, $J_{b\rightarrow a}$ p = 0.011) with butyric acid supplementation but there was no overall increase in sulfate conjugates ($J_{a\rightarrow b}$ p = 0.216 $J_{b\rightarrow a}$ p = 0.334) with butyric acid supplementation. Acute supplementation only increased ferulic acid sulfate levels on the basolateral side, increased dihydroferulic acid on the apical

side, when ferulic acid was applied apically, and decreased cellular levels of ferulic acid glucuronide when applied basolaterally (figure 4.8).

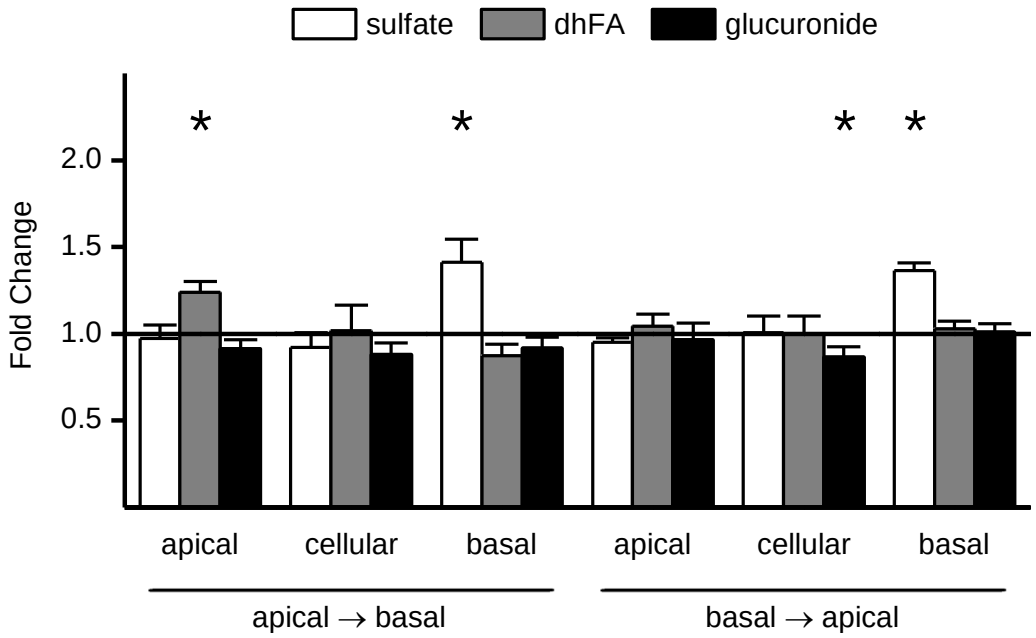

Figure 4.8, Ferulic acid metabolism by Caco-2 cells. Change in metabolite formation after acute butyric acid (1000 µM) treatment. Ferulic acid metabolite content was analysed in apical, basolateral and cell lysate samples after ferulic acid (500 µM) transport in apical → basal ($J_{a\rightarrow b}$) or basal → apical ($J_{b\rightarrow a}$) direction. n = 6, N = 1; * = $p \leq 0.05$; For details see sections 2.3, 2.4 and 2.7.

4.3.3 Butyric acid impact on transporter expression

As mentioned above, it has previously been reported that butyric acid increases expression of MCT1 and transport experiments with phloretin indicated that a change in MCT1 activity or abundance is responsible for the increase in ferulic acid absorption. Therefore, the impact of chronic and acute butyric acid supplementation on MCT1 gene expression in the Caco-2 model was tested. As phloretin is not only an inhibitor of MCT1 but also of other MCT isoforms, the second and third most abundant MCT isoforms in the colon, MCT4 and MCT5, were also investigated, as well as SMCT which has also been suggested to play a role in ferulic acid transport.

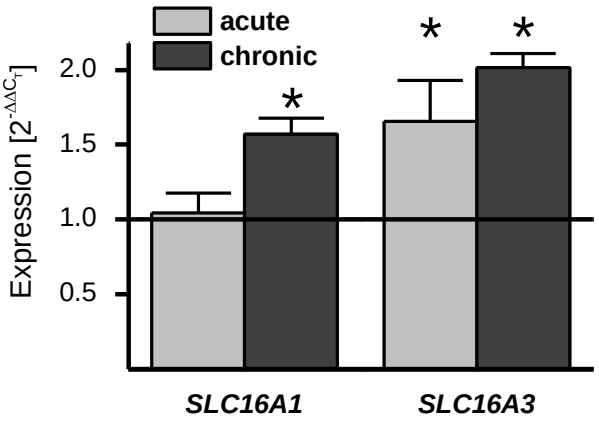

Figure 4.9; Impact of chronic and acute 1 mM butyric acid supplementation on gene expression of SLC16A1 (MCT1) and SLC16A3 (MCT4) in Caco-2 cells. n = 5, N = 1; * = $p \leq 0.05$; For details see sections 2.3 and 2.8.

Figure 4.9 shows the impact of butyric acid treatment on MCT1 and MCT4 expression. MCT1 was upregulated by chronic but not acute treatment whereas MCT4 was upregulated by chronic as well as acute treatment. MCT5 was not affected by chronic butyric acid supplementation. No SMCT mRNA could be detected in Caco-2 cells. The fact that MCT1 was not upregulated with acute treatment but MCT4 was and that with acute treatment there was also an increase in ferulic acid transport indicates that not only MCT1 but also MCT4 is involved in ferulic acid transport.

To detect localisation of those two transporters, indirect immunofluorescence staining of Caco-2 monolayers was carried out. Figure 4.10 shows differentiated Caco-2 cells stained for MCT1 and figure 4.11 shows cells stained for MCT4.

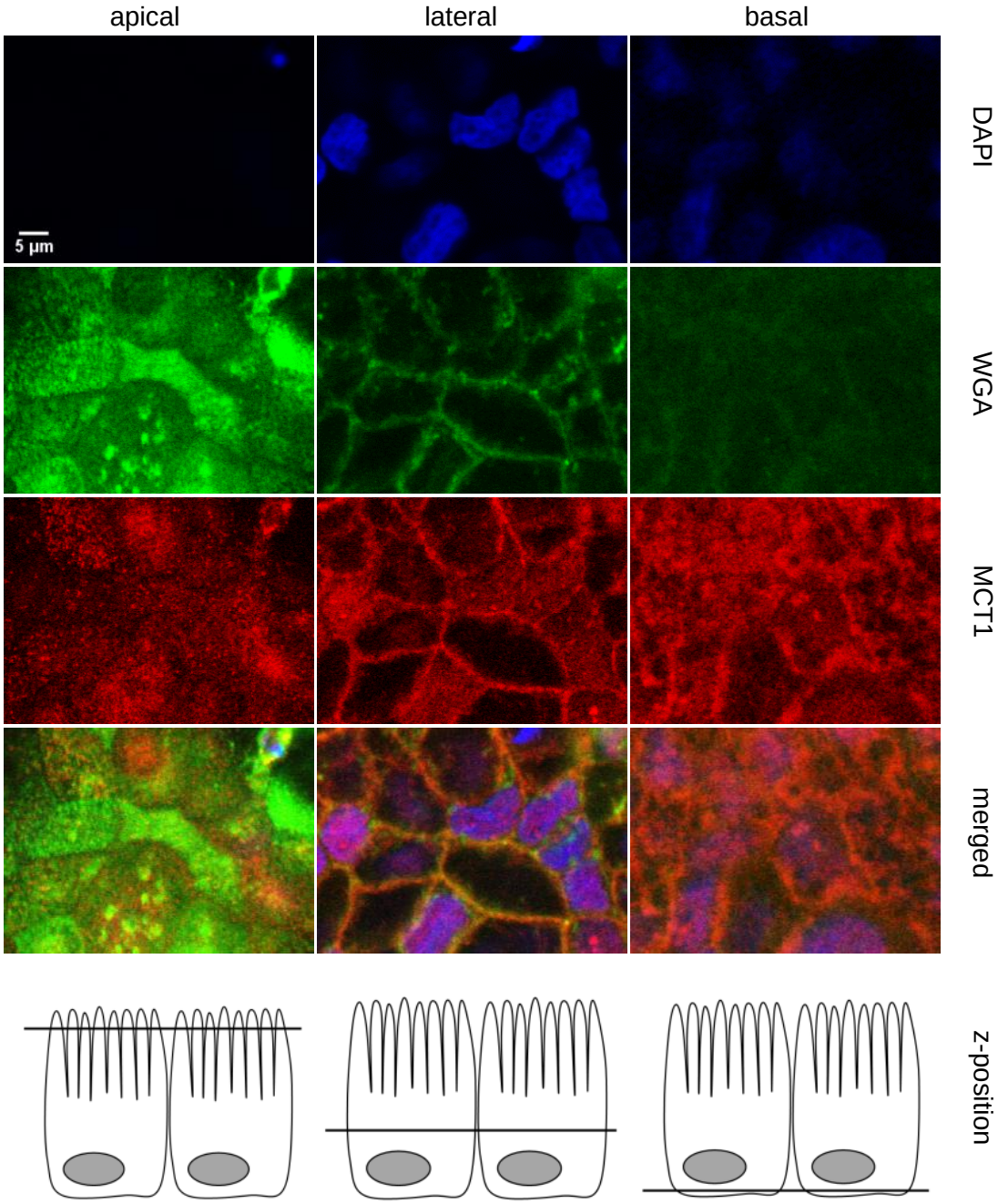

Figure 4.10; Indirect immunofluorescence detection of MCT1 in differentiated Caco-2 monolayers. Cells were incubated with DAPI, membrane marker wheatgerm agglutinin (WGA) and mouse anti-hMCT1 primary antibody and Cy3-conjugated donkey anti-mouse secondary antibody. MCT1 is shown in red, appearing orange when co-localising with WGA shown in green and appearing purple when co-localising with DAPI shown in blue. n = 3, N = 1; For details see sections 2.3 and 2.10.

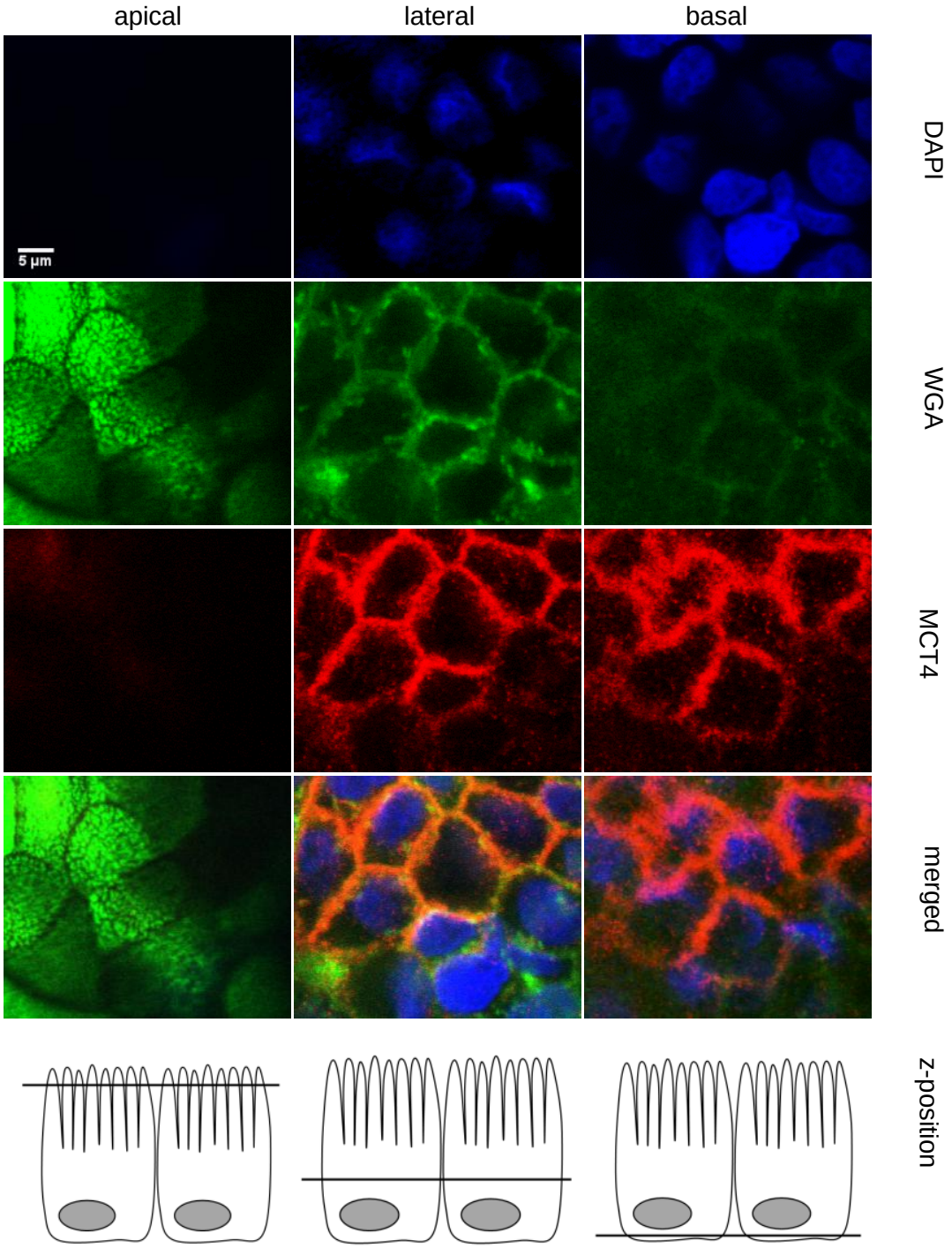

Figure 4.11; Indirect immunofluorescence detection of MCT4 in differentiated Caco-2 monolayers. Cells were incubated with DAPI, membrane marker wheatgerm agglutinin (WGA) and mouse anti-hMCT4 primary antibody and Cy3-conjugated donkey anti-mouse secondary antibody. MCT4 is shown in red, appearing orange when co-localising with WGA shown in green. n = 3, N = 1; For details see sections 2.3 and 2.10

MCT1 (in red) was detected in the plasma membrane on the apical, lateral and basal side, co-localising with the plasma membrane marker WGA (shown in green, appearing orange in the merged fluorescence images when co-localising with red MCT1). The signal intensity of MCT1 detected in the apical plasma membrane varied between cells. Such an effect could either stem from a heterogeneous cell population with different MCT1 expression levels or from the fact that cells did not grow to exactly the same height. This means that some cells are in the plane of focus, and appear brighter than others that are not. MCT1 was also detected in the nuclear envelope co-localising with DAPI (shown in blue, appearing purple in merged images when co-localising with red MCT1). MCT4 was almost exclusively localised in the lateral plasma membrane with only very low signal originating from the apical and basal membrane. No intracellular MCT4 signal could be observed.

To investigate whether the changes in metabolite concentrations detected in the apical well could stem from an impact of butyric acid on the expression of apical efflux transporters, mRNA levels of the most abundant apical ATP-binding cassette transporters, that were described to recognise xenobiotics and phase II metabolites as allocrites in Caco-2 cells (discussed further in chapter 6), ABCB1, ABCC2 and ABCG2 where investigated (figure 4.11).

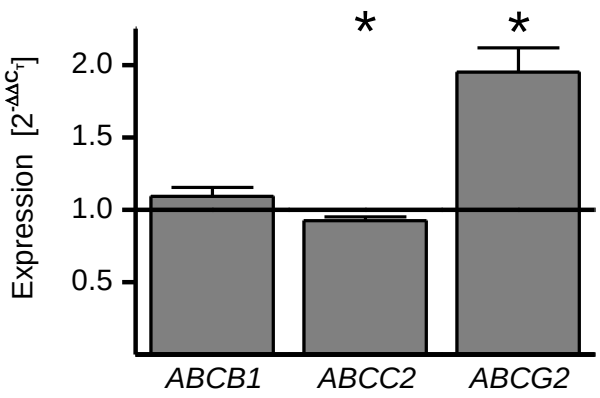

Figure 4.12; Impact of chronic and acute 1 mM butyric acid supplementation on gene expression of ABC-efflux transporters in Caco-2. n = 4, N = 1, * = $p \leq 0.05$; For details see sections 2.3 and 2.8.

Gene expression of ABCG2 was greatly increased after long term butyric acid treatment whereas ABCC2 expression was slightly reduced. ABCB1 expression was not affected.

4.4 Discussion

MCT1 was shown to act either as a symporter, facilitating proton coupled transport of monocarboxylates, or as an antiporter exchanging one monocarboxylate against another without proton movement (224). *In vivo*, such proton coupled transport in the small intestine is driven by the acidic microclimate of pH 6.1 to pH 6.8 in the unstirred water layer at the surface of the brush border (236). This acidic microclimate is sometimes simulated in Caco-2 transport studies by using an apical incubation buffer with the corresponding lower pH, but such set-up was not employed in the current study. MCT1 expression has been reported to increase in the presence of the short chain fatty acid butyric acid, a microbial metabolite reaching high concentrations of up to 25 mM in the colon (219). In the current study it was shown that pre-treatment of intestinal Caco-2 cells with butyric acid resulted in increased transepithelial transport of ferulic acid, an effect that was abolished when the MCT inhibitor phloretin was added to the transport buffer on both sides of the cell monolayer. It has been suggested that ferulic acid is an allocrite of MCT1, and in the current study, upregulation of MCT1 by chronic butyric acid supplementation did correlate with an increase in ferulic acid uptake into the cell. However, ferulic acid transport across the cell monolayer was increased even when MCT1 expression was not, suggesting that it is not only MCT1 that facilitates ferulic acid transport. Another transporter that was upregulated by butyric acid treatment is MCT4, which can also be inhibited by phloretin and which is highly expressed in the colon and in Caco-2 cells (220, 237, 238). It therefore seems that either MCT4 on its own, or both MCT1 and MCT4 together, is the underlying cause of the effect observed here related to butyric acid treatment. Immunofluorescence staining of Caco-2 cells revealed the presence of MCT4 solely in the lateral plasma membrane and the presence of MCT1 in all parts of the plasma membrane, but with the strongest signal originating from the basal membrane.

Taken together, these results suggest the following mechanism: ferulic acid, applied to either the apical or basolateral side, is taken up into the cell by MCT1, which is more abundant after chronic butyric acid treatment, resulting in increased intracellular concentrations of the aglycone. After acute butyric acid treatment, there is no increase in intracellular concentration, as MCT1 expression is unchanged. MCT1 is only able to import ferulic acid into the cell, as there is no increase in ferulic acid transport to the apical side after chronic supplementation with butyric acid, even though MCT1 is also localised in the apical plasma membrane and it's expression is upregulated. MCT4, on the other hand, only exports ferulic acid from the cytosol to the basolateral side and not in the reverse direction, as intracellular ferulic acid concentrations are unchanged when the aglycone is applied to the basolateral side after acute butyric acid treatment, even though MCT4 is upregulated. The lack of MCT4 in the apical plasma membrane has the consequence that only apical to basolateral transport is affected by butyric acid and not basolateral to apical transport. However, this observation, that MCT1 only imports and MCT4 only exports ferulic acid, disagrees with the idea that both transporters can translocate monocarboxylates in and out of the cell, only depending on the concentration gradient of the allocrite (239). However, bidirectional transport by MCT1 and MCT4 has mostly been investigated in non-differentiating cell lines and oocytes using small endogenous compounds like lactic acid, which might have different transport kinetics than larger phenolics like ferulic acid. Also, the asymmetrical nature of MCT facilitated transport in Caco-2 cells has been observed previously. Neuhoff *et al.* found that the transport of salicylic acid, another substrate of MCT1, could be inhibited by phloretin in the apical to basolateral transport direction, but not in the basolateral to apical direction (240).

The increase in metabolism of ferulic acid, after chronic but not acute butyric acid treatment, confirms the observations from transport experiments. As the upregulation of MCT1 with chronic treatment resulted in increased intracellular

ferulic acid concentrations, the formation rate of ferulic acid metabolites was also increased, as there were higher levels of substrate available. Using human intestinal S9 homogenates, the K_m for the formation of ferulic acid glucuronide was recently determined as 4610 ± 100 µM and the K_m for the formation of ferulic acid sulfate was 62.9 ± 7.2 µM (143). This data could explain why an increase in intracellular ferulic acid concentration by butyric acid treatment from 70 µM to 89 µM did not significantly increase the overall amount of sulfoconjugate, but had a significant impact on the formation of ferulic acid glucuronide. Since it is not known which enzyme catalyses the formation of dhFA, no pharmacokinetic data is available on that. The export of ferulic acid sulfate to the apical side was decreased with chronic butyric acid supplementation. This could be due to decreased expression of the apical efflux transporter ABCC2, indicating that ferulic acid sulfate is an allocrite of ABCC2. ABCG2 is strongly upregulated with butyric acid treatment, which might also contribute to the increase in metabolite concentrations in samples collected from the apical reservoir.

With acute butyric acid treatment no increase in metabolite levels was observed, because without upregulation of MCT1, there is no increase in the intracellular concentration of ferulic acid. Only sulfate transport to the basolateral side was enhanced, which could be the result of an impact of butyric acid on a basolateral efflux transporter, maybe also of the ABCC family.

Reports on the intestinal localisation of MCT1 vary in their conclusion. The transporter was found in the apical membrane of Caco-2 cells (241) and once almost exclusively in the apical (237) and once entirely in the basolateral (242) membrane of enterocytes of the human large intestine. It was observed in the apical membrane of pig (243) and rat (232), but in the basolateral membrane of hamster (244) and cow (245) colon enterocytes. In the current study, MCT1 was found to be uniformly distributed in Caco-2 cells. MCT4 on the other hand, has only been reported to localise in the basolateral membrane of human mucosal cells (237) and

was also only detected in the basolateral membrane here. A possible explanation for this variation in reports on MCT1 but not MCT4 localisation has recently been addressed and the authors suggested that the answer might lie in the ability of different tissues to recognise certain targeting signals in the nascent protein. Both MCT1 and MCT4 are associated with the chaperone protein CD147. CD147 knock down studies have shown that without the chaperone CD147 neither MCT1 nor MCT4 will localise in the plasma membrane, but instead those transporters accumulate in the Golgi, which indicates that MCT1 and MCT4 are dependent on CD147 for correct membrane targeting (246, 247). MCT4 contains a strong C-terminal sorting signal, targeting the protein to the basolateral membrane of epithelial cells. MCT1, on the other hand, does not contain any sorting signal but CD147 does. It has a strong targeting sequence for basolateral sorting, as well as a weak apical targeting signal. Through the tight association between MCT1 and CD147, MCT1 localisation is determined by the localisation of CD147. In tissues that recognise the basolateral targeting motif, CD147 and MCT1 will be inserted into the basolateral membrane, in tissues that do not recognise this sequence, they will be localised in the apical plasma membrane. CD147 is a highly glycosylated protein and it has been suggested that the degree of glycosylation in different tissues may play a role in its apical or basolateral targeting (248-250).

SMCT has also been proposed to facilitate ferulic acid transport and expression of the transporter at the mRNA level has been described for Caco-2 cells (230). In contrast to that, there was no SLC5A8 (SMCT) mRNA detected in the current study. The silencing of SLC5A8, in the Caco-2 batch used in the experiments described here, could be related to reports of SLC5A8 silencing in other colon cancer cell lines. Exon 1 of SLC5A8 was found to be hypermethylated in over 50% of primary colon cancers, adenomas and colon cancer cell lines, resulting in non-transcription of the gene (251). As the Caco-2 cell line is derived from colon adenoma, perhaps the same has happened here.

In summary, results described in this chapter demonstrate that short chain fatty acids produced by the colon microflora can influence the absorption of polyphenols and that not MCT1 but MCT4 expression might be crucial for transepithelial transport of ferulic acid in the colon. Moreover, butyric acid increased the amount of ferulic acid metabolites that were produced. Human studies on the pharmacokinetics of ferulic acid and it's metabolites have shown that the concentration of metabolites in plasma is higher than the concentration of the aglycone and also that metabolites have a longer half life than the aglycone (252). Therefore butyric acid could enhance the bioavailability of ferulic acid, and with that, increase the potential of positive health effects.

Chapter 5: Impact of chronic fatty acid supplementation on transepithelial transport of phenolic acids

5.1 Abstract

In this chapter, supplementation of the Caco-2 cell model with fatty acids was employed to identify a possible impact of dietary lipids on caffeic and ferulic acid transport. Chronic supplementation with PUFA increased uptake of both phenolics. Caffeic acid permeation correlated with permeation rates of the paracellular transport marker lucifer yellow. The increase in ferulic acid transport neither correlated with permeation rates of the paracellular marker nor with plasma membrane fluidity changes. Passive transcellular diffusion of metoprolol and hesperetin was also unaffected by lipid treatment. Ferulic acid uptake was only increased in the apical to basolateral but not in the basolateral to apical direction, which indicates the involvement of a transporter mediated pathway. Phloretin, an inhibitor of MCT, did not affect DHA-induced increase in transport, but estrone-3-sulfate lowered permeation rates of ferulic acid across fatty acid treated and untreated Caco-2 cells. Transport to the basolateral side was decreased by estrone-3-sulfate but intracellular ferulic acid concentrations were unchanged and DHA also had no significant impact on intracellular ferulic acid concentrations. Both DHA and estrone-3-sulfate affected metabolism of ferulic acid, but not due to changes in aglycone transport but by direct impact on the activity of the metabolising enzymes. In conclusion, caffeic acid transport is affected by dietary fatty acids through an increase in paracellular absorption and ferulic acid uptake through impact on an unidentified transporter.

5.2 Introduction

In chapter 4, the transporter-mediated component of ferulic acid absorption in the large intestine, where high levels of SCFA induced enhanced expression of MCT, was investigated. In the small intestine, where MCTs are less abundant, passive diffusion is reported to constitute the major route of uptake (135, 234). In chapter 3 it was shown that chronic supplementation of Caco-2 cells with different dietary fatty acids would modulate plasma membrane fluidity. For many *in vitro* studies with membrane vesicles and model organisms, it has been reported that lipid composition and fluidity are crucial factors determining passive diffusion (113, 253-256). For example, in yeast mutant strains, differing in plasma membrane fluidity, drug uptake through passive diffusion correlated with that parameter (257). In animal models, PUFA feeding and incorporation into plasma cell membranes resulted in decreased uptake of the passive transcellular diffusion marker diazepam (181). This chapter explores the impact of dietary lipids on transepithelial transport and metabolism of the coffee phenolics caffeic and ferulic acid *in vitro*.

5.3 Results

5.3.1 Impact of chronic fatty acid treatment on transepithelial transport of phenolic acids

The results described in chapter 3 indicated that the cellular fatty acid content can be modified by addition of free fatty acids to FBS-containing medium and that chronic treatment results in greater changes than acute treatment. Therefore, to screen for the impact of different fatty acids on the transepithelial transport of phenolics in the intestinal Caco-2 model, chronic supplementation was used. Figure 5.1 shows the effect of fatty acid treatment on absorption of caffeic acid and ferulic acid.

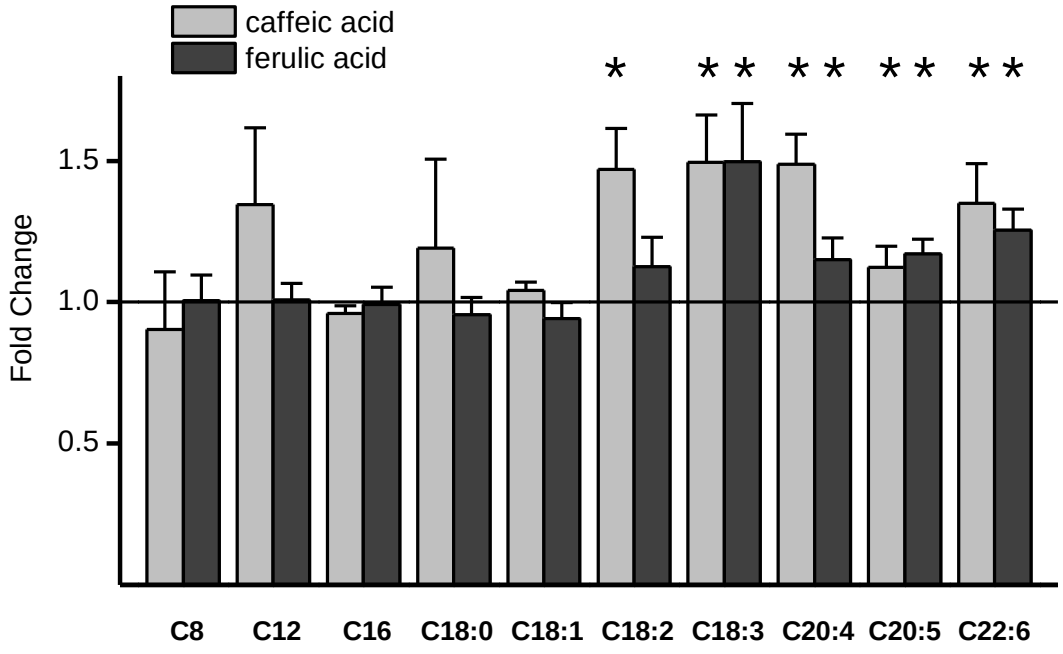

Figure 5.1; Impact of dietary fatty acids on absorption of phenolic acids. Transport of caffeic and ferulic acid (both 500 µM) across chronically fatty acid supplemented (50 µM) Caco-2 monolayers was assessed. For details on transport and analysis see sections 2.3, 2.4 and 2.6. C8 = octanoic acid, C12 = lauric acid, C16 = palmitic acid, C16:1 = palmitoleic acid, C18:0 = stearic acid, C18:1 = oleic acid, C18:2 = linoleic acid, C18:3 = linolenic acid, C20:4 = arachidonic acid, C20:5 = EPA, C22:6 = DHA; n = 6, N = 1; * = $p \leq 0.05$

A similar pattern of transport changes was observed for both phenolic acids. Neither medium chain nor long chain SFA had an impact on transport. Only supplementation with PUFA increased the transepithelial transport. A-linolenic acid, arachidonic acid, EPA and DHA increased caffeic as well as ferulic acid transport, whereas linoleic acid significantly increased caffeic acid transport only.

The fact that both caffeic and ferulic acid transport is increased with the same treatment suggests that both changes in transport rate are the result of PUFA affecting the same mechanism. Caffeic acid is thought to cross the intestinal epithelium by paracellular diffusion only, whereas ferulic acid is mainly transported up by passive diffusion and also by facilitated diffusion via MCT, as described in chapter 4. To investigate the mechanism further, supplementation with the PUFA DHA was selected. Figure 5.2 shows the apparent permeability of the two phenolics acids in comparison to the paracellular transport marker lucifer yellow.

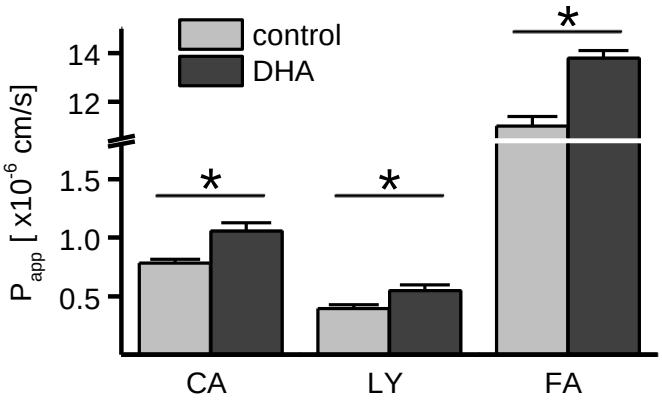

Figure 5.2; Impact of chronic DHA supplementation on apical to basolateral transepithelial transport of caffeic and ferulic acid (both 500 µM) and lucifer yellow (100 µM) across Caco-2 monolayers. For details on transport and analysis see sections 2.3, 2.4 and 2.6. n = 6, N = 1; * = $p \leq 0.05$

Caffeic acid (MW = 180 g/mol) and lucifer yellow (MW = 457 g/mol) have very similar permeation rates of 0.8 x 10^{-6} cm/s and 0.4 x 10^{-6} cm/s respectively, whereas the permeation rate of ferulic acid (MW = 194 g/mol) is considerably higher at

11 x 10^{-6} cm/s. Treatment with the PUFA DHA increased transport of both caffeic acid and lucifer yellow by 0.3 x 10^{-6} cm/s and transport of ferulic acid by 3 x 10^{-6} cm/s. That means the increase in permeability of ferulic acid alone is eight times higher than the overall transport rate of the paracellular marker lucifer yellow. It is very unlikely that such high transport rates as observed for ferulic acid could stem from paracellular diffusion, especially since there is no decrease in TEER with DHA treatment (see chapter 3, figure 3.9) and yet there is such a great change in permeability of the compound. To test whether a change in tight junction integrity could affect the transport rate of ferulic acid in such a way, differentiated Caco-2 cell monolayers were treated with methyl-β-cyclodextrin to decrease plasma membrane cholesterol content and reduce tight junction integrity (258).

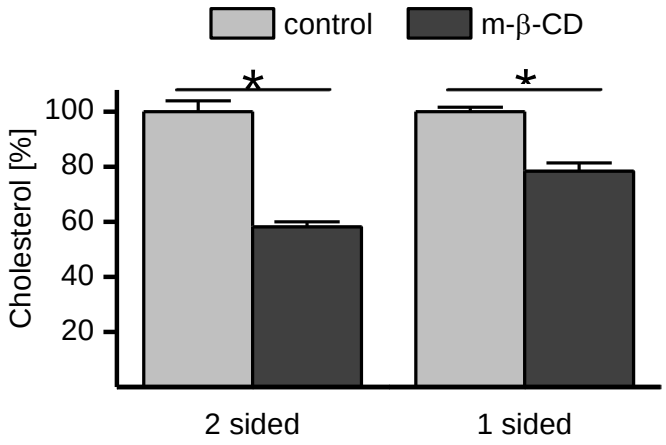

Figure 5.3; Impact of cholesterol removal by 30 min methyl-β-cyclodextrin (10 mM) treatment of differentiated Caco-2 monolayers on cellular cholesterol content. Cells were either incubated from the apical side only (1 sided) or from both apical and basolateral side (2 sided). Methyl-β-cyclodextrin was dissolved in HBSS + 1.8 mM $CaCl_2$, control cells were treated with buffer only. Cholesterol content of untreated cells was set as 100 %. For further conditions and analysis see sections 2.2 and 2.13. n = 6, N = 1; * = $p \leq 0.05$

As shown in figure 5.3, one-sided incubation of Caco-2 cells with methyl-β-cyclodextrin resulted in removal of 39% of cellular cholesterol, two-sided incubation resulted in removal of 57% of cellular cholesterol.

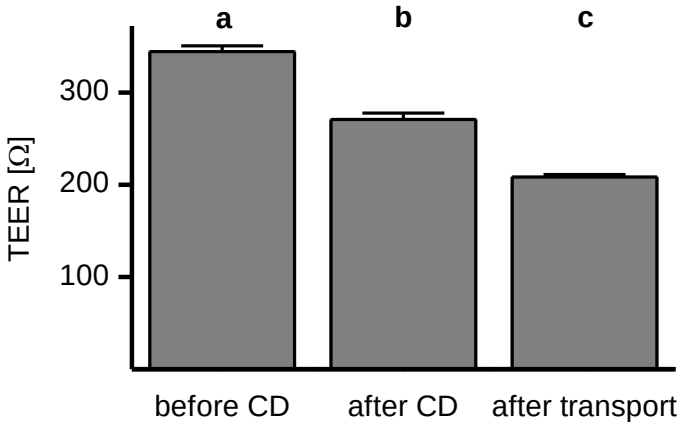

Figure 5.4; Impact of 30 min methyl-β-cyclodextrin (10 mM) treatment and transport study on transepithelial electrical resistance. Different letters indicate statistically significant differences determined by one-way ANOVA. a vs. b: p = 2.96E-7, a vs. c: p = 6.32E-11, b vs. c: p = 2.43E-6; n = 6, N = 1; For details on conditions and analysis see sections 2.2, 2.3 and 2.13.

The treatment with methyl-β-cyclodextrin also resulted in a significant decrease in TEER, which was even further reduced after the transport experiment (figure 5.4).

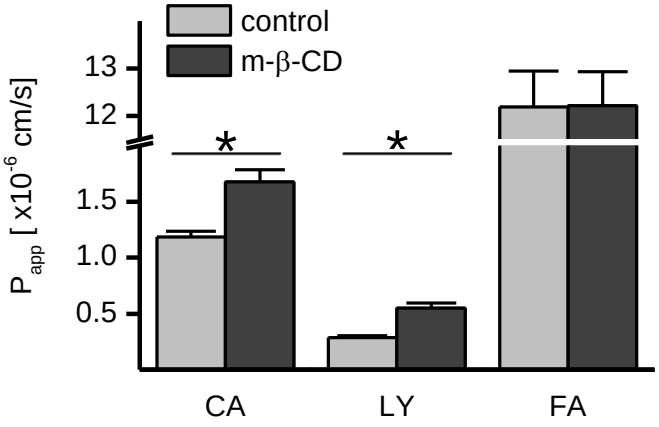

Figure 5.5; Impact of 2-sided cholesterol removal by methyl-β-cyclodextrin on paracellular transport of caffeic acid, ferulic acid and lucifer yellow. For further conditions and analysis see sections 2.3, 2.4 and 2.6. n = 6; * = $p \leq 0.05$

Methyl-β-cyclodextrin treatment increased paracellular diffusion of caffeic acid and lucifer yellow but had no impact on ferulic acid transport (figure 5.5). These results

indicate that the increase in ferulic acid transport, caused by PUFA supplementation, is not the result of an increase in paracellular diffusion.

PUFA supplementation of Caco-2 cells results in a modulation of plasma membrane fluidity as described in section 3.3.5. Linoleic, α-linolenic and arachidonic acid resulted in an increase in membrane fluidity whereas EPA and DHA resulted in a decrease in plasma membrane fluidity. Supplementation with these five fatty acids also resulted in an increase in ferulic acid transport. But since EPA and DHA have the opposite effect on fluidity compared to the other three PUFA, but all five had the same effect on transport, it is unlikely that the change in fluidity is the cause for the observed change in ferulic acid absorption.

5.3.2 Impact of PUFA on transporter mediated absorption of ferulic acid

Transepithelial permeation of a compound can occur via four different mechanisms, paracellular diffusion, transcellular passive diffusion, carrier mediated diffusion or active transport involving plasma membrane spanning transporters (see chapter 1). Since the modification of membrane fluidity by fatty acid supplementation did not correlate with the increase in ferulic acid transport rate, and paracellular transport was also ruled out as the cause of the observed change in apparent permeability, it was assumed that a membrane spanning transporter was involved in the observed change in ferulic acid transport. Therefore, in the next step the PUFA DHA was selected to investigate the mechanism of transepithelial transport of ferulic acid further. Figure 5.6 shows the impact of DHA treatment on uptake transport (apical to basolateral side) of hesperetin, metoprolol and ferulic acid and also transport of ferulic acid in the efflux direction (basolateral to apical).

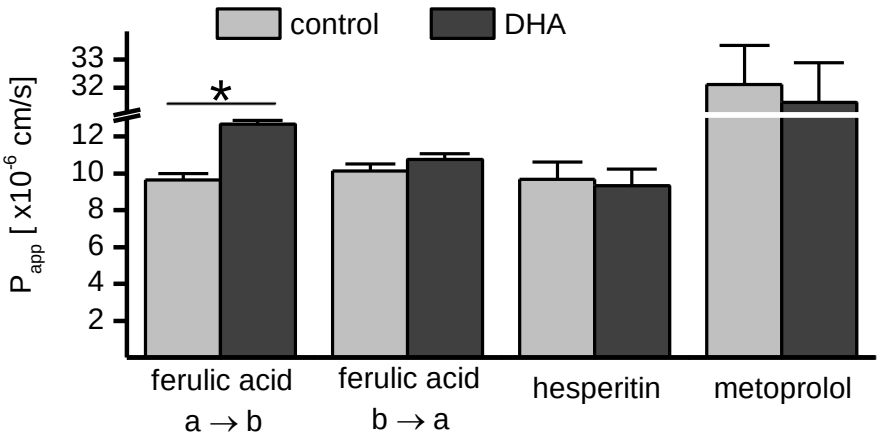

Figure 5.6; Impact of chronic DHA supplementation on transepithelial transport of ferulic acid, hesperetin and metoprolol in apical to basolateral direction (a → b) and of ferulic acid in basolateral to apical direction (b → a). For details on transport and analysis see sections 2.3, 2.4 and 2.6. n = 6, N = 1; * = $p \leq 0.05$

Transepithelial transport of hesperetin and metoprolol, which are both absorbed by passive diffusion (259, 260), was unaffected by DHA supplementation of Caco-2 cells, confirming that a change in passive diffusion is not the cause for the increase in permeability of ferulic acid. DHA treatment only significantly increased apical to basolateral transport of ferulic acid ($J_{a\rightarrow b}$ control vs. $J_{a\rightarrow b}$ DHA: p = 6.48E-6, $J_{b\rightarrow a}$ control vs. $J_{a\rightarrow b}$ DHA: p = 7.36E-5, $J_{b\rightarrow a}$ DHA vs. $J_{a\rightarrow b}$ DHA: p = 0.00195) but not in basolateral to apical transport direction ($J_{b\rightarrow a}$ DHA vs. $J_{a\rightarrow b}$ control: p = 0.11, $J_{b\rightarrow a}$ DHA vs. $J_{b\rightarrow a}$ control: p = 1). Such an asymmetric effect suggests that DHA has an impact on a transporter-mediated process. In chapter 4, a change in facilitated diffusion of ferulic acid via modulation of the expression of MCT1 and MCT4, by the microbial metabolite butyric acid, was reported. There, the effect of butyric acid on ferulic acid transport was abolished by the presence of the MCT inhibitor phloretin in the transport buffer. It was therefore tested whether phloretin would also inhibit the effect of DHA on ferulic acid transport. Figure 5.7 shows that the presence of phloretin in the transport buffer had no significant impact on ferulic acid transport.

A

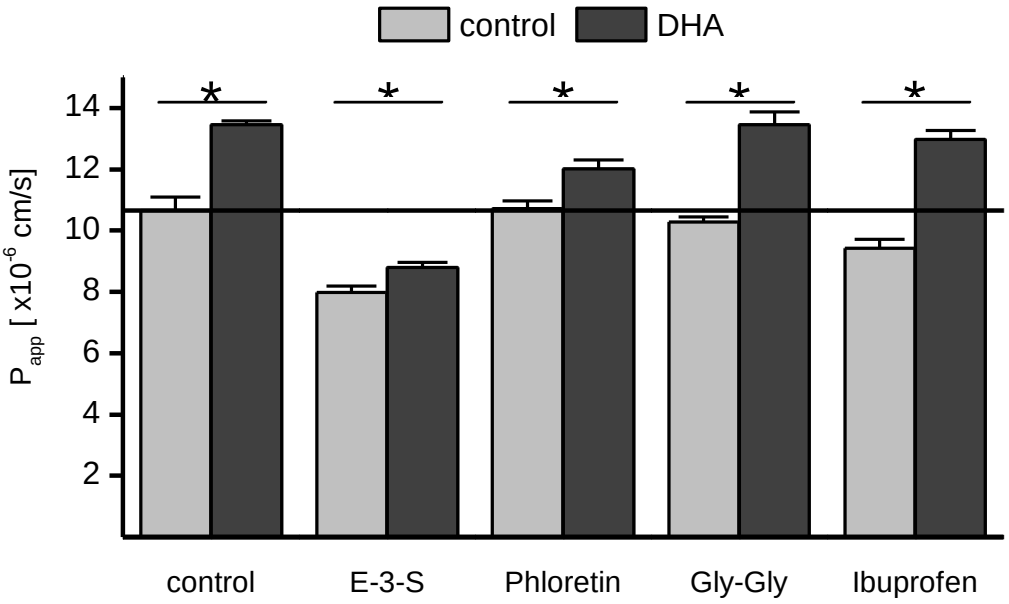

B

treatment	control	DHA	E-3-S DHA	Phloretin DHA	Gly-Gly DHA	Ibuprofen DHA
control		4.9E-4	3.2E-4	1.7E-4	0.03	0.08
DHA	4.9E-4		2.8E-10	1	0.222	0.084
E-3-S control	2.8E-6	1.6E-11	0.241			
Phloretin control	0.085	0.223		0.081		
Gly-Gly control	1	5.6E-4			0.066	
Ibuprofen control	1	1.5E-4				0.030

Figure 5.7; **A** Impact of different transport inhibitors on apical to basolateral transport of ferulic acid (500µM). **B** Corresponding p-values determined by one-way ANOVA. For details on transport and analysis see sections 2.3, 2.4 and 2.6. n = 6, N = 1 for phloretin and estrone-3-sulfate (E-3-S) and n = 3, N = 1 for Diglycine (Gly-Gly) and Ibuprofen; * = $p \leq 0.05$

Since phloretin did not reduce transport across DHA treated cell monolayers to the level of controls, other transport inhibitors were tested, which target some of the most abundant uptake transporters in the apical membrane of Caco-2 cells, according to the literature (18, 147). Diglycine (Gly-Gly), an inhibitor of

Peptide transporter 1 (PepT1) (137, 261), and ibuprofen, an inhibitor of PepT1 (136) and Organic anion transporting polypeptide B (OATPB) (136), had no impact on ferulic acid transport, but estrone-3-sulfate, an inhibitor of Organic anion transporter 2 (OAT2) (138, 262), Sodium-dependent organic anion transporter (SOAT) (263) and several members of the OATP family (264), significantly reduced transepithelial transport across DHA treated and untreated cells. To test whether DHA has an impact on gene expression of the phloretin and estrone-3-sulfate sensitive transporters MCT and OAT2, changes in mRNA levels of those transporters in chronically supplemented Caco-2 cells were assessed.

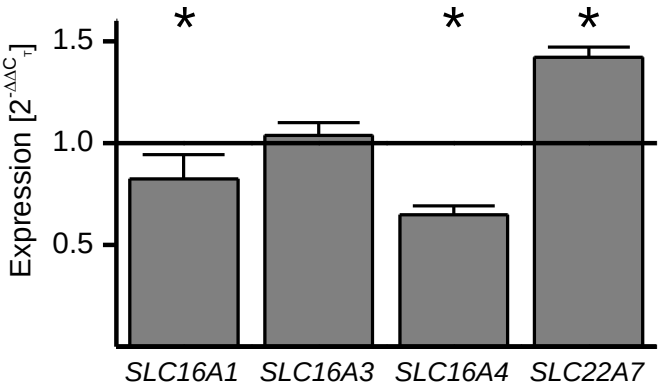

Figure 5.8; Impact of chronic DHA supplementation on gene expression of selected transporters in Caco-2 cells. For details on treatment and analysis see sections 2.3 and 2.8. n = 6, N = 1; * = $p \leq 0.05$

The expression of the three most abundant MCT isoforms in Caco-2 cells was not increased with DHA treatment; on the contrary, expression of MCT1 (SLC16A1) and MCT5 (SLC16A4) even decreased, which argues against a role of MCT transporters in the increase in ferulic acid transport after DHA treatment. Expression of OAT2 (SLC22A7) was upregulated after DHA supplementation.

5.3.3 Impact of fatty acid supplementation on ferulic acid metabolism by Caco-2 cells

The mechanism of ferulic acid transport described in chapter 4 was investigated by comparing transport and gene expression data with changes in metabolism. This approach was employed again, this time to draw conclusions on the impact of DHA on ferulic acid transport.

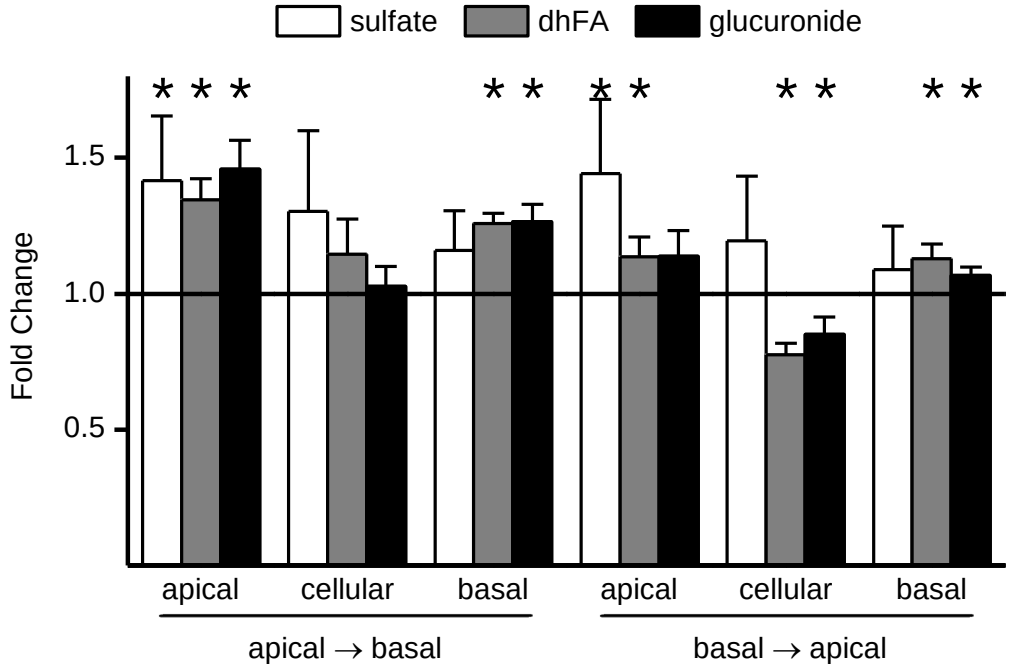

Figure 5.9; Impact of chronic DHA supplementation on metabolism of ferulic acid by Caco-2 cells. The aglycone was either applied to the apical side (apical → basal) or to the basolateral side (basal → apical) at a concentration of 500 µM. For details on treatment and analysis see sections 2.3 and 2.7. n = 6, N = 1; * = $p \leq 0.05$

DHA supplementation increased the concentration of all metabolites on the apical side, when ferulic acid was applied to the apical side but did not significantly change intracellular metabolite concentrations and significantly increased dihydroferulic acid and ferulic acid glucuronide concentrations in the basolateral chamber. DHA supplementation significantly increased ferulic acid sulfate and dihydroferulic acid concentrations on the apical side, decreased concentrations of dihydroferulic acid

and ferulic acid glucuronide intracellularly and significantly increased concentrations of dihydroferulic acid and ferulic acid glucuronide in the basolateral well, when ferulic acid was applied to the basolateral side (figure 5.9). For metabolite concentrations, see figure 4.6.

The conclusions on the impact of DHA on ferulic acid metabolism are not as clear as with the impact of butyric acid. Generally, metabolite levels are increased in the apical and basolateral chamber but not intracellularly. DHA also had no influence on the concentration of ferulic acid in the cell lysate, so there is no correlation of intracellular aglycone concentration with metabolism increase (figure 5.12).

Since it was not possible to draw definite conclusions from the data presented in figure 5.9, regarding the transport mechanism that is affected by PUFA supplementation, the metabolism of ferulic acid was also investigated in DHA treated and untreated cells in the presence and absence of the transport inhibitor estrone-3-sulfate. Since estrone-3-sulfate reduced transepithelial transport of ferulic acid (figure 5.6), most likely through inhibition of apical aglycone uptake, the resulting lower intracellular concentration of ferulic acid should be reflected in metabolite formation.

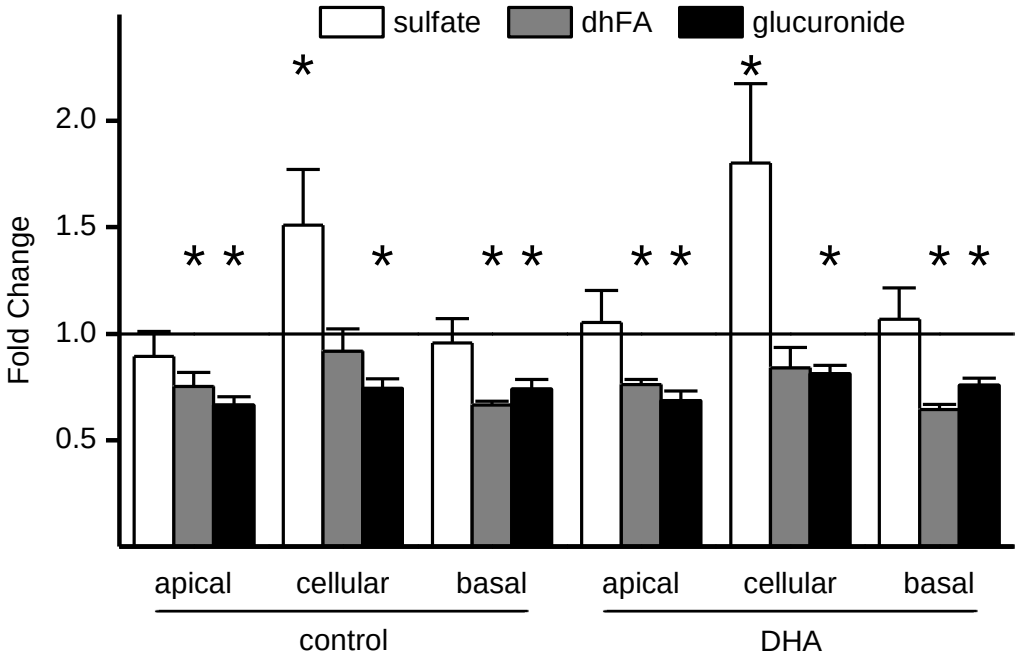

Figure 5.10; Impact of estrone-3-sulfate on metabolism of ferulic acid by control and chronically DHA treated Caco-2 cells. A fold change of amount of metabolites produced in the presence of estrone-3-sulfate is shown normalised to the amount of metabolites produced in the absence of estrone-3-sulfate. For details on treatment and analysis see sections 2.3 and 2.7. n = 6, N = 1; * = $p \leq 0.05$

The impact of DHA supplementation on metabolism was compared between incubations with and without estrone-3-sulfate. The inhibitor showed the same effect on metabolism by DHA-supplemented and control cells. It decreased the amount of dihydroferulic acid and feruloyl-glucuronide and increased the amount of feruloyl-sulfate that was produced (figure 5.10).

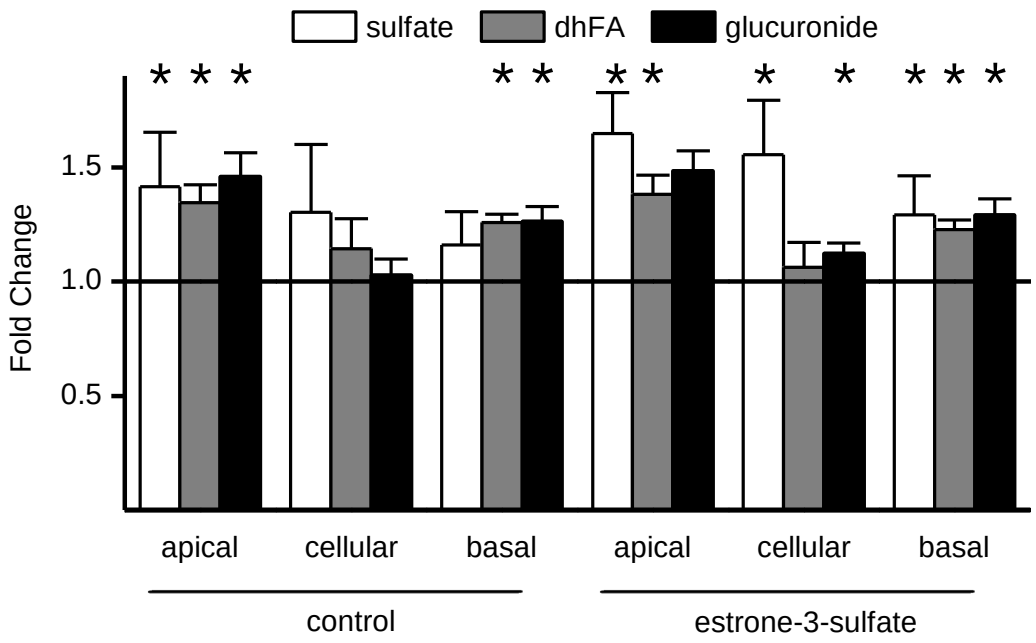

Figure 5.11; Impact of estrone-3-sulfate on metabolism of ferulic acid by control and chronically DHA treated Caco-2 cells. A fold change of amount of metabolites produced in DHA treated cells is shown normalised to the amount of metabolites produced in untreated cells. Note that this data is the same as already presented in figure 5.11, but plotted differently to show a different effect. For details on treatment and analysis see sections 2.3 and 2.7. n = 6, N = 1; * = $p \leq 0.05$

Comparing the impact of estrone-3-sulfate treatment on ferulic acid metabolism in DHA supplementated and non-supplemented cells shows that, while the inhibitor reduces metabolite formation in Caco-2 cells, it has no impact on the pattern of changes induced by DHA treatment (figure 5.11). There was a general increase of metabolite concentration after DHA supplementation in the presence and absence of estrone-3-sulfate. There also was a very slight but non-significant increase in intracellular concentrations of ferulic acid after DHA treatment, but the presence of estrone-3-sulfate in the incubation medium did not affect intracellular concentrations of ferulic acid (figure 5.12)

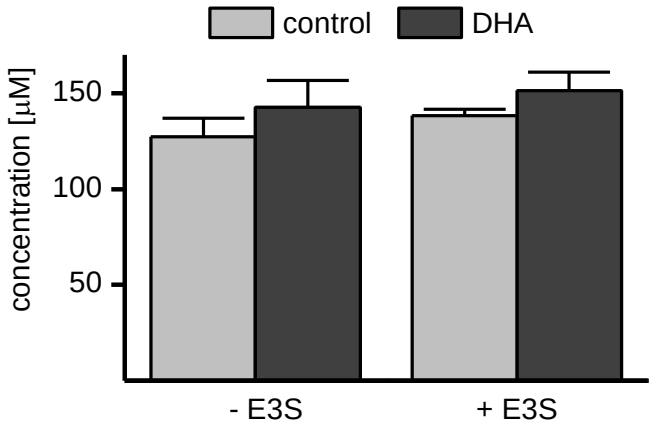

Figure 5.12; Impact of DHA supplementation and the presence of estrone-3-sulfate (E-3-S) on intracellular concentrations of ferulic acid in Caco-2 cells. For details on treatment and analysis see sections 2.3 and 2.7. n = 6, N = 1;

Even though paracellular and transcellular passive diffusion have been ruled out as the cause of ferulic acid transport increase induced by PUFA supplementation on the basis of experiments described above, it was still interesting to investigate a possible impact of these physical changes on ferulic acid metabolism. Therefore it was tested whether treatment of Caco-2 cells with methyl-β-cyclodextrin has an impact on ferulic acid metabolism.

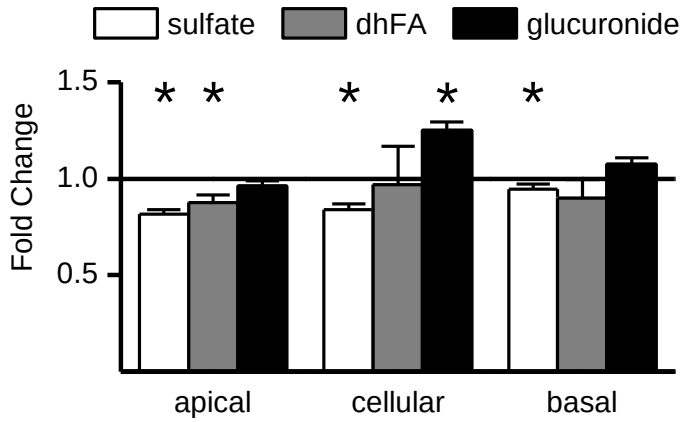

Figure 5.13, Impact of methyl-β-cyclodextrin treatment of Caco-2 cells on metabolism of ferulic acid. For details on treatment and analysis see sections 2.2 and 2.13. n = 6, N = 1; * = $p \leq 0.05$

Figure 5.13 shows that methyl-β-cyclodextrin treatment induced in a unique pattern of metabolism changes, that was different from previously observed effects, with decreased levels of feruloyl-sulfate in all compartments and dihydroferulic acid in the apical well, but increased levels of feruloyl-glucuronide intracellularly.

5.3.4 Impact of fatty acid supplementation on ferulic acid metabolism in HepG2 cells.

The metabolism of ferulic acid described in section 5.3.3 gives no clear picture of the impact of fatty acids on ferulic acid transport. It is quite possible that several effects overlay each other here, for example PUFA could also have an impact on the metabolism itself by affecting the expression or activity of enzymes that catalyse those reactions. Caco-2 cells are a complex model in this respect because they are a differentiating cell line and there are three compartments in which metabolites can accumulate. Therefore a much simpler model was sought to investigate the impact of fatty acids on metabolism of ferulic acid further. Differential fatty acid feeding in animal models will not only change the composition of the intestinal cells but also of other tissues and organs. The liver is usually thought to be the crucial organ for metabolism of xenobiotics, since many key phase II enzymes are particularly expressed here. The lipid composition of liver cells was also shown to change with fatty acid supplementation *in vivo* (265, 266). Therefore, for further experiments the hepatoblastoma HepG2 cell line was chosen, as this cell line is a much simpler model since it is non-polarising. It does however express many efflux transporters, therefore what fraction of the metabolites produced is exported into the medium and how much is retained intracellularly was investigated first.

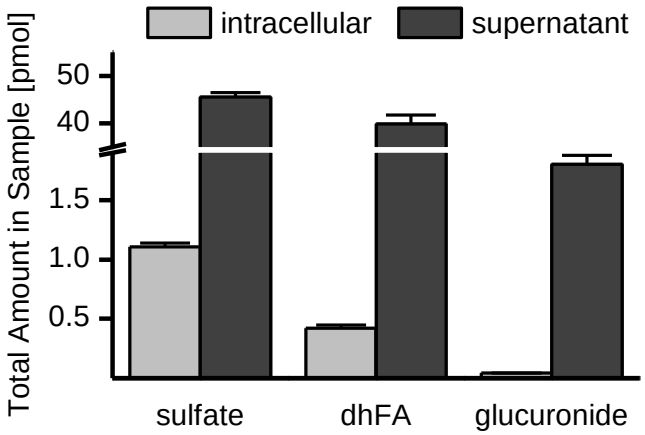

Figure 5.14; Distribution of ferulic acid metabolites in HepG2 cultures. Results are given as the total amount of compound summed up over the 100 µL of cell lysate or 2000 µL of supernatant. Cells were incubated with 1 µmol ferulic acid in 2000 µL buffer for 120 min and the supernatant and cell lysate were analysed as described in section 2.13. n = 6, N = 1

Figure 5.14 shows that the largest portion of metabolites was exported into the supernatant and only 1 - 2 % could be found intracellularly. For that reason, only the supernatant was analysed in all further experiments.

Next, the impact of a five day treatment of HepG2 cells with different long chain fatty acids on ferulic acid metabolism was investigated.

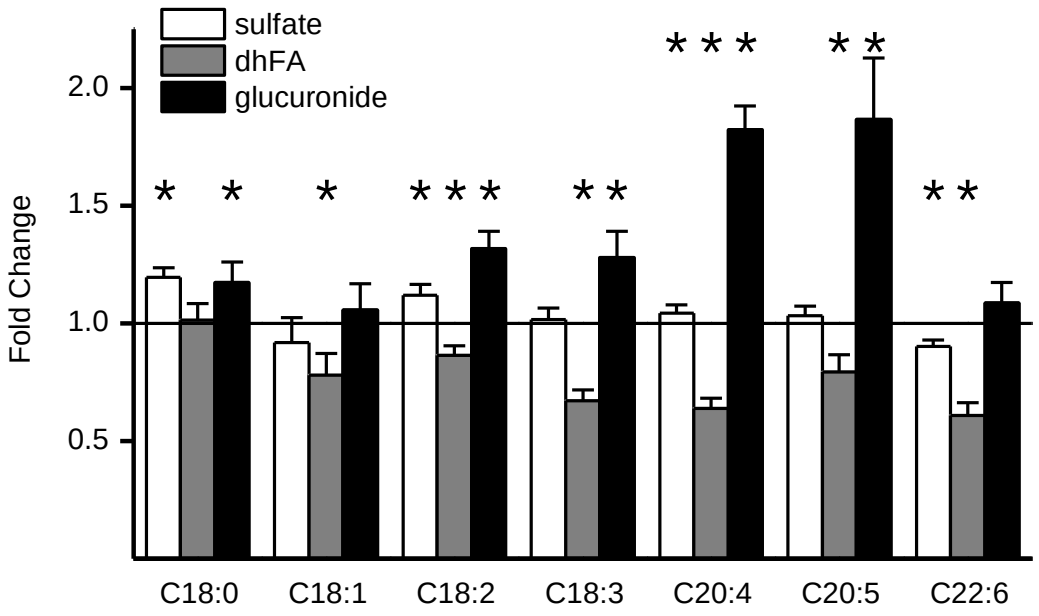

Figure 5.15; Impact of different long chain fatty acids on ferulic acid metabolism in HepG2 cells. Cells were treated with 50 µM fatty acid for 5 days and metabolism was analysed as described in sections 2.3 and 2.7. C18:0 = stearic acid, C18:1 = oleic acid, C18:2 = linoleic acid, C18:3 = linolenic acid, C20:4 = arachidonic acid, C20:5 = EPA, C22:6 = DHA; n = 6, N = 1; * = $p \leq 0.05$

As figure 5.15 shows, there is a clear impact of PUFA on the formation of dihydroferulic acid and feruloyl-glucuronide. Glucuronide levels increased and dihydroferulic acid levels decreased. The impact of fatty acids on sulfoconjugation is not as clear, as there is an increase in that metabolite with stearic, linoleic and arachidonic acid and a slight decrease with DHA supplementation.

Since DHA has been selected for most of the experiments described above, it was again chosen to investigate a long term impact of fatty acids. HepG2 cells were cultured in the renewed presence of 50 µM DHA over several passages and ferulic acid metabolism was tested at different time points.

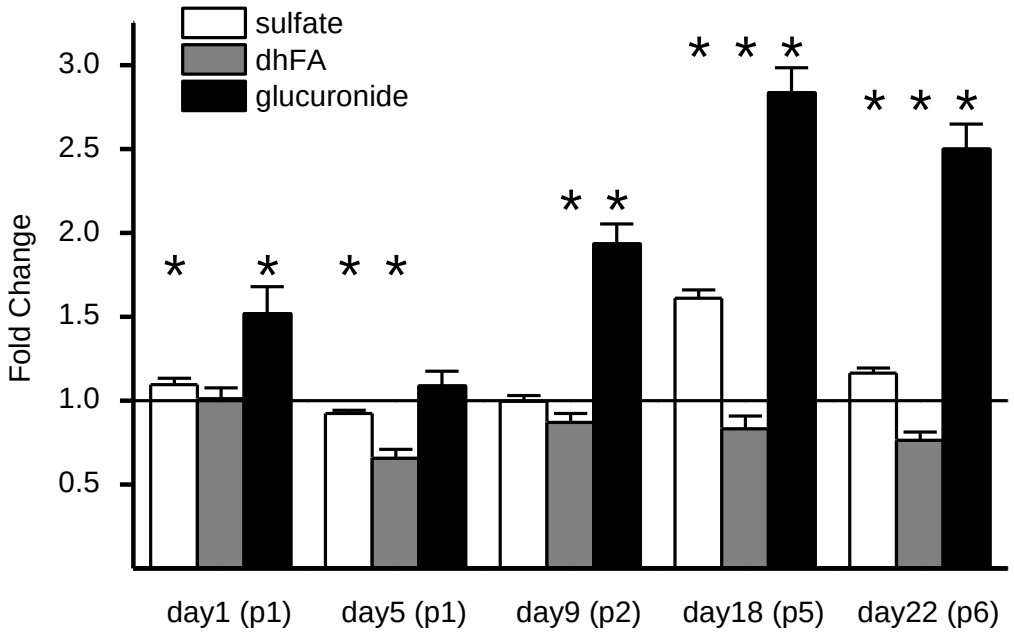

Figure 5.16, Impact of long term supplementation of HepG2 cells with 50 µM DHA on ferulic acid (500 µM) metabolism. X-axis indicates day after lipid supplementation commenced and number of passages in lipid supplemented medium. For details on conditions and analysis see sections 2.3 and 2.7. n = 6, N = 1; * = $p \leq 0.05$

The continuous presence of DHA in the growth medium over several passages increased the formation of glucuronic acid conjugates up to three times the amount found in control cells. Dihyhodroferulic acid production remained lower than in untreated cells and sulfoconjugation, although decreased at day five, was actually increased after two weeks of supplementation (figure 5.16).

5.4 Discussion

The impact of different dietary patterns, concerning the type of lipid that is consumed, on phenolic acid bioavailability, was investigated. An enterocyte cell culture model with chronic supplementation of low concentrations of dietary fatty acids was used to study this possible interaction.

Chronic supplementation with several different PUFAs resulted in an increase in caffeic and ferulic acid uptake. Since fatty acid treatment did not decrease cell viability or TEER (see figure 3.9), such an effect does not seem to be due to a weakening of the cell layer integrity caused by lipid cytotoxicity. Choosing DHA to investigate the mechanism of uptake increase further, it was found that caffeic acid but not ferulic acid transport correlated with an increase in permeability of the paracellular diffusion marker lucifer yellow. Paracellular diffusion is regulated by proteins of the tight junction complex. Very early in the history of tight junction research, the great abundance of cholesterol in the tight junction complex and disturbance of the tight junction assembly with cholesterol removal, was noted (267). More recently the presence of some of the tight junction proteins in special cholesterol rich membrane domains, that can be selectively extracted using certain detergents, was confirmed (268, 269). When fractionated by sucrose gradient centrifugation, the tight junction proteins occludin, claudin 1, claudin 3, claudin 4, claudin 7 and JAM-A, but not the ZO proteins, co-localised with the detergent resistant membrane (DRM) marker flotillin. After lowering the membrane cholesterol content using methyl-β-cyclodextrin, these proteins became detergent soluble and no longer localised in DRM fractions. Methyl-β-cyclodextrin treatment of Caco-2 cells resulted in time dependent removal of cholesterol, a decrease in TEER and an increase in permeability of the paracellular diffusion marker dextran (269). Cholesterol removal also resulted in a redistribution of tight junction proteins occludin, claudin 3 and claudin 4 from the lateral plasma membrane to the cytosol (269, 270), thereby causing a decrease in tight junction integrity and an increase in

paracellular diffusion. Supplementation with dietary PUFA has also been shown to modulate DRM composition and functioning (271-273), which could explain the impairment of tight junction integrity observed here. The description of the impact of PUFA on paracellular diffusion in the literature varies depending on the incubation conditions and the cell line employed. In most studies, where 24 h of exposure time were chosen, either no effect on TEER and diffusion rate of paracellular markers lucifer yellow, mannitol, fluorescein and dextran, or an increase in permeability only with very high concentrations of PUFA in the millimolar range, was found (177, 274-279). The long term impact of physiological concentrations of fatty acids, as investigated in the current study, has not been described before.

As methyl-β-cyclodextrin treatment of Caco-2 cell monolayers resulted in an increase in transport of caffeic acid but not ferulic acid, it was concluded that caffeic acid uptake is due to increased paracellular diffusion but ferulic acid uptake is not. The fact that transport of ferulic acid did not correlate with changes in paracellular nor passive transcellular diffusion suggests that it was transporter mediated uptake that was affected by PUFA supplementation. Previous reports (234) and the work described in chapter 4 have shown a possible role of MCT1 in the uptake of ferulic acid in Caco-2 cells. Therefore it was tested, whether the PUFA DHA has a similar effect as butyric acid in modulation of MCT expression. Ferulic acid transport was not sensitive to the MCT inhibitor phloretin, and expression of MCT1, MCT4 and MCT5 was not enhanced with DHA supplementation, and therefore MCT is not involved in PUFA upregulation of ferulic acid transepithelial transport. The impact of other transport inhibitors affecting some of the most abundant uptake transporters in the apical membrane of Caco-2 cells, which could have ferulic acid as an allocrite (19, 147, 280), was investigated, and it was found that estrone-3-sulfate decreased transport across fatty acid supplemented and non-supplemented cell layers. Estrone-3-sulfate is reported to be an inhibitor of OAT2 and OAT2 expression was also found to be increased in DHA supplemented cells. However, previous reports

have not found ferulic acid to be an allocrite of OAT2 but only of OAT1 (281). There is no information available whether estrone-3-sulfate is also inhibiting OAT1, so it would be interesting to explore this possible interaction further.

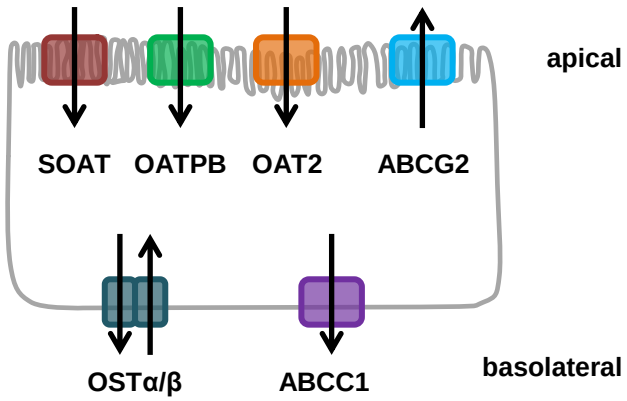

Figure 5.17, Cellular localisation of estrone-3-sulfate sensitive transporters in Caco-2 cells.

Estrone-3-sulfate is also an inhibitor of other apical uptake transporters expressed in Caco-2 cells. It inhibits OATPB, but since ibuprofen, which is an inhibitor of OATPB as well, had no effect on ferulic acid transport, OATPB is unlikely to be involved in ferulic acid uptake. The only other apical uptake transporter that is known to be inhibited by estrone-3-sulfate, is SOAT (263). Instead of apical uptake, basolateral efflux transporters could also be responsible for the observed effect of estrone-3-sulfate on ferulic acid transport. Here the inhibitor has an impact on ABCC1 and OSTα/β (282). To determine the exact mechanism of estrone-3-sulfate action in this context, all four transporters, OAT1, SOAT, ABCC1 and OSTα/β, would have to be investigated concerning their ability to transport ferulic acid. But it is not entirely clear whether the target of estrone-3-sulfate is actually the same transporter that is responsible for the increase in ferulic acid transport after PUFA supplementation. Looking closely at the transport and metabolism data presented in figures 5.6 and 5.10, it can be observed that the presence of estrone-3-sulfate neither abolishes the significant increase in ferulic acid uptake induced by fatty acid treatment, nor does it alter the change in metabolism pattern induced by chronic

DHA supplementation. It could therefore also be that ferulic acid is the allocrite of a third, unknown transporter that is neither sensitive to phloretin nor to estrone-3-sulfate and which has not been considered or reported so far.

Even though co-incubation of ferulic acid with the transport inhibitor estrone-3-sulfate resulted in a decrease of the metabolites dihydroferulic acid and ferulic acid glucuronide, it is not likely that this effect was due to a decreased uptake of ferulic acid into the cell, as intracellular concentrations of ferulic acid were unchanged. Most likely it is a direct effect of estrone-3-sulfate on metabolism. Caco-2 cells exhibit steroid sulfatase activity (283, 284), meaning that the inhibitor estrone-3-sulfate can be deconjugated intracellularly and the free steroid then constitutes a competing substrate for phase II metabolism enzymes that also conjugate ferulic acid. Thus the decrease in feruloyl-glucuronide can be explained as estrone is a substrate of the same UGTs as ferulic acid, namely UGT1A1, UGT1A8, UGT1A9 and UGT1A10 (143, 285). Which enzyme catalyses the reduction of ferulic acid to dihydroferulic acid has not been characterised, but since the formation of this metabolite is also decreased with estrone-3-sulfate co-application, it can be assumed, that there is also an overlapping enzyme specificity of these two compounds. Which sulfatase isoform catalyses the hydrolysis of feruloyl-sulfate has also not been reported, but perhaps here as well is a overlap in enzyme specificity with esterone-3-sulfate which would result in a decreased desulfation of the ferulic acid metabolites and consequent raised levels of this conjugate in the presence of estrone-3-sulfate. Estrone-3-sulfate deconjugation is catalysed by steroid sulfatase, which also has a weak affinity for non-steroidal substrates, for example, p-nitrophenol (286). Alternatively, the desulfation of estrone-3-sulfate would lead to increased intracellular levels of sulfate which might shift the equilibrium of the desulfation reaction a little from the product to the reactant side and result in increased levels of that conjugate.

Fatty acid supplementation induced changes in ferulic acid metabolism were also compared between intestinal enterocytes and hepatocytes to assess how different tissues are affected by different dietary lipids. In both cell lines, fatty acid supplementation induced an increase in glucuronide formation. This effect of lipids on UGT activity and expression has been described before (287-289), and is discussed further in chapter 7. Sulfoconjugation was also increased in chronically DHA supplemented Caco-2 cells and in HepG2 cells that have been treated for more than nine days. Ferulic acid is sulfoconjugated mainly by SULT1E1 but also by SULT1A1, SULT1A2 and SULT1A3 (143). There is no report on SULT regulation by dietary lipids, but SULT1E1 is highly expressed in adipose tissue (290). Since the main function of adipose tissue is to store lipids, there is a potential connection here that would be interesting to explore further. SULT1E1 expression and activity in HepG2 cells are very low (291, 292). In Caco-2 cells, SULT1E1 is also expressed at low levels, but SULT1A3 is very highly expressed, over 1000 times more than SULT1E1 (293). Therefore, even though ferulic acid has a much higher affinity for SULT1E1, SULT1A3 could have a dominating impact on ferulic acid sulfoconjugation due to the much higher expression. Formation of dihydroferulic acid was increased in intestinal cells but decreased in hepatocytes, which indicates a mechanism that is differentially regulated in different tissues. From comparison of metabolism in enterocytes and hepatocytes it can be concluded that the impact of fatty acid supplementation of Caco-2 cells on ferulic acid metabolism is more likely due to a direct impact on metabolising enzymes and not connected to the change in transport.

The ability of methyl-β-cyclodextrin treatment to modulate ferulic acid metabolism in Caco-2 cells was also investigated. This was interesting as any observed changes would not stem from changes in gene expression but purely from the physical impact of lowered membrane cholesterol content. This impact could either be direct through reduced/enhanced diffusion of a hydrophobic compound across the plasma

membrane or indirect, affecting endocytosis or exocytosis pathways or DRM resident transporters (discussed further in chapter 6). Transport of ferulic acid glucuronide- and sulfoconjugates will rely on the latter mechanisms, as they are too large and polar to freely diffuse across the lipophilic core of the plasma membrane. Many transporters, such as PepT1 (294) or ABCB1 (295), are reported to locate to DRM. DRM are rich in cholesterol and lowering plasma membrane cholesterol content by methyl-β-cyclodextrin treatment results in disturbance of these structures and consequent altered transporter activity (296). DRM are also involved in endo-/exocytosis pathways which are sensitive to cholesterol depletion and either mediate direct uptake of compounds by endocytosis or regulate the abundance of transporters on the cell surface (297, 298). The decrease in apical efflux of feruloyl-sulfate and dihydroferulic acid after methyl-β-cyclodextrin treatment could be the result of the impact of cholesterol removal affecting DRM residing efflux transporters, as discussed further in chapter 6. The increase in feruloyl-glucuronide will most likely be due to activation of the ER residing UGT enzyme, as discussed further in chapter 7.

In conclusion, it was shown that paracellular diffusion of caffeic acid in the intestinal Caco-2 cell culture model can be enhanced by fatty acid supplementation that weakens tight junction integrity. Ferulic acid transport is also enhanced by this treatment but through a different mechanism, which does not correlate with membrane fluidity changes. Most likely the PUFA sensitive mechanism of ferulic acid transport involves a carrier mediated process, perhaps one that is inhibited by estrone-3-sulfate, but which is not of the MCT family. Further work will need to be carried out to determine the identity of such transporter.

Chapter 6: Impact of the fatty acid DHA on transepithelial transport of epicatechin and its phase II metabolites in the Caco-2 model

6.1 Abstract

The influence of chronic dietary fatty acid treatment of Caco-2 cells on epicatechin transport was investigated. Several fatty acids were tested but only DHA and arachidonic acid were able to reduce efflux to the apical side, which indicates an interference with the previously reported mechanism of epicatechin efflux by apical ABC-transporter. SiRNA silencing of ABCB1, ABCC2 and ABCG2 revealed that epicatechin is probably an allocrite of ABCC2, whereas the phase II conjugates *O*-methyl-epicatechin, epicatechin-sulfate and *O*-methyl-epicatechin-sulfate seem to be transported by ABCG2. DHA treatment decreased the transport of the *O*-methyl- and *O*-methyl-sulfo-conjugates and increased formation of sulfate metabolites. Glucuronic acid conjugates were only detected after transport in basolateral to apical direction and all other conjugates were also much more abundant when efflux transport was investigated. This behaviour agrees with the observation that epicatechin accumulates intracellularly when applied to the basolateral side but not when loaded in the apical well. Lowering membrane cholesterol content by methyl-β-cyclodextrin treatment of cells also reduced efflux of aglycone and metabolites. Epicatechin transport in apical to basolateral direction correlated very well with lucifer yellow permeation rates, which indicates that epicatechin absorption probably occurs by paracellular diffusion.

6.2 Introduction

As reviewed in chapter 1, the flavanol epicatechin belongs to a group of polyphenols whose beneficial properties have received a lot of attention over the recent years. When the mechanism of epicatechin uptake at the intestinal epithelium was investigated in the Caco-2 enterocyte model, either no (299) or only very little (300) transport from the apical to the basolateral side was observed, whereas efflux of that compound from the basolateral to the apical compartment was much higher. Uptake rates increased and efflux decreased when the experiment was conducted in the presence of the compound MK571, an inhibitor of the apical efflux pump ABCC2. Such behaviour would indicate that epicatechin is an allocrite of apical efflux transporters of the ABC-family. This group of transporters, especially ABCB1, has been reported to localise in specific domains that are found in the outer leaflet of the plasma membrane called DRM or lipid rafts (301, 302). These structures contain many membrane receptors and transporters at a much higher density than the surrounding plasma membrane (303, 304) and modulation of their lipid composition by dietary fatty acids was shown to alter the activity of raft residing proteins (256, 305-307). Since ABC-transporters are DRM resident, for this chapter the hypothesis that dietary fatty acids can affect epicatechin bioavailability through modulation of the plasma membrane composition and consequent interference with ABC-transporter activity, was investigated.

6.3 Results

6.3.1 Impact of chronic fatty acid supplementation on transepithelial transport of epicatechin

To screen for a possible modification of epicatechin absorption by dietary lipids, Caco-2 cells were chronically supplemented with 50 µM fatty acid and after 22 days, transepithelial transport of epicatechin was assessed in uptake (apical to basolateral) and efflux direction (basolateral to apical).

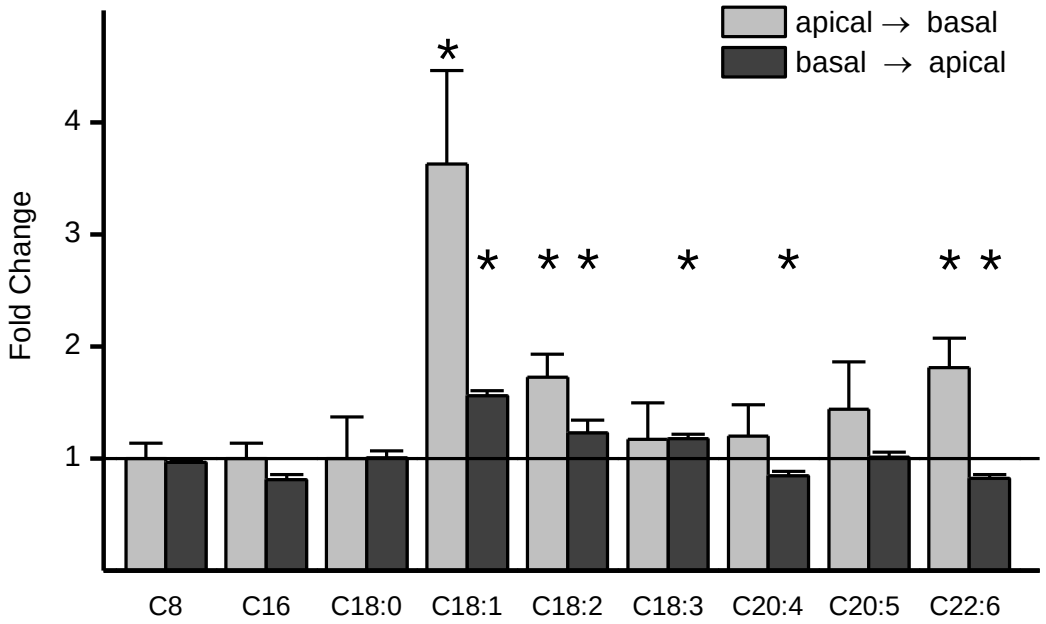

Figure 6.1; Impact of chronic fatty acid supplementation of Caco-2 cells on epicatechin transport. Cells were treated with 50 µM fatty acid for 22 days and transport of epicatechin (200 µM) was assessed in uptake (apical → basal) and efflux direction (basal → apical). For details on conditions and analysis see sections 2.3, 2.4 and 2.6. C8 = octanoic acid, C16 = palmitic acid, C18:0 = stearic acid, C18:1 = oleic acid, C18:2 = linoleic acid, C18:3 = linolenic acid, C20:4 = arachidonic acid, C20:5 = EPA, C22:6 = DHA; n = 6, N = 1; * = $p \leq 0.05$

Figure 6.1 shows that all unsaturated fatty acids tested had an impact on epicatechin transport. Oleic, linoleic and α-linolenic acid increased epicatechin

efflux, which would either correspond to a stimulation of efflux transporter activity or an impact on paracellular diffusion. Only arachidonic acid and DHA decreased efflux of epicatechin while increasing uptake (though with arachidonic acid this increase was not significant), which could be due to decreased efflux transporter activity. Supplementation with DHA decreased the uptake : efflux ratio of epicatechin from 1 : 10 to 1 : 5 (figure 6.2).

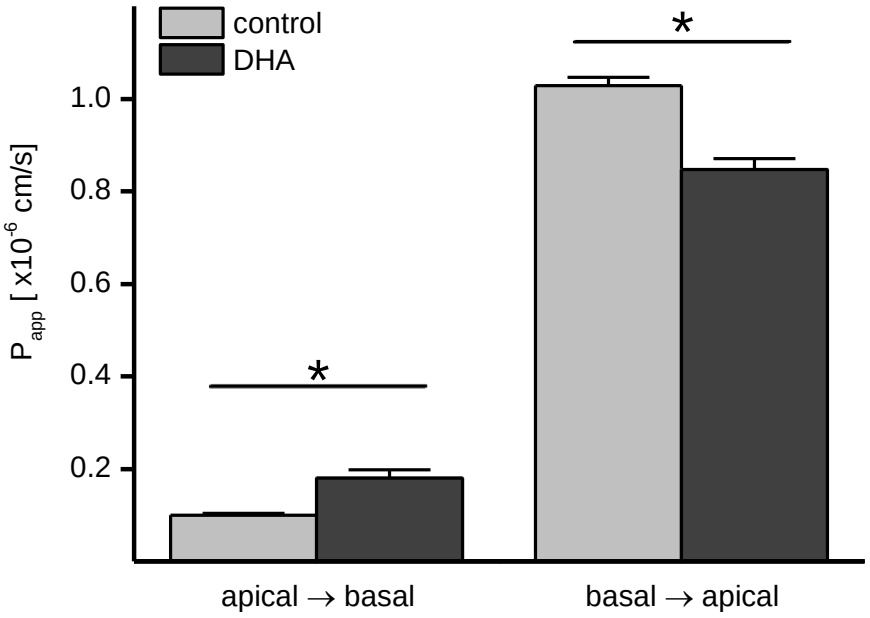

Figure 6.2; Apparent permeability rate of epicatechin across chronically DHA supplemented Caco-2 monolayers in uptake (apical → basal) and efflux (basal → apical)) direction. For details on conditions and analysis, see sections 2.3, 2.4 and 2.6. n = 6, N = 1; * = $p \leq 0.05$

To test whether the observed changes in epicatechin transport rate after DHA supplementation were due to a change in efflux transporter activity, transport was assessed in the presence and absence of a mix of three different inhibitors that target ABC efflux transporters. Cyclosporin A was included as an ABCB1 inhibitor (308), MK571 is reported to inhibit different transporters of the ABCC family (309) and apigenin is an inhibitor of ABCG2 (310). The presence of a combination of these three compounds reduced efflux of epicatechin across non-treated cell monolayers, but not across DHA treated Caco-2 cells, indicating that DHA treatment

already reduced activity of efflux transporters and the inhibitor mix was not able to reduce it further (figure 6.3).

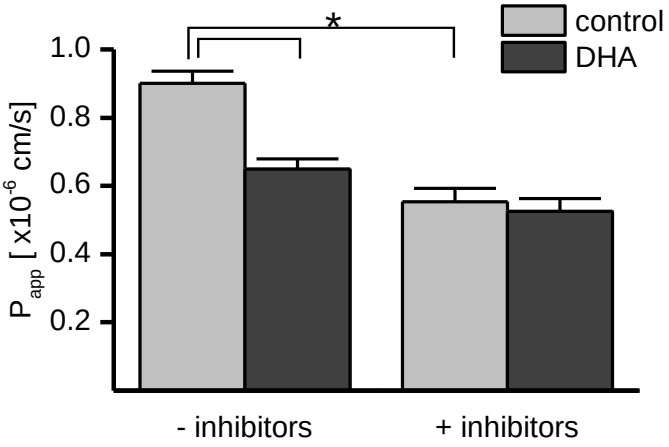

Figure 6.3; Impact of the presence of ABC transporter inhibitors apigenin (10 µM), MK571 (25 µM) and cyclosporine A (25 µM) on the basolateral to apical transport of epicatechin (200 µM) across DHA treated and non-treated Caco-2 monolayers. For details on conditions and analysis, see sections 2.3, 2.4 and 2.6. n = 3, N = 1; * = p ≤ 0.05

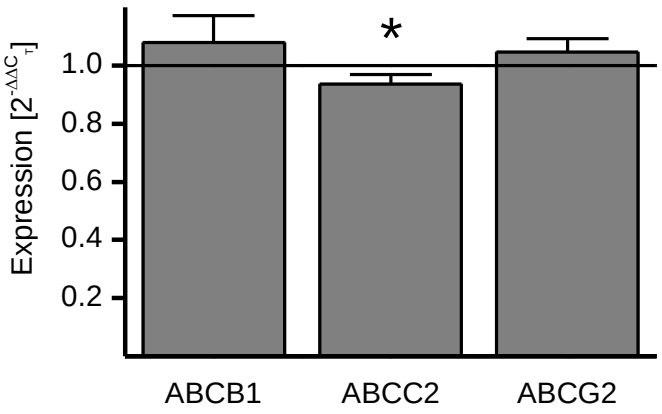

Figure 6.4; Impact of chronic DHA treatment on efflux transporter expression in Caco-2 cells. For details on conditions and analysis, see sections 2.3 and 2.8. n = 6, N = 1; * = p ≤ 0.05

There are different ways that DHA treatment could affect the efflux of epicatechin by ABC-transporters. One of them is downregulation of gene transcription. Figure 6.4

shows that chronic DHA supplementation had no significant impact on ABCB1 and ABCG2 mRNA levels but slightly reduced expression of ABCC2 by 6 ± 3 %.

6.3.2 Impact of ABC-transporter siRNA silencing on intracellular concentrations of epicatechin

As described above, it has previously been suggested that epicatechin is an allocrite of the apical efflux transporter ABCC2, mostly on the basis that co-application of the ABCC inhibitor MK571 increased epicatechin uptake. To investigate the involvement of ABCC2 but also of ABCB1 and ABCG2 in epicatechin transport further, expression of those three transporters was reduced by siRNA treatment of Caco-2 cells and the impact of transporter expression decrease on epicatechin uptake was investigated.

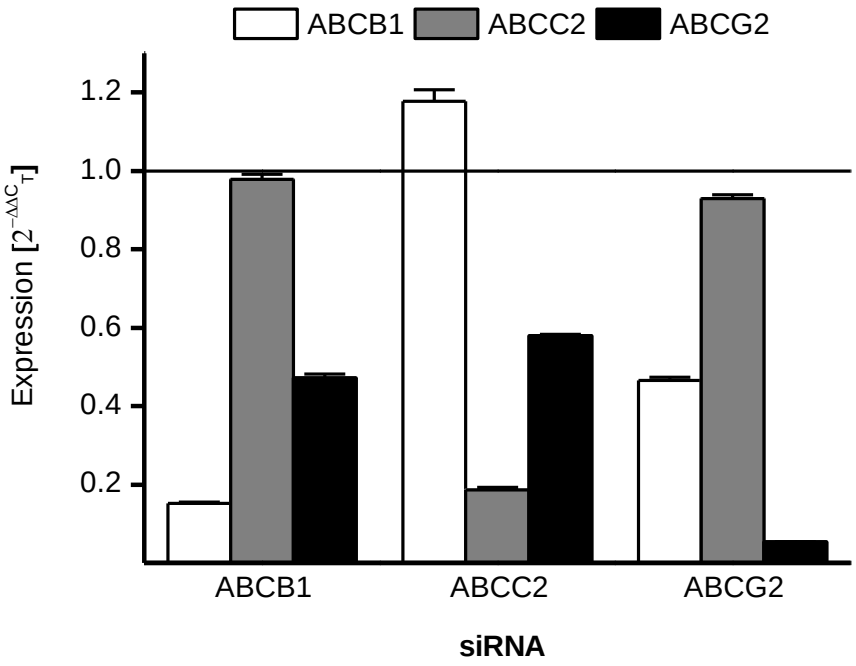

Figure 6.5; Impact of ABCB1, ABCC2 and ABCG2 siRNA treatment on gene expression of those transporters in Caco-2 cells. Gene expression was normalised to reference gene GAPDH and expression of the gene of interest in control incubations with negative control siRNA. For details on conditions and analysis, see sections 2.8 and 2.9. n = 3, N = 1

As shown in figure 6.5, there was an overlap in target specificity of the siRNA probes. They did not only repress mRNA levels of the one gene they were supposed to target, but siRNA targeted at ABCB1 also affected ABCG2 and vice versa. With ABCC2 siRNA treatment, mRNA levels of ABCG2 were also reduced whereas transcription of ABCB1 was slightly enhanced, perhaps a cellular mechanism to counteract the impact of siRNA treatment.

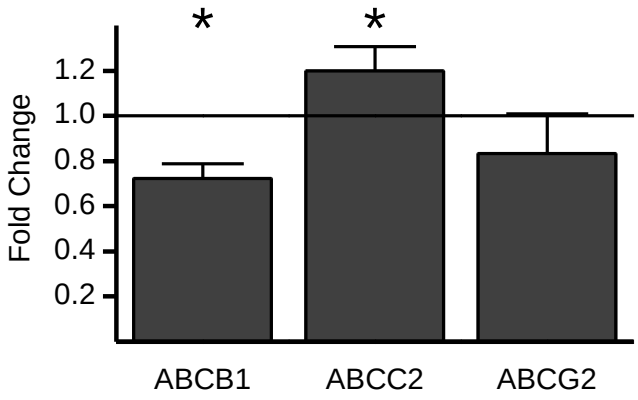

Figure 6.6; Impact of siRNA silencing of ABC-transporter expression on intracellular concentration of epicatechin. For details on conditions and analysis, see sections 2.6 and 2.9. n = 6, N = 1

Silencing of ABCC2 resulted in enhanced intracellular retention of epicatechin, compared to cells treated with negative control siRNA, indicating that this transporter is indeed involved in the efflux of epicatechin from Caco-2 cells (figure 6.6).

6.3.3 Identification of epicatechin metabolite transport by ABC-transporters through siRNA silencing

SiRNA silencing of ABC-transporters will not only affect efflux of epicatechin itself, but also its phase II metabolites. In chapter 5 it has already been shown that investigating metabolite transport using transport inhibitors can lead to misinterpretation, if the inhibitor has an effect on the formation of the metabolite itself and that fact is not taken into consideration. Assessing distribution of

metabolites between the cell lysate and supernatant after siRNA silencing of transporters is a more reliable way of studying the efflux mechanism of epicatechin metabolites. To achieve this, an LC-MS/MS method for analysis of green tea catechin metabolites in urine (140) was adopted and optimised for analysis of epicatechin metabolites in cell culture samples. Figure 6.7 shows sample chromatograms of different epicatechin conjugate traces.

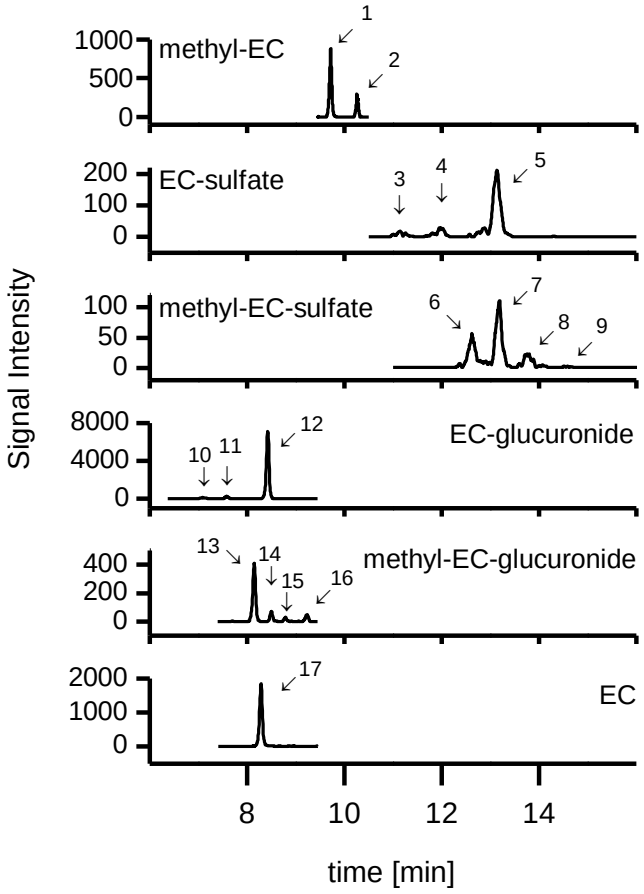

Figure 6.7; Traces of epicatechin metabolites analysed by LC-MS/MS. (1) 3′-*O*-methyl-EC, (2) 4′-*O*-methyl-EC [both m/z = 303 → 137], (3) EC-4′-sulfate, (4) EC-5-sulfate, (5) EC-3′-sulfate [all three m/z = 369 → 289], (6) 3′-*O*-methyl-EC-5-sulfate, (7) 3′-*O*-methyl-EC-7-sulfate, (8) 4′-*O*-methyl-EC-5-sulfate, (9) 4′-*O*-methyl-EC-7-sulfate [all four m/z = 383 → 303], (10) EC-7-β-D-glucuronide, (11) EC-4′-β-D-glucuronide, (12) EC-3′-β-D-glucuronide [all three m/z = 465 → 289], (13) 3′-*O*-methyl-EC-7-β-D-glucuronide, (14) 4′-*O*-methyl-EC-5-β-D-glucuronide, (15) 4′-*O*-methyl-EC-7-β-D-glucuronide, (16) 4′-*O*-methyl-EC-3′-β-D-glucuronide [all four m/z = 465 → 289], (17) EC (10 pmol loaded) [m/z = 289 → 245], For details on conditions and analysis, see sections 2.4 and 2.7.

As no original standards were available, identification of structural isomers was achieved by comparison to publications where they were so and which employed similar chromatographic conditions as used here, namely Kuhnle et al. 2000 (311) and Actis-Goretta et al. 2012 (312). Also, no absolute quantification of metabolites was possible, only relative quantification by comparing peak areas between different

treatments. Figure 6.8 gives the structure of (-)-epicatechin and the preferred sides of conjugation.

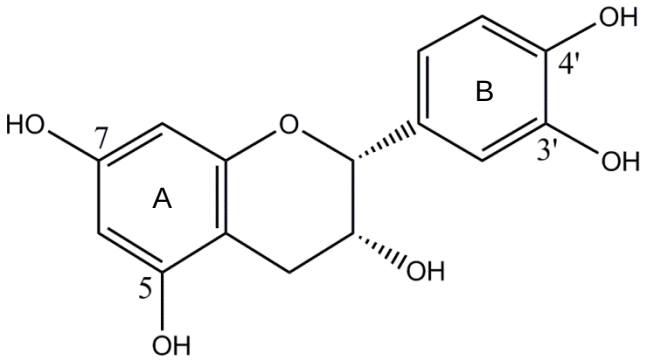

Figure 6.8; Structure of (-)-epicatechin with preferred sides of conjugation labelled.

Transport of epicatechin metabolites grown on solid supports was investigated by comparing efflux of metabolites from the cytosol to the apical side ($J_{c \rightarrow a}$) and intracellular metabolite concentrations.

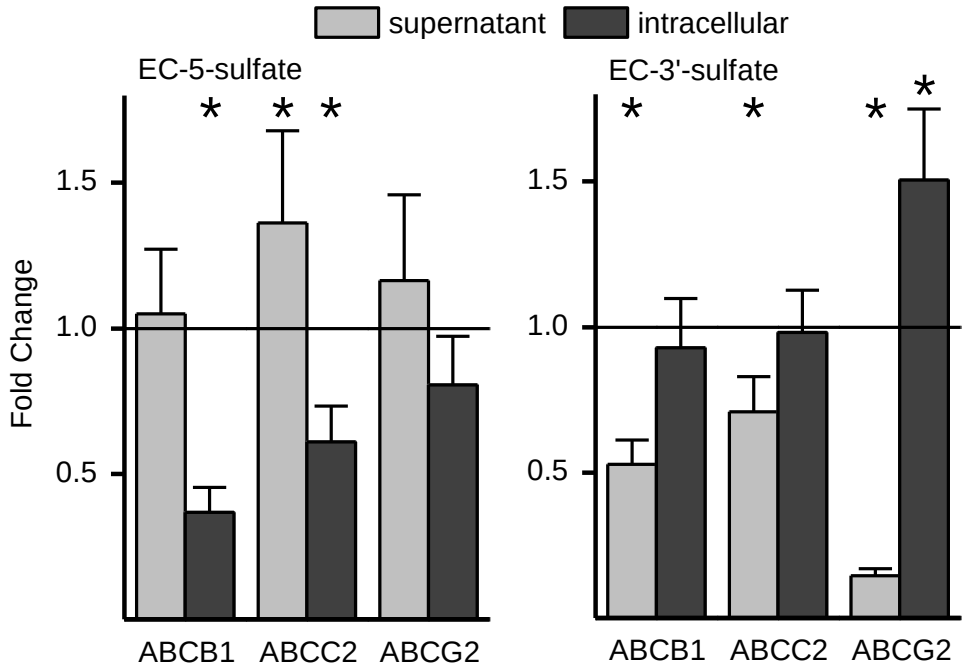

Figure 6.9; Impact of efflux transporter siRNA silencing on epicatechin-sulfate levels in Caco-2 cell lysate and cell culture supernatant. For details on conditions and analysis, see sections 2.7 and 2.9. n = 6, N = 1; * = $p \leq 0.05$

Silencing of ABCG2 resulted in a decreased epicatechin-3ˈ-sulfate efflux and increased intracellular retention, indicating that this compound is an allocrite of ABCG2. The decrease in efflux with ABCB1 and ABCC2 siRNA treatment will most likely stem from reduced ABCG2 expression that is a side effect of those two probes. Levels of epicatechin-5-sulfate are much lower than those of the 3ˈ-isomer and siRNA silencing did not indicate involvement of either transporter in efflux of that compound. The third stereoisomer, epicatechin-4ˈ-sulfate was not detected in the supernatant of five day old cultures and therefore not taken into consideration (figure 6.9).

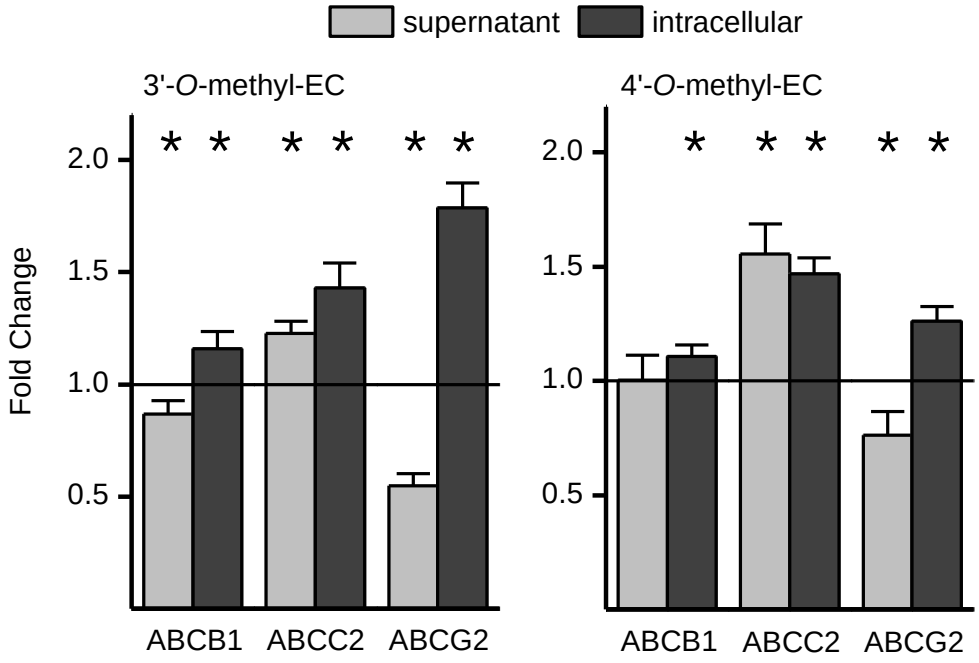

Figure 6.10; Impact of efflux transporter siRNA silencing on *O*-methyl-epicatechin levels in Caco-2 cell lysate and cell culture supernatant. For details on conditions and analysis, see sections 2.7 and 2.9. n = 6, N = 1; * = p ≤ 0.05

Both levels of the 3ˈ- and the 4ˈ-*O*-methyl-epicatechin form were reduced in the supernatant and elevated in cell lysate samples after siRNA silencing of ABCG2. The increase of methyl forms in both types of sample after ABCC2 silencing could stem from the increased intracellular levels of the aglycone with that treatment.

Decreased efflux of 3ˈ-*O*-methyl-epicatechin after ABCB1 silencing could again be due to decreased ABCG2 expression with that treatment (figure 6.10).

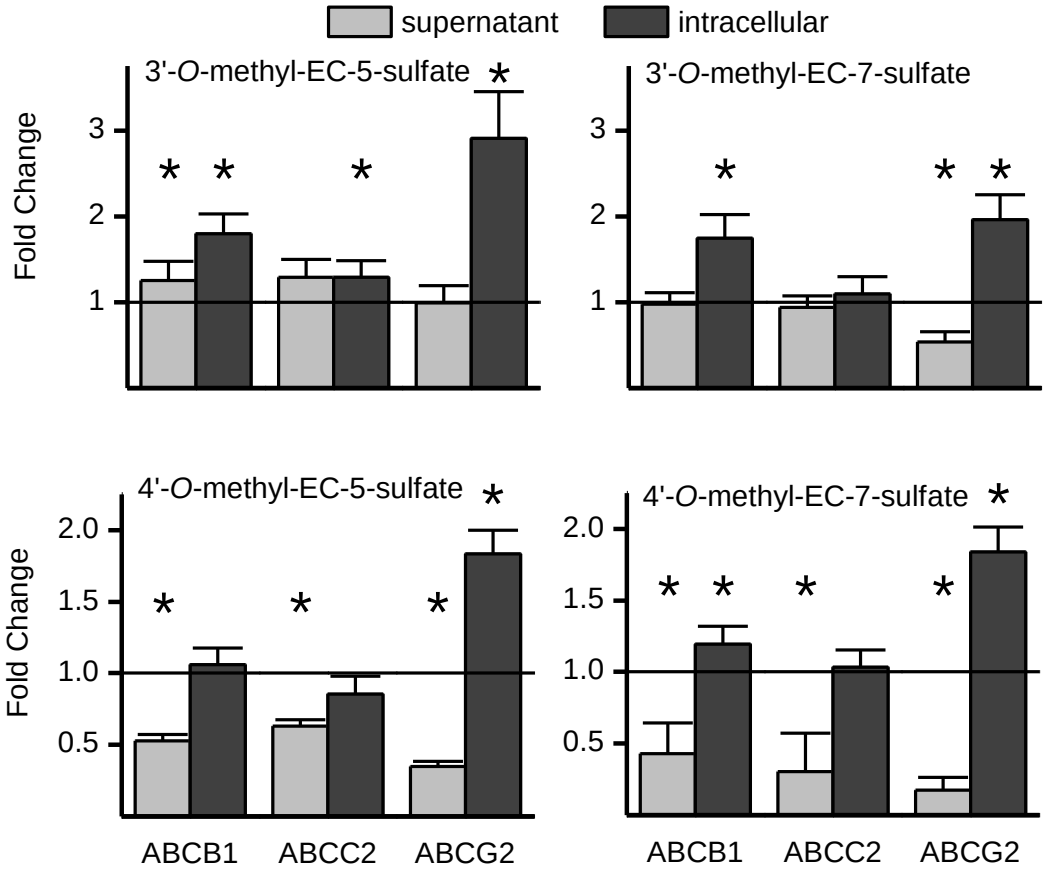

Figure 6.11; Impact of efflux transporter siRNA silencing on *O*-methyl-epicatechin-sulfate levels in Caco-2 cell lysate and cell culture supernatant. For details on conditions and analysis, see sections 2.7 and 2.9. n = 6, N = 1; * = $p \leq 0.05$

Distribution of three out of the four *O*-methyl-epicatechin-sulfate isomers, detected in Caco-2 cell culture samples, was sensitive to ABCG2 silencing, only 3ˈ-*O*-methyl-epicatechin-5-sulfate levels were elevated in cell samples but not decreased in the supernatant (figure 3.11).

In summary, it appears that all three types of epicatechin metabolites presented here are allocrites of ABCG2. Two other types of epicatechin metabolite, the glucuronic acid conjugate and the *O*-methyl-epicatechin-β-D-glucuronide, were not investigated in this context as they are mainly found intracellularly and in the

basolateral well of Caco-2 cells grown on transwell inserts (see below). Determining an impact of apical efflux transporter silencing on these compounds is difficult as they are either found not at all, or only in very low amounts in the apical supernatant, and it is also physiologically irrelevant, as these transporters don't seem to affect the bioavailability of those conjugates.

6.3.4 Impact of chronic DHA treatment on transport of epicatechin metabolites.

Metabolism of epicatechin by chronically DHA treated Caco-2 cells was assessed to gain an insight into how the fatty acid affects metabolite transport, and with that, bioavailability of the compound.

The impact of transporter silencing, described in section 6.3.3, was investigated in Caco-2 cultures five days after seeding. As already described in chapter 3, the expression and activity of many metabolising enzymes changes during cell differentiation. Therefore, metabolism of epicatechin was now compared between Caco-2 cultures five and 22 days after seeding. The change in relative concentration (see section 2.7 for calculations) of metabolites in intracellular and supernatant samples over time is presented for the most abundant conjugate of each of the three types of epicatechin metabolite presented above.

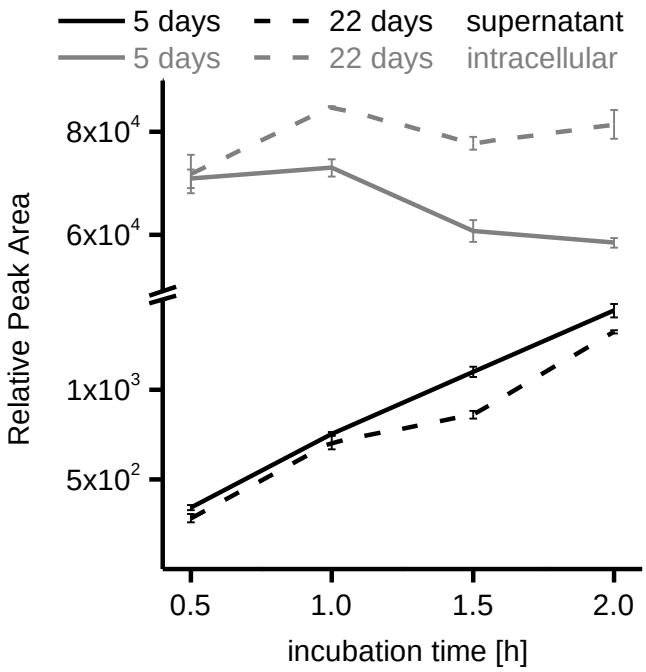

Figure 6.12; Formation of 3'-*O*-methyl-epicatechin in non-differentiated (5 days) and differentiated (22 days) Caco-2 cells. For details on conditions and analysis, see sections 2.3, 2.4 and 2.7. n = 3, N = 1

Relative 3'-*O*-methyl-epicatechin concentrations in the supernatant steadily increased over time, with slightly higher levels in cultures of non-differentiated cells. Intracellular conjugate levels did not consistently rise after the first time point, in non-differentiated cells 3'-*O*-methyl-epicatechin concentrations even slightly decreased over time (figure 6.12).

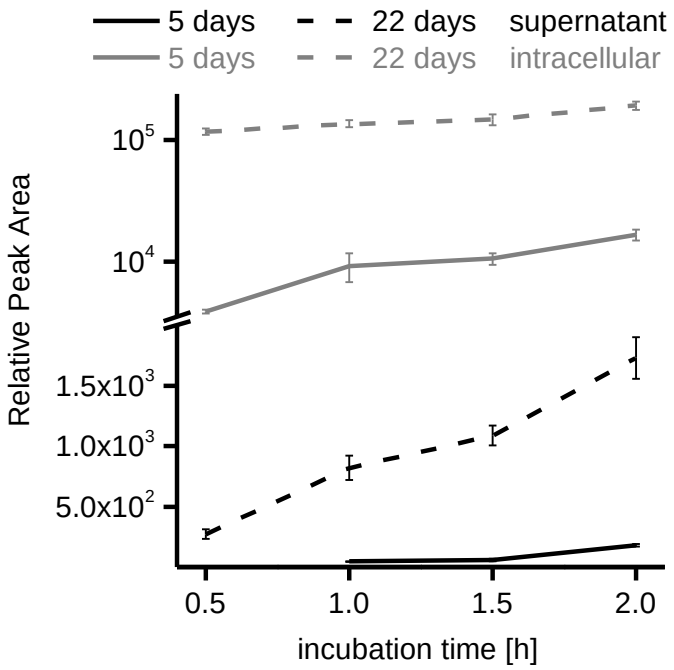

Figure 6.13; Formation of epicatechin-3′-sulfate in non-differentiated (5 days) and differentiated (22 days) Caco-2 cells. For details on conditions and analysis, see sections 2.3, 2.4 and 2.7. n = 3, N = 1

In contrast to *O*-methyl-epicatechin, levels of epicatechin-3′-sulfate were much higher in differentiated Caco-2 cultures, compared to cultures 5 days after seeding. As with *O*-methyl-epicatechin, sulphate levels in the supernatant steadily increased over time whereas intracellular concentrations were more stable. In five day old cultures, the conjugates were only detected in the supernatant after 1 h of incubation (figure 6.13).

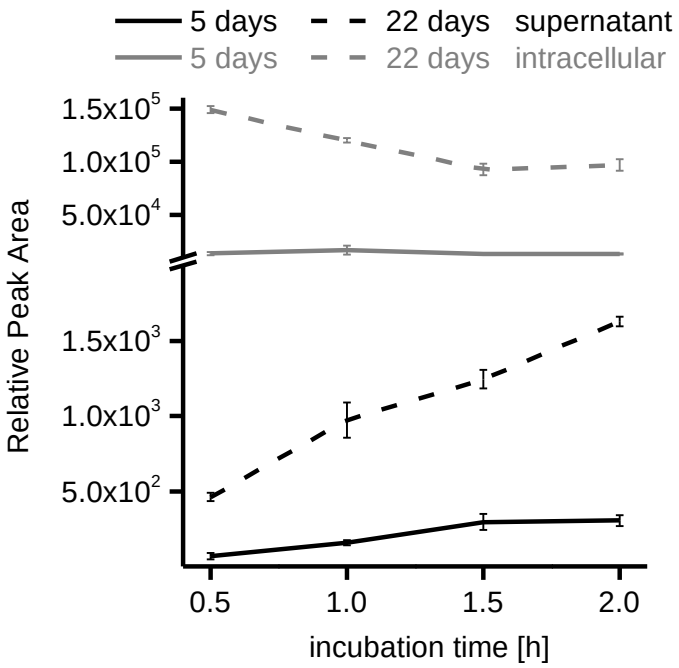

Figure 6.14; Formation of 3'-*O*-methyl-epicatechin-5-sulfate in non-differentiated (5 days) and differentiated (22 days) Caco-2 cells. For details on conditions and analysis, see sections 2.3, 2.4 and 2.7. n = 3, N = 1

Just like with sulfoconjugates, levels of 3'-*O*-methyl-epicatechin-5-sulfate were higher in differentiated cultures than in non-differentiated cultures. As with O-methyl-epicatechin, intracellular levels were very stable over time, and in 22 day old cultures, they even decreased slightly. In the supernatant, conjugate concentrations increased over time (figure 6.14).

In conclusion, comparison of epicatechin metabolism in Caco-2 cells five and 22 days after seeding has shown that COMT activity does not change with cell differentiation whereas SULT activity or expression increases.

Next, the impact of chronic DHA supplementation on epicatechin metabolism was investigated.

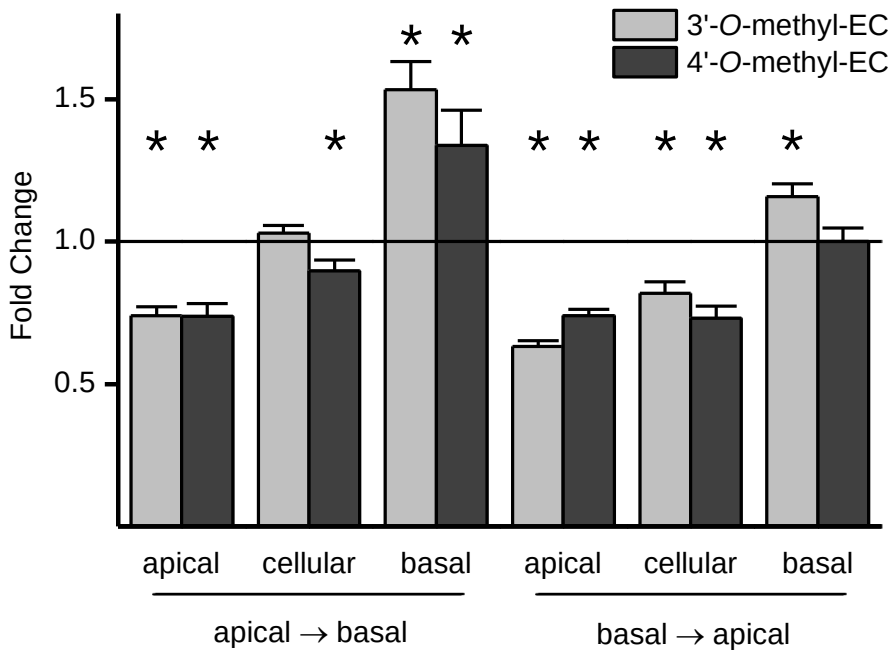

Figure 6.15; Impact of chronic DHA supplementation on levels of *O*-methyl-epicatechin in different compartments. Epicatechin (200 µM) was applied either to the apical side (apical → basal) or to the basolateral side (basal → apical). For details on conditions and analysis, see sections 2.3, 2.4 and 2.7. n = 6, N = 1; * = p ≤ 0.05

DHA treatment reduced efflux of *O*-methyl-conjugates to the apical side and increased levels in the basolateral compartment. It also decreased intracellular levels of *O*-methyl-epicatechin when the aglycone was applied to the basolateral side (figure 6.15).

0

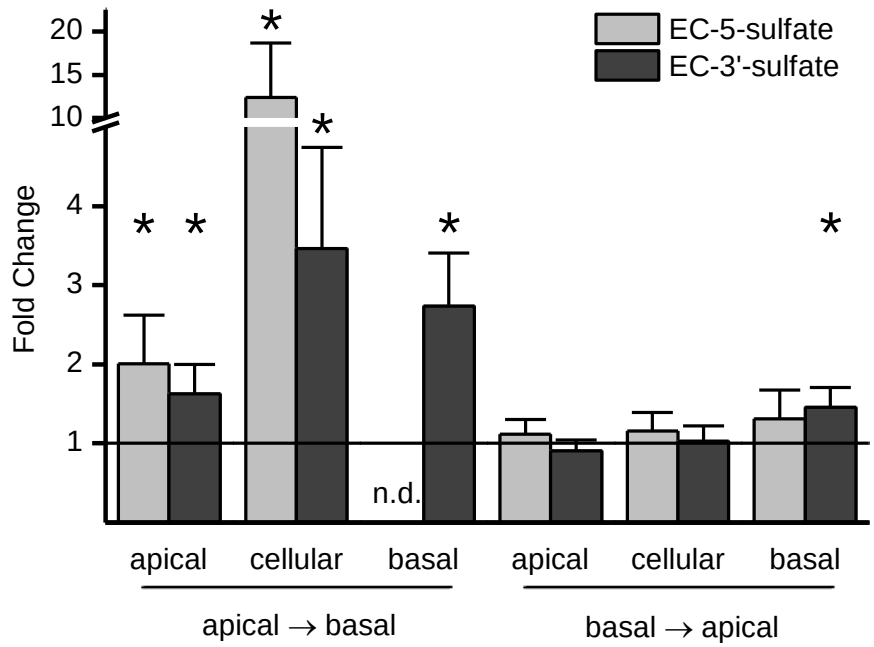

Figure 6.16; Impact of chronic DHA supplementation on levels of epicatechin-sulfate in different compartments. Epicatechin (200 µM) was applied either to the apical side (apical → basal) or to the basolateral side (basal → apical). For details on conditions and analysis, see sections 2.3, 2.4 and 2.7. n.d. = not detected; n = 6, N = 1; * = $p \leq 0.05$

DHA treatment greatly increased epicatechin-sulfate levels in all compartments when the aglycone was applied apically, but not when applied to the basolateral side (figure 6.16).

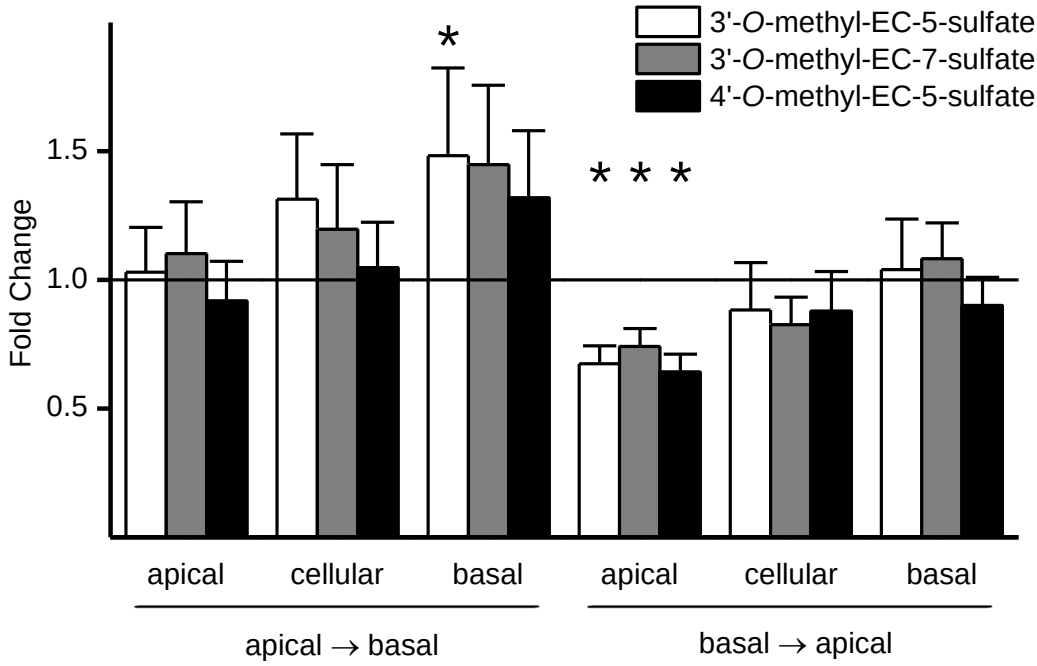

Figure 6.17; Impact of chronic DHA supplementation on levels of *O*-methyl-epicatechin-sulfate in different compartments. Epicatechin (200 µM) was applied either to the apical side (apical → basal) or to the basolateral side (basal → apical). For details on conditions and analysis, see sections 2.3, 2.4 and 2.7. n = 6, N = 1; * = $p \leq 0.05$

O-methyl-epicatechin-sulfate export to the apical side was decreased when epicatechin was applied to the basolateral side and levels were increased in the basolateral chamber when the aglycone was applied to the apical side (figure 6.17).

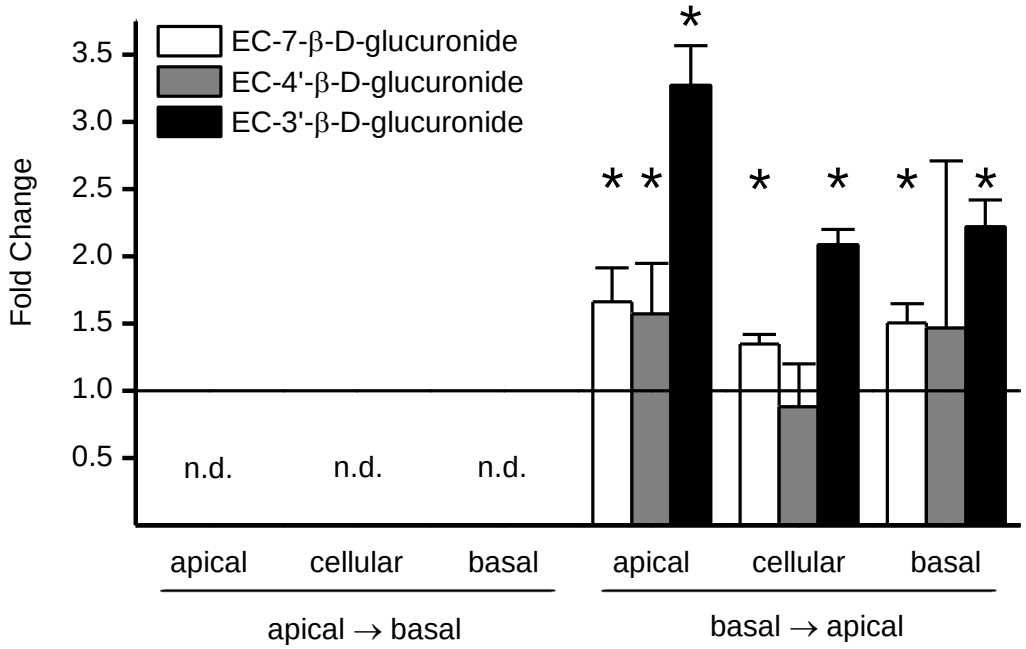

Figure 6.18; Impact of chronic DHA supplementation on levels of epicatechin-β-D-glucuronide in different compartments. Epicatechin (200 µM) was applied either to the apical side (apical → basal) or to the basolateral side (basal → apical). For details on conditions and analysis, see sections 2.3, 2.4 and 2.7. n.d. = not detected; n = 6, N = 1; * = $p \leq 0.05$

No epicatechin-β-D-glucuronide forms were detected when the aglycone was applied to the apical side, only when applied to the basolateral side. DHA treatment increased levels in all compartments. After chronic DHA supplementation, the most abundant form, epicatechin-3ˈ-β-D-glucuronide, was also detected intracellularly when the aglycone was applied apically but not without fatty acid treatment.

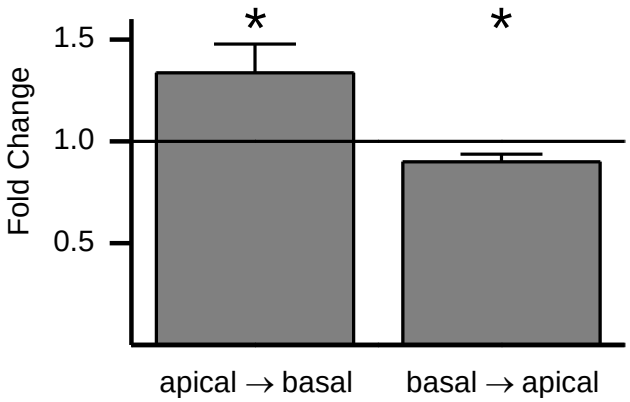

Figure 6.19; Impact of chronic DHA supplementation on intracellular concentration of epicatechin. Epicatechin (200 µM) was applied either to the apical side (apical → basal) or to the basolateral side (basal → apical). For details on conditions and analysis, see sections 2.3, 2.4 and 2.7. n = 6, N = 1; * = $p \leq 0.05$

Chronic DHA supplementation decreased intracellular epicatechin levels when applied to the basolateral side, but increased intracellular levels, when applied to the apical side. This behaviour agrees with the transport of epicatechin, where DHA has the same effect of lowering efflux and increasing uptake transport. But if that effect really is caused by a change in efflux transporter activity, then it would be expected that in both cases, uptake and efflux transport, intracellular levels of epicatechin would increase. Decreased intracellular aglycone levels, after transport in the basolateral to apical direction, could be explained by either increased apical efflux or decreased basolateral uptake. Since apical levels are also decreased with DHA treatment, the first explanation is highly unlikely. The results presented in figure 6.19 do therefore support a mechanism of decreased basolateral uptake. Figure 6.20 shows epicatechin concentrations detected in Caco-2 cells after uptake and efflux transport (for calculation of intracellular concentrations see section 2.7). In both cases, a 200 µM solution of epicatechin was applied. After apical to basolateral transport ($J_{a \rightarrow b}$), an intracellular epicatechin concentration of 54 µM ± 3 µM was detected and after basolateral to apical transport ($J_{b \rightarrow a}$) it was 632 µM ± 6 µM (figure 6.20). It is very hard to reconcile the concept of a reduced bioavailability of

epicatechin due to its strong affinity for active efflux transporters with an intracellular accumulation of that compound to over three times the extracellular concentration. If those two mechanisms should co-exist, and the fact that inhibition or silencing of efflux transporters does indeed reduce epicatechin transport to the apical side is in support of the theory, than it must be assumed that epicatechin taken up from the basolateral side is localised intracellularly in a way that the aglycone is not within reach of apical membrane transporters.

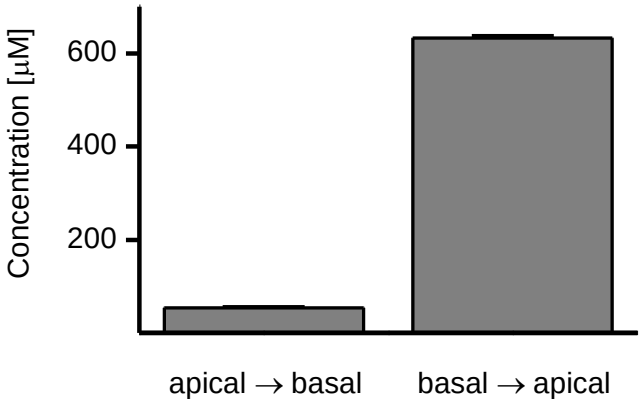

Figure 6.20; Impact of transport direction on intracellular concentrations of epicatechin. Epicatechin (200 µM) was applied either to the apical side (apical → basal) or to the basolateral side (basal → apical). For details on conditions and analysis, see sections 2.4 and 2.7. n = 6, N = 1

If epicatechin taken up from the basolateral side is distributed within the cells in the same way as epicatechin taken up from the apical side, than substrate concentrations for phase II enzymes would be over ten times higher in the efflux transport direction than the uptake direction. Consequently, levels of metabolites would be expected to reflect this difference. Figures 6.21 to 6.23 show the relative concentrations of metabolites detected after efflux transport (aglycone applied to the basolateral side) normalised to concentrations after uptake transport (aglycone applied to the apical side).

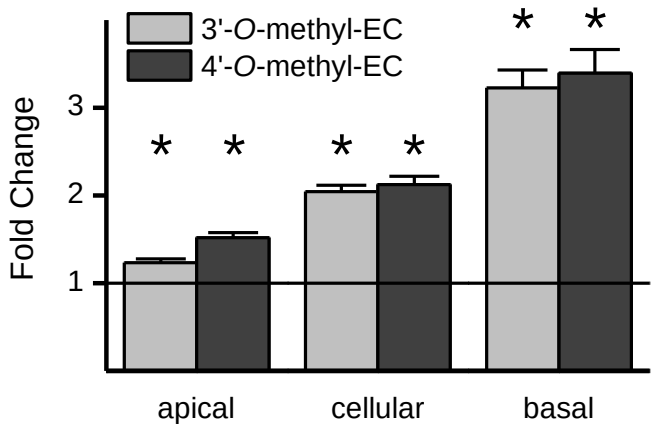

Figure 6.21; Impact of transport direction on concentrations of *O*-methyl-epicatechin. Metabolite levels detected after efflux transport were normalised to levels detected after uptake transport. For details on conditions and analysis, see sections 2.4 and 2.7. n = 6, N = 1; * = p ≤ 0.05

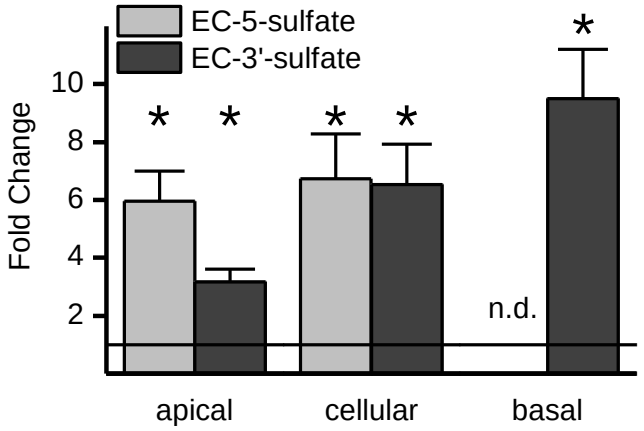

Figure 6.22; Impact of transport direction on concentrations of epicatechin-sulfate. Metabolite levels detected after efflux transport were normalised to levels detected after uptake transport. For details on conditions and analysis, see sections 2.4 and 2.7. n.d. = not detected; n = 6, N = 1; * = p ≤ 0.05

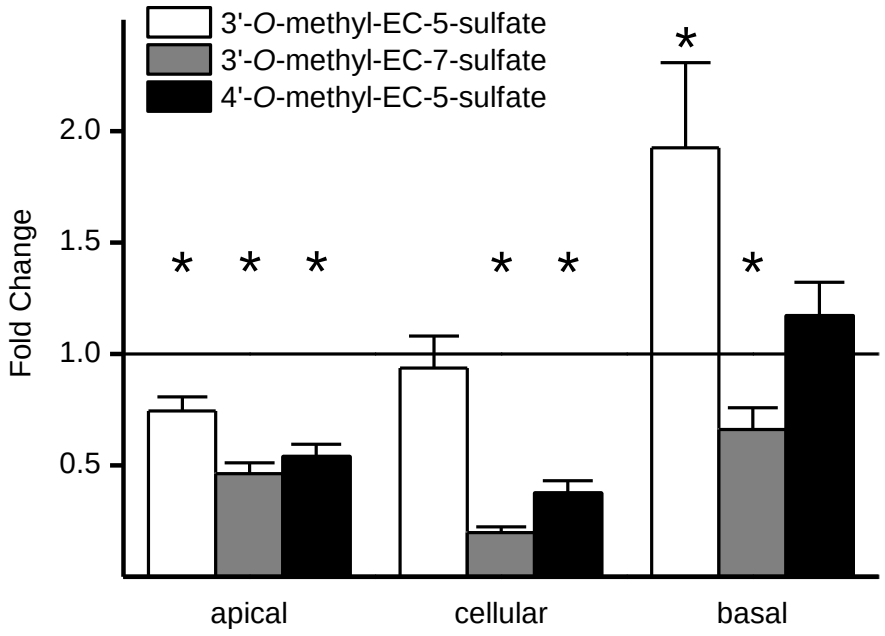

Figure 6.23; Impact of transport direction on concentrations of *O*-methyl-epicatechin-sulfate. Metabolite levels detected after efflux transport were normalised to levels detected after uptake transport. For details on conditions and analysis, see sections 2.4 and 2.7. n = 6, N = 1; * = $p \leq 0.05$

On average, *O*-methyl-conjugates were two times more abundant when Caco-2 cells were incubated with epicatechin from the basolateral side, than when incubated from the apical side (figure 6.21). Sulfoconjugates were six times more abundant after efflux transport (figure 6.22) but only half the amount of double-conjugated forms were detected (figure 6.23). Therefore, overall metabolite formation does not reflect the much greater abundance of substrate in efflux direction. Only sulfonation of epicatechin increased to an extent that would correlate with ten times higher intracellular substrate concentrations.

There also is no obvious link between the impact of DHA on intracellular epicatechin concentrations and metabolism. As shown in figure 6.19, DHA supplementation increases intracellular epicatechin concentrations with uptake transport, but decreases them with efflux transport. Sulfoconjugate levels are also increased after uptake transport, but not decreased after efflux. *O*-methyl-epicatechin levels show reduced efflux to the apical side, which corresponds with a decrease in apical efflux

transporter activity by DHA treatment, and overall reduced conjugate levels after efflux transport. Perhaps the increase in SULT activity is again due to a direct impact of DHA on enzyme expression, as already discussed in chapter 5. Epicatechin and ferulic acid sulfonation are both catalysed by SULT1A1 and SULT1A3 (313). Since DHA supplementation increased production of sulfoconjugates of both phenolics, the impact of that fatty acid on expression of SULT1A1, which has a much higher affinity for epicatechin than SULT1A3, was investigated. But although DHA treatment increased sulfoconjugation, the expression of SULT1A1 was actually decreased by 14 ± 11 %. Therefore, either SULT1A3 is greatly affected by DHA treatment, which still needs to be investigated, or DHA has an impact on protein translation or substrate accessibility. Both SULT and COMT enzymes exist as cytosolic and membrane bound forms. Xenobiotic conjugating SULTs, such as SULT1A1 and SULT1A3, are cytosolic (314). Both cytosolic COMT (S-COMT) and membrane bound COMT (MB-COMT) are translated from the same gene, regulated by differential promoter activity (315). In all tissues, except brain, COMT is predominantly expressed as the cytosolic form. Since both SULT and COMT are cytosolic, they should both encounter the same substrate levels. But SULT seems to be much more susceptible to changing substrate levels due to DHA treatment. In this respect, sulfoconjugates behave just as glucuronic acid conjugates, which are found in very low amounts intracellularly when epicatechin is applied to the apical side, but in much higher amounts and in all compartments when epicatechin is applied to the basolateral side. The UGT enzyme is not cytosolic but ER membrane resident. So in summary, UGT and SULT are sensitive to intracellular concentration changes, COMT much less so. Interestingly, formation of the double conjugate is actually decreased with the much higher intracellular epicatechin levels after efflux transport, even though levels of the individual conjugates are increased.

6.3.5 Impact of methyl-β-cyclodextrin treatment on epicatechin transport.

The original assumption that DHA supplementation decreases epicatechin efflux by affecting apical transporter activity was tested further through incubation of Caco-2 cells with methyl-β-cyclodextrin. As already mentioned in chapter 4 and 5, methyl-β-cyclodextrin treatment removes membrane cholesterol which results in disruption of DRM and reduced activity of DRM residing transporters. Figure 6.24 summarises the impact of that treatment on epicatechin metabolite levels.

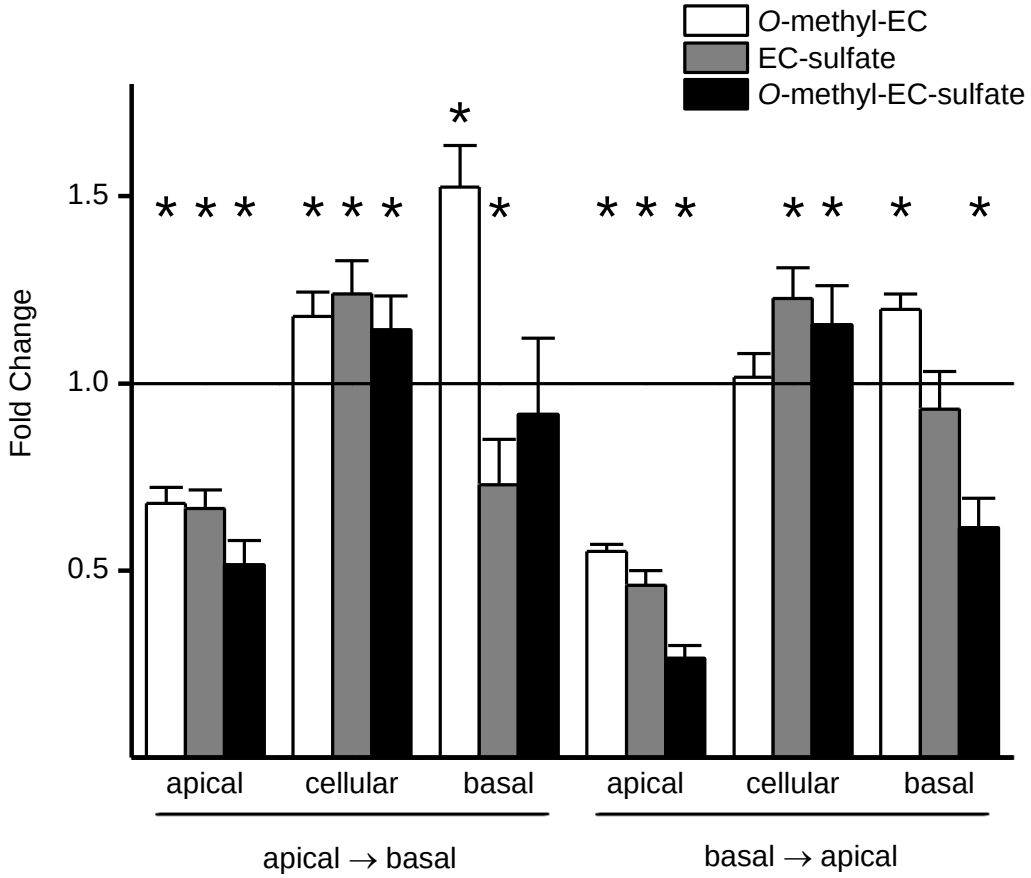

Figure 6.24; Impact of methyl-β-cyclodextrin pre-treatment on transport of epicatechin metabolites. For details on conditions and analysis, see sections 2.4, 2.7 and 2.13. n = 6, N = 1; * = $p \leq 0.05$

Apical efflux of all metabolites was strongly inhibited, just as would be assumed with decreased efflux transporter activity. Intracellular metabolite levels were increased, which could stem from an accumulation of metabolites due to decreased efflux or

from increased substrate levels. Figure 6.25 shows changes in epicatechin levels induced by methyl-β-cyclodextrin treatment.

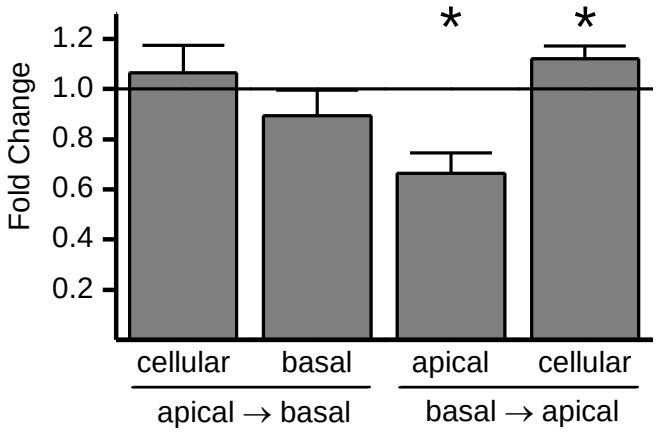

Figure 6.25; Impact of methyl-β-cyclodextrin pre-treatment on transport of epicatechin. For details on conditions and analysis, see sections 2.4, 2.7 and 2.13. n = 6; * = p ≤ 0.05

Cyclodextrin treatment did not significantly change epicatechin transport in uptake direction but reduced apical efflux and increased intracellular levels in the efflux direction.

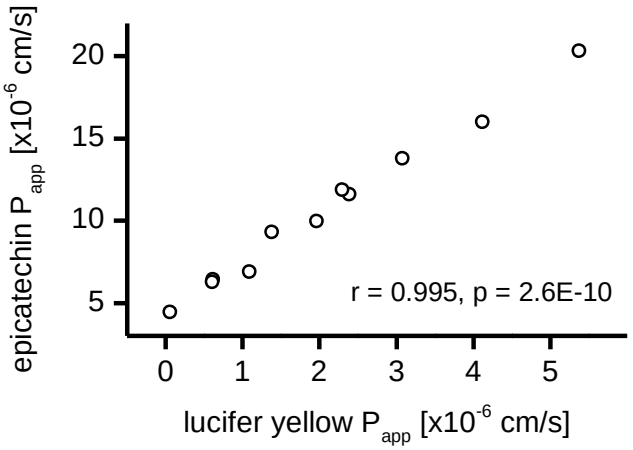

Figure 6.26; Correlation of epicatechin uptake with lucifer yellow transport. For details on transport and analysis, see sections 2.4, 2.6 and 2.13.

As already shown in chapter 5, cyclodextrin treatment increased diffusion rates of the paracellular marker lucifer yellow. Epicatechin permeation rates in uptake direction correlated very well with lucifer yellow permeation rates, which indicates that epicatechin absorption occurs paracellularly (figure 6.26).

6.4 Discussion

For this chapter, the impact of dietary fatty acids on epicatechin basolateral to apical and apical to basolateral transport in the Caco-2 enterocyte model was investigated. The reported limitation of epicatechin bioavailability due to active efflux by ABC-transporters was addressed by first screening fatty acids for their ability to increase uptake and to decrease efflux. Only chronic supplementation with arachidonic acid and DHA resulted in the desired effect. Interestingly, when modification of the cellular lipid composition was investigated, treatment of cells with those two fatty acids resulted in an almost identical lipid profile regarding acyl chain saturation (see figures 3.6 to 3.8). DHA was chosen to study the mechanism of the observed effect further. Epicatechin permeation rate was ten times higher in efflux than in uptake direction which agrees with previous reports on this topic. Zhang *et al.* even found a 22 times higher efflux than uptake rate for epicatechin in Caco-2 cells and pre-incubation with the ABCC2 inhibitor MK571 reduced efflux to only 1.5 times the uptake rate, which concurrently increased 2.5 fold (300). However, a different study conducted by Tian *et al.* found an almost equal transport rate for uptake and efflux in the same cell line with apparent permeability rates that lie between the ones that were observed here and in the above cited study (316). Tian and colleagues reported a P_{app} of 0.6×10^{-6} cm/s for uptake and a P_{app} of 0.7×10^{-6} cm/s for efflux, whereas Zhang *et al.* observed an uptake rate of $P_{app} = 0.14 \times 10^{-6}$ cm/s and an efflux rate of $P_{app} = 3 \times 10^{-6}$ cm/s, which agrees with the epicatechin transport rates reported in the current chapter of $P_{app} = 0.1 \times 10^{-6}$ cm/s in uptake direction and $P_{app} = 1 \times 10^{-6}$ cm/s in efflux direction. Since Tian et al also observed an intracellular accumulation of epicatechin of 5 % of the applied dose in uptake direction but the intracellular amount presented in figure 6.20 is only 0.1 % of the applied dose at the same incubation time, it seems that the batch of Caco-2 cells used by Tian *et al.* exhibit much higher apical uptake or lower apical efflux than the batch used here. ABC efflux transporter expression increases

in Caco-2 cells with time in culture but not with passage number (317). As both studies cited above as well as the work described in this chapter were carried out 22 days after seeding, a difference in differentiation status should not be the reason for different uptake rates. The only major difference in experimental set-up is that Tian *et al.* cultured Caco-2 cells on membranes with a pore diameter of 3 µm whereas most transport studies use permeable supports with a pore diameter of 0.4 µm. The larger pore diameter is more typically used for cell migration assays (318, 319), and so perhaps this is the reason for the different transport rates observed.

The transport profile of epicatechin described here for the Caco-2 cell model fits very well with the hypothesis that apical efflux transporters are the cause for a limited uptake of that compound in the small intestine. Also, the impact of DHA treatment on transport seems to agree with the idea that a modification of membrane lipids results in an activity decrease of efflux transporters which enhances epicatechin bioavailability. However, the fact that epicatechin accumulates intracellularly up to six times the extracellular concentration seems to stand in sharp contrast to the above described mechanism. In that case, uptake into cell to such high concentration occurs against the concentration gradient which indicates that active transport is required to achieve this. The only other explanation would be a mechanism of different local concentrations within the cell which would require low concentrations of the compound towards the cell membrane so that passive diffusion can occur along the concentration gradient. The ChEMBL Database gives the calculated partition coefficient of epicatechin as logP = 2.02 (320) and the dissociation constants of the four hydroxyl group protons at the A and B phenyl-rings were determined experimentally as $pK_{a1} = 8.72$, $pK_{a2} = 9.49$, $pK_{a3} = 11.23$ and $pK_{a4} = 13.4$ (321). All transport studies described in this and previous chapters were carried out at pH = 7.4, which means that epicatechin will have been almost entirely protonated and thus should be able to cross the plasma membrane by passive diffusion. Inside the cell, the compound would then have to

accumulate in a restricted area to a much higher concentrations than detected in whole cell lysate, perhaps through binding to certain structures or uptake into specific organelles. Since epicatechin is able to emit a fluorescence signal, it would be of great interest to image epicatechin loaded cells and observe whether this compound does indeed accumulate in certain cellular structures. The limitation to this approach is the low excitation wavelength of epicatechin of around λ = 230 nm. Most fluorescence microscopes have a laser at 405 nm as the lowest excitation wavelength, which unfortunately is too high to carry out this experiment. Uptake from both the apical and basolateral side can occur by cytosis. There are different mechanisms how this process is initiated but they all have in common that they start with an invagination at the plasma membrane that is loaded with cargo, which could be membrane proteins, extracellular particles or fluid, and that then buds of and fuses with the early endosome. From the early endosome vesicles are either directed to the late endosome or lysosome, recycled back to the place of origin, sorted in the trans-Golgi network or, in polarised cells, routed towards the opposite membrane (322).

Uptake of nutrients in the intestine can occur via transcytosis. An example is cobalamin or vitamin B12, which is taken up at the luminal side bound to the cobalamin gastric intrinsic factor and then transferred to transcobalamin in the late endosomal compartment from which it is released when it reaches the serosal side (323, 324). But although endo- or transcytosis originating from the apical membrane has been investigated much more extensively than transport from the basolateral side, the latter one is by no means less important. Especially in cells with a polarised morphology, like the Caco-2 cell line, transcytosis is crucial for establishing and maintaining the specific distribution of receptors and transporters between the apical and basolateral membrane. In undifferentiated Caco-2 cells, membrane proteins are still uniformly distributed in the plasma membrane but after connection of tight junctions and with increasing time in culture, polarity is established by shuttling

proteins to either apical or basolateral side via transcytosis (284, 325). Newly synthesised membrane proteins are mostly sorted in the trans-Golgi network and packed into vesicles that eventually fuse with their destination membrane. But there is also an 'indirect pathway' in which apically targeted proteins are first transported to the basolateral side and then re-routed to their final destination through transcytosis (326, 327). As cytotic transport is an important factor in polarised cells, such a mechanism may account for the intracellular accumulation of epicatechin. It was shown that basolaterally endocytosed compounds can accumulate in intracellular compartments if their release to the apical side or into the lysosome is disturbed (325, 328). Marsh *et al.* measured the uptake rate of fluid phase by endocytosis in Baby Hamster Kidney (BHK) cells with the help of labelled solutes and found it to be ~ 0.37 µL per h and per 10^7 cells (329). In Caco-2 cell monolayers, as used for results presented in figure 6.20, there are approximately 10^6 cells per well, which would equal to an uptake of 0.037 µL per well. With a calculated cell layer volume of 7 µL, this would result in an intracellular epicatechin concentration of ~ 1 µM due to pinocytosis. Even if one considers differences in endocytosis rates for different cell types, it is unlikely that this transport mechanism is a major contribution to the ~ 600 µM epicatechin found intracellularly after efflux transport. Therefore another mechanism must be responsible for epicatechin uptake at the basolateral membrane.

After 90 min of epicatechin transport, none of the compartments had reached equilibrium. Figure 6.27 depicts the concentrations detected in the apical and basolateral well and in the cell lysate.

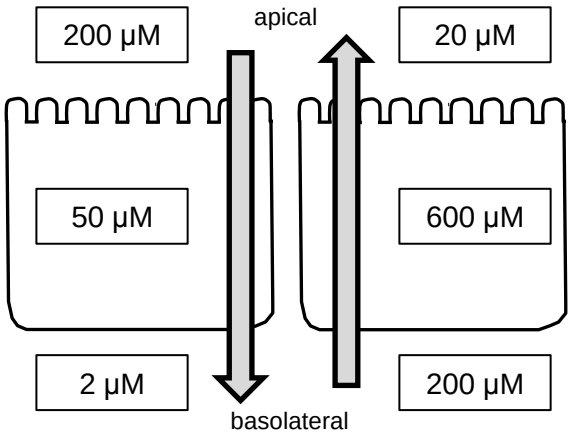

Figure 6.27; Epicatechin concentrations after 90 min of uptake or efflux transport. Arrows indicate transport direction.

With apical to basolateral transport there is a downward slope in epicatechin concentration from compartment to compartment which could indicate a simple diffusion of the compound through the cell. However, since there is a very potent uptake mechanism from the basolateral side, epicatechin which reaches the basolateral side by, for example, paracellular diffusion would be readily taken up at the receiver side, lowering the apparent diffusion rate and increasing intracellular concentrations through indirect influx (figure 6.28). Since transport rates of epicatechin and lucifer yellow correlate very well (figure 6.26), paracellular diffusion is a likely mechanism of epicatechin uptake. Similar results were obtained by Kosińska and Andlauer who measured epicatechin permeation across Caco-2 cells as P_{app} = 4.5 x10^{-6} cm/s and a corresponding permeation rate of P_{app} = 6 x10^{-6} cm/s for lucifer yellow (330). Both rates are more than ten times higher than what is usually reported for paracellular diffusion, but they do confirm that an increase in paracellular diffusion, as shown by increase in lucifer yellow permeation rate, correlates with increased epicatechin permeation in uptake direction.

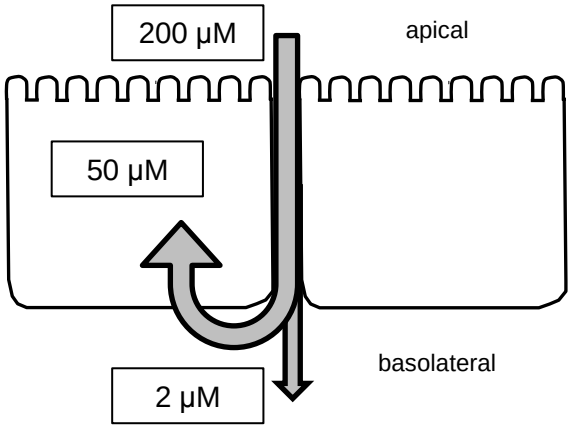

Figure 6.28; A possible mechanism of epicatechin uptake.

The involvement of apical efflux transporters in epicatechin transport was investigated by siRNA silencing and with the help of transport inhibitors. Efflux at the intestinal brush border is mediated by ABC-transporters. The most abundant ABC-transporters in the apical plasma membrane of Caco-2 cells, that have been shown to be involved in excretion of xenobiotics and their phase II metabolites, are ABCB1 (331), ABCC2 (332), and ABCG2 (333). Other xenobiotic transporters that facilitate translocation across the basolateral membrane are closely related to ABCC2. ABCC1 (334) and ABCC3 (335) consistently localise to the basolateral membrane in polarised cells of different types of tissue, whereas ABCC4 is reported to locate in either the basolateral or the apical membrane, but seems to locate to the basolateral membrane in Caco-2 cells (336). Other members of the ABC-transporter family are also present in enterocytes but they exhibit different substrate specificities, for example, several transporters of that superfamily are involved in maintaining the lipid asymmetry of the outer and inner membrane leaflet (337, 338).

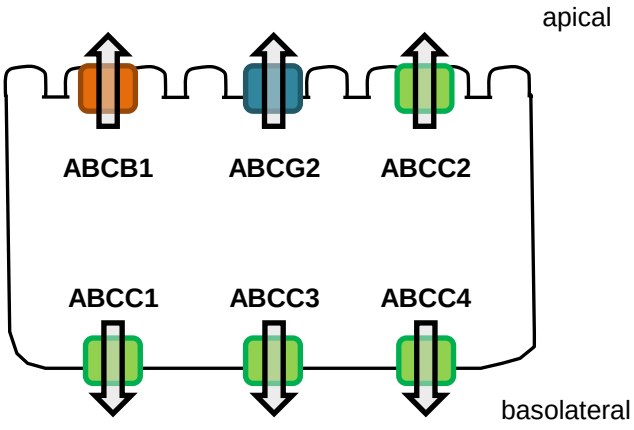

Figure 6.29; Localisation of ABC-transporters in Caco-2 cells.

All of the xenobiotic transporting members of the ABC-family are among the most highly expressed transporters in Caco-2 cells, but reports on their expression pattern vary concerning their relative abundance compared to one another. Especially ABCG2 expression seems to vary among Caco-2 batches in different laboratories. Presented below is a list of expression patterns that have been reported for that cell line.

ABC**C2** > ABC**G2** > ABC**C3** > ABC**B1** > ABC**C4** > ABC**C1** (18)

ABC**C2** > ABC**B1** > ABC**C3** > ABC**C4** > ABC**G2** > ABC**C1** (280)

ABC**C3** > ABC**C2** > ABC**B1** > ABC**C4** > ABC**G2** > ABC**C1** (339)

ABC**C2** > ABC**C3** > ABC**B1** > ABC**G2** > ABC**C4** > ABC**C1** (147)

ABC**C4** > ABC**C3** > ABC**B1** > ABC**C2** > ABC**C1** > ABC**G2** (340)

In the Caco-2 cells used for the work presented in this chapter, the order of expression was ABCC2 (C_T = 23.6) > ABCB1 (C_T = 25.6)> ABCG2 (C_T = 28.8, all determined at a concentration of 5 ng cDNA/µL).

Reduction of transporter expression by siRNA silencing has shown that epicatechin is a likely allocrite of ABCC2, as reported previously, and that most epicatechin conjugates are allocrites of ABCG2. The most extensively investigated efflux transporter of that group though, is ABCB1. This transporter especially has been associated with the symptom of multiple drug resistance (MDR) that is feature of

many cancer cells and cell lines. MDR involves several mechanisms, among them is the upregulation of drug transporting efflux transporters of the ABC-family, which greatly limits the concentration of anti-cancer drugs that can be achieved in those cells and thus diminishes success of therapy. One such drug that is an allocrite of ABCB1 is vinblastine. When vinblastine transport was investigated in the ABCB1 expressing Madin-Darby-Canine-Kidney (MDCK) cell line, another cell line that is routinely used for *in vitro* drug bioavailability prediction, it was reported to behave in the same way as epicatechin did here. Transepithelial transport of vinblastine was much greater in efflux than in uptake direction and the drug accumulated intracellularly when it was applied to the basolateral side, but intracellular levels were low when it was applied to the apical side. ABCB1 inhibition increased intracellular drug concentrations further and reduced efflux to the apical compartment (341). The authors of that report suggested that the disposition of vinblastine was mainly due to the unusual ability of ABCB1 to pick up allocrites from inside the inner leaflet of the plasma membrane and release them in the outer leaflet from where they then diffuse to the extracellular space. When this model was originally described by Higgins and Gottesman in 1992, the authors prominently described ABCB1 to function as a ‘hydrophobic vacuum cleaner’ that keeps the inner membrane leaflet clean of xenobiotics (342). Such function could explain why vinblastine is very effectively prevented from entering the cell from the apical side, but the transporter is much less able to reduce drug concentration once it reaches the cyosol. The authors also suggested that there is some unidentified uptake mechanism for vinblastine at the basolateral membrane and that the drug then binds intracellularly and thus accumulates to high concentrations (341). SiRNA silencing of ABCB1 did not show an involvement of that transporter in epicatechin efflux and there is no report that ABCC2 is also able to take up allocrites from inside the plasma membrane. But since all ABC-transporters are very similar in their structure,

it would be interesting to investigate whether ABCC2 could exhibit an uptake mechanism that is analogue to that of ABCB1.

Independent of the phenomenon of intracellular accumulation, the involvement of ABC-transporters, most likely ABCC2, in apical epicatechin efflux has been demonstrated by transporter silencing and inhibition. Expression of ABCC2 was slightly reduced after chronic DHA supplementation. However, the decrease in epicatechin efflux three times exceeds the decrease in mRNA transcript levels. To confirm whether a decrease in efflux transporter abundance really could be the cause for DHA induced epicatechin transport inhibition, protein levels of the transporter will have to be investigated. The original hypothesis that fatty acids can affect transporter mediated epicatechin efflux by modulation of transporter activity, could still play a role though. This modulation was thought to occur through interference of DHA with the structure of DRM or lipid rafts. These lipid domains within the outer leaflet of the plasma membrane are enriched in cholesterol, sphingolipids, glucosylceramide and phospholipids with saturated acyl-moieties. The term DRM results from their property of being insoluble in cold detergent solutions, traditionally that detergent was Triton X-100, but different extraction methods have been developed since, among them also detergent free procedures that employ sonification in cold buffer. Each extraction technique will result in DRM with a slightly different lipid and protein composition (301, 343). Transport of epicatechin across methyl-β-cyclodextrin treated cells, as described in this chapter, has shown that the efflux rate of the aglycone and its conjugates can be reduced by physical changes of the plasma membrane. Decrease in the transport of epicatechin and its metabolites to the apical side indicates that cholesterol removal from the plasma membrane reduces ABCC2 and ABCG2 activity, which could be based on a disruption of DRM due to the lower cholesterol content. ABCC2 is the least investigated of the three apical efflux transporters in Caco-2 cells. It is highly expressed in the canalicular membrane of hepatocytes and most studies on that transporter have been

conducted using this cell type. In one such study, the authors showed that membrane cholesterol removal by methyl-β-cyclodextrin resulted in a diffusion of ABCC2 out of DRM fractions and an inhibition of ABCC2 mediated efflux (344). Another group has shown the same behaviour for ABCG2 in MDCK cells (345). It has also been reported that ABCC2 resides in membrane domains that are resistant to extraction by the detergent Lubrol WX and different bile salts but not resistant to extraction by Triton X-100 (346, 347). DHA was shown to specifically incorporate into DRM but much more into Triton X-100 insoluble (DHA content increased from 1.2 to 31.7 %) and less into Lubrol XW insoluble (DHA content increased from 1.2 to only 5 %) domains (174). There are contradicting reports on the action of DHA on raft structure. On the one hand it was shown that DHA increase raft size by inducing fusion of these structures (273), on the other hand, it was also reported that DHA prevents raft clustering in plasma membranes of ethanol treated cells (348). But since that fatty acid is mostly incorporated into raft domains that do not contain ABCC2, the impact of DHA on ABC-transporter function might not be through modulation of raft structure but perhaps through alteration of the plasma membrane cholesterol content, as n-3 PUFA feeding of mice and MDR cell lines has shown to reduce the content of cholesterol and sphingolipids in raft fractions (123, 207, 273). And as mentioned above, results presented in this chapter and in previously published reports have shown that a decrease in membrane cholesterol content resulted in a decrease in ABCC2 and ABCG2 activity.

A direct impact of FFA on ABC-transporter activity was also investigated but the presence of neither DHA nor α-linolenic acid had a direct inhibitory effect on ABCB1 (349). This transporter, together with ABCC1, has been shown to transport xenobiotics as well as lipids (337, 338). So a chronic fatty acid supplementation of cells could theoretically lead to a competitive inhibition of xenobiotic transport. But as this has not been observed for either transporter with a known affinity for lipids, it

is also unlikely that lipid treatment will cause a direct inhibition of epicatechin efflux via ABCC2.

Another mechanism that could contribute to the abundance of ABCC2 at the plasma membrane is the release of that transporter from intracellular ABCC2 pools. It was reported that the protein is abundant in a vesicular compartment just below the apical membrane and that plasma membrane fusion or retrieval of those vesicles can be rapidly induced through several signalling pathways (350). There is no report on interaction of lipids with this mechanism, but it does comprise a further possible interface between gene regulation and transporter abundance at the cell surface and stresses the need to investigate transporter protein levels, not only of whole cell lysate samples, but ideally of isolated plasma membranes.

Metabolism of epicatechin by Caco-2 cells resulted mainly in the formation of *O*-methyl-, sulfate- and double conjugates. All three types of metabolites were preferentially exported to the apical side. These results are in accordance with previous reports, where these conjugates were also mainly found in the apical chamber after apical aglycone loading (300, 351). After basolateral loading, another phase II metabolite, epicatechin-β-D-glucuronide, was detected mainly in the basolateral well and also in cell lysate. O-methyl-epicatechin-β-D-glucuronide was only detected in trace amounts. None of the studies cited above reported the formation of glucuronic acid conjugates.

The main difference between epicatechin metabolite formation in the Caco-2 cell line and in human studies is the great abundance of the *O*-methyl-conjugate in *in vitro* studies, but which is not at all found *in vivo*. Even though no chemical standards of epicatechin conjugates were available for the work presented here, comparison of peak areas can indicate the relative abundance of metabolites. The largest peak areas were found for 3ʹ-*O*-methyl-epicatechin. Just as it was shown for ferulic acid conjugates, it would be expected that sulfate- or glucuronic acid conjugates will be ionised more easily in the ion source of the mass spectrometer

and therefore will result in a stronger signal and larger peak areas than *O*-methyl-epicatechin at the same concentration. Since 3ˈ-*O*-methyl-epicatechin consistently reaches the largest peak areas, it can be assumed with confidence that this conjugate represents the most abundant epicatechin metabolite produced by Caco-2 cells. Therefore, the conjugate which is most abundant *in vitro* is completely absent *in vivo* in human samples (55, 351-354). Also, after incubation of the Caco-2 model with epicatechin, no glucuronic acid and sulfate double-conjugated forms were detected and no triple conjugates either, whereas they were detected in plasma and urine after feeding either green tea, cocoa or epicatechin to rats or humans (55, 353, 354).

In this chapter it was shown that chronic supplementation of Caco-2 cells with the fatty acid DHA is able to reduce transport of epicatechin and its conjugates towards the apical side, which *in vivo* corresponds to the intestinal lumen. It was also demonstrated that a reduction in expression of the apical efflux transporter ABCC2 has the same effect on epicatechin transport as DHA treatment and that reduced expression of ABCG2 reduced apical efflux of epicatechin conjugates. DHA could exert its effect on aglycone transport either through reduction of ABCC2 expression or through modulation of the lipid environment of that transporter when inserted into the plasma membrane which would results in reduced transporter activity. It could not be determined via which mechanism epicatechin crosses the basolateral plasma membrane and why it accumulates intracellularly. More work is required to clarify these aspects of epicatechin transport across the intestinal epithelium.

Chapter 7: Increase of glucuronic acid conjugation of epicatechin by UGT1A8 in DHA supplemented intestinal goblet cells

7.1 Abstract

Previous reports have shown that dietary fatty acids are able to modify glucuronic acid conjugation rates *in vitro* and *in vivo*. Using recombinant human UGT isoforms it was shown in this chapter that glucuronidation of epicatechin is mainly catalysed by UGT1A1, UGT1A8 and UGT1A9. In HepG2 cells, pre-treatment with PUFA, but not stearic acid, increased epicatechin glucuronidation. In the intestinal Caco-2/HT29-MTX co-culture model, overall glucuronidation rates were much higher than in hepatocytes and enterocytes alone, and epicatechin was much more readily conjugated when cells were incubated from the basolateral side than when incubated from the apical side. The highest amount of glucuronide was also found in the basolateral well, whereas the highest concentration was detected in the cell lysate. None of the other epicatechin metabolites shared this distribution pattern. HT29-MTX cells contained over 1000 fold higher mRNA levels of UGT1A8 than Caco-2 or HepG2 cells and expression of UGT1A1 and UGT1A8 was increased after treatment of cells with DHA. DHA also doubled UGT1A(8) protein levels detected in HT29-MTX cell lysate and immunofluorescence staining revealed the presence of UGT1A(8) at the plasma membrane of that cell line. These results suggest that in the HT29-MTX cells at least some of the UGT1A8 enzyme is not ER resident but plasma membrane spanning and facilitates conjugation of epicatechin much more efficiently from the basolateral than from the luminal side.

7.2 Introduction

In the previous chapter, the metabolism of epicatechin by Caco-2 cells was described. Only very low levels of epicatechin-β-D-glucuronide were detected in the cell culture model although *in vivo* these conjugates were found to be much more abundant (351, 355). UGT expression varies between different tissue and cell lines. Enzyme levels are high in tissues involved in xenobiotic metabolism. The greatest abundance and also the highest variety of different UGT isoforms is found in liver, intestine and kidney (36). Overall, most cell lines reflect the enzyme expression pattern of the type of tissue they were derived from, but levels of some individual isoforms can differ significantly between tissue and *in vitro* model. For example, the hepatic HepG2 cell line does not express UGT1A4 although this enzyme is highly abundant in liver samples and the intestinal cell line Caco-2 only contains low mRNA levels of UGT1A10, which is very well expressed in the small intestine (356). Dietary lipids have been shown to affect glucuronic acid conjugation *in vitro* and *in vivo* (357), but reports differ on the outcome of this effect. Some studies found that fatty acids enhance activity (358) and some found that they inhibit glucuronidation (359). To investigate the effect of dietary lipids on UGT activity further, the impact of chronic fatty acid supplementation of different cell lines on formation of epicatechin-β-D-glucuronide was assessed.

7.3 Results

7.3.1 PUFA increase epicatechin glucuronic acid conjugation in HepG2 cells

Liver and intestinal tissue have been reported to exhibit high glucuronic acid conjugation activity. Incubation of the intestinal Caco-2 cell line with epicatechin only resulted in the production of low amounts of the conjugate (see chapter 6) and therefore, the HepG2 hepatocyte cell line was chosen to investigate the effect of supplementation with different fatty acids on glucuronic acid conjugation further (figure 7.1).

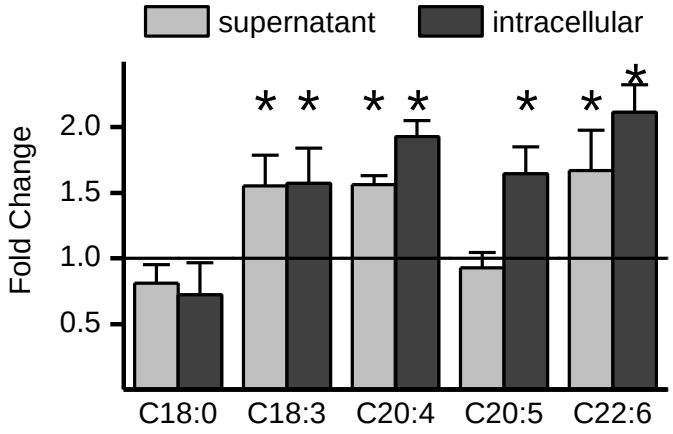

Figure 7.1; Impact of chronic fatty acid supplementation on epicatechin glucuronic acid conjugation in HepG2 cells. The amount of epicatechin-3ˈ-β-D-glucuronide concentration detected in fatty acid supplemented cells was compared to the amount detected in untreated cells. For details on conditions and analysis see sections 2.2, 2.3 and 2.7 C18:0 = stearic acid, C18:2 = linoleic acid, C18:3 = linolenic acid, C20:4 = arachidonic acid, C20:5 = EPA, C22:6 = DHA * = $p \leq 0.05$, n = 6, N = 1

Stearic acid had no effect on glucuronic acid conjugation but PUFA increased levels of the most abundant metabolite epicatechin-3'-β-D-glucuronide. EPA increased only intracellular epicatechin-3'-β-D-glucuronide levels but α-linolenic acid, arachidonic acid and DHA increased intra- as well as extracellular epicatechin-3'-β-D-glucuronide concentrations. However, overall amounts of

glucuronic acid conjugate were also low in HepG2 cells. Three structural isomers were detected but the less abundant epicatechin-7-β-D-glucuronide and epicatechin-4'-β-D-glucuronide were only present in trace amounts in the supernatant.

7.3.2 Epicatechin metabolism by Caco-2/HT29-MTX co-cultures

Apart from the liver, the small intestine has also been shown to have high glucuronidation activity. Since Caco-2 cells have only shown little glucuronidation activity towards epicatechin (see chapter 6), an improved *in vitro* model of the small intestine, the co-culture of enterocytes (Caco-2 cells) and goblet cells (HT29-MTX cells) was employed to investigate epicatechin conjugation. TEER indicated that tight junctions were formed between the two different cell types, but values for the mixed model were lower than for Caco-2 monolayers alone and did not reach 300 Ω. But even though co-cultures only reached TEER values between 250 and 300 Ω, these monolayers were used for transport experiments. The PUFA DHA doubled glucuronide levels in HepG2 cells and was therefore selected to assess glucuronidation in the Caco-2/HT29-MTX co-culture model. Cells were treated with DHA for their entire differentiation time of 22 days. Controls were treated with vehicle only. Conjugation rates were much higher in the intestinal co-culture model than in HepG2 cells and Caco-2 cells alone. Figure 7.2 shows the relative concentration of glucuronic acid conjugates compared to the total amount in different compartments of the cell model and figure 7.3 shows the same comparison for each of the most abundant forms of the non-glucuronic acid conjugates *O*-methyl-epicatechin, epicatechin-sulfate and *O*-methyl-epicatechin-sulfate. Individual graphs show the relative amount/concentration of a metabolite detected in the apical and basolateral well and in the cell lysate. Epicatechin was applied either to the apical (a → b) or the basolateral (b→ a) side. All epicatechin glucuronide forms showed the same pattern of distribution: the highest concentration was found

intracellularly whereas the highest amount was found in the basolateral well when epicatechin was applied basolaterally.

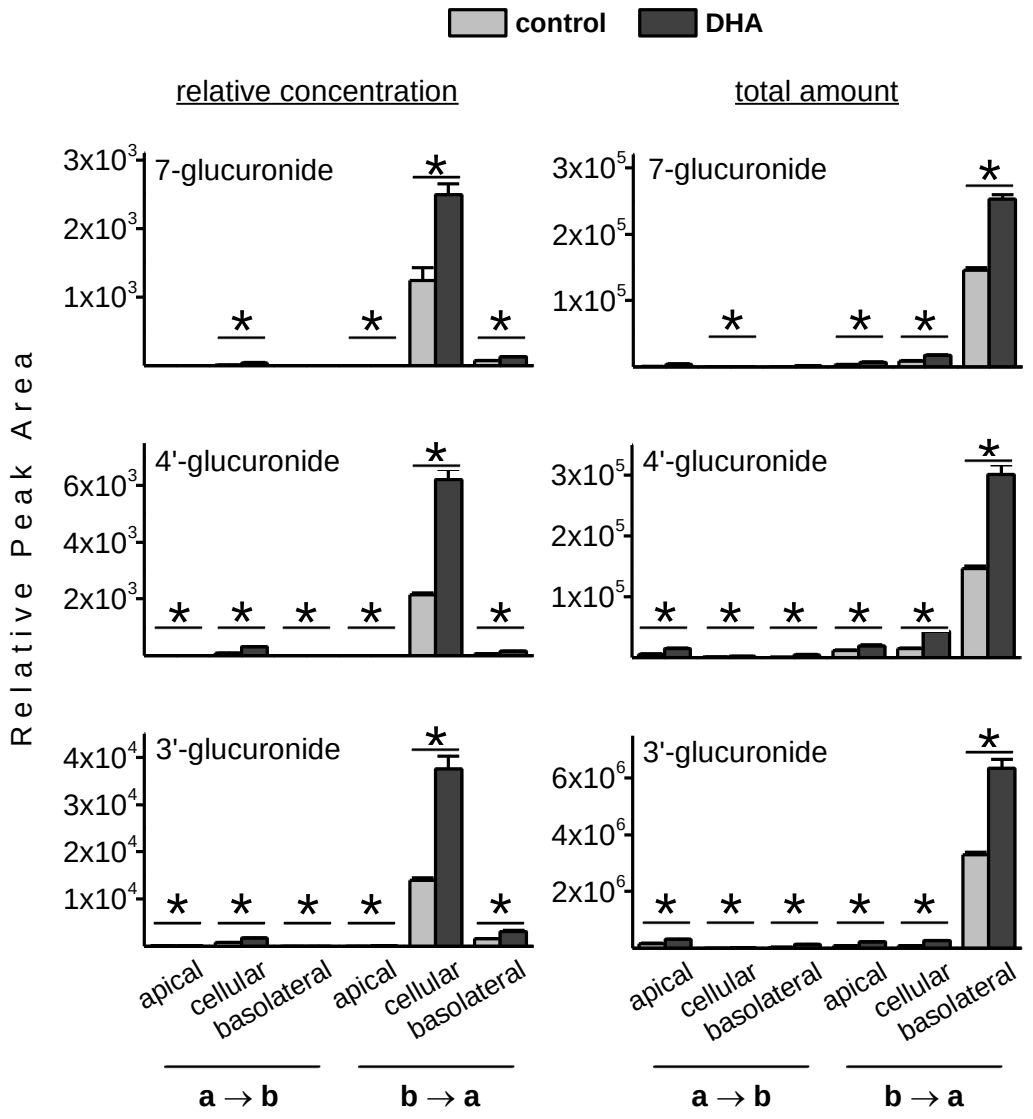

Figure 7.2; Impact of chronic DHA supplementation on epicatechin glucuronidation in Caco-2/HT29-MTX co-cultures. Cells were seeded onto permeable supports at a ratio of Caco-2:HT29-MTX 76:24 and supplemented with 50 µM DHA or vehicle for their entire differentiation time of 22 days. For metabolism experiments, cells were incubated with epicatechin from either the apical (a → b) or basolateral (b → a) side. For graphs in column 'relative concentration' peak areas were adjusted to represent the concentration of metabolite in the compartment they were drawn from, for graphs in the column 'total amount' results were adjusted for the overall sample volume, as described in section 2.7. For details on conditions and analysis see sections 2.2, 2.3 and 2.7. * = ≤ 0.05, n = 6, N = 1

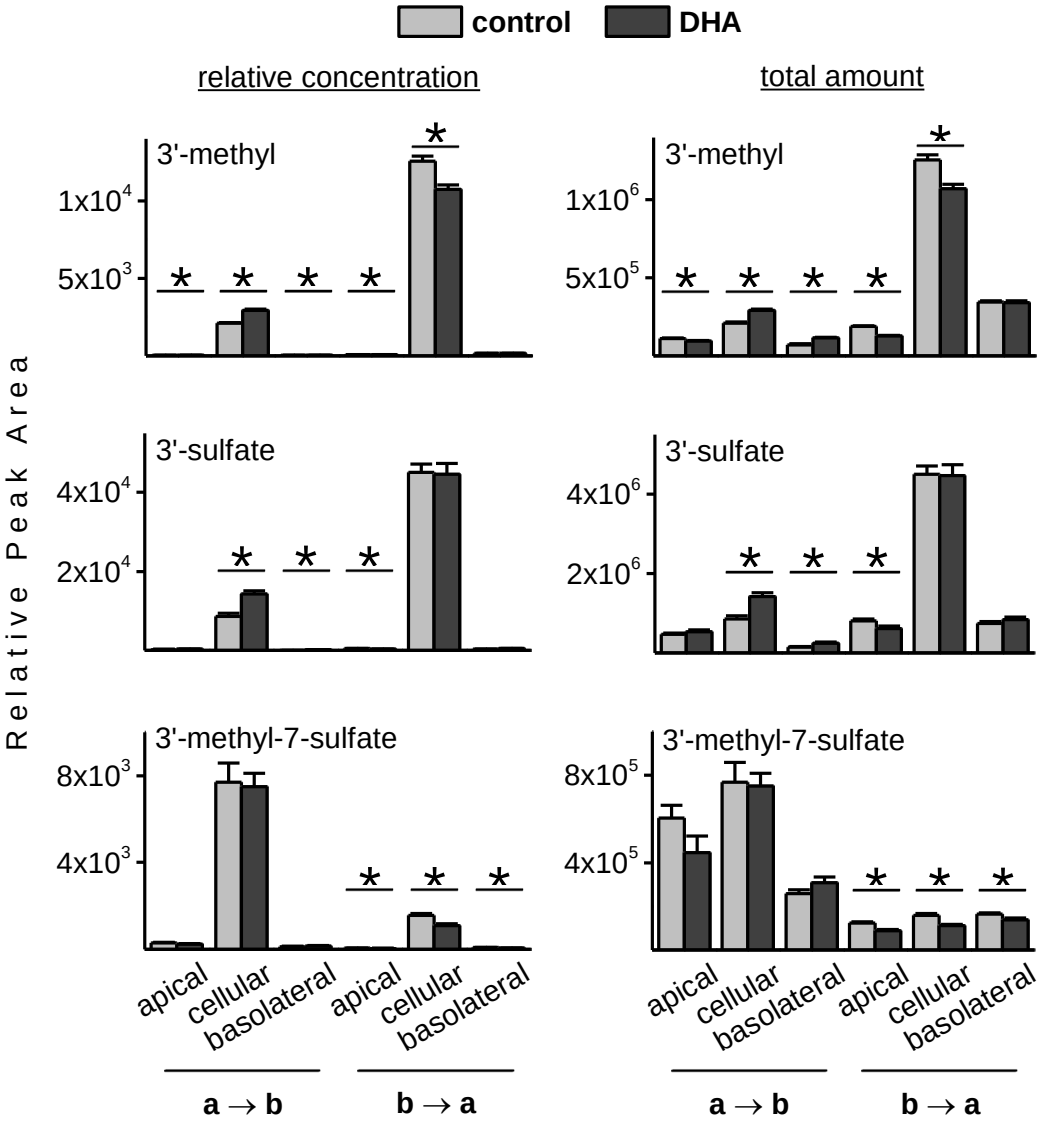

Figure 7.3; Impact of chronic DHA supplementation on epicatechin metabolism in Caco-2/HT29-MTX co-cultures. Cells were seeded onto permeable supports at a ratio of Caco-2:HT29-MTX 76:24 and supplemented with 50 µM DHA or vehicle for their entire differentiation time of 22 days. For metabolism experiments, cells were incubated with epicatechin from either the apical (a → b) or basolateral (b → a) side. For graphs in column 'relative concentration' peak areas were adjusted to represent the concentration of metabolite in the compartment they were drawn from. For graphs in the column 'total amount' results were adjusted for the overall sample volume as described in section 2.7. For details on conditions and analysis see sections 2.2, 2.3 and 2.7. * = ≤ 0.05, n = 6, N = 1

The transport direction had a dramatic impact on the formation of glucuronic acid conjugates. When epicatechin was applied to the basolateral side, the concentration of epicatechin glucuronide was up to fifty times greater in all compartments than

when cells were incubated from the apical side. DHA treatment was able to further increase glucuronide levels up to four fold in all compartments. None of the other metabolites showed the same pattern of distribution as epicatechin glucuronide. Figure 7.3 shows representative graphs for *O*-methyl-epicatechin, epicatechin-sulphate and *O*-methyl-epicatechin-sulphate. With all non-glucuronide metabolites, the highest concentration was detected intracellularly, but in contrast to epicatechin glucuronide, the highest amount was not found in samples drawn from the basolateral well but also in the cell lysate. Epicatechin applied basolaterally instead of apically resulted in a slight increase in methyl- and sulphate-conjugate concentrations but not as pronounced as with glucuronic acid conjugates. The *O*-methyl-sulphate double conjugate even showed opposite behaviour, with higher amounts produced when epicatechin was applied apically. None of the non-glucuronide metabolites showed a pronounced difference regarding their distribution between the apical and basolateral well. These results indicate that DHA treatment did not increase activity of COMT or SULT but that it does increase the formation UGT products. The fact that DHA increased the amount of only one type of metabolites shows that there is a direct impact of DHA on that enzyme and not just a generic mechanism that is affected. Also the great difference in glucuronide production depending on the epicatechin transport direction (a → b vs. b → a) is unique to UGT catalysed reactions and does therefore not stem from an increased uptake of epicatechin and consequent increase in substrate availability from the basolateral side, as described in chapter 6, since in that case the relative concentration of SULT and COMT products would have been increased to a similar magnitude. Therefore, in the intestinal co-culture model, epicatechin glucuronidation by UGT seems to occur through a unique mechanism that is asymmetrical regarding the cellular localisation and responds to DHA supplementation of cells, a mechanism that cannot be explained by the current model of an ER residing enzyme.

7.3.3 HT29-MTX cells are the main source of UGT activity in co-culture

The Caco-2/HT29-MTX seeding ratio of 76/24, used for the experiments presented above, was chosen to represent the percentage of goblet cells in the small intestine.

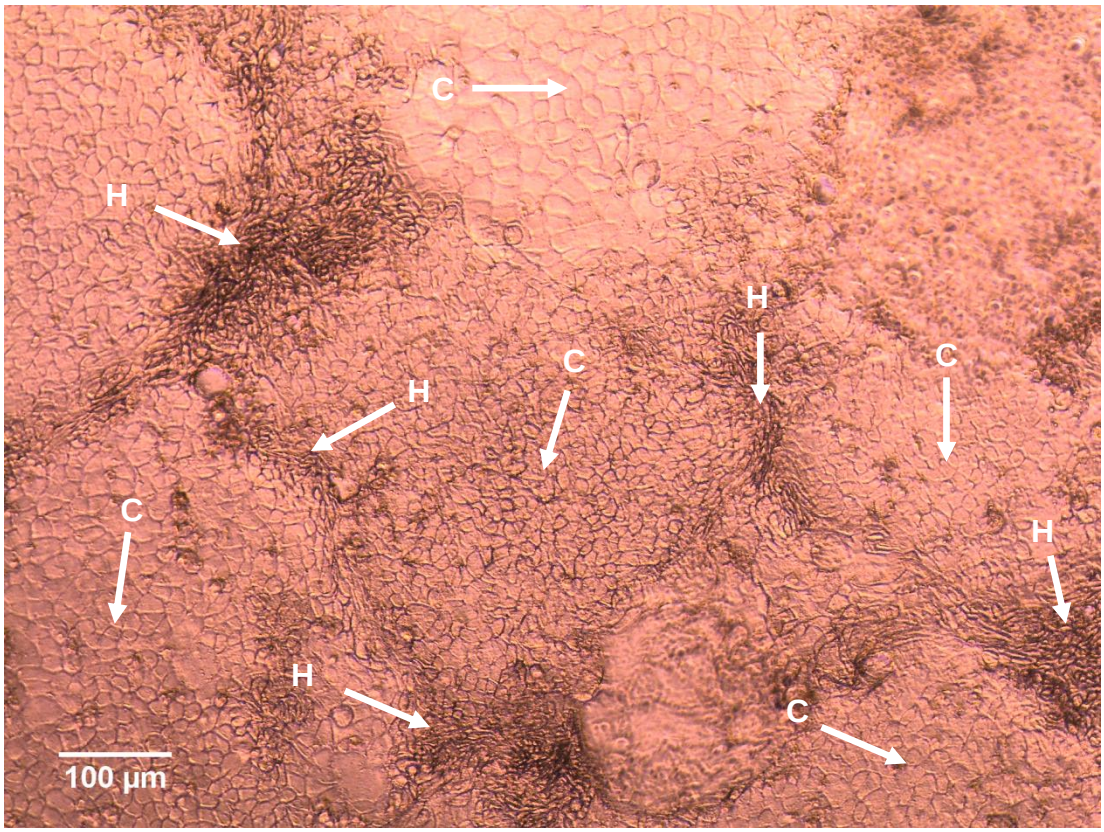

Figure 7.4; Representative image of Caco-2/HT29-MTX co-cultures 22 days after seeding. The two cell lines were seeded at a ratio of Caco-2:HT29-MTX 76:24. Streaks of HT29-MTX cells are labelled 'H' and patches of Caco-2 cells are labelled 'C'. For details on culture conditions and image acquirement, see sections 2.2 and 2.10.

As Caco-2 cells grow more rapidly than HT29-MTX cells, seeding 24 % of the goblet cell line typically resulted in 13 ± 2% of those in the monolayer after differentiation. Even though the two different cell types were extensively mixed before plating, they always grew in the same pattern of patches of Caco-2 cells with ribbons of HT29-MTX running through (figure 7.4). To investigate how glucuronidation activity of co-cultures changes with different seeding ratios of the two cell lines, epicatechin metabolism was investigated with varying percentages of goblet cells in the model.

Figure 7.5 shows the impact of increasing amounts of HT29-MTX cells on glucuronic acid conjugation rates. There is an almost linear relationship between epicatechin-3'-β-D-glucuronide production and the percentage of goblet cells seeded. This indicates that Caco-2 cells contribute very little to the overall glucuronide formation and that either the activity or the abundance of UGT is much greater in HT29-MTX cells. For that reason, all following cell experiments were carried out with HT29-MTX cultures only.

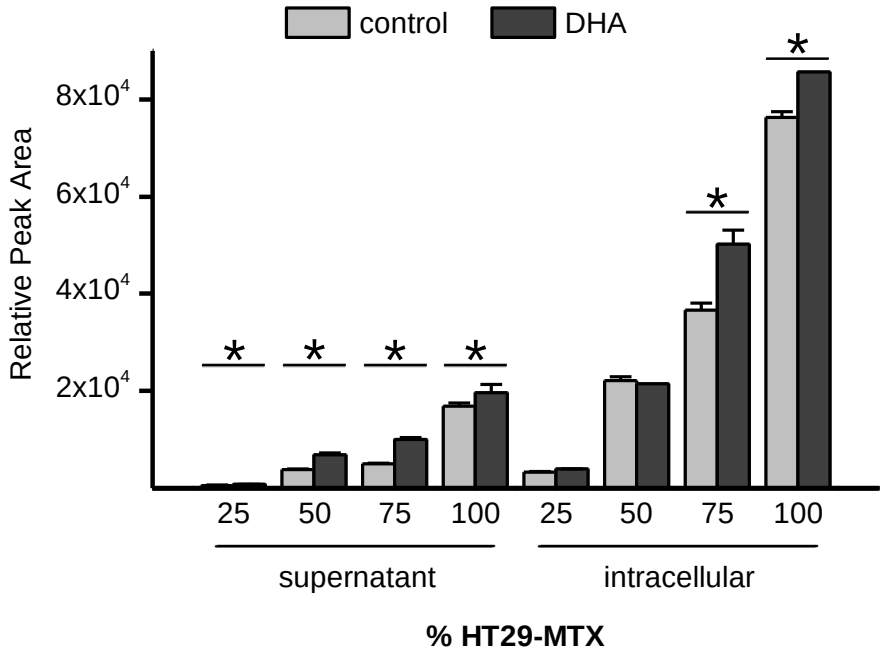

Figure 7.5; Impact of increasing percentage of HT29-MTX cells (25, 50, 75 and 100%) in the co-culture model on formation of epicatechin-3'-β-D-glucuronide. For conditions and analysis see sections 2.2, 2.3 and 2.7. * = $p \leq 0.05$, n = 3, N = 1

7.3.4 *In vitro* glucuronidation of epicatechin

There is only one published report of *in vitro* conjugation of epicatechin by individual UGT isoforms. This study conducted by Blount *et al.* used four different UGT1A enzymes to investigate the formation of epicatechin-3'-β-D-glucuronide (360). To acquire a more extensive picture of this conjugation reaction, epicatechin

glucuronidation was now assessed using a wider range of 12 different UGTs of the 1A and 2B family and the formation of all three glucuronide forms detected in cell culture samples was monitored.

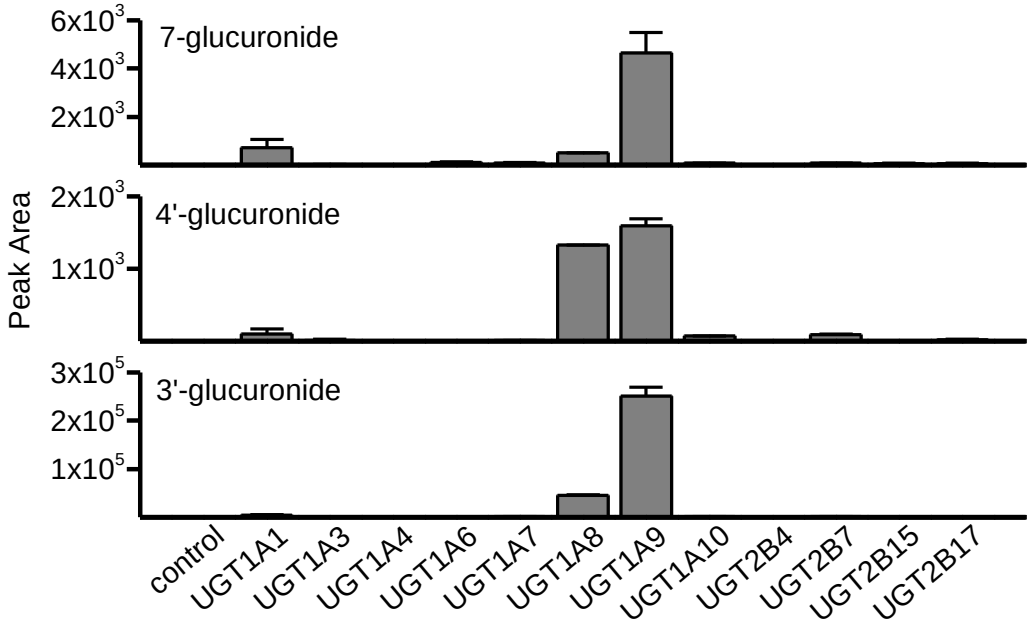

Figure 7.6; *In vitro* glucuronidation of epicatechin by recombinant human UGT isoforms expressed in insect microsomes. Microsomes corresponding to 0.5 mg/mL protein were incubated with 50 µM epicatechin for 60 min at 37°C in the presence of 0.025 mg/mL alamethicin, 100 µM ascorbic acid and 1 mM UDPGA in phosphate buffer. Conjugates were analysed by LC-MS/MS. For conditions and analysis see sections 2.7 and 2.15. n = 2, N = 1

Three UGT of the 1A family were able to glucuronidate epicatechin: UGT1A1, UGT1A8 and UGT1A9 (figure 7.6). As already observed with epicatechin metabolism by liver and intestinal cell lines, epicatechin-3'-β-D-glucuronide was the most abundant product, followed by epicatechin-7-β-D-glucuronide and epicatechin-4'-β-D-glucuronide.

7.3.5 DHA treatment increases UGT1A gene expression and protein levels

Gene expression of the three UGT isoforms, that were identified to recognise epicatechin as a substrate, was investigated in HepG2, Caco-2 and HT29-MTX

cells. Figure 7.7 shows their relative mRNA abundance, normalised to the housekeeping gene GAPDH, in the different cell lines.

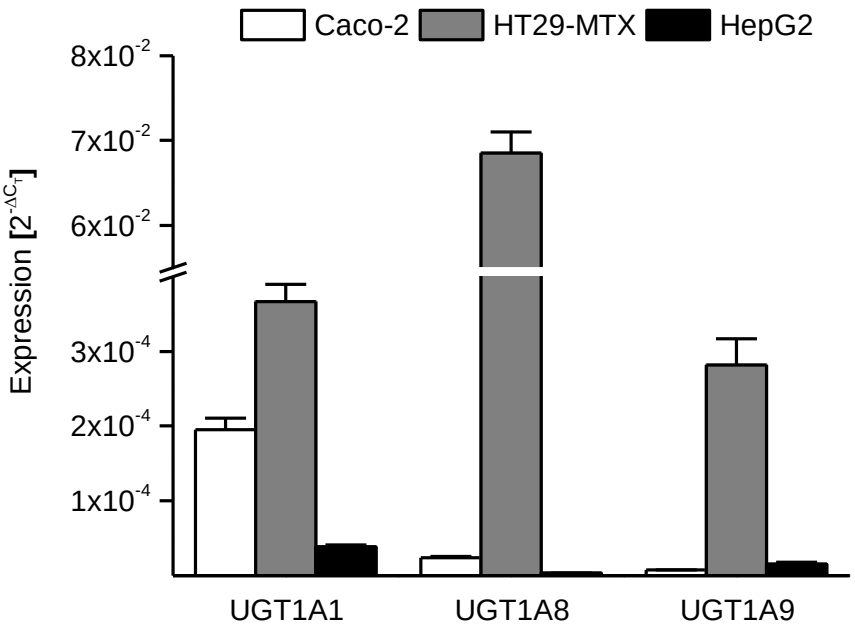

Figure 7.7; Relative expression levels of epicatechin glucuronidating UGT isoforms in Caco-2, HT29-MTX and HepG2 cells, normalised to levels of the housekeeping gene GAPDH and expressed as $2^{-\Delta C_T}$). For details on conditions and analysis see sections 2.2, 2.3 and 2.9. n = 5, N = 1

For all three UGT isoforms, similar mRNA levels were found in Caco-2 and HepG2 cells, but HT29-MTX cells contained about 1000 fold higher levels of UGT1A8 mRNA, therefore this isoform will most likely be the dominant epicatechin conjugating isoform in Caco-2/HT29-MTX co-cultures. The impact of chronic DHA treatment on UGT gene expression was assessed after 22 day treatment in Caco-2 and HT29-MTX cells grown separately and after 5 day treatment in HepG2 cells. UGT1A1 expression was upregulated in Caco-2 and HT29-MTX cells and UGT1A8 was upregulated in HT29-MTX and HepG2 cells (figure 7.8).

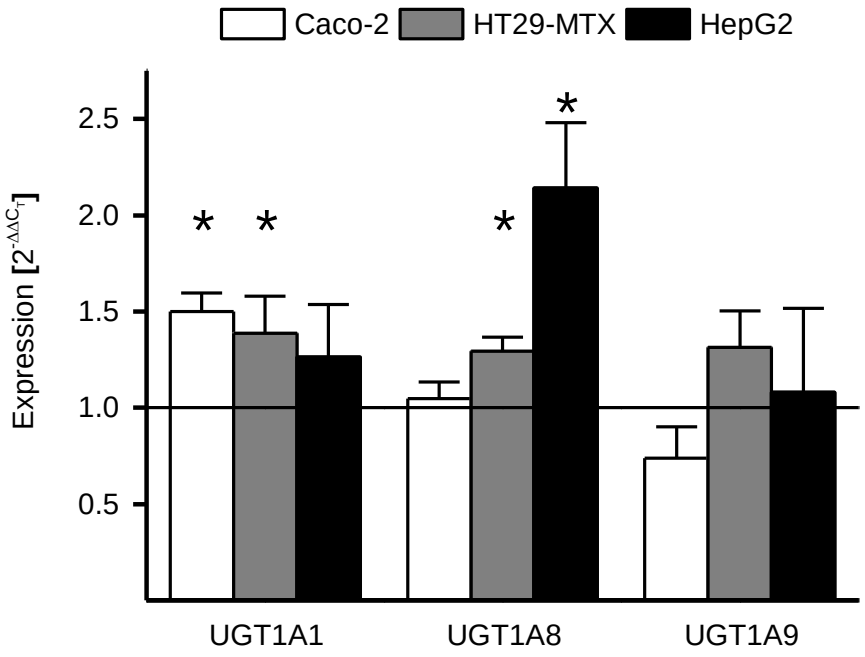

Figure 7.8; Impact of chronic DHA supplementation (50 µM and 22 days for Caco-2 and HT29-MTX and 5 days for HepG2) on UGT expression. For details on conditions and analysis see sections 2.2, 2.3 and 2.9. * = $p \leq 0.05$, n = 5, N = 1

Unfortunately, no specific UGT1A8 antibody was commercially available, therefore a generic UGT1A antibody recognising all isoforms of that family was used to assess the impact of DHA on protein levels of UGT1A8 in HT29-MTX cells. However, having shown that UGT1A8 is potentially about 1000 fold more abundant in that cell line than the other UGTs investigated, it was assumed that the UGT1A protein detected by that antibody will be mainly UGT1A8 with the other isoforms contributing only little to the signal. Twice the amount of UGT1A(8) protein was detected in cell lysates of chronically DHA supplemented HT29-MTX cells than in the lysate of cells treated with vehicle only (figure 7.9)

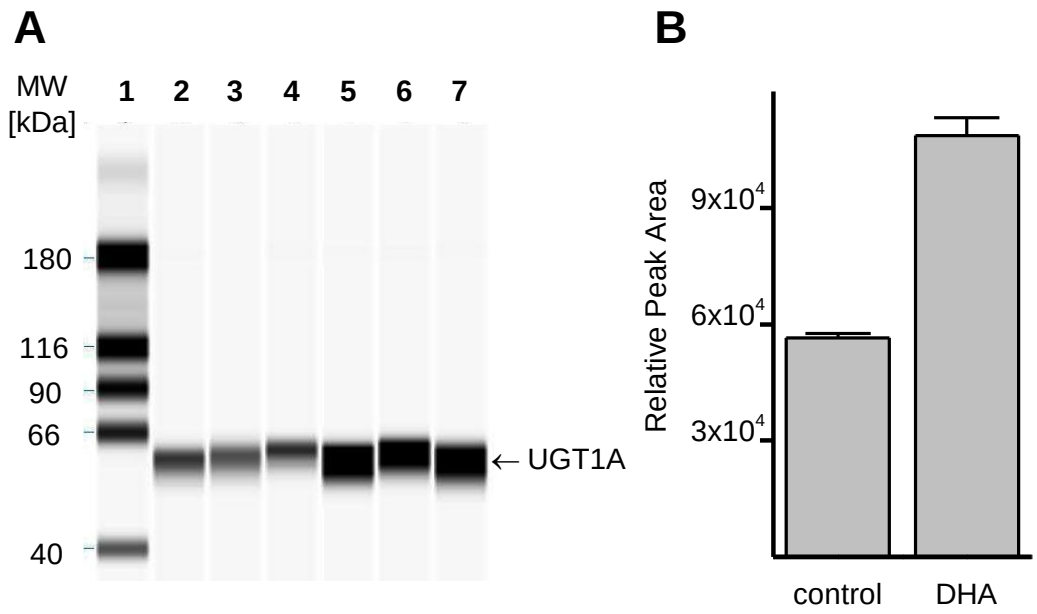

Figure 7.9; Impact of chronic DHA supplementation on UGT1A protein levels in HT29-MTX cells. (A) Image of capillaries with immunodetection of UGT1A. lane 1 = molecular weight (MW) standards, lane 2-4 = control samples, lane 5 – 7 = DHA treatment. (B) Average peak areas of UGT1A protein in samples shown in (A). For conditions and analysis see sections 2.2, 2.3 and 2.11. n = 3, N = 1

7.3.6 UGT1A(8) localises in the plasma membrane in HT29-MTX cells

It is difficult to imagine how the current model of UGT as an ER membrane residing enzyme would result in a pattern of product distribution and asymmetrical formation rates as described in section 7.3.2. To investigate intracellular localisation of the UGT1A(8) protein, indirect immunofluorescence staining of HT29-MTX cells grown on permeable supports was performed. Figure 7.10 shows representative images of 24 independent experiments.

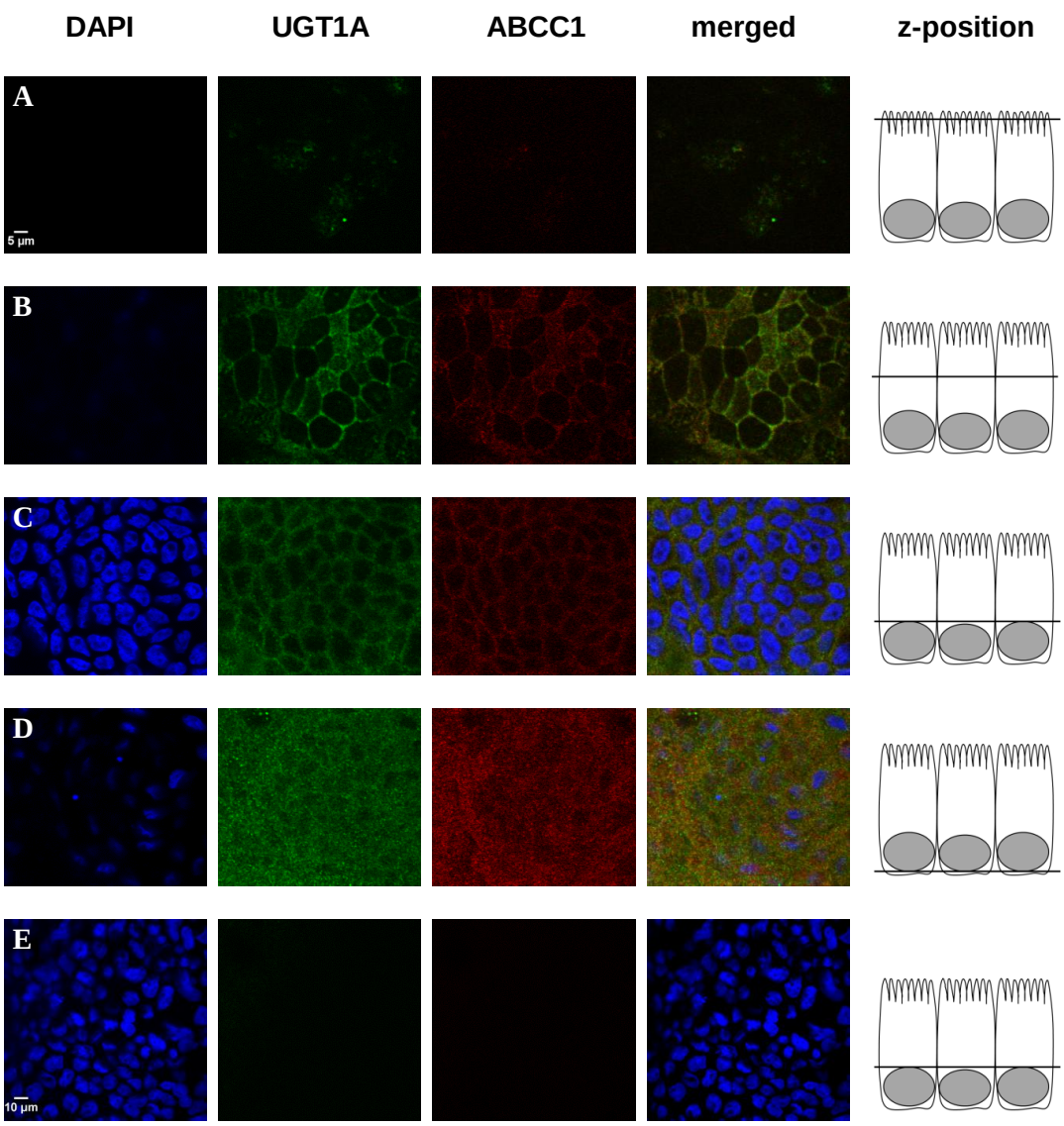

Figure 7.10; Indirect immunofluorescence staining of UGT1A and ABCC1 in HT29-MTX cells grown on permeable supports. Representative images of 24 independent experiments are shown. For images presented in rows A to D, cells were incubated with primary rat anti-human UGT1A, mouse anti-human ABCC1 and secondary Cy3 conjugated donkey anti-mouse and Alexa Fluor 488 conjugated donkey anti-rat antibody. For images presented in row E, cells were incubated with secondary antibody only. For further details on conditions and image acquirement see sections 2.2, 2.3 and 2.10.

UGT1A(8) was observed in the plasma membrane, co-localising with the plasma membrane marker ABCC1. The signal was more pronounced in lateral and basal sections of the plasma membrane than on the apical side. So far, most UGT

isoforms have been described to localise to the ER. Goblet cells such as the cell line HT29-MTX have a very unique structure with most of the apical lumen being filled with mucus granules and the basolateral lumen containing the nucleus (361). This conformation leaves little room for cytosolic organelles like the Golgi and the ER, which are consequently very much marginalised towards the peripheral space of the cell, close to the plasma membrane. Considering this spatial peculiarity, it might be that the apparent co-localisation of UGT and membrane marker ABCC1 is due to the ER residing UGT being localised just below the plasma membrane.

To confirm whether UGT1A(8) really is plasma membrane spanning in HT29-MTX cells, cell surface biotinylation and pull down with streptavidin resin was performed.

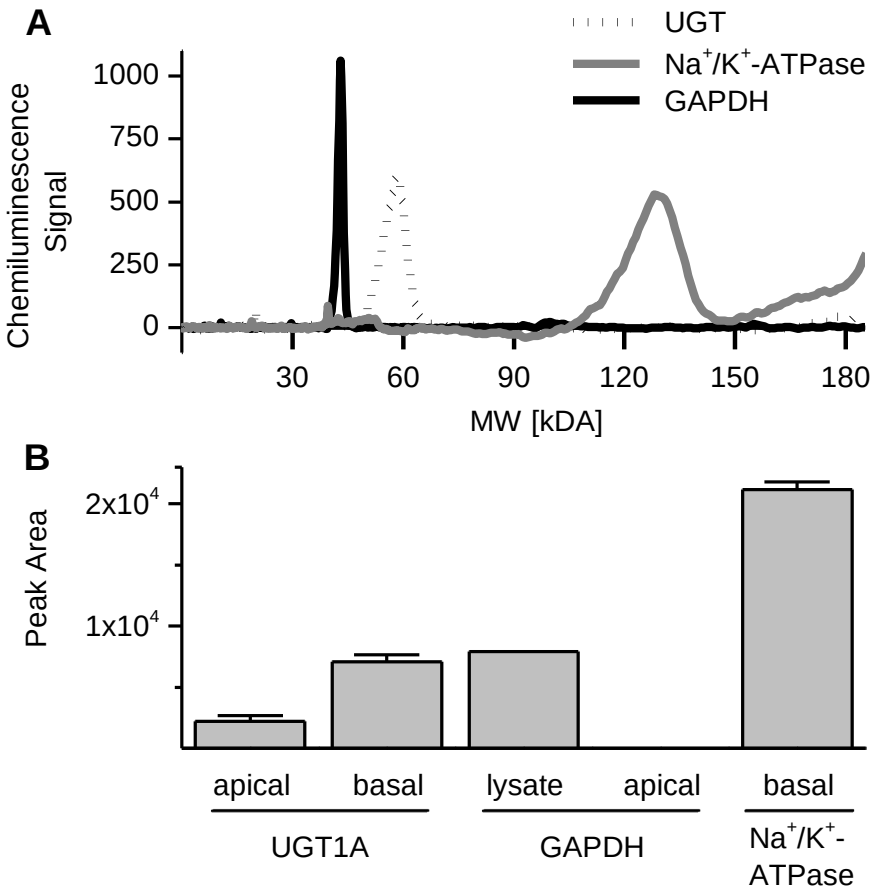

Figure 7.11; Cell surface biotinylation and pull down of UGT1A(8) in HT29-MTX cells. (A) Specificity of antibodies used for UGT1A and controls analysed by capillary electrophoresis and immunodetection. (B) Peak areas of protein levels detected in cell surface biotinylation samples after streptavidin pull down (UGT1A, only basolateral for Na^+/K^+-ATPase) and in whole cell lysate (GAPDH). For conditions and analysis see sections 2.2, 2.3 and 2.11. n = 2, N = 1

UGT1A(8) protein was detected in samples containing apical or basolateral plasma membrane proteins, but the enzyme was more abundant in samples from cells incubated with biotin from the basolateral side than in samples of cells incubated from the apical side (figure 7.11). Intracellular protein GAPDH was used as a negative control to monitor cell membrane integrity during biotinylation and plasma membrane spanning Na^+/K^+-ATPase was used as a positive control for successful biotinylation and pull down. No GAPDH could be detected in the apical surface lysate, which confirms the presence of UGT1A in the plasma membrane.

7.3.7 Extracellular UDPGA has no impact on epicatechin glucuronidation

The results described above show that at least some of the UGT1A(8) pool resides in the plasma membrane of HT29-MTX cells. It is not clear however, what the orientation of the enzyme in the plasma membrane is. If it was inserted the same way as into the ER membrane, the enzyme's active site would be facing the extracellular space. If it was inserted the opposite way, the usually cytoplasmic tail would be outside the cell. In the first case, with the active site facing the extracellular space, the availability of the co-factor UDPGA would be the rate limiting step of the enzyme reaction when investigated in a cell culture model. High concentrations of substrate are in contact with the cell surface in transport experiments but the co-factor would have to be exported from the cytosol to reach the active site of the enzyme. To test whether the active site is exposed to the extracellular space, the glucuronidation rate of substrate epicatechin was measured with and without externally supplied co-factor.

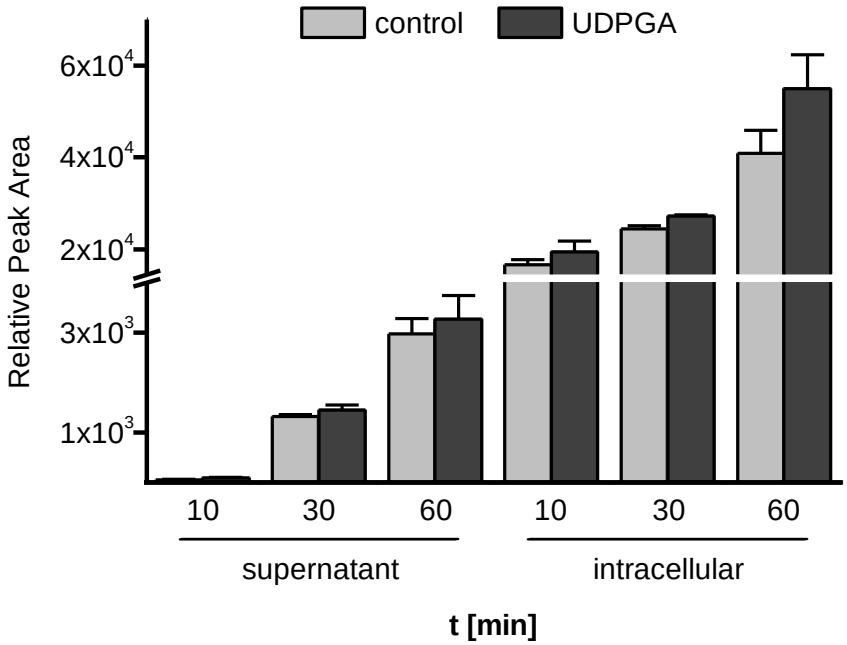

Figure 7.12; Impact of extracellular UDPGA on EC-3'-glc formation by HT29-MTX cells. Cells grown on solid supports were incubated with 200 µM epicatechin and 200 µM UDPGA and controls were incubated with epicatechin only. For conditions and analysis see sections 2.2, 2.3 and 2.7. n = 3, N = 1

Adding UDPGA to the incubation buffer together with the substrate epicatechin did not increase epicatechin-3'-β-D-glucuronide levels in either the supernatant or the cytosol (figure 7.12), indicating that the active site of the enzyme is not exposed at the apical cell surface.

7.4 Discussion

In this chapter an enhanced tissue culture model of the intestinal epithelium was employed to further elucidate the impact of lipids on glucuronic acid conjugation. Using recombinant human UGT isoforms it was first shown that epicatechin was preferentially glucuronidated by UGT1A9 which is mainly expressed in liver and also by UGT1A8 which is extrahepatic and mainly expressed in the small intestine and kidney (358, 362-366). In the intestinal Caco-2/HT29-MTX co-culture model, UGT1A8 mRNA was much more abundant in HT29-MTX cells than in Caco-2 cells, and also more abundant than has been reported for the small intestine where UGT1A1 and UGT1A10 are the predominant isoforms of the UGT1A family (36, 367). This difference between the intestine and an intestinal cell line could be explained by the fact that in studies looking at enzyme expression in tissue samples, mRNA is extracted from whole tissue and not from specific cell types. HT29-MTX cells are goblet cells, only one of five different cell types present in the intestine, which amounts to about 10% of the mucosa (4). In total mRNA extracts of intestinal tissue samples, the expression pattern of enterocytes would be predominant, as they are the major cell type present in that tissue and therefore high levels of a particular gene transcript originating from one of the less occurring cell types would be much diluted in the overall mRNA pool. To date how the gene expression profile of enzymes involved in phase II metabolism differs in the individual intestinal cell types has not been reported. Goblet cells are generally not regarded to be involved in nutrient or xenobiotic metabolism. Instead, their main function is to produce and excrete mucus that will act as a diffusion barrier and protect the intestinal epithelium from pathogen invasion, mechanical stress and injury (368). However, it might be possible that some UGT isoforms have a different function in mucus secreting cells than in enterocytes, as has been described for other metabolising enzymes. SULTs also conjugate xenobiotics in most cell types, but in goblet cells enzymes of that family sulfo-conjugate mucin molecules and the increase of SULT protein levels

along the length of the intestine is the cause for increasing acidity of the intestinal mucus layer towards the colon (369-371). It might therefore be possible that UGT isoforms also participate in processes beyond xenobiotic conjugation in goblet cells such as the HT29-MTX cell line. To investigate whether it is their function as mucus producing cells that causes the here observed departure from previous reports on UGT expression and localisation, it would be interesting to compare the UGT expression profile of the mucus producing cell line HT29-MTX with its non-mucus producing parent cell line HT29 and also with other types of goblet cells.

The impact of dietary fatty acids on UGT activity has been investigated with contradicting results. Some groups found that fatty acids inhibited UGT activity, some found that they increase conjugation rates. Zakim and Dannenberg published a series of studies investigating the impact of the phospholipid environment on UGT activity. They found that different membrane modifying agents such as phospholipase or Triton X can modulate enzyme function (372-374). Feeding animals increasing amounts of certain fatty acids (n-3 or n-6 PUFA, MUFA or SFA) changed UGT protein levels in microsomes prepared from different tissues and also resulted in a direct modulation of UGT activity (287, 288, 375). These results were corroborated by another group who found that feeding rats an n-3 or n-6 PUFA rich diet increased UGT activity in liver microsomes by increasing abundance of UGT1A protein (376). The cytosolic concentration of free fatty acids is very low. Upon entering the cell, fatty acids are bound by FABP and are then either esterified and stored as triglycerides or coenzyme A conjugated and used for energy production (77). Okamura *et al*. have shown that acyl-CoAs added to an *in vitro* system can either inhibit or enhance UGT activity depending on concentration and whether microsomes have been pre-treated with de-latency agents (e.g. detergents or alamethicin). High acyl-CoA concentrations inhibited, lower concentrations enhanced activity. In intact microsomes, acyl-CoAs and free unsaturated fatty acids resulted in activity enhancement, whereas in detergent treated microsomes activity

was reduced (358). Unsaturated fatty acids could inhibit glucuronidation of 4-methylumbelliferone by human kidney cortical microsomes and recombinant UGT1A9 and UGT2B7 enzymes. The greater the degree of fatty acid unsaturation, the greater the inhibition (359). Shibuya et al. extensively investigated the impact of different free fatty acids on UGT1A1 activity *in vitro* and *in vivo*. Using recombinant enzyme, they found that all PUFA tested inhibited UGT1A1 glucuronidation of estradiol *in vitro*. The most potent inhibitor was DHA. DHA also inhibited enzyme activity *in vivo*, increasing bilirubin levels 48 h after oral administration of low concentrations of DHA. In contrast, bilirubin levels were decreased when high concentrations of DHA were administered. The authors also showed that feeding fatty acids could greatly increase mRNA levels of UGT1A1 in weaning mice (357). In the current study DHA was found to increase conjugation of epicatechin, most likely through increasing levels of UGT1A8 protein.

It has been shown that some UGT isoforms can be upregulated by PUFA metabolites of the lipoxygenase and the cyclooxygenase pathway and even by some free fatty acids. These metabolites and fatty acids are able to activate peroxisome proliferator-activated receptors α and γ (PPARα, PPARγ) which then dimerise with the retinoid X receptor (RXR) and bind to PPAR response elements in the promoter region of the gene, thus stimulating UGT gene transcription (377-379). Interestingly, in the work presented here DHA supplementation increased expression of UGT1A8 in HepG2 and HT29-MTX cells but not of UGT1A9, even though DHA has been shown to increase activity of transcription factor PPARα in the Caco-2 model (380) and UGT1A9 expression was shown to be upregulated with increased PPARα activity (377).

The *in vitro* data reported here suggests that *in vivo* glucuronidation of epicatechin occurs mainly in the small intestine and less in liver. In one of the first publications on epicatechin conjugation, Vaidyanathan and Walle did not find any UGT activity towards epicatechin neither with human liver microsomes nor with human small or

large intestinal microsomes but they did find that epicatechin was readily glucuronidated by rat microsomes using the same protocol (313). Similar results were reported by Shrestha *et al*. using mouse liver microsomes (381). Natsume *et al.* compared epicatechin metabolites in urine and plasma of human and rat origin and found that in rat samples, epicatechin was preferentially glucuronidated at the 7-position whereas human samples mainly contained epicatechin glucuronidated at the 3'-position (382) which corresponds to the findings presented here, where epicatechin was also found primarily conjugated at the 3'-position using human liver and intestinal cell lines. A very recent study conducted by Rodriguez-Mateos *et al*. also compared glucuronidation of epicatechin by Caco-2 and HepG2 cells and found only very little activity towards that compound in Caco-2 cells and no epicatechin-β-D-glucuronide formation in HepG2 cells. There is no previous report on glucuronic acid conjugation of epicatechin in HT29 or HT29-MTX cells.

In metabolism experiments using the Caco-2/HT29-MTX co-culture model an interesting distribution pattern of epicatechin glucuronide was observed which was later found to stem from the glucuronidation activity of the HT29-MTX cell line. There was a dramatic impact of the transport direction on UGT product formation. When epicatechin was applied to the apical side of the cell layer, which *in vivo* corresponds to epicatechin reaching the intestinal mucosa from the gut lumen, glucuronidation was much lower than when epicatechin was applied to the basolateral side, which *in vivo* would correspond to epicatechin taken up into the mucosa from the submucosa. Also, epicatechin glucuronide was preferentially transported to the side of aglycone application, meaning that when epicatechin was applied apically, glucuronide levels were higher on the apical side, when epicatechin was applied basolaterally, glucuronide levels were higher in the basolateral compartment. These observations from metabolism experiments agree well with results obtained by immunofluorescence staining of HT29-MTX cells for UGT1A(8). Here, high levels of UGT1A(8) were observed in the lateral and basal parts of the

plasma membrane. As mentioned above, all UGT isoforms are assumed to localise to the ER but there are some reports that have also detected UGT protein or activity in the nuclear envelope and the Golgi (383-385). Early reports even found UGT activity in the plasma membrane of liver cells. (386-388). Also, immunofluorescence staining of intestinal tissue samples for UGT1A resulted in an asymmetrical staining pattern similar to the one shown in figure 7.10, but with the strongest signal towards the apical surface of crypt cells (389, 390). In immunofluorescence images presented here, it was the basolateral membrane where a stronger signal and activity was observed. Some of these differences could be caused by the mucus layer produced by HT29-MTX cells, which inhibits diffusion of substrate and antibody to the apical but not the basolateral cell surface. Though intestinal samples will also have a mucus layer at the luminal side, this will not interfere with staining as tissue is sliced and stained along the lateral axis. From the results described in the current chapter it seems that epicatechin, after entering the cell, is readily glucuronidated by UGT localised at the plasma membrane and quickly exported to the extracellular space by basolaterally located efflux transporters. This distribution of UGT enzyme has never been described before, so far most studies found UGT localised in the ER. All UGT1A isoforms are alternative splice variants from a single gene locus with only the first, N-terminal exon being unique for each isoform and exons 2-5 shared among all UGT1A forms. The N-terminal region contains a signal peptide that targets the nascent protein to the ER. This signal peptide is cleaved off after insertion into the ER membrane. The C-terminus contains an ER retention signal which is the same for all isoforms since it is translated from the shared exon 5. A number of different alleles have been reported for all UGT isoforms. For UGT1A8 eight different mutations have been described leading to three allelic variants. All three alleles were cloned and expressed in HEK293 cells but none of them localised in the plasma membrane (391). Several studies observed that the enzymes translated from the three different alleles had different glucuronidation

activity. UGT1A8*1 and UGT1A8*2 ($A^{173}G$) exhibit similar conjugation rates whereas UGT1A8*3 ($C^{277}Y$) hardly shows any activity at all (29, 391) and has been identified as a risk factor in colorectal cancer (392). One mutation in the signal peptide region ($T^{4}A$) has been reported but not cloned and expressed *in vitro* (393). It would be of interest to analyse which allele is expressed in which cell line, especially with regard to UGT1A8*3, which occurs with low frequency in the general population but is much more abundant in tumour cells. Since most cell lines are carcinoma derived, such increased abundance of this low activity allele might help to explain some disagreements between *in viv*o and *in vitro* results. Also a possible impact of the $A^{4}T$ mutation on ER targeting could be investigated.

It is not entirely resolved which sequence elements retain the UGT protein in the ER membrane. On the one hand, it has been shown that the transmembrane domain (TMD) and the cytosolic tail (CT) together anchor the enzyme in the ER membrane and in addition to that, the CT also contains a retrieval signal that targets any escaped protein for transport from the Golgi back to the ER. When TMD and CT were fused with the extracellular domain of CD4 this plasma membrane protein became ER resident (394). On the other hand, a different group found that neither deleting the N-terminal signal peptide nor removing the CT and TMD had an impact on UGT1A6 ER localisation. Instead this group showed an internal membrane anchoring region to play a vital role in UGT ER localisation (395, 396).

In summary, it was shown that HT29-MTX cells display a, so far, unique distribution of UGT1A(8) protein in the plasma membrane and a corresponding distribution of epicatechin-β-D-glucuronide in the cell model. Further studies will have to show whether this is a distinctive feature of that individual cell line or whether it is a common attribute of mucus cells that has so far been overlooked because most studies on UGT activity and localisation have been conducted using liver cells where this particular isoform is not well expressed.

Chapter 8: Conclusions and outlook

The current work describes the impact of lipids on absorption and metabolism of phenolics. Several mechanisms of interaction between those two groups of compounds were identified. Both dietary fatty acids and short chain fatty acids, which are metabolic products of the intestinal microflora, were able to modulate expression or activity of transmembrane transporters in models of the intestinal epithelium. Chronic treatment with butyric acid, at physiological concentrations as prevalent in the large intestine, increased expression of MCT1 and MCT4 which resulted in enhanced uptake of ferulic acid into the cell, and consequent elevated levels of phase II metabolites due to increased substrate availability, and also increased transepithelial transport of the aglycone. PUFA supplementation of Caco-2 cells resulted in enhanced paracellular diffusion of caffeic acid and epicatechin in the apical to basolateral transport direction, and efflux of epicatechin was reduced, most likely through an impact of PUFA on either expression or activity of apical transporter ABCC2. Uptake of epicatechin into the cell was much greater from the basolateral than from the apical side and intracellular epicatechin concentrations exceeding the extracellular concentration were reached with basolateral incubation. This uptake of aglycone against the concentration gradient indicates an active mechanism of epicatechin uptake at the basolateral plasma membrane of Caco-2 cells. A similar pathway mechanism was also observed for glucuronic acid conjugation of epicatechin by UGT1A8 in the HT29-MTX intestinal goblet cell line. Epicatechin conjugation was much greater when cells were incubated from the basolateral side than when incubated from the apical side, perhaps due to the presence of UGT1A8 in the basolateral plasma membrane. PUFA supplementation of cells also affected transport of ferulic acid in the apical to basolateral direction, but not, as originally hypothesised, through a change in passive diffusion rate. Even though the modulation of cellular lipid composition, by chronic fatty acid supplementation of the Caco-2 model, resulted in altered plasma

membrane fluidity, these physical changes did not correlate with the observed increase in ferulic acid transport. Instead it was demonstrated that the transport of ferulic acid could be inhibited by the compound estrone-3-sulfate, which argues for a transporter mediated pathway. More work is required to elucidate how these *in vitro* findings are linked to *in vivo* observations and whether the biological impact of phenolics can be enhanced through mechanisms identified in the current work.

Understanding the uptake mechanism and subsequent metabolism is crucial to predict the bioavailability of a compound. *In vitro* cell culture studies are helpful tools to examine isolated effects and mechanisms. *In vivo,* individual effects are much harder to follow because whole organisms, be it mouse, pig or human, are incredibly complex and a compound can exert its effect on many different processes simultaneously. As a result often only an overall impact on certain parameters can be identified *in vivo* and the molecular mechanism behind that impact can then be isolated and investigated *in vitro*. To achieve this, the *in vitro* model needs to replicate *in vivo* conditions as closely as possible. The work described here was carried out using a model that was intended to represent a chronic exposure to certain fatty acids as would be expected with different dietary patterns, as opposed to acute high doses of something that is not regularly consumed. Therefore a chronic supplementation with 50 µM fatty acid was chosen to represent lipid concentrations in the small intestine. Lipids are hydrolysed and absorbed in the distal duodenum and proximal ileum. Reports on the concentration of FFA in the small intestine of healthy participants are scarce. One study determined the FFA concentration in the distal duodenum, after consumption of a meal replacement drink which contained 24 g of fat, as 42 mM (397). Most of the experiments conducted for the current work were performed using DHA. The best dietary source for this compound is fatty fish. According to the USDA National Nutrient Database (99), 100 g of salmon, which is also the weight of a small to average portion that would be consumed in a meal, contain 4.65 g of fat, of which 0.65 g are DHA.

Putting this information in relation to the study cited above reveals that one portion of salmon fillet would result in a concentration of DHA of about 245 µM at its site of absorption. DHA from fish is not only consumed as part of a meal but also in form of nutritional supplements, traditionally in form of cod liver oil, but now also more specifically as omega 3 fish oil. According to the National Diet and Nutrition Survey of 2011, 11 % of man end women in the UK over the age of 19 are taking cod liver oil or other fish oil supplements, among the over 65s the number of people taking these supplements even increases to 24 % (398). The more traditional cod liver oil supplements contain about 11 % w/w DHA, specific omega 3 fish oil supplements are often more concentrated and contain higher amounts of PUFA (99). Supplement are often sold as capsules of 1000 mg fish oil which, assuming will undergo the same dilution as in the study cited above were 1 g of fat resulted in a concentration of 1.75 mM in the duodenum, translates to a FFA concentration in the distal duodenum of about 1.75 mM of which about 190 µM (11%) would be DHA. Of course these are only approximate estimations and do not take into account any matrix effects or meal sizes, but they do demonstrate that a 50 µM concentration of DHA at the site of absorption could be easily achieved in a population with regular fish consumption or people taking fish oil supplements.

The lipid induced changes in absorption and metabolism, which were identified in the current work, might contribute to some of the variations encountered in pharmacokinetic studies. High interindividual variation is often observed in human studies investigating absorption and metabolism of polyphenols (399-403). For such investigations, volunteers are asked to consume a defined amount of a phenolic compound and then plasma and/or urine samples are taken at regular intervals to monitor the absorption and excretion of the compounds of interest. Participants are required to abstain from polyphenol rich food before and during the study and a specified test meal is usually provided on the day of the study, but modulation of cellular composition and transporter expression by dietary fatty acids, as described

in the current work, could persist throughout pre-trial wash-out phase. Also, since meals are generally not regulated regarding non-polyphenol components before a study, lipids consumed during the wash-out phase could affect absorption during the trial. It would be of great interest to investigate whether such an interaction does indeed happen *in vivo*. For this purpose a human study could be conducted that tests the absorption of phenolics, for example, catechins from green tea or chocolate, before and after a supplementation period with fish oil or the impact of high and low fibre diets on absorption of ferulic acid from wheat bran.

The work described here concentrated on the long term effect of lipids as modulators of intestinal absorption. There are only very few reports that look at dietary lipids in this context, but there are a great number of publications on the use of lipids as acute absorption enhancers. Medium and long chain fatty acids especially were found to have a high potential to increase the *in vivo* bioavailability of a range of compounds. For example, co-administration of capric acid increased peptide transport (404) and lauric acid increased transport of the paracellular marker phenol red in a concentration dependent manner (405). When a lipophilic drug was administered in an oil matrix rich in either long, medium or short chain fatty acids, the drug concentration in lymph was greatly increased by long chain fatty acids but plasma concentrations were much higher when the drug was ingested together with medium chain fatty acids. Short chain fatty acids did not affect drug absorption (406). High concentrations of DHA in a drug suspension were shown to increase plasma levels of model compounds as well (407, 408). The influence of the lipid matrix has also been investigated for polyphenol bioavailability. In pigs, quercetin absorption was increased with concomitant feeding of medium chain, but not long chain fatty acids (409). Adding different oils to tomato sauce stimulated re-absorption of naringenin in humans. Especially the addition of olive oil resulted in a second plasma concentration peak of the glucuronic acid conjugate most likely due to enterohepatic recycling (410). A well-known case of direct impact of lipids on

absorption of lipophilic compounds is the uptake of carotenoids from vegetables consumed with or without added lipids. Adding oil to salad enhances absorption of lipid soluble vitamins, but not all types of oil have an equally strong effect. Soybean and coconut oil were shown to increase carotenoid uptake, whereas safflower oil, canola oil and butter had little impact (411, 412).

Epidemiological studies have revealed a link between fruit and vegetable intake and health, which in part is thought to be due to the polyphenol content of these foods (413-415). However, direct health improvement by phenolics has mostly been demonstrated using nutritional supplements containing high doses of individual compounds. Many fatty acids themselves have also been extensively investigated in the same context. DHA, for example, has been shown to possess many beneficial properties such as anti-inflammatory and immunomodulatory capacity, and being able to induce cell differentiation and apoptosis in cancer cells (416-418). There are areas where polyphenols and PUFA have overlapping effects. For instance, both polyphenols (419-421) and PUFA (422-424) have been demonstrated to protect against colorectal cancer and also polyphenols (425-427) and PUFA (428-431) have been shown to help reduce the risk of CVD. Perhaps this overlap in biological action could be exploited for the use of these food components in a medical context, as neutraceuticals. Not only do both substances have an individual effect but in combination they might work in synergy potentiating their impact and in addition, the work described here has shown that PUFA can enhance absorption of polyphenols thus increasing the potential health benefit of a combination of these substances even further. A recent study investigated the impact of such a combination of fish oil and polyphenols together with vitamins on mouse models of CVD. The authors showed that this mixture of compounds was able to significantly reduce atherosclerotic lesions in mice on a high cholesterol diet (432). Such synergistic effects might also play a small role in the context of polyphenols and lipids as part of a healthy diet. In particular, the ‘Mediterranean diet’ is defined by a high content of

fresh fruit and vegetables (good sources of polyphenols) and also a high intake of fish and olive oil (sources of unsaturated fatty acids) (433). Therefore a small part of the success of the Mediterranean diet in preventing CVD and other diseases associated with a ‘Western’ nutrition and lifestyle, could be due to the circumstance that it is based on a combination of foods that is especially well suited to improve absorption of bioactive phenolic compounds.

Chapter 9: Reference

1. Scalbert, A. and Williamson, G. Dietary intake and bioavailability of polyphenols. *Journal of Nutrition.* 2000, **130**(8), pp.2073S-2085S.
2. Manach, C. et al. Polyphenols: food sources and bioavailability. *American Journal of Clinical Nutrition.* 2004, **79**(5), pp.727-747.
3. Shin, K. et al. Tight junctions and cell polarity. In: *Annual Review of Cell and Developmental Biology*. 2006, pp.207-235.
4. Noah, T.K. et al. Intestinal development and differentiation. *Experimental Cell Research.* 2011, **317**(19), pp.2702-2710.
5. Yu, Q.-H. and Yang, Q. Diversity of tight junctions (TJs) between gastrointestinal epithelial cells and their function in maintaining the mucosal barrier. *Cell Biology International.* 2009, **33**(1), pp.78-82.
6. Collett, A. et al. Influence of morphometric factors on quantitation of paracellular permeability of intestinal epithelia in vitro. *Pharmaceutical Research.* 1997, **14**(6), pp.767-773.
7. Suzuki, T. Regulation of intestinal epithelial permeability by tight junctions. *Cellular and Molecular Life Sciences.* 2013, **70**(4), pp.631-659.
8. Krug, S.M. et al. Charge-selective claudin channels. *Barriers and Channels Formed by Tight Junction Proteins I.* 2012, **1257**, pp.20-28.
9. Turner, J.R. et al. The role of molecular remodeling in differential regulation of tight junction permeability. *Seminars in Cell & Developmental Biology.* 2014, **36**, pp.204-212.
10. Watson, C.J. et al. Functional modeling of tight junctions in intestinal cell monolayers using polyethylene glycol oligomers. *American Journal of Physiology-Cell Physiology.* 2001, **281**(2), pp.C388-C397.
11. Weber, C.R. Dynamic properties of the tight junction barrier. *Barriers and Channels Formed by Tight Junction Proteins I.* 2012, **1257**, pp.77-84.

12. Garrido-Urbani, S. et al. Tight junction dynamics: the role of junctional adhesion molecules (JAMs). *Cell and Tissue Research.* 2014, **355**(3), pp.701-715.

13. Maeda, S. and Tsukihara, T. Structure of the gap junction channel and its implications for its biological functions. *Cellular and Molecular Life Sciences.* 2011, **68**(7), pp.1115-1129.

14. Giepmans, B.N.G. and van Ijzendoorn, S.C.D. Epithelial cell-cell junctions and plasma membrane domains. *Biochimica Et Biophysica Acta-Biomembranes.* 2009, **1788**(4), pp.820-831.

15. Garrod, D. and Chidgey, M. Desmosome structure, composition and function. *Biochimica Et Biophysica Acta-Biomembranes.* 2008, **1778**(3), pp.572-587.

16. Konishi, Y. et al. Transepithelial transport of p-coumaric acid and gallic acid in caco-2 cell monolayers. *Bioscience Biotechnology and Biochemistry.* 2003, **67**(11), pp.2317-2324.

17. Konishi, Y. and Kobayashi, S. Transepithelial transport of chlorogenic acid, caffeic acid, and their colonic metabolites in intestinal Caco-2 cell monolayers. *Journal of Agricultural and Food Chemistry.* 2004, **52**(9), pp.2518-2526.

18. Hilgendorf, C. et al. Expression of thirty-six drug transporter genes in human intestine, liver, kidney, and organotypic cell lines. *Drug Metabolism and Disposition.* 2007, **35**(8), pp.1333-1340.

19. Oostendorp, R.L. et al. The biological and clinical role of drug transporters at the intestinal barrier. *Cancer Treatment Reviews.* 2009, **35**(2), pp.137-147.

20. Estudante, M. et al. Intestinal drug transporters: An overview. *Advanced Drug Delivery Reviews.* 2013, **64**(10), pp.1340-1356.

21. Rouleau, M. et al. Protein-protein interactions between the bilirubin-conjugating UDPglucuronosyltransferase UGT1A1 and its shorter isoform 2

regulatory partner derived from alternative splicing. *Biochemical Journal.* 2013, **450**, pp.107-114.

22. Rowland, A. et al. The UDP-glucuronosyltransferases: Their role in drug metabolism and detoxification. *International Journal of Biochemistry & Cell Biology.* 2013, **45**(6), pp.1121-1132.

23. Grosse, L. et al. Enantiomer Selective Glucuronidation of the Non-Steroidal Pure Anti-Androgen Bicalutamide by Human Liver and Kidney: Role of the Human UDP-Glucuronosyltransferase (UGT)1A9 Enzyme. *Basic & Clinical Pharmacology & Toxicology.* 2013, **113**(2), pp.92-102.

24. Gill, K.L. et al. Characterization of In Vitro Glucuronidation Clearance of a Range of Drugs in Human Kidney Microsomes: Comparison with Liver and Intestinal Glucuronidation and Impact of Albumin. *Drug Metabolism and Disposition.* 2012, **40**(4), pp.825-835.

25. Malfatti, M.A. et al. The effect of UDP-glucuronosyltransferase 1A1 expression on the mutagenicity and metabolism of the cooked-food carcinogen 2-amino-1-methyl-6-phenylimidazo 4,5-b pyridine in CHO cells. *Mutation Research-Fundamental and Molecular Mechanisms of Mutagenesis.* 2005, **570**(2), pp.205-214.

26. Leung, H.Y. et al. Differential effect of over-expressing UGT1A1 and CYP1A1 on xenobiotic assault in MCF-7 cells. *Toxicology.* 2007, **242**(1-3), pp.153-159.

27. Xu, L. et al. N-glucuronidation of perfluorooctanesulfonamide by human, rat, dog, and monkey liver microsomes and by expressed rat and human UDP-glucuronosyltransferases. *Drug Metabolism and Disposition.* 2006, **34**(8), pp.1406-1410.

28. Jenkinson, C. et al. Effects of Dietary Components on Testosterone Metabolism via UDP-Glucuronosyltransferase. *Frontiers in endocrinology.* 2013, **4**, pp.80-80.

29. Thibaudeau, J. et al. Characterization of common UGT1A8, UGT1A9, and UGT2B7 variants with different capacities to inactivate mutagenic 4-hydroxylated metabolites of estradiol and estrone. *Cancer Research.* 2006, **66**(1), pp.125-133.

30. Kato, Y. et al. Hepatic UDP-glucuronosyltransferases responsible for glucuronidation of thyroxine in humans. *Drug Metabolism and Disposition.* 2008, **36**(1), pp.51-55.

31. Cheng, Z.Q. et al. Studies on the substrate specificity of human intestinal UDP-glucuronosyltransferases 1A8 and 1A10. *Drug Metabolism and Disposition.* 1999, **27**(10), pp.1165-1170.

32. Wu, B. et al. First-Pass Metabolism via UDP-Glucuronosyltransferase: a Barrier to Oral Bioavailability of Phenolics. *Journal of Pharmaceutical Sciences.* 2011, **100**(9), pp.3655-3681.

33. Ng, S.P. et al. Evaluation of the first-pass glucuronidation of selected flavones in gut by Caco-2 monolayer model. *Journal of Pharmacy and Pharmaceutical Sciences.* 2005, **8**(1), pp.1-9.

34. Singh, R. et al. Uridine Diphosphate Glucuronosyltransferase Isoform-Dependent Regiospecificity of Glucuronidation of Flavonoids. *Journal of Agricultural and Food Chemistry.* 2011, **59**(13), pp.7452-7464.

35. Meech, R. et al. The glycosidation of xenobiotics and endogenous compounds: Versatility and redundancy in the UDP glycosyltransferase superfamily. *Pharmacology & Therapeutics.* 2012, **134**(2), pp.200-218.

36. Ohno, S. and Nakajin, S. Determination of mRNA Expression of Human UDP-Glucuronosyltransferases and Application for Localization in Various Human Tissues by Real-Time Reverse Transcriptase-Polymerase Chain Reaction. *Drug Metabolism and Disposition.* 2009, **37**(1), pp.32-40.

37. Glatt, H. et al. Human cytosolic sulphotransferases: genetics, characteristics, toxicological aspects. *Mutation Research-Fundamental and Molecular Mechanisms of Mutagenesis.* 2001, **482**(1-2), pp.27-40.

38. Blanchard, R.L. et al. A proposed nomenclature system for the cytosolic sulfotransferase (SULT) superfamily. *Pharmacogenetics.* 2004, **14**(3), pp.199-211.

39. Nishimura, M. and Naito, S. Tissue-specific mRNA expression profiles of human carbohydrate sulfotransferase and tyrosylprotein sulfotransferase. *Biological & Pharmaceutical Bulletin.* 2007, **30**(4), pp.821-825.

40. Jancova, P. et al. Phase II Drug Metabolizing Enzymes. *Biomedical Papers-Olomouc.* 2010, **154**(2), pp.103-116.

41. Rothwell, J.A. et al. Phenol-Explorer 3.0: a major update of the Phenol-Explorer database to incorporate data on the effects of food processing on polyphenol content. *Database.* 2013, **2013**.

42. El-Seedi, H.R. et al. Biosynthesis, Natural Sources, Dietary Intake, Pharmacokinetic Properties, and Biological Activities of Hydroxycinnamic Acids. *Journal of Agricultural and Food Chemistry.* 2012, **60**(44), pp.10877-10895.

43. Klepacka, J. and Fornal, L. Ferulic acid and its position among the phenolic compounds of wheat. *Critical Reviews in Food Science and Nutrition.* 2006, **46**(8), pp.639-647.

44. Lempereur, I. et al. Genetic and agronomic variation in arabinoxylan and ferulic acid contents of durum wheat (Triticum durum L.) grain and its milling fractions. *Journal of Cereal Science.* 1997, **25**(2), pp.103-110.

45. Mancuso, C. and Santangelo, R. Ferulic acid: Pharmacological and toxicological aspects. *Food and Chemical Toxicology.* 2014, **65**, pp.185-195.

46. Andreasen, M.F. et al. Esterase activity able to hydrolyze dietary antioxidant hydroxycinnamates is distributed along the intestine of mammals. *J Agric Food Chem.* 2001, **49**(11), pp.5679-5684.

47. Nordlund, E. et al. Formation of Phenolic Microbial Metabolites and Short-Chain Fatty Acids from Rye, Wheat, and Oat Bran and Their Fractions in the Metabolical in Vitro Colon Model. *J Agric Food Chem.* 2012, **60**(33), pp.8134-8145.

48. Kroon, P.A. et al. Release of covalently bound ferulic acid from fiber in the human colon. *J Agric Food Chem.* 1997, **45**(3), pp.661-667.

49. Hatcher, D.W. and Kruger, J.E. Simple phenolic acids in flours prepared from Canadian wheat: Relationship to ash content, color, and polyphenol oxidase activity. *Cereal Chemistry.* 1997, **74**(3), pp.337-343.

50. Rodriguez-Duran, L.V. et al. Soluble and Bound Hydroxycinnamates in Coffee Pulp (Coffea arabica) from Seven Cultivars at Three Ripening Stages. *Journal of Agricultural and Food Chemistry.* 2014, **62**(31), pp.7869-7876.

51. Renouf, M. et al. Dose-response plasma appearance of coffee chlorogenic and phenolic acids in adults. *Molecular Nutrition & Food Research.* 2014, **58**(2), pp.301-309.

52. DuPont, M.S. et al. Polyphenols from Alcoholic Apple Cider Are Absorbed, Metabolized and Excreted by Humans. *The Journal of nutrition.* 2002, **132**(2), pp.172-175.

53. Renouf, M. et al. Measurement of caffeic and ferulic acid equivalents in plasma after coffee consumption: Small intestine and colon are key sites for coffee metabolism. *Molecular Nutrition & Food Research.* 2010, **54**(6), pp.760-766.

54. Warden, B.A. et al. Catechins are bioavailable in men and women drinking black tea throughout the day. *Journal of Nutrition.* 2001, **131**(6), pp.1731-1737.

55. Del Rio, D. et al. Bioavailability and catabolism of green tea flavan-3-ols in humans. *Nutrition.* 2010, **26**(11-12), pp.1110-1116.

56. Yang, C.S. et al. Blood and urine levels of tea catechins after ingestion of different amounts of green tea by human volunteers. *Cancer Epidemiology Biomarkers & Prevention.* 1998, **7**(4), pp.351-354.

57. Lee, M.J. et al. Pharmacokinetics of tea catechins after ingestion of green tea and (-)-epigallocatechin-3-gallate by humans: formation of different metabolites and individual variability. *Cancer Epidemiology Biomarkers & Prevention.* 2002, **11**(10), pp.1025-1032.

58. Renouf, M. et al. Dose-response plasma appearance of green tea catechins in adults. *Molecular Nutrition & Food Research.* 2013, **57**(5), pp.833-839.

59. Narumi, K. et al. Simultaneous detection of green tea catechins and gallic acid in human serum after ingestion of green tea tablets using ion-pair high-performance liquid chromatography with electrochemical detection. *Journal of Chromatography B-Analytical Technologies in the Biomedical and Life Sciences.* 2014, **945**, pp.147-153.

60. Masukawa, Y. et al. Determination of green tea catechins in human plasma using liquid chromatography-electrospray ionization mass spectrometry. *Journal of Chromatography B-Analytical Technologies in the Biomedical and Life Sciences.* 2006, **834**(1-2), pp.26-34.

61. Richelle, M. et al. Plasma kinetics in man of epicatechin from black chocolate. *European Journal of Clinical Nutrition.* 1999, **53**(1), pp.22-26.

62. Li, C. et al. Structural identification of two metabolites of catechins and their kinetics in human urine and blood after tea ingestion. *Chemical Research in Toxicology.* 2000, **13**(3), pp.177-184.

63. Zhou, B.F. et al. Nutrient intakes of middle-aged men and women in China, Japan, United Kingdom, and United States in the late 1990s: the INTERMAP study. *Journal of Human Hypertension.* 2003, **17**(9), pp.623-630.

64. Murtaugh, M.A. et al. Diet composition and risk of overweight and obesity in women living in the southwestern United States. *Journal of the American Dietetic Association.* 2007, **107**(8), pp.1311-1321.

65. Ambring, A. et al. Effects of a Mediterranean-inspired diet on blood lipids, vascular function and oxidative stress in healthy subjects. *Clinical Science.* 2004, **106**(5), pp.519-525.

66. Vinknes, K.J. et al. Dietary Intake of Protein Is Positively Associated with Percent Body Fat in Middle-Aged and Older Adults. *Journal of Nutrition.* 2011, **141**(3), pp.440-446.

67. Bujnowski, D. et al. Longitudinal Association between Animal and Vegetable Protein Intake and Obesity among Men in the United States: The Chicago Western Electric Study. *Journal of the American Dietetic Association.* 2011, **111**(8), pp.1150-1155.

68. Iqbal, J. and Hussain, M.M. Intestinal lipid absorption. *American Journal of Physiology-Endocrinology and Metabolism.* 2009, **296**(6), pp.E1183-E1194.

69. Kulkarni, B.V. and Mattes, R.D. Lingual lipase activity in the orosensory detection of fat by humans. *American Journal of Physiology-Regulatory Integrative and Comparative Physiology.* 2014, **306**(12), pp.R879-R885.

70. Aloulou, A. and Carriere, F. Gastric lipase: an extremophilic interfacial enzyme with medical applications. *Cellular and Molecular Life Sciences.* 2008, **65**(6), pp.851-854.

71. *Servier medical art.* [Online]. [Accessed 16.11.2014]. Available from: http://www.servier.com/Powerpoint-image-bank.

72. Dawson, P.A. et al. Bile acid transporters. *Journal of Lipid Research.* 2009, **50**(12), pp.2340-2357.

73. Martinez-Augustin, O. and Sanchez de Medina, F. Intestinal bile acid physiology and pathophysiology. *World Journal of Gastroenterology.* 2008, **14**(37), pp.5630-5640.

74. Nanjwade, B.K. et al. Functions of lipids for enhancement of oral bioavailability of poorly water-soluble drugs. *Scientia pharmaceutica.* 2011, **79**(4), pp.705-27.

75. Demignot, S. et al. Triglyceride-rich lipoproteins and cytosolic lipid droplets in enterocytes: Key players in intestinal physiology and metabolic disorders. *Biochimie.* 2014, **96C**, pp.48-55.

76. McKimmie, R.L. et al. Acyl chain length, saturation, and hydrophobicity modulate the efficiency of dietary fatty acid absorption in adult humans. *American Journal of Physiology-Gastrointestinal and Liver Physiology.* 2013, **305**(9), pp.G620-G627.

77. Abumrad, N.A. and Davidson, N.O. Role of the Gut in Lipid Homeostasis. *Physiological Reviews.* 2012, **92**(3), pp.1061-1085.

78. Buttet, M. et al. From fatty-acid sensing to chylomicron synthesis: role of intestinal lipid-binding proteins. *Biochimie.* 2014, **96**, pp.37-47.

79. Takeuchi, K. and Reue, K. Biochemistry, physiology, and genetics of GPAT, AGPAT, and lipin enzymes in triglyceride synthesis. *Am J Physiol Endocrinol Metab.* 2009, **296**(6), pp.E1195-209.

80. Pan, X. and Hussain, M.M. Gut triglyceride production. *Biochimica Et Biophysica Acta-Molecular and Cell Biology of Lipids.* 2012, **1821**(5), pp.727-735.

81. Coleman, R.A. and Lee, D.P. Enzymes of triacylglycerol synthesis and their regulation. *Progress in Lipid Research.* 2004, **43**(2), pp.134-176.

82. Mitsche, M.A. et al. Surface Tensiometry of Apolipoprotein B Domains at Lipid Interfaces Suggests a New Model for the Initial Steps in Triglyceride-

rich Lipoprotein Assembly. *Journal of Biological Chemistry.* 2014, **289**(13), pp.9000-9012.

83. Pepino, M.Y. et al. Structure-function of CD36 and importance of fatty acid signal transduction in fat metabolism. *Annual Review of Nutrition.* 2014, **34**, pp.281-303.

84. Kalantari, F. et al. Biogenesis of lipid droplets - how cells get fatter. *Molecular Membrane Biology.* 2010, **27**(8), pp.462-468.

85. Beilstein, F. et al. Proteomic Analysis of Lipid Droplets from Caco-2/TC7 Enterocytes Identifies Novel Modulators of Lipid Secretion. *Plos One.* 2013, **8**(1).

86. Walther, T.C. and Farese, R.V., Jr. Lipid Droplets and Cellular Lipid Metabolism. *Annual Review of Biochemistry, Vol 81.* 2012, **81**, pp.687-714.

87. Bouchoux, J. et al. The proteome of cytosolic lipid droplets isolated from differentiated Caco-2/TC7 enterocytes reveals cell-specific characteristics. *Biology of the Cell.* 2011, **103**(11), pp.499-517.

88. Sewell, G.W. et al. Lipidomic profiling in Crohn's disease: Abnormalities in phosphatidylinositols, with preservation of ceramide, phosphatidylcholine and phosphatidylserine composition. *International Journal of Biochemistry & Cell Biology.* 2012, **44**(11), pp.1839-1846.

89. Holthuis, J.C.M. and Menon, A.K. Lipid landscapes and pipelines in membrane homeostasis. *Nature.* 2014, **510**(7503), pp.48-57.

90. Storch, J. et al. Metabolism of apical versus basolateral sn-2-monoacylglycerol and fatty acids in rodent small intestine. *Journal of Lipid Research.* 2008, **49**(8), pp.1762-1769.

91. Ho, S.Y. et al. Monoacylglycerol metabolism in human intestinal Caco-2 cells - Evidence for metabolic compartmentation and hydrolysis. *Journal of Biological Chemistry.* 2002, **277**(3), pp.1816-1823.

92. Trotter, P.J. and Storch, J. Fatty acid uptake and metabolism in a human intestinal cell line (Caco-2): comparison of apical and basolateral incubation *Journal of Lipid Research.* 1991, **32**(2), pp.293-304.

93. Jakobsson, A. et al. Fatty acid elongases in mammals: Their regulation and roles in metabolism. *Progress in Lipid Research.* 2006, **45**(3), pp.237-249.

94. Leonard, A.E. et al. Elongation of long-chain fatty acids. *Progress in Lipid Research.* 2004, **43**(1), pp.36-54.

95. Pauter, A.M. et al. Elovl2 ablation demonstrates that systemic DHA is endogenously produced and is essential for lipid homeostasis in mice. *Journal of Lipid Research.* 2014, **55**(4), pp.718-728.

96. Moon, Y.A. et al. Deletion of ELOVL5 leads to fatty liver through activation of SREBP-1c in mice. *J Lipid Res.* 2009, **50**(3), pp.412-23.

97. den Besten, G. et al. The role of short-chain fatty acids in the interplay between diet, gut microbiota, and host energy metabolism. *Journal of Lipid Research.* 2013, **54**(9), pp.2325-2340.

98. den Besten, G. et al. Gut-derived short-chain fatty acids are vividly assimilated into host carbohydrates and lipids. *American Journal of Physiology-Gastrointestinal and Liver Physiology.* 2013, **305**(12), pp.G900-G910.

99. U.S. Department of Agriculture, A.R.S. *USDA National Nutrient Database for Standard Reference, Release 26.* [Online]. 2013. [Accessed 08/11/2014]. Available from: http://www.ars.usda.gov/ba/bhnrc/ndl.

100. Gabrielsson, B.G. et al. Dietary herring improves plasma lipid profiles and reduces atherosclerosis in obese low-density lipoprotein receptor-deficient mice. *International Journal of Molecular Medicine.* 2012, **29**(3), pp.331-337.

101. Heemskerk, J.W.M. et al. Influence of Dietary Fatty-Acids on Membrane Fluidity and Activation of Rat Platelets. *Biochimica Et Biophysica Acta.* 1989, **1004**(2), pp.252-260.

102. Browning, L.M. et al. Incorporation of eicosapentaenoic and docosahexaenoic acids into lipid pools when given as supplements providing doses equivalent to typical intakes of oily fish. *American Journal of Clinical Nutrition.* 2012, **96**(4), pp.748-758.

103. Krul, E.S. et al. Effects of duration of treatment and dosage of eicosapentaenoic acid and stearidonic acid on red blood cell eicosapentaenoic acid content. *Prostaglandins Leukotrienes and Essential Fatty Acids.* 2012, **86**(1-2), pp.51-59.

104. Dawczynski, C. et al. Incorporation of n-3 PUFA and gamma-linolenic acid in blood lipids and red blood cell lipids together with their influence on disease activity in patients with chronic inflammatory arthritis - a randomized controlled human intervention trial. *Lipids in Health and Disease.* 2011, **10**.

105. Faber, J. et al. Supplementation with a Fish Oil-Enriched, High-Protein Medical Food Leads to Rapid Incorporation of EPA into White Blood Cells and Modulates Immune Responses within One Week in Healthy Men and Women. *Journal of Nutrition.* 2011, **141**(5), pp.964-970.

106. Witt, P.M. et al. The incorporation of marine n-3 PUFA into platelets and adipose tissue in pre- and postmenopausal women: a randomised, double-blind, placebo-controlled trial. *British Journal of Nutrition.* 2010, **104**(3), pp.318-325.

107. Haugaard, S.B. et al. Dietary intervention increases n-3 long-chain polyunsaturated fatty acids in skeletal muscle membrane phospholipids of obese subjects. Implications for insulin sensitivity. *Clinical Endocrinology.* 2006, **64**(2), pp.169-178.

108. Harris, W.S. et al. Omega-3 fatty acids in cardiac biopsies from heart transplantation patients - Correlation with erythrocytes and response to supplementation. *Circulation.* 2004, **110**(12), pp.1645-1649.

109. Berlin, E. et al. Effects of Omega-3 Fatty Acid and Vitamin-E Supplementation on Erythrocyte Membrane Fluidity, Tocopherols, Insulin Binding, and Lipid Composition in Adult Men. *Journal of Nutritional Biochemistry.* 1992, **3**(8), pp.392-400.

110. Browning, L.M. et al. Compared with Daily, Weekly n-3 PUFA Intake Affects the Incorporation of Eicosapentaenoic Acid and Docosahexaenoic Acid into Platelets and Mononuclear Cells in Humans. *Journal of Nutrition.* 2014, **144**(5), pp.667-672.

111. Gillingham, L.G. et al. High-oleic rapeseed (canola) and flaxseed oils modulate serum lipids and inflammatory biomarkers in hypercholesterolaemic subjects. *British Journal of Nutrition.* 2011, **105**(3), pp.417-427.

112. Charman, W.N. et al. Physicochemical and physiological mechanisms for the effects of food on drug absorption: The role of lipids and pH. *Journal of Pharmaceutical Sciences.* 1997, **86**(3), pp.269-282.

113. van Hell, A.J. et al. Membrane organization determines barrier properties of endothelial cells and short-chain sphingolipid-facilitated doxorubicin influx. *Biochimica Et Biophysica Acta-Molecular and Cell Biology of Lipids.* 2014, **1841**(9), pp.1301-1307.

114. Narayanan, N.K. et al. Liposome encapsulation of curcumin and resveratrol in combination reduces prostate cancer incidence in PTEN knockout mice. *International Journal of Cancer.* 2009, **125**(1), pp.1-8.

115. Yuan, Z.P. et al. Liposomal quercetin efficiently suppresses growth of solid tumors in murine models. *Clinical Cancer Research.* 2006, **12**(10), pp.3193-3199.

116. Daveloose, D. et al. Simultaneous changes in lipid composition, fluidity and enzyme activity in piglet intestinal brush border membrane as affected by

dietary polyunsaturated fatty acid deficiency *Biochimica Et Biophysica Acta.* 1993, **1166**(2-3), pp.229-237.

117. Masaoka, Y. et al. Site of drug absorption after oral administration: Assessment of membrane permeability and luminal concentration of drugs in each segment of gastrointestinal tract. *European Journal of Pharmaceutical Sciences.* 2006, **29**(3-4), pp.240-250.

118. Stubbs, C.D. and Smith, A.D. The modification of mammalian membrane polyunsaturated fatty acid composition in relation to membrane fluidity. *Biochimica Et Biophysica Acta.* 1984, **779**(1), pp.89-137.

119. Breton, M. et al. Linoleate Incorporation into Rat Liver Membranes Phospholipids: Effect on Plasma Membrane ATPase Activities and Physical Properties. *Biochemical and Biophysical Research Communications.* 1983, **117**(3), pp.809-816.

120. Yuli, I. et al. GLUCOSE-TRANSPORT THROUGH CELL-MEMBRANES OF MODIFIED LIPID FLUIDITY. *Biochemistry.* 1981, **20**(15), pp.4250-4256.

121. Merrill, A.R. et al. Relation Between Ca-2+ Uptake and Fluidity of Brush Border Membranes Isolated From Rabbit Small-Intestine and Incubated with Fatty-AcidsaAnd Methyl Oleate. *Biochimica Et Biophysica Acta.* 1987, **896**(1), pp.89-95.

122. Meyer dos Santos, S. et al. Cholesterol: Coupling between membrane microenvironment and ABC transporter activity. *Biochemical and Biophysical Research Communications.* 2007, **354**(1), pp.216-221.

123. Ma, D.W.L. et al. n-3 PUFA Alter caveolae lipid composition and resident protein localization in mouse colon. *Faseb Journal.* 2004, **18**(6), pp.1040-+.

124. Modok, S. et al. P-glycoprotein retains function when reconstituted into a sphingolipid- and cholesterol-rich environment. *Journal of Lipid Research.* 2004, **45**(10), pp.1910-1918.

125. Warren, G.B. et al. Cholesterol is Excluded from Phospholipid Annulus Surrounding an Active Calcium-Transport Protein. *Nature.* 1975, **255**(5511), pp.684-687.

126. Lee, A.G. How lipids and proteins interact in a membrane: a molecular approach. *Molecular BioSystems.* 2005, **1**(3), pp.203-212.

127. Powl, A.M. et al. Different effects of lipid chain length on the two sides of a membrane and the lipid annulus of MscL. *Biophysical Journal.* 2007, **93**(1), pp.113-122.

128. Lee, A.G. Lipid–protein interactions in biological membranes: a structural perspective. *Biochimica et Biophysica Acta (BBA) - Biomembranes.* 2003, **1612**(1), pp.1-40.

129. Mahoney, E.M. et al. Influence of Fatty Acyl Substitution on The Composition and Function of Macrophage Membranes. *Journal of Biological Chemistry.* 1980, **255**(10), pp.4910-4917.

130. Lesuffleur, T. et al. Growth adaptation to methotrexate of ht-29 human colon-carcinoma cells is associated with their ability to differentiate into columnar absorptive and mucus-secreting cells. *Cancer Research.* 1990, **50**(19), pp.6334-6343.

131. ATCC. *Caco-2 [Caco2] (ATCC® HTB-37™) Culture Method.* [Online]. [Accessed 02/03/2015]. Available from: https://www.lgcstandards-atcc.org/Products/All/HTB-37.aspx?slp=1#culturemethod.

132. Ivanov, A.I. et al. Endocytosis of epithelial apical junctional proteins by a clathrin-mediated pathway into a unique storage compartment. *Molecular Biology of the Cell.* 2004, **15**(1), pp.176-188.

133. Salucci, M. et al. Flavonoids uptake and their effect on cell cycle of human colon adenocarcinoma cells (Caco2). *British Journal of Cancer.* 2002, **86**(10), pp.1645-1651.

134. Garcia, C.K. et al. Molecular Characterization of a Membrane Transporter for Lactate, Pyruvate, and other Monocarboxylates - Implications for the Cori Cycle. *Cell.* 1994, **76**(5), pp.865-873.

135. Farrell, T.L. et al. Predicting Phenolic Acid Absorption in Caco-2 Cells: A Theoretical Permeability Model and Mechanistic Study. *Drug Metabolism and Disposition.* 2012, **40**(2), pp.397-406.

136. Omkvist, D.H. et al. Ibuprofen is a non-competitive inhibitor of the peptide transporter hPEPT1 (SLC15A1): possible interactions between hPEPT1 substrates and ibuprofen. *British Journal of Pharmacology.* 2010, **161**(8), pp.1793-1805.

137. Nakanishi, T. et al. Carrier-mediated transport of oligopeptides in the human fibrosarcoma cell line HT1080. *Cancer Research.* 1997, **57**(18), pp.4118-4122.

138. Grandvuinet, A.S. and Steffansen, B. Interactions Between Organic Anions on Multiple Transporters in Caco-2 Cells. *Journal of Pharmaceutical Sciences.* 2011, **100**(9), pp.3817-3830.

139. Farrell, T. et al. Characterization of hydroxycinnamic acid glucuronide and sulfate conjugates by HPLC-DAD-MS2: Enhancing chromatographic quantification and application in Caco-2 cell metabolism. *J Pharm Biomed Anal.* 2011, **55**(5), pp.1245-1254.

140. Clarke, K.A. et al. High performance liquid chromatography tandem mass spectrometry dual extraction method for identification of green tea catechin metabolites excreted in human urine. *Journal of Chromatography B.* 2014, **972**(0), pp.29-37.

141. Shirazibeechey, S.P. et al. Preparation and Properties of Brush-Border Membrane-Vesicles from Human Small-Intestine. *Gastroenterology.* 1990, **98**(3), pp.676-685.

142. Cruz-Hernandez, C. et al. Direct quantification of fatty acids in human milk by gas chromatography. *Journal of Chromatography A.* 2013, **1284**, pp.174-179.

143. Wong, C.C. et al. In vitro and in vivo conjugation of dietary hydroxycinnamic acids by UDP-glucuronosyltransferases and sulfotransferases in humans. *Journal of Nutritional Biochemistry.* 2010, **21**(11), pp.1060-1068.

144. Pinto, M. et al. Enterocyte Like Differentiation and Polarization of the Human Colon Carcinoma Cell Line Caco-2 in Culture. *Biology of the Cell.* 1983, **47**(3), pp.323-330.

145. Mehran, M. et al. Lipid, apolipoprotein, and lipoprotein synthesis and secretion during cellular differentiation in CACO-2 cells. *In Vitro Cellular & Developmental Biology-Animal.* 1997, **33**(2), pp.118-128.

146. Meunier, V. et al. The Human Intestinal Epithelial Cell Line Caco-2; Pharmacological and Pharmacokinetic Applications. *Cell Biology and Toxicology.* 1995, **11**(3-4), pp.187-194.

147. Hayeshi, R. et al. Comparison of drug transporter gene expression and functionality in Caco-2 cells from 10 different laboratories. *Eur J Pharm Sci.* 2008, **35**(5), pp.383-396.

148. Jahn, K.A. et al. GM1 expression in caco-2 cells: Characterisation of a fundamental passage-dependent transformation of a cell line. *Journal of Pharmaceutical Sciences.* 2011, **100**(9), pp.3751-3762.

149. Walter, E. and Kissel, T. Heterogeneity in the human intestinal cell line Caco-2 leads to differences in transepithelial transport. *European Journal of Pharmaceutical Sciences.* 1995, **3**(4), pp.215-230.

150. Roth, W.J. et al. The effects of intralaboratory modifications to media composition and cell source on the expression of pharmaceutically relevant transporters and metabolizing genes in the Caco-2 cell line. *Journal of Pharmaceutical Sciences.* 2012, **101**(10), pp.3962-3978.

151. Murota, K. and Storch, J. Uptake of micellar long-chain fatty acid and sn-2-monoacylglycerol into human intestinal Caco-2 cells exhibits characteristics of protein-mediated transport. *Journal of Nutrition.* 2005, **135**(7), pp.1626-1630.

152. Trotter, P.J. et al. Fatty acid uptake by Caco-2 human intestinal cells. *Journal of Lipid Research.* 1996, **37**(2), pp.336-346.

153. Gil-Zamorano, J. et al. Docosahexaenoic Acid Modulates the Enterocyte Caco-2 Cell Expression of MicroRNAs Involved in Lipid Metabolism. *Journal of Nutrition.* 2014, **144**(5), pp.575-585.

154. Bateman, P.A. et al. Differences in cell morphology, lipid and apo B secretory capacity in caco-2 cells following long term treatment with saturated and monounsaturated fatty acids. *Biochimica Et Biophysica Acta-Molecular and Cell Biology of Lipids.* 2007, **1771**(4), pp.475-485.

155. Nano, J.L. et al. Effects of fatty acids on the growth of Caco-2 cells. *Prostaglandins Leukotrienes and Essential Fatty Acids.* 2003, **69**(4), pp.207-215.

156. Dias, V.C. and Parsons, H.G. Modulation in delta 9, delta 6, and delta 5 fatty acid desaturase activity in the human intestinal CaCo-2 cell line. *Journal of Lipid Research.* 1995, **36**(3), pp.552-63.

157. Barber, E. et al. Comparative actions of omega-3 fatty acids on in-vitro lipid droplet formation. *Prostaglandins, Leukotriens and Essential Fatty Acids.* 2013, **89**(5), pp.359-66.

158. Greenspan, P. et al. Nile red: a selective fluorescent stain for intracellular lipid droplets. *Journal of Cell Biology.* 1985, **100**(3), pp.965-73.

159. Luchoomun, J. and Hussain, M.M. Assembly and secretion of chylomicrons by differentiated Caco-2 cells - Nascent triglycerides and preformed phospholipids are preferentially used for lipoprotein assembly. *Journal of Biological Chemistry.* 1999, **274**(28), pp.19565-19572.

160. Collins, J.M. and Grogan, W.M. Comparisons of Steady-State Anisotropy of The Plasma-Membrane of Living Cells with Different Probes. *Biochimica Et Biophysica Acta.* 1991, **1067**(2), pp.171-176.

161. Tóth, M.E. et al. Alcohol stress, membranes, and chaperones. *Cell Stress Chaperones.* 2014, **19**(3), pp.299-309.

162. Ranheim, T. et al. Fatty acid uptake and metabolism in CaCo-2 cells: eicosapentaenoic acid (20:5(n - 3)) and oleic acid (18: l(IZ - 9)) presented in association with micelles or albumin *Biochimica Et Biophysica Acta-Lipids and Lipid Metabolism.* 1994, **1212**(3), pp.295-304.

163. Ho, S.P. and Storch, J. Common mechanisms of monoacylglycerol and fatty acid uptake by human intestinal Caco-2 cells. *American Journal of Physiology-Cell Physiology.* 2001, **281**(4), pp.C1106-C1117.

164. Levin, M.S. et al. Trafficking of exogenous fatty acids within Caco-2 cells *Journal of Lipid Research.* 1992, **33**(1), pp.9-19.

165. Inaba, M. et al. Extracellular metabolism-dependent uptake of lysolipids through cultured monolayer of differentiated Caco-2 cells. *Biochimica Et Biophysica Acta-Molecular and Cell Biology of Lipids.* 2014, **1841**(1), pp.121-131.

166. Wiesenfeld, P.W. et al. Effect of long-chain fatty acids in the culture medium on fatty acid composition of WEHI-3 and J774A.1 cells. *Comparative Biochemistry and Physiology Part B: Biochemistry and Molecular Biology.* 2001, **128**(1), pp.123-34.

167. Spector, A.A. et al. Binding of Long Chain Fatty Acids to Bovine Serum Albumin. *Journal of Lipid Research.* 1969, **10**(1), pp.56-&.

168. Gstraunthaler, G. Alternatives to the use of fetal bovine serum: Serum-free cell culture. *Altex-Alternativen Zu Tierexperimenten.* 2003, **20**(4), pp.275-281.

169. Sambuy, Y. et al. The Caco-2 cell line as a model of the intestinal barrier: influence of cell and culture-related factors on Caco-2 cell functional characteristics. *Cell Biology and Toxicology.* 2005, **21**(1), pp.1-26.

170. Trotter, P.J. and Storch, J. Esterification During Differentiation of the Human Intestinal Cell Line Caco-2. *Journal of Biological Chemistry.* 1993, **268**(14), pp.10017-10023.

171. Tahin, Q.S. et al. The Fatty Acid Composition of Subcellular Membranes of Rat Liver, Heart, and Brain: Diet-Induced Modifications. *European Journal of Biochemistry.* 1981, **121**(1), pp.5-13.

172. Christon, R. et al. Effects of a Low Dietary Linoleic-Acid Level on Intestinal Morphology and Enterocyte Brush-Border Membrane Lipid-Composition. *Reproduction Nutrition Development.* 1991, **31**(6), pp.691-701.

173. Roig-Perez, S. et al. Correlation of Taurine Transport with Membrane Lipid Composition and Peroxidation in DHA-Enriched Caco-2 Cells. *Journal of Membrane Biology.* 2009, **228**(3), pp.141-150.

174. Duraisamy, Y. et al. Differential incorporation of docosahexaenoic acid into distinct cholesterol-rich membrane raft domains. *Biochemical and Biophysical Research Communications.* 2007, **360**(4), pp.885-890.

175. Black, I.L. et al. Acute-on-chronic effects of fatty acids on intestinal triacylglycerol-rich lipoprotein metabolism. *British Journal of Nutrition.* 2002, **88**(6), pp.661-669.

176. Gurzell, E.A. et al. Is the omega-3 index a valid marker of intestinal membrane phospholipid EPA+DHA content? *Prostaglandins, Leukotriens and Essential Fatty Acids.* 2014, **91**, pp.87-96.

177. Beguin, P. et al. Effect of polyunsaturated fatty acids on tight junctions in a model of the human intestinal epithelium under normal and inflammatory conditions. *Food & function.* 2013, **4**(6), pp.923-931.

178. Tu, W.C. et al. Omega-3 long chain fatty acid synthesis is regulated more by substrate levels than gene expression. *Prostaglandins Leukotrienes and Essential Fatty Acids.* 2010, **83**(2), pp.61-68.

179. Gronn, M. et al. Dietary n-6 Fatty-Acids Inhibit the Incorporation Of Dietary n-3 Fatty-Acids in Thrombocyte and Serum Phospholipids In Humans - a Controlled Dietetic Study. *Scandinavian Journal of Clinical & Laboratory Investigation.* 1991, **51**(3), pp.255-263.

180. Conquer, J.A. and Holub, B.J. Effect of supplementation with different doses of DHA on the levels of circulating DHA as non-esterified fatty acid in subjects of Asian Indian background. *Journal of Lipid Research.* 1998, **39**(2), pp.286-92.

181. Vine, D.F. et al. Effect of dietary fatty acids on the intestinal permeability of marker drug compounds in excised rat jejunum. *Journal of Pharmacy and Pharmacology.* 2002, **54**(6), pp.809-819.

182. Engler, M.M. et al. Dietary docosahexaenoic acid affects stearic acid desaturation in spontaneously hypertensive rats. *Lipids.* 2000, **35**(9), pp.1011-1015.

183. Poudyal, H. et al. Effects of ALA, EPA and DHA in high-carbohydrate, high-fat diet-induced metabolic syndrome in rats. *Journal of Nutritional Biochemistry.* 2013, **24**(6), pp.1041-1052.

184. Lamaziere, A. et al. Lipidomics of hepatic lipogenesis inhibition by omega 3 fatty acids. *Prostaglandins Leukotrienes and Essential Fatty Acids.* 2013, **88**(2), pp.149-154.

185. Gronn, M. et al. Peroxisomal Retroconversion of Docosahexaenoic Acid (22-6(N-3)) to Eicosapentaenoic Acid (20-5(N-3)) Studied in Isolated Rat-Liver Cells. *Biochimica Et Biophysica Acta.* 1991, **1081**(1), pp.85-91.

186. Caligiuri, S.P.B. et al. Dietary Linoleic Acid and a-Linolenic Acid Differentially Affect Renal Oxylipins and Phospholipid Fatty Acids in Diet-Induced Obese Rats. *Journal of Nutrition.* 2013, **143**(9), pp.1421-1431.

187. Kim, H.K. and Choi, H. Dietary alpha-linolenic acid lowers postprandial lipid levels with increase of eicosapentaenoic and docosahexaenoic acid contents in rat hepatic membrane. *Lipids.* 2001, **36**(12), pp.1331-1336.

188. Danielsen, E.M. et al. Permeabilization of enterocytes induced by absorption of dietary fat. *Molecular Membrane Biology.* 2013, **30**(3), pp.261-272.

189. Schneeberger, E.E. et al. Formation and Disappearance of Triglyceride Droplets in Strain L Fibroblasts - Electron Microscopic Study. *Experimental Cell Research.* 1971, **69**(1), pp.193-&.

190. Wang, Y. et al. Effects of Eicosapentaenoic Acid and Docosahexaenoic Acid on Chylomicron and VLDL Synthesis and Secretion in Caco-2 Cells. *Biomedical Research International.* 2014.

191. Calder, P.C. et al. Incorporation of fatty acids by concanavalin A-stimulated lymphocytes and the effect on fatty acid composition and membrane fluidity. *Biochemical Journal.* 1994, **300**, pp.509-518.

192. Stubbs, C.D. et al. Incubation of Exogenous Fatty Acids with Lymphocytes. Changes in Fatty Acid Composition and Effects on the Rotational Relaxation Time of 1,6-Diphenyl-1,3,5-hexatriene. *Biochemistry.* 1980, **19**(12), pp.2756-2762.

193. Pazouki, S. et al. Utilization of Extracellular Lipids by HT29/219 Cancer Cells in Culture. *Lipids.* 1992, **27**(11), pp.827-834.

194. Rosenthal, M.D. Accumulation of Neutral Lipids by Human Skin Fibroblasts: Differential Effects of Saturated and Unsaturated Fatty Acids. *Lipids.* 1981, **16**(3), pp.173-182.

195. Hatala, M.A. et al. Comparison of Linoleic-Acid and Eicosapentaenoic Acid Incorporation into Human Breast-Cancer Cells. *Lipids.* 1994, **29**(12), pp.831-837.

196. Pessin, J.E. et al. Use of a Fluorescent Probe to Compare Plasma Membrane Properties in Normal and Transformed Cells. Evaluation of Interference by Triacylglycerols and Alkyldiacylglycerols. *Biochemistry.* 1978, **17**(10), pp.1997-2004.

197. Dimancheboitrel, M.T. et al. Confluence-Dependent Resistance in Human Colon Cancer-Cells - Role of Reduced Drug Accumulation and Low Intrinsic Chemosensitivity of Resting Cells. *International Journal of Cancer.* 1992, **50**(5), pp.677-682.

198. D'Souza, V.M. et al. High glucose concentration in isotonic media alters Caco-2 cell permeability. *Aaps Pharmsci.* 2003, **5**(3).

199. Mengeaud, V. et al. Effects of Eicosapentaenoic Acid, Gamma-Linolenic Acid and Prostaglandin-E1 on 3 Human Colon-Carcinoma Cell-Lines. *Prostaglandins Leukotrienes and Essential Fatty Acids.* 1992, **47**(4), pp.313-319.

200. Berlin, E. et al. Fatty acid modification of membrane fluidity in Chinese hamster ovary (TR715-19) cells. *International Journal of Biochemistry & Cell Biology.* 1996, **28**(10), pp.1131-1139.

201. Meehan, E. et al. Influence of an n-6 polyunsaturated fatty acid-enriched diet on the development of tolerance during chronic ethanol administration in rats. *Alcoholism-Clinical and Experimental Research.* 1995, **19**(6), pp.1441-1446.

202. Calderon, R.O. and Eynard, A.R. Fatty acids specifically related to the anisotropic properties of plasma membrane from rat urothelium. *Biochimica Et Biophysica Acta-Molecular and Cell Biology of Lipids.* 2000, **1483**(1), pp.174-184.

203. Xu, J. et al. Dietary polyunsaturated fats regulate rat liver sterol regulatory element binding proteins-1 and-2 in three distinct stages and by different mechanisms. *Journal of Nutrition.* 2002, **132**(11), pp.3333-3339.

204. Zhang, J. et al. Alpha-linolenic acid increases cholesterol efflux in macrophage-derived foam cells by decreasing stearoyl CoA desaturase 1 expression: evidence for a farnesoid-X-receptor mechanism of action. *Journal of Nutritional Biochemistry.* 2012, **23**(4), pp.400-409.

205. Schmidt, S. et al. Regulation of lipid metabolism-related gene expression in whole blood cells of normo- and dyslipidemic men after fish oil supplementation. *Lipids in Health and Disease.* 2012, **11**.

206. Karanth, S. et al. Polyunsaturated fatty acyl-coenzyme As are inhibitors of cholesterol biosynthesis in zebrafish and mice. *Disease Models & Mechanisms.* 2013, **6**(6), pp.1365-1377.

207. Gelsomino, G. et al. Omega 3 fatty acids chemosensitize multidrug resistant colon cancer cells by down-regulating cholesterol synthesis and altering detergent resistant membranes composition. *Molecular Cancer.* 2013, **12**.

208. Slater, T.F. et al. Studies on Succinate-Tetrazolium Reductase Systems .3. Points of Coupling of 4 Different Tetrazolium Salts. *Biochimica Et Biophysica Acta.* 1963, **77**(3), pp.383-&.

209. Hess, R. et al. The Cytochemical Localization of Oxidative Enzymes .2. Pyridine Nucleotide-linked Dehydrogenases. *Journal of Biophysical and Biochemical Cytology.* 1958, **4**(6), pp.753-&.

210. Takahashi, S. et al. Substrate-dependence of reduction of MTT: a tetrazolium dye differs in cultured astroglia and neurons. *Neurochemistry International.* 2002, **40**(5), pp.441-448.

211. Berridge, M.V. and Tan, A.S. Characterization of the Cellular Reduction of 3-(4,5-Dimethylthiazol-2-Yl)-2,5-Diphenyltetrazolium Bromide (MTT) - Subcellular-Localization, Substrate Dependence, and Involvement of

Mitochondrial Electron-Transport in MTT Reduction. *Archives of Biochemistry and Biophysics.* 1993, **303**(2), pp.474-482.

212. Bernas, T. and Dobrucki, J. Mitochondrial and nonmitochondrial reduction of MTT: Interaction of MTT with TMRE, JC-1, and NAO mitochondrial fluorescent probes. *Cytometry.* 2002, **47**(4), pp.236-242.

213. Stockert, J.C. et al. MTT assay for cell viability: Intracellular localization of the formazan product is in lipid droplets. *Acta Histochemica.* 2012, **114**(8), pp.785-796.

214. Loveland, B.E. et al. Validation of the MTT Dye Assay for Enumeration of Cells in Proliferative and Antiproliferative Assays. *Biochemistry International.* 1992, **27**(3), pp.501-510.

215. York, J.L. et al. Reduction of MTT by glutathione S-Transferase. *Biotechniques.* 1998, **25**(4), pp.622-+.

216. Di Nunzio, M. et al. Pro- and anti-oxidant effects of polyunsaturated fatty acid supplementation in HepG2 cells. *Prostaglandins Leukotrienes and Essential Fatty Acids.* 2011, **85**(3-4), pp.121-127.

217. Vellonen, K.S. et al. Substrates and inhibitors of efflux proteins interfere with the MTT assay in cells and may lead to underestimation of drug toxicity. *European Journal of Pharmaceutical Sciences.* 2004, **23**(2), pp.181-188.

218. Kuan, C.-Y. et al. Long-Chain Polyunsaturated Fatty Acids Promote Paclitaxel Cytotoxicity via Inhibition of the MDR1 Gene in the Human Colon Cancer Caco-2 Cell Line. *Journal of the American College of Nutrition.* 2011, **30**(4), pp.265-273.

219. Koecher, K.J. et al. Estimation and Interpretation of Fermentation in the Gut: Coupling Results from a 24 h Batch in Vitro System with Fecal Measurements from a Human Intervention Feeding Study Using Fructooligosaccharides, Inulin, Gum Acacia, and Pea Fiber. *Journal of Agricultural and Food Chemistry.* 2014, **62**(6), pp.1332-1337.

220. Hadjiagapiou, C. et al. Mechanism(s) of butyrate transport in Caco-2 cells: role of monocarboxylate transporter 1. *Am J Physiol Gastrointest Liver Physiol.* 2000, **279**(4), pp.G775-G780.

221. Goncalves, P. et al. Inhibition of butyrate uptake by the primary bile salt chenodeoxycholic acid in intestinal epithelial cells. *Journal of Cellular Biochemistry.* 2012, **113**(9), pp.2937-2947.

222. Clausen, M.R. and Mortensen, P.B. Kinetic Studies on Colonocyte Metabolism of Short Chain Fatty Acids and Glucose In Ulcerative Colitis. *Gut.* 1995, **37**(5), pp.684-689.

223. Roediger, W.E.W. Utilization of Nutrients by Isolated Epithelial Cells of the Rat Colon. *Gastroenterology.* 1982, **83**(2), pp.424-429.

224. Halestrap, A.P. The monocarboxylate transporter family - Structure and functional characterization. *Iubmb Life.* 2012, **64**(1), pp.1-9.

225. Wright, E.M. Glucose transport families SLC5 and SLC50. *Molecular Aspects of Medicine.* 2013, **34**(2-3), pp.183-196.

226. Fung, K.Y.C. et al. A review of the potential mechanisms for the lowering of colorectal oncogenesis by butyrate. *British Journal of Nutrition.* 2012, **108**(5), pp.820-831.

227. Hamer, H.M. et al. Review article: the role of butyrate on colonic function. *Alimentary Pharmacology & Therapeutics.* 2008, **27**(2), pp.104-119.

228. Cuff, M.A. et al. Substrate-induced regulation of the human colonic monocarboxylate transporter, MCT1. *Journal of Physiology-London.* 2002, **539**(2), pp.361-371.

229. Kirat, D. et al. Dietary pectin up-regulates monocaboxylate transporter 1 in the rat gastrointestinal tract. *Exp Physiol.* 2009, **94**(4), pp.422-433.

230. Lecona, E. et al. Kinetic analysis of butyrate transport in human colon adenocarcinoma cells reveals two different carrier-mediated mechanisms. *Biochem J.* 2008, **409**, pp.311-320.

231. Haenen, D. et al. A Diet High in Resistant Starch Modulates Microbiota Composition, SCFA Concentrations, and Gene Expression in Pig Intestine. *Journal of Nutrition.* 2013, **143**(3), pp.274-283.

232. Borthakur, A. et al. A novel nutrient sensing mechanism underlies substrate-induced regulation of monocarboxylate transporter-1. *American Journal of Physiology-Gastrointestinal and Liver Physiology.* 2012, **303**(10), pp.G1126-G1133.

233. Englund, G. et al. Regional levels of drug transporters along the human intestinal tract: Co-expression of ABC and SLC transporters and comparison with Caco-2 cells. *Eur J Pharm Sci.* 2006, **29**(3-4), pp.269-277.

234. Poquet, L. et al. Transport and metabolism of ferulic acid through the colonic epithelium. *Drug Metab Dispos.* 2008, **36**(1), pp.190-197.

235. Konishi, Y. and Shimizu, M. Transepithelial transport of ferulic acid by monocarboxylic acid transporter in Caco-2 cell monolayers. *Biosci Biotechnol Biochem.* 2003, **67**(4), pp.856-862.

236. Anderson, C.M.H. and Thwaites, D.T. *Hijacking Solute Carriers for Proton-Coupled Drug Transport.* 2010.

237. Gill, R.K. et al. Expression and membrane localization of MCT isoforms along the length of the human intestine. *Am J Physiol Cell Physiol.* 2005, **289**(4), pp.C846-C852.

238. Lam, W.K. et al. Monocarboxylate Transporter-Mediated Transport of gamma-Hydroxybutyric Acid in Human Intestinal Caco-2 Cells. *Drug Metab Dispos.* 2010, **38**(3), pp.441-447.

239. Halestrap, A.P. and Wilson, M.C. The monocarboxylate transporter family - Role and regulation. *Iubmb Life.* 2012, **64**(2), pp.109-119.

240. Neuhoff, S. et al. pH-Dependent passive and active transport of acidic drugs across Caco-2 cell monolayers. *European Journal of Pharmaceutical Sciences.* 2005, **25**(2-3), pp.211-220.

241. Saksena, S. et al. Mechanisms underlying modulation of monocarboxylate transporter 1 (MCT1) by somatostatin in human intestinal epithelial cells. *American Journal of Physiology-Gastrointestinal and Liver Physiology.* 2009, **297**(5), pp.G878-G885.

242. Iwanaga, T. et al. Cellular expression of monocarboxylate transporters (MCT) in the digestive tract of the mouse, rat, and humans, with special reference to slc5a8. *Biomedical Research-Tokyo.* 2006, **27**(5), pp.243-254.

243. Welter, H. and Claus, R. Expression of the monocarboxylate transporter 1 (MCT1) in cells of the porcine intestine. *Cell Biology International.* 2008, **32**(6), pp.638-645.

244. Garcia, C.K. et al. CDNA Cloning of MCT2, a Second Monocarboxylate Transporter Expressed In Different Cells than MCT1. *Journal of Biological Chemistry.* 1995, **270**(4), pp.1843-1849.

245. Kirat, D. and Kato, S. Monocarboxylate transporter 1 (MCT1) mediates transport of short-chain fatty acids in bovine caecum. *Experimental Physiology.* 2006, **91**(5), pp.835-844.

246. Wilson, M.C. et al. Basigin (CD147) is the target for organomercurial inhibition of monocarboxylate transporter isoforms 1 and 4 - The ancillary protein for the insensitive MCT2 is embigin (gp70). *Journal of Biological Chemistry.* 2005, **280**(29), pp.27213-27221.

247. Kirk, P. et al. CD147 is tightly associated with lactate transporters MCT1 and MCT4 and facilitates their cell surface expression. *Embo Journal.* 2000, **19**(15), pp.3896-3904.

248. Deora, A.A. et al. Mechanisms regulating tissue-specific polarity of monocarboxylate transporters and their chaperone CD147 in kidney and retinal epithelia. *Proceedings of the National Academy of Sciences of the United States of America.* 2005, **102**(45), pp.16245-16250.

249. Castorino, J.J. et al. Basolateral Sorting Signals Regulating Tissue-Specific Polarity of Heteromeric Monocarboxylate Transporters in Epithelia. *Traffic.* 2011, **12**(4), pp.483-498.

250. Gallagher, S.M. et al. Monocarboxylate transporter 4 regulates maturation and trafficking of CD147 to the plasma membrane in the metastatic breast cancer cell line MDA-MB-231. *Cancer Research.* 2007, **67**(9), pp.4182-4189.

251. Li, H. et al. SLC5A8, a sodium transporter, is a tumor suppressor gene silenced by methylation in human colon aberrant crypt foci and cancers. *Proceedings of the National Academy of Sciences of the United States of America.* 2003, **100**(14), pp.8412-8417.

252. Lang, R. et al. Bioappearance and pharmacokinetics of bioactives upon coffee consumption. *Analytical and Bioanalytical Chemistry.* 2013, **405**(26), pp.8487-8503.

253. Eze, M.O. and McElhaney, R.N. The Effect of Alterations in the Fluidity and Phase State of the Membrane Lipids on the Passive Permeation and Facilitated Diffusion of Glycerol in Escherichia coli. *Journal of General Microbiology.* 1981, **124**(JUN), pp.299-307.

254. Casey, D. et al. Amphiphilic drug interactions with model cellular membranes are influenced by lipid chain-melting temperature. *Journal of the Royal Society Interface.* 2014, **11**(94).

255. Campbell, S.D. et al. Significance of Lipid Composition in a Blood-Brain Barrier-Mimetic PAMPA Assay. *Journal of Biomolecular Screening.* 2014, **19**(3), pp.437-444.

256. Vijayaraghavalu, S. et al. Epigenetic Modulation of the Biophysical Properties of Drug-Resistant Cell Lipids to Restore Drug Transport and Endocytic Functions. *Molecular Pharmaceutics.* 2012, **9**(9), pp.2730-2742.

257. Mukhopadhyay, K. et al. Drug susceptibilities of yeast cells are affected by membrane lipid composition. *Antimicrobial Agents and Chemotherapy.* 2002, **46**(12), pp.3695-3705.

258. Francis, S.A. et al. Rapid reduction of MDCK cell cholesterol by methyl-beta-cyclodextrin alters steady state transepithelial electrical resistance. *European Journal of Cell Biology.* 1999, **78**(7), pp.473-484.

259. Doan, K.M.M. et al. Passive permeability and P-glycoprotein-mediated efflux differentiate central nervous system (CNS) and non-CNS marketed drugs. *Journal of Pharmacology and Experimental Therapeutics.* 2002, **303**(3), pp.1029-1037.

260. Brand, W. et al. Metabolism and transport of the citrus flavonoid hesperetin in Caco-2 cell monolayers. *Drug Metabolism and Disposition.* 2008, **36**(9), pp.1794-1802.

261. Frolund, S. et al. The proton-coupled amino acid transporter, SLC36A1 (hPAT1), transports Gly-Gly, Gly-Sar and other Gly-Gly mimetics. *British Journal of Pharmacology.* 2010, **161**(3), pp.589-600.

262. Rolsted, K. et al. Simulating kinetic parameters in transporter mediated permeability across Caco-2 cells. A case study of estrone-3-sulfate. *European Journal of Pharmaceutical Sciences.* 2011, **44**(3), pp.218-226.

263. Grosser, G. et al. Cloning and functional characterization of the mouse sodium-dependent organic anion transporter Soat (Slc10a6). *Journal of Steroid Biochemistry and Molecular Biology.* 2013, **138**, pp.90-99.

264. Hagenbuch, B. and Meier, P.J. Organic anion transporting polypeptides of the OATP/SLC21 family: phylogenetic classification as OATP/SLCO superfamily, new nomenclature and molecular/functional properties. *Pflugers Archiv-European Journal of Physiology.* 2004, **447**(5), pp.653-665.

265. Mohrhauer, H. et al. Metabolism of Linoleic Acid in Relation to Dietary Monoenoic Fatty Acids in Rat. *Journal of Nutrition.* 1967, **91**(4), pp.521-&.

266. Ide, T. et al. Stimulation of the activities of hepatic fatty acid oxidation enzymes by dietary fat rich in alpha-linolenic acid in rats. *Journal of Lipid Research.* 1996, **37**(3), pp.448-463.

267. Feltkamp, C.A. and Vanderwaerden, A.W.M. Junction Formation between Cultured Normal Rat Hepatocytes - an Ultrastructural-Study on the Presence of Cholesterol and The Structure of Developing Tight-Junction Strands. *Journal of Cell Science.* 1983, **63**(SEP), pp.271-286.

268. Lambert, D. et al. Methyl-beta-cyclodextrin increases permeability of Caco-2 cell monolayers by displacing specific claudins from cholesterol rich domains associated with tight junctions. *Cell Physiol Biochem.* 2007, **20**(5), pp.495-506.

269. Lambert, D. et al. Depletion of Caco-2 cell cholesterol disrupts barrier function by altering the detergent solubility and distribution of specific tight-junction proteins. *Biochemical Journal.* 2005, **387**, pp.553-560.

270. Nusrat, A. et al. Tight junctions are membrane microdomains. *Journal of Cell Science.* 2000, **113**(10), pp.1771-1781.

271. Stulnig, T.M. et al. Polyunsaturated fatty acids inhibit T cell signal transduction by modification of detergent-insoluble membrane domains. *Journal of Cell Biology.* 1998, **143**(3), pp.637-644.

272. Briolay, A. et al. Myogenic differentiation and lipid-raft composition of L6 skeletal muscle cells are modulated by PUFAs. *Biochimica Et Biophysica Acta-Biomembranes.* 2013, **1828**(2), pp.602-613.

273. Turk, H.F. and Chapkin, R.S. Membrane lipid raft organization is uniquely modified by n-3 polyunsaturated fatty acids. *Prostaglandins Leukot Essent Fatty Acids.* 2013, **88**(1), pp.43-7.

274. Roig-Perez, S. et al. Intracellular Mechanisms Involved in Docosahexaenoic Acid-Induced Increases in Tight Junction Permeability in Caco-2 Cell Monolayers. *Journal of Nutrition.* 2010, **140**(9), pp.1557-1563.

275. Willemsen, L.E.M. et al. Polyunsaturated fatty acids support epithelial barrier integrity and reduce IL-4 mediated permeability in vitro. *European Journal of Nutrition.* 2008, **47**(4), pp.183-191.

276. Li, Q. et al. N-3 polyunsaturated fatty acids prevent disruption of epithelial barrier function induced by proinflammatory cytokines. *Molecular Immunology.* 2008, **45**(5), pp.1356-1365.

277. Jiang, W.G. et al. Regulation of tight junction permeability and occludin expression by polyunsaturated fatty acids. *Biochemical and Biophysical Research Communications.* 1998, **244**(2), pp.414-420.

278. Usami, M. et al. Effect of gamma-linolenic acid or docosahexaenoic acid on tight junction permeability in intestinal monolayer cells and their mechanism by protein kinase C activation and/or eicosanoid formation. *Nutrition.* 2003, **19**(2), pp.150-156.

279. Usami, M. et al. Effect of eicosapentaenoic acid (EPA) on tight junction permeability in intestinal monolayer cells. *Clinical Nutrition.* 2001, **20**(4), pp.351-359.

280. Ahlin, G. et al. Endogenous Gene and Protein Expression of Drug-Transporting Proteins in Cell Lines Routinely Used in Drug Discovery Programs. *Drug Metabolism and Disposition.* 2009, **37**(12), pp.2275-2283.

281. Wong, C.C. et al. Interaction of hydroxycinnamic acids and their conjugates with organic anion transporters and ATP-binding cassette transporters. *Molecular Nutrition & Food Research.* 2011, **55**(7), pp.979-988.

282. Ballatori, N. et al. The heteromeric organic solute transporter, OST alpha-OST beta/SLC51: A transporter for steroid-derived molecules. *Molecular Aspects of Medicine.* 2013, **34**(2-3), pp.683-692.

283. Yang, B. et al. Exposure to common food additive carrageenan leads to reduced sulfatase activity and increase in sulfated glycosaminoglycans in human epithelial cells. *Biochimie.* 2012, **94**(6), pp.1309-1316.

284. Hughes, P.J. et al. Up-regulation of steroid sulphatase activity in HL60 promyelocytic cells by retinoids and 1 alpha,25-dihydroxyvitamin D-3. *Biochemical Journal.* 2001, **355**, pp.361-371.

285. Lepine, J. et al. Specificity and regioselectivity of the conjugation of estradiol, estrone, and their catecholestrogen and methoxyestrogen metabolites by human uridine diphospho-glucuronosyltransferases expressed in endometrium. *Journal of Clinical Endocrinology & Metabolism.* 2004, **89**(10), pp.5222-5232.

286. Mostafa, Y.A. and Taylor, S.D. Steroid derivatives as inhibitors of steroid sulfatase. *Journal of Steroid Biochemistry and Molecular Biology.* 2013, **137**, pp.183-198.

287. Dannenberg, A.J. et al. Dietary Lipids Induce Phase 2 Enzymes in Rat Small-Intestine. *Biochimica Et Biophysica Acta.* 1993, **1210**(1), pp.8-12.

288. Dannenberg, A.J. and Zakim, D. Dietary Lipid Regulates the Amount and Functional State of UDP-Glucuronosyltransferase in Rat Liver. *Journal of Nutrition.* 1992, **122**(8), pp.1607-1613.

289. de Vogel-van den Bosch, H.M. et al. PPARalpha-mediated effects of dietary lipids on intestinal barrier gene expression. *Bmc Genomics.* 2008, **9**.

290. Ihunnah, C.A. et al. Estrogen Sulfotransferase/SULT1E1 Promotes Human Adipogenesis. *Molecular and Cellular Biology.* 2014, **34**(9), pp.1682-1694.

291. Smuc, T. and Rizner, T.L. Expression of 17 beta-hydroxysteroid dehydrogenases and other estrogen-metabolizing enzymes in different cancer cell lines. *Chemico-Biological Interactions.* 2009, **178**(1-3), pp.228-233.

292. Li, L. et al. Increased SULT1E1 activity in HepG2 hepatocytes decreases growth hormone stimulation of STAT5b phosphorylation. *Steroids.* 2009, **74**(1), pp.20-29.

293. Meinl, W. et al. Sulfotransferase forms expressed in human intestinal Caco-2 and TC7 cells at varying stages of differentiation and role in benzo a pyrene metabolism. *Drug Metabolism and Disposition.* 2008, **36**(2), pp.276-283.

294. Nguyen, H.T.T. et al. Association of PepT1 with lipid rafts differently modulates its transport activity in polarized and nonpolarized cells. *American journal of physiology. Gastrointestinal and liver physiology.* 2007, **293**(6), pp.G1155-65.

295. Radeva, G. et al. P-glycoprotein is localized in intermediate-density membrane microdomains distinct from classical lipid rafts and caveolar domains. *Febs Journal.* 2005, **272**(19), pp.4924-4937.

296. Zidovetzki, R. and Levitan, I. Use of cyclodextrins to manipulate plasma membrane cholesterol content: Evidence, misconceptions and control strategies. *Biochimica Et Biophysica Acta-Biomembranes.* 2007, **1768**(6), pp.1311-1324.

297. Caliceti, C. et al. Effect of Plasma Membrane Cholesterol Depletion on Glucose Transport Regulation in Leukemia Cells. *Plos One.* 2012, **7**(7).

298. Karnik, R. et al. Endocytosis of hERG Is Clathrin-Independent and Involves Arf6. *Plos One.* 2013, **8**(12).

299. Vaidyanathan, J.B. and Walle, T. Transport and metabolism of the tea flavonoid (-)-epicatechin by the human intestinal cell line Caco-2. *Pharmaceutical Research.* 2001, **18**(10), pp.1420-1425.

300. Zhang, L. et al. Investigation of intestinal absorption and disposition of green tea catechins by Caco-2 monolayer model. *International Journal of Pharmaceutics.* 2004, **287**(1-2), pp.1-12.

301. Hinrichs, J.W.J. et al. ATP-binding cassette transporters are enriched in non-caveolar detergent-insoluble glycosphingolipid-enriched membrane domains (DIGs) in human multidrug-resistant cancer cells. *Journal of Biological Chemistry.* 2004, **279**(7), pp.5734-5738.

302. Orlowski, S. et al. P-glycoprotein and 'lipid rafts': some ambiguous mutual relationships (floating on them, building them or meeting them by chance?). *Cellular and Molecular Life Sciences.* 2006, **63**(9), pp.1038-1059.

303. Pike, L.J. Lipid rafts: bringing order to chaos. *Journal of Lipid Research.* 2003, **44**(4), pp.655-667.

304. Brown, D.A. Lipid rafts, detergent-resistant membranes, and raft targeting signals. *Physiology.* 2006, **21**, pp.430-439.

305. Kim, W. et al. A Novel Role for Nutrition in the Alteration of Functional Microdomains on the Cell Surface. *Lipidomics: Vol 1: Methods and Protocols.* 2009, pp.261-270.

306. Basiouni, S. et al. Polyunsaturated fatty acid supplements modulate mast cell membrane microdomain composition. *Cellular Immunology.* 2012, **275**(1-2), pp.42-46.

307. Chapkin, R.S. et al. Bioactive dietary long-chain fatty acids: emerging mechanisms of action. *British Journal of Nutrition.* 2008, **100**(6), pp.1152-1157.

308. Loor, F. et al. Cyclosporins: Structure-activity relationships for the inhibition of the human MDR1 P-glycoprotein ABC transporter. *Journal of Medicinal Chemistry.* 2002, **45**(21), pp.4598-4612.

309. Gutmann, H. et al. Evidence for different ABC-transporters in Caco-2 cells modulating drug uptake. *Pharmaceutical Research.* 1999, **16**(3), pp.402-407.

310. Zhang, S.Z. et al. Combined effects of multiple flavonoids on breast cancer resistance protein (ABCG2)-mediated transport. *Pharmaceutical Research.* 2004, **21**(7), pp.1263-1273.

311. Ottaviani, J.I. et al. Structurally related (-)-epicatechin metabolites in humans: Assessment using de novo chemically synthesized authentic standards. *Free Radical Biology and Medicine.* 2012, **52**(8), pp.1403-1412.

312. Actis-Goretta, L. et al. Elucidation of (-)-epicatechin metabolites after ingestion of chocolate by healthy humans. *Free Radical Biology and Medicine.* 2012, **53**(4), pp.787-795.

313. Vaidyanathan, J.B. and Walle, T. Glucuronidation and sulfation of the tea flavonoid (-)-epicatechin by the human and rat enzymes. *Drug Metabolism and Disposition.* 2002, **30**(8), pp.897-903.

314. Gamage, N. et al. Human sulfotransferases and their role in chemical metabolism. *Toxicological Sciences.* 2006, **90**(1), pp.5-22.

315. Mannisto, P.T. and Kaakkola, S. Catechol-O-methyltransferase (COMT): Biochemistry, molecular biology, pharmacology, and clinical efficacy of the new selective COMT inhibitors. *Pharmacological Reviews.* 1999, **51**(4), pp.593-628.

316. Tian, X.-J. et al. Studies of intestinal permeability of 36 flavonoids using Caco-2 cell monolayer model. *International Journal of Pharmaceutics.* 2009, **367**(1-2), pp.58-64.

317. Seithel, A. et al. Variability in mRNA expression of ABC- and SLC-transporters in human intestinal cells: Comparison between human segments and Caco-2 cells. *European Journal of Pharmaceutical Sciences.* 2006, **28**(4), pp.291-299.

318. Auguste, K.I. et al. Greatly impaired migration of implanted aquaporin-4-deficient astroglial cells in mouse brain toward a site of injury. *Faseb Journal.* 2007, **21**(1), pp.108-116.

319. Luehrmann, A. et al. The alveolar epithelial type I-like cell line as an adequate model for leukocyte migration studies in vitro. *Experimental and Toxicologic Pathology.* 2007, **58**(5), pp.277-283.

320. Bento, A.P. et al. The ChEMBL bioactivity database: an update. *Nucleic acids research.* 2014, **42**(Database issue), pp.D1083-90.

321. Kennedy, J.A. et al. The Protonation Reactions of Catechin, Epicatechin and Related Compounds. *Australian Journal of Chemistry.* 1984, **37**(4), pp.885-892.

322. Fujita, M. et al. Convergence of Apical and Basolateral Endocytic Pathways at Apical Late Endosomes in Absorptive Cells of Suckling Rat Ileum In Vivo. *Journal of Cell Science.* 1990, **97**, pp.385-394.

323. Dan, N. and Cutler, D.F. Transcytosis and Processing of Intrinsic Factor-Cobalamin in Caco-2 Cells. *Journal of Biological Chemistry.* 1994, **269**(29), pp.18849-18855.

324. Brada, N. et al. Transfer of cobalamin from intrinsic factor to transcobalamin II. *Journal of Nutritional Biochemistry.* 2001, **12**(4), pp.200-206.

325. Shah, D. and Shen, W.C. The Establishment of Polarity and Enhanced Transcytosis of Transferrin Receptors in Enterocyte-Like Caco-2 Cells. *Journal of Drug Targeting.* 1994, **2**(2), pp.93-99.

326. Schaerer, E. et al. Molecular and Cellular Mechanisms Involved in Transepithelial Transport. *Journal of Membrane Biology.* 1991, **123**(2), pp.93-103.

327. Lebivic, A. et al. Biogenetic Pathways of Plasma-Membrane Proteins in Caco-2, a Human Intestinal Epithelial Cell Line. *Journal of Cell Biology.* 1990, **111**(4), pp.1351-1361.

328. Barroso, M. and Sztul, E.S. Basolateral to Apical Transcytosis in Polarized Cells is Indirect and Involves BFA and Trimeric-G Protein Sensitive Passage Through the Apical Endosome. *Journal of Cell Biology.* 1994, **124**(1-2), pp.83-100.

329. Marsh, M. and Helenius, A. Adsorptive Endocytosis of Semliki Forest Virus. *Journal of Molecular Biology.* 1980, **142**(3), pp.439-454.

330. Kosinska, A. and Andlauer, W. Cocoa polyphenols are absorbed in Caco-2 cell model of intestinal epithelium. *Food Chemistry.* 2012, **135**(3), pp.999-1005.

331. Anderle, P. et al. P-glycoprotein (P-gp) mediated efflux in Caco-2 cell monolayers: The influence of culturing conditions and drug exposure on P-gp expression levels. *Journal of Pharmaceutical Sciences.* 1998, **87**(6), pp.757-762.

332. Emi, Y. et al. A cis-acting five-amino-acid motif controls targeting of ABCC2 to the apical plasma membrane domain. *Journal of Cell Science.* 2012, **125**(13), pp.3133-3143.

333. Xia, C.Q. et al. Expression, localization, and functional characteristics of breast cancer resistance protein in Caco-2 cells. *Drug Metabolism and Disposition.* 2005, **33**(5), pp.637-643.

334. Emi, Y. et al. Involvement of a di-leucine motif in targeting of ABCC1 to the basolateral plasma membrane of polarized epithelial cells. *Biochemical and Biophysical Research Communications.* 2013, **441**(1), pp.89-95.

335. Prime-Chapman, H.M. et al. Differential multidrug resistance-associated protein 1 through 6 isoform expression and function in human intestinal epithelial Caco-2 cells. *Journal of Pharmacology and Experimental Therapeutics.* 2004, **311**(2), pp.476-484.

336. Ming, X. and Thakker, D.R. Role of basolateral efflux transporter MRP4 in the intestinal absorption of the antiviral drug adefovir dipivoxil. *Biochemical Pharmacology.* 2010, **79**(3), pp.455-462.

337. Quazi, F. and Molday, R.S. Lipid transport by mammalian ABC proteins. In: Sharom, F.J. ed. *Essays in Biochemistry: Abc Transporters*. 2011, pp.265-290.

338. Borst, P. et al. ABC transporters in lipid transport. *Biochimica Et Biophysica Acta-Molecular and Cell Biology of Lipids.* 2000, **1486**(1), pp.128-144.

339. Maubon, N. et al. Analysis of drug transporter expression in human intestinal Caco-2 cells by real-time PCR. *Fundam Clin Pharmacol.* 2007, **21**(6), pp.659-663.

340. Taipalensuu, J. et al. Correlation of gene expression of ten drug efflux proteins of the ATP-binding cassette transporter family in normal human jejunum and in human intestinal epithelial Caco-2 cell monolayers. *Journal of Pharmacology and Experimental Therapeutics.* 2001, **299**(1), pp.164-170.

341. Hunter, J. et al. Transepithelial Secretion, Cellular Accumulation and Cytotoxicity of Vinblastine in Defined MDCK Cell Strains. *Biochimica Et Biophysica Acta.* 1993, **1179**(1), pp.1-10.

342. Higgins, C.F. and Gottesman, M.M. Is the Multidrug Transporter a Flippase? *Trends in Biochemical Sciences.* 1992, **17**(1), pp.18-21.

343. Quinn, P.J. A lipid matrix model of membrane raft structure. *Progress in Lipid Research.* 2010, **49**(4), pp.390-406.

344. Ito, K. et al. Cholesterol but not association with detergent resistant membranes is necessary for the transport function of MRP2/ABCC2. *Febs Letters.* 2008, **582**(30), pp.4153-4157.

345. Storch, C.H. et al. Localization of the human breast cancer resistance protein (BCRP/ABCG2) in lipid rafts/caveolae and modulation of its activity by cholesterol in vitro. *Journal of Pharmacology and Experimental Therapeutics.* 2007, **323**(1), pp.257-264.

346. Guyot, C. and Stieger, B. Interaction of bile salts with rat canalicular membrane vesicles: Evidence for bile salt resistant microdomains. *Journal of Hepatology.* 2011, **55**(6), pp.1368-1376.

347. Ismair, M.G. et al. ABC-transporters are localized in caveolin-1-positive and reggie-1-negative and reggie-2-negative microdomains of the canalicular membrane in rat hepatocytes. *Hepatology.* 2009, **49**(5), pp.1673-82.

348. Aliche-Djoudi, F. et al. A role for lipid rafts in the protection afforded by docosahexaenoic acid against ethanol toxicity in primary rat hepatocytes. *Food and Chemical Toxicology.* 2013, **60**, pp.286-296.

349. Simon, S. and Schubert, R. Inhibitory effect of phospholipids on P-glycoprotein: Cellular studies in Caco-2, MDCKII mdr1 and MDCKII wildtype cells and P-gp ATPase activity measurements. *Biochimica Et Biophysica Acta-Molecular and Cell Biology of Lipids.* 2012, **1821**(9), pp.1211-1223.

350. Gerk, P.M. and Vore, M. Regulation of expression of the multidrug resistance associated protein 2 (MRP2) and its role in drug disposition. *Journal of Pharmacology and Experimental Therapeutics.* 2002, **302**(2), pp.407-415.

351. Actis-Goretta, L. et al. Intestinal absorption, metabolism, and excretion of (-)-epicatechin in healthy humans assessed by using an intestinal perfusion technique. *American Journal of Clinical Nutrition.* 2013, **98**(4), pp.924-933.

352. Roura, E. et al. Rapid liquid chromatography tandem mass spectrometry assay to quantify plasma (-)-epicatechin metabolites after ingestion of a standard portion of cocoa beverage in humans. *Journal of Agricultural and Food Chemistry.* 2005, **53**(16), pp.6190-6194.

353. Baba, S. et al. Bioavailability of (-)-epicatechin upon intake of chocolate and cocoa in human volunteers. *Free Radical Research.* 2000, **33**(5), pp.635-641.

354. Piskula, M.K. and Terao, J. Accumulation of (-)-epicatechin metabolites in rat plasma after oral administration and distribution of conjugation enzymes in rat tissues. *Journal of Nutrition.* 1998, **128**(7), pp.1172-1178.

355. Rodriguez-Mateos, A. et al. Uptake and metabolism of (-)-epicatechin in endothelial cells. *Archives of Biochemistry and Biophysics.* 2014, **559**, pp.17-23.

356. Nakamura, A. et al. Expression of UGT1A and UGT2B mRNA in human normal tissues and various cell lines. *Drug Metabolism and Disposition.* 2008, **36**(8), pp.1461-1464.

357. Shibuya, A. et al. Impact of fatty acids on human UDP-glucuronosyltransferase 1A1 activity and its expression in neonatal hyperbilirubinemia. *Scientific Reports.* 2013, **3**.

358. Okamura, K. et al. Fatty acyl-CoA as an endogenous activator of UDP-glucuronosyltransferases. *Biochemical and Biophysical Research Communications.* 2006, **345**(4), pp.1649-1656.

359. Tsoutsikos, P. et al. Evidence that unsaturated fatty acids are potent inhibitors of renal UDP-glucuronosyltransferases (UGT): kinetic studies using human kidney cortical microsomes and recombinant UGT1A9 and UGT2B7. *Biochemical Pharmacology.* 2004, **67**(1), pp.191-199.

360. Blount, J.W. et al. Enzymatic synthesis of substituted epicatechins for bioactivity studies in neurological disorders. *Biochemical and Biophysical Research Communications.* 2012, **417**(1), pp.457-461.

361. Specian, R.D. and Oliver, M.G. Functional Biology of Intestinal Goblet Cells. *American Journal of Physiology.* 1991, **260**(2), pp.C183-C193.

362. Fallon, J.K. et al. Targeted Quantitative Proteomics for the Analysis of 14 UGT1As and-2Bs in Human Liver Using NanoUPLC-MS/MS with Selected Reaction Monitoring. *Journal of Proteome Research.* 2013, **12**(10), pp.4402-4413.

363. Izukawa, T. et al. Quantitative Analysis of UDP-Glucuronosyltransferase (UGT) 1A and UGT2B Expression Levels in Human Livers. *Drug Metabolism and Disposition.* 2009, **37**(8), pp.1759-1768.

364. Sato, Y. et al. Optimized methods for targeted Peptide-based quantification of human uridine 5'-diphosphate-glucuronosyltransferases in biological specimens using liquid chromatography-tandem mass spectrometry. *Drug*

metabolism and disposition: the biological fate of chemicals. 2014, **42**(5), pp.885-9.

365. Hanioka, N. et al. Effect of aflatoxin B1 on UDP-glucuronosyltransferase mRNA expression in HepG2 cells. *Chemosphere.* 2012, **89**(5), pp.526-529.

366. Harbourt, D.E. et al. Quantification of Human Uridine-Diphosphate Glucuronosyl Transferase 1A Isoforms in Liver, Intestine, and Kidney Using Nanobore Liquid Chromatography-Tandem Mass Spectrometry. *Analytical Chemistry.* 2012, **84**(1), pp.98-105.

367. Court, M.H. et al. Quantitative distribution of mRNAs encoding the 19 human UDP-glucuronosyltransferase enzymes in 26 adult and 3 fetal tissues. *Xenobiotica.* 2012, **42**(3), pp.266-277.

368. Johansson, M.E.V. et al. The gastrointestinal mucus system in health and disease. *Nature Reviews Gastroenterology & Hepatology.* 2013, **10**(6), pp.352-361.

369. Croix, J.A. et al. Inflammatory cues modulate the expression of secretory product genes, Golgi sulfotransferases and sulfomucin production in LS174T cells. *Experimental Biology and Medicine.* 2011, **236**(12), pp.1402-1412.

370. Campbell, B.J. et al. Increasing the intra-Golgi pH of cultured LS174T goblet-differentiated cells mimics the decreased mucin sulfation and increased Thomsen-Friedenreich antigen (Gal beta 1-3GalNac alpha-) expression seen in colon cancer. *Glycobiology.* 2001, **11**(5), pp.385-393.

371. Forstner, J. et al. Effect of Reserpine on the Histochemical and Biochemical-Properties of Rat Intestinal Mucin. *Experimental and Molecular Pathology.* 1991, **54**(2), pp.129-143.

372. Zakim, D. et al. Influence of Membrane Lipids on Regulatory Properties of UDP-Glucuronyltransferase. *European Journal of Biochemistry.* 1973, **38**(1), pp.59-63.

373. Zakim, D. Regulation of Microsomal Enzymes by Phospholipids: 1. Effect of Phospholipases and Phospholipids on Glucose-6-Phosphatase. *Journal of Biological Chemistry.* 1970, **245**(19), pp.4953-&.

374. Vessey, D.A. and Zakim, D. Regulation of Microsomal Enzymes by Phospholipids: 2. Activation of Hepatic Uridine Diphosphate-Glucuronyltransferase. *Journal of Biological Chemistry.* 1971, **246**(15), pp.4649-&.

375. Dannenberg, A.J. and Yang, E.K. Effect of Dietary Lipids on Levels Of UDP-Glucuronosyltransferase in Liver. *Biochemical Pharmacology.* 1992, **44**(2), pp.335-340.

376. Kato, J. et al. The effect of dietary fatty acids on the expression levels and activities of hepatic drug metabolizing enzymes. *Journal of Health Science.* 2003, **49**(2), pp.105-114.

377. Barbier, O. et al. The UDP-glucuronosyltransferase 1A9 enzyme is a peroxisome proliferator-activated receptor alpha and gamma target gene. *Journal of Biological Chemistry.* 2003, **278**(16), pp.13975-13983.

378. Forman, B.M. et al. Hypolipidemic drugs, polyunsaturated fatty acids, and eicosanoids are ligands for peroxisome proliferator-activated receptors alpha and delta. *Proceedings of the National Academy of Sciences of the United States of America.* 1997, **94**(9), pp.4312-4317.

379. Kliewer, S.A. et al. Fatty acids and eicosanoids regulate gene expression through direct interactions with peroxisome proliferator-activated receptors alpha and gamma. *Proceedings of the National Academy of Sciences of the United States of America.* 1997, **94**(9), pp.4318-4323.

380. Kimura, R. et al. DHA attenuates postprandial hyperlipidemia via activating PPAR alpha in intestinal epithelial cells. *Journal of Lipid Research.* 2013, **54**(12), pp.3258-3268.

381. Shrestha, S.P. et al. Glucuronidation and Methylation of Procyanidin Dimers B2 and 3,3 ''-Di-O-Galloyl-B2 and Corresponding Monomers Epicatechin and 3-O-Galloyl-Epicatechin in Mouse Liver. *Pharmaceutical Research.* 2012, **29**(3), pp.856-865.

382. Natsume, M. et al. Structures of (-)-epicatechin glucuronide identified from plasma and urine after oral ingestion of (-)-epicatechin: Differences between human and rat. *Free Radical Biology and Medicine.* 2003, **34**(7), pp.840-849.

383. Zaleski, J. et al. Nuclear Membrane-Bound UDP-Glucuronsyltransferase of Rat-Liver. *Canadian Journal of Biochemistry.* 1982, **60**(10), pp.972-979.

384. Chowdhury, J.R. et al. Distribution Of UDPglucuronosyltransferase in Rat-Tissue. *Proceedings of the National Academy of Sciences of the United States of America.* 1985, **82**(9), pp.2990-2994.

385. Hauser, S.C. et al. Subcellular Distribution and Regulation of Hepatic Bilirubin UDP-Glucuronyltransferase. *Journal of Biological Chemistry.* 1984, **259**(7), pp.4527-4533.

386. Antoine, B. et al. Functional-Heterogeneity Of UDP-Glucuronosyltransferases in Different Membranes of Rat-Liver. *Biochemical Pharmacology.* 1983, **32**(17), pp.2629-2632.

387. Antoine, B. et al. Kinetic-Properties of UDP-Glucuronosyltransferase(S) In Different Membranes of Rat-Liver Cells. *Xenobiotica.* 1984, **14**(7), pp.575-579.

388. Magdalou, J. et al. Phenobarbital Induction of Cytochrome-P-450 And UDP-Glucuronosyltransferase in Rabbit Liver Plasma-Membranes. *Enzyme.* 1982, **28**(1), pp.41-47.

389. Strassburg, C.P. et al. Polymorphic gene regulation and interindividual variation of UDP-glucuronosyltransferase activity in human small intestine. *Journal of Biological Chemistry.* 2000, **275**(46), pp.36164-36171.

390. Strassburg, C.P. et al. UDP-glucuronosyltransferase activity in human liver and colon. *Gastroenterology.* 1999, **116**(1), pp.149-160.

391. Huang, Y.H. et al. Identification and functional characterization of UDP-glucuronosyltransferases UGT1A8*1, UGT1A8*2 and UGT1A8*3. *Pharmacogenetics.* 2002, **12**(4), pp.287-297.

392. Wang, M. et al. Polymorphic Expression of UDP-Glucuronosyltransferase UGTlA Gene in Human Colorectal Cancer. *Plos One.* 2013, **8**(2).

393. Mojarrabi, B. and Mackenzie, P.I. Characterization of two UDP glucuronosyltransferases that are predominantly expressed in human colon. *Biochemical and Biophysical Research Communications.* 1998, **247**(3), pp.704-709.

394. Barre, L. et al. The stop transfer sequence of the human UDP-glucuronosyltransferase 1A determines localization to the endoplasmic reticulum by both static retention and retrieval mechanisms. *Febs Journal.* 2005, **272**(4), pp.1063-1071.

395. Ouzzine, M. et al. An internal signal sequence mediates the targeting and retention of the human UDP-glucuronosyltransferase 1A6 to the endoplasmic reticulum. *Journal of Biological Chemistry.* 1999, **274**(44), pp.31401-31409.

396. Ouzzine, M. et al. Expression of a functionally active human hepatic UDP-glucuronosyltransferase (UGT1A6) lacking the N-terminal signal sequence in the endoplasmic reticulum. *Febs Letters.* 1999, **454**(3), pp.187-191.

397. Kalantzi, L. et al. Canine intestinal contents vs. simulated media for the assessment of solubility of two weak bases in the human small intestinal contents. *Pharmaceutical Research.* 2006, **23**(6), pp.1373-1381.

398. *The National Diet and Nutrition Survey Results from Years 1, 2, 3 and 4 (combined) of the Rolling Programme (2008/2009 – 2011/2012).* Public Health England and the Food Standards Agency, 2014.

399. DuPont, M.S. et al. Absorption of kaempferol from endive, a source of kaempferol-3-glucuronide, in humans. *European Journal of Clinical Nutrition.* 2004, **58**(6), pp.947-954.

400. Brett, G.M. et al. Absorption, metabolism and excretion of flavanones from single portions of orange fruit and juice and effects of anthropometric variables and contraceptive pill use on flavanone excretion. *British Journal of Nutrition.* 2009, **101**(5), pp.664-675.

401. Milbury, P.E. et al. Anthocyanins are Bioavailable in Humans following an Acute Dose of Cranberry Juice. *Journal of Nutrition.* 2010, **140**(6), pp.1099-1104.

402. Kaushik, D. et al. Comparison of Quercetin Pharmacokinetics Following Oral Supplementation in Humans. *Journal of Food Science.* 2012, **77**(11), pp.H231-H238.

403. Czank, C. et al. Human metabolism and elimination of the anthocyanin, cyanidin-3-glucoside: a C-13-tracer study. *American Journal of Clinical Nutrition.* 2013, **97**(5), pp.995-1003.

404. Chao, A.C. et al. In vitro and in vivo evaluation of effects of sodium caprate on enteral peptide absorption and on mucosal morphology. *International Journal of Pharmaceutics.* 1999, **191**(1), pp.15-24.

405. Yata, T. et al. Amino acids protect epithelial cells from local toxicity by absorption enhancer, sodium laurate. *Journal of Pharmaceutical Sciences.* 2001, **90**(10), pp.1456-1465.

406. Caliph, S.M. et al. Effect of short-, medium-, and long-chain fatty acid-based vehicles on the absolute oral bioavailability and intestinal lymphatic transport of halofantrine and assessment of mass balance in lymph-cannulated and non-cannulated rats. *Journal of Pharmaceutical Sciences.* 2000, **89**(8), pp.1073-1084.

407. Hirunpanich, V. et al. Demonstration of docosahexaenoic acid as a bioavailability enhancer for CYP3A substrates: In vitro and in vivo evidence using cyclosporin in rats. *Drug Metabolism and Disposition.* 2006, **34**(2), pp.305-310.

408. Hirunpanich, V. et al. Inhibitory effect of docosahexaenoic acid (DHA) on the intestinal metabolism of midazolam: In vitro and in vivo studies in rats. *International Journal of Pharmaceutics.* 2008, **351**(1-2), pp.133-143.

409. Lesser, S. et al. The fatty acid pattern of dietary fat influences the oral bioavailability of the flavonol quercetin in pigs. *British Journal of Nutrition.* 2006, **96**(6), pp.1047-1052.

410. Tulipani, S. et al. Oil matrix effects on plasma exposure and urinary excretion of phenolic compounds from tomato sauces: Evidence from a human pilot study. *Food Chemistry.* 2012, **130**(3), pp.581-590.

411. Conlon, L.E. et al. Coconut Oil Enhances Tomato Carotenoid Tissue Accumulation Compared to Safflower Oil in the Mongolian Gerbil (Meriones unguiculatus). *Journal of Agricultural and Food Chemistry.* 2012, **60**(34), pp.8386-8394.

412. Goltz, S.R. et al. Meal triacylglycerol profile modulates postprandial absorption of carotenoids in humans. *Molecular Nutrition & Food Research.* 2012, **56**(6), pp.866-877.

413. Bazzano, L.A. et al. Fruit and vegetable intake and risk of cardiovascular disease in US adults: the first National Health and Nutrition Examination Survey Epidemiologic Follow-up Study. *American Journal of Clinical Nutrition.* 2002, **76**(1), pp.93-99.

414. Wedick, N.M. et al. Dietary flavonoid intakes and risk of type 2 diabetes in US men and women. *American Journal of Clinical Nutrition.* 2012, **95**(4), pp.925-933.

415. Oude Griep, L.M. et al. Raw and Processed Fruit and Vegetable Consumption and 10-Year Coronary Heart Disease Incidence in a Population-Based Cohort Study in the Netherlands. *Plos One.* 2010, **5**(10).

416. Skender, B. et al. Docosahexaenoic fatty acid (DHA) in the regulation of colon cell growth and cell death: A review. *Biomedical Papers-Olomouc.* 2012, **156**(3), pp.186-199.

417. van den Elsen, L. et al. Long Chain n-3 Polyunsaturated Fatty Acids in the Prevention of Allergic and Cardiovascular Disease. *Current Pharmaceutical Design.* 2012, **18**(16), pp.2375-2392.

418. Swanson, D. et al. Omega-3 Fatty Acids EPA and DHA: Health Benefits Throughout Life. *Advances in Nutrition.* 2012, **3**(1), pp.1-7.

419. Zamora-Ros, R. et al. Association between habitual dietary flavonoid and lignan intake and colorectal cancer in a Spanish case-control study (the Bellvitge Colorectal Cancer Study). *Cancer Causes & Control.* 2013, **24**(3), pp.549-557.

420. Galeone, C. et al. Coffee consumption and risk of colorectal cancer: a meta-analysis of case-control studies. *Cancer Causes & Control.* 2010, **21**(11), pp.1949-1959.

421. Pericleous, M. et al. Diet and supplements and their impact on colorectal cancer. *Journal of gastrointestinal oncology.* 2013, **4**(4), pp.409-23.

422. Song, M. et al. Dietary intake of fish, omega-3 and omega-6 fatty acids and risk of colorectal cancer: A prospective study in U.S. men and women. *International Journal of Cancer.* 2014, **135**(10), pp.2413-2423.

423. Piazzi, G. et al. Eicosapentaenoic acid free fatty acid prevents and suppresses colonic neoplasia in colitis-associated colorectal cancer acting on Notch signaling and gut microbiota. *International Journal of Cancer.* 2014, **135**(9), pp.2004-2013.

424. Murff, H.J. et al. Dietary intake of PUFAs and colorectal polyp risk. *American Journal of Clinical Nutrition.* 2012, **95**(3), pp.703-712.

425. Tome-Carneiro, J. et al. One-Year Consumption of a Grape Nutraceutical Containing Resveratrol Improves the Inflammatory and Fibrinolytic Status of Patients in Primary Prevention of Cardiovascular Disease. *American Journal of Cardiology.* 2012, **110**(3), pp.356-363.

426. Kay, C.D. et al. Relative impact of flavonoid composition, dose and structure on vascular function: A systematic review of randomised controlled trials of flavonoid-rich food products. *Molecular Nutrition & Food Research.* 2012, **56**(11), pp.1605-1616.

427. Khan, N. et al. Cocoa Polyphenols and Inflammatory Markers of Cardiovascular Disease. *Nutrients.* 2014, **6**(2), pp.844-880.

428. Kondo, K. et al. A fish-based diet intervention improves endothelial function in postmenopausal women with type 2 diabetes mellitus: A randomized crossover trial. *Metabolism-Clinical and Experimental.* 2014, **63**(7), pp.930-940.

429. Miyagawa, N. et al. Long-chain n-3 polyunsaturated fatty acids intake and cardiovascular disease mortality risk in Japanese: A 24-year follow-up of NIPPON DATA80. *Atherosclerosis.* 2014, **232**(2), pp.384-389.

430. Otto, M.C.d.O. et al. Circulating and Dietary Omega-3 and Omega-6 Polyunsaturated Fatty Acids and Incidence of CVD in the Multi-Ethnic Study of Atherosclerosis. *Journal of the American Heart Association.* 2013, **2**(6).

431. Kaikkonen, J.E. et al. Fatty acids as determinants of in-vivo lipid peroxidation: The EFFGE study in Eastern Finnish hypertensive and non-hypertensive subjects. *Annals of Medicine.* 2013, **45**(5-6), pp.455-464.

432. Verschuren, L. et al. A Dietary Mixture Containing Fish Oil, Resveratrol, Lycopene, Catechins, and Vitamins E and C Reduces Atherosclerosis in Transgenic Mice. *Journal of Nutrition.* 2011, **141**(5), pp.863-869.

433. Hoffman, R. and Gerber, M. Evaluating and adapting the Mediterranean diet for non-Mediterranean populations: A critical appraisal. *Nutrition Reviews.* 2013, **71**(9), pp.573-584.